

Nitrothiazole-thiazolidinone hybrids: Synthesis and *in vitro* antimicrobial evaluation

D Hart

 **orcid.org/0000-0002-7379-9250**

Dissertation accepted in fulfilment of the requirements for the degree Master of Science in Pharmaceutical Chemistry at the North-West University

Supervisor: Dr R Beteck
Co-Supervisor: Prof L Legoabe
Assist-Supervisor: Dr O J Jesumoroti

Graduation: June 2023
Student number: 27105083

D Hart Dissertation

ORIGINALITY REPORT

20%

SIMILARITY INDEX

6%

INTERNET SOURCES

18%

PUBLICATIONS

%

STUDENT PAPERS

PRIMARY SOURCES

1

Dylan Hart, Lesetja J. Legoabe, Omobolanle J. Jesumoroti, Audrey Jordaan, Digby F. Warner, Rebecca Steventon, Richard Beteck.

"Nitrothiazole - thiazolidinone hybrids: Synthesis and in vitro antimicrobial evaluation", Chemistry & Biodiversity, 2022

Publication

7%

2

Dylan Hart, Lesetja J. Legoabe, Omobolanle J. Jesumoroti, Audrey Jordaan, Digby F. Warner, Rebecca Steventon, Richard M. Beteck. "

Nitrothiazole - Thiazolidinone Hybrids: Synthesis and Antimicrobial Evaluation ", Chemistry & Biodiversity, 2022

Publication

5%

3

epdf.pub

Internet Source

1%

4

archive.org

Internet Source

1%

5

www.science.gov

Internet Source

<1%

6	Antibiotic Discovery and Development, 2012. Publication	<1 %
7	Zubair Shanib Bhat, Muzafar Ahmad Rather, Mubashir Maqbool, Zahoor Ahmad. "Drug targets exploited in Mycobacterium tuberculosis : Pitfalls and promises on the horizon", Biomedicine & Pharmacotherapy, 2018 Publication	<1 %
8	Steingart, Karen R, Ian Schiller, David J Horne, Madhukar Pai, Catharina C Boehme, Nandini Dendukuri, and Karen R Steingart. "Xpert® MTB/RIF assay for pulmonary tuberculosis and rifampicin resistance in adults", Cochrane Database of Systematic Reviews, 2014. Publication	<1 %
9	Stephen D Lawn, Mark P Nicol. " Xpert MTB/RIF assay: development, evaluation and implementation of a new rapid molecular diagnostic for tuberculosis and rifampicin resistance ", Future Microbiology, 2011 Publication	<1 %
10	"Posters", Clinical Microbiology and Infection, 5/2008 Publication	<1 %
11	opencommons.uconn.edu Internet Source	<1 %

12	Jiyong Jian, Xinyu Yang, Jun Yang, Liang Chen. "Evaluation of the GenoType MTBDR _{plus} and MTBDR _{s/l} for the detection of drug-resistant <i>Mycobacterium tuberculosis</i> on isolates from Beijing, China", Infection and Drug Resistance, 2018 Publication	<1 %
13	uknowledge.uky.edu Internet Source	<1 %
14	www.ncbi.nlm.nih.gov Internet Source	<1 %
15	"Posters", Clinical Microbiology and Infection, 4/2007 Publication	<1 %
16	mist-meme.com Internet Source	<1 %
17	library.unisel.edu.my Internet Source	<1 %
18	mdpi-res.com Internet Source	<1 %
19	open.uct.ac.za Internet Source	<1 %
20	Jian Xu, Bin Wang, Minghao Hu, Fengmin Huo, Shaochen Guo, Wei Jing, Eric Nuermberger, Yu Lu. "Primary Clofazimine and Bedaquiline Resistance among Isolates from Patients with	<1 %

Multidrug-Resistant Tuberculosis",
Antimicrobial Agents and Chemotherapy,
2017

Publication

-
- | | | |
|----|---|------|
| 21 | perspectivesinmedicine.cshlp.org
Internet Source | <1 % |
|----|---|------|
-
- | | | |
|----|---|------|
| 22 | series.publisso.de
Internet Source | <1 % |
|----|---|------|
-
- | | | |
|----|---|------|
| 23 | www.gulfcoastconsortia.org
Internet Source | <1 % |
|----|---|------|
-
- | | | |
|----|---|------|
| 24 | Jeong Seong Yang, Kyung Jong Kim, Hongjo Choi, Seung Heon Lee. "Delamanid, Bedaquiline, and Linezolid Minimum Inhibitory Concentration Distributions and Resistance-related Gene Mutations in Multidrug-resistant and Extensively Drug-resistant Tuberculosis in Korea", <i>Annals of Laboratory Medicine</i> , 2018
Publication | <1 % |
|----|---|------|
-
- | | | |
|----|--|------|
| 25 | Hend A. A. Ezelarab, Samar H. Abbas, Heba A. Hassan, Gamal El-Din A. Abuo-Rahma. "Recent updates of fluoroquinolones as antibacterial agents", <i>Archiv der Pharmazie</i> , 2018
Publication | <1 % |
|----|--|------|
-
- | | | |
|----|--|------|
| 26 | Schmitz F.-J., Higgins P., Mayer S., Fluit A., Dalhoff A.. "Activity of Quinolones Against Gram-Positive Cocci: Mechanisms of Drug | <1 % |
|----|--|------|

Action and Bacterial Resistance", European Journal of Clinical Microbiology & Infectious Diseases, 2002

Publication

27	fems-microbiology.org Internet Source	<1 %
28	journals.lww.com Internet Source	<1 %
29	"Abstracts cont.", Clinical Microbiology and Infection, 2004 Publication	<1 %
30	Coker, Richard, Atun, Rifat, McKee, Martin. "EBOOK: Health Systems and the Challenge of Communicable Diseases: Experiences from Europe and Latin America", EBOOK: Health Systems and the Challenge of Communicable Diseases: Experiences from Europe and Latin America, 2008 Publication	<1 %
31	Igor B. Levshin, Nina A. Rastorgueva, Alexey V. Kiselev, Alexandr S. Vedenkin et al. "Thiazolidine-2,4-dione in benzoylation reaction", Chemistry of Heterocyclic Compounds, 2019 Publication	<1 %
32	Taryn Hassinger, Robert Sawyer. "Should We Immediately Start Antibiotics in Every Patient	<1 %

with a Clinical Suspicion of HAP/VAP?",
Seminars in Respiratory and Critical Care
Medicine, 2017

Publication

33 docserv.uni-duesseldorf.de <1 %
Internet Source

34 www.e-trd.org <1 %
Internet Source

35 Jinying Gu, Qiuyu Wu, Qiuyue Zhang, Qidong You, Lei Wang. "A decade of approved first-in-class small molecule orphan drugs: Achievements, challenges and perspectives", European Journal of Medicinal Chemistry, 2022
Publication

36 www.communitymedical.org <1 %
Internet Source

37 S.-M. Lim. "Nosocomial bacterial infections in Intensive Care Units. I: Organisms and mechanisms of antibiotic resistance", Anaesthesia, 9/2005
Publication

38 Xiaoyun Lu, Zoe Williams, Kiel Hards, Jian Tang et al. " Pyrazolo[1,5-]pyridine Inhibitor of the Respiratory Cytochrome Complex for the Treatment of Drug-Resistant Tuberculosis ", ACS Infectious Diseases, 2018
Publication

39	www.nursingcenter.com Internet Source	<1 %
40	basicmedicalkey.com Internet Source	<1 %
41	res.mdpi.com Internet Source	<1 %
42	www.ahcmedia.com Internet Source	<1 %
43	www.cdc.gov Internet Source	<1 %
44	Azar Dokht Khosravi, Nayereh Etemad, Mohammad Hashemzadeh, Solmaz Khandan Dezfuli, Hamed Goodarzi. "Frequency of rrs and rpsL mutations in streptomycin-resistant Mycobacterium tuberculosis isolates from Iranian patients", Journal of Global Antimicrobial Resistance, 2017 Publication	<1 %
45	doctor-ru.org Internet Source	<1 %
46	fjfsdata01prod.blob.core.windows.net Internet Source	<1 %
47	ijddt.com Internet Source	<1 %

livrepository.liverpool.ac.uk

48	Internet Source	<1 %
49	onlinelibrary.wiley.com Internet Source	<1 %
50	repository.nwu.ac.za Internet Source	<1 %
51	www.ahrq.gov Internet Source	<1 %
52	www.nature.com Internet Source	<1 %
53	www.rspublication.com Internet Source	<1 %
54	Payam Nahid, Susan E. Dorman, Narges Alipanah, Pennan M. Barry et al. "Official American Thoracic Society/Centers for Disease Control and Prevention/Infectious Diseases Society of America Clinical Practice Guidelines: Treatment of Drug-Susceptible Tuberculosis", Clinical Infectious Diseases, 2016 Publication	<1 %
55	wikimili.com Internet Source	<1 %
56	www.rdworldonline.com Internet Source	<1 %

57 Joseph E Marturano, Thomas J Lowery. "ESKAPE Pathogens in Bloodstream Infections Are Associated With Higher Cost and Mortality but Can Be Predicted Using Diagnoses Upon Admission", Open Forum Infectious Diseases, 2019
Publication <1 %

58 agris.fao.org
Internet Source <1 %

59 link.springer.com
Internet Source <1 %

60 publikationen.bibliothek.kit.edu
Internet Source <1 %

61 www.scribd.com
Internet Source <1 %

This study is based on research funded in part by the Medical Research Council (MRC-SIR granted to RMB) and the National Research Foundation (NRF) of South Africa (UID: 137776). The grant holders recognise that the views, opinions, results, and conclusions expressed in this work are those of the authors and do not reflect those of the NRF. The NRF accepts no responsibility in this respect.

PREFACE

This thesis is presented in article format in compliance with the North-West University's General Academic Rules (A.13.7.3).

Chapter 1: Introduction and problem statement

Chapter 2: Literature review

Chapter 3: Article

Nitrothiazole-thiazolidinone hybrids: Synthesis and *in vitro* antimicrobial evaluation

This article has been accepted and published in Chemistry & Biodiversity, which is available at Wiley Online Library: <https://doi.org/10.1002/cbdv.202200729>

This manuscript was written in accordance with the journal's author guidelines, which can be accessed on the journal's webpage.

<https://onlinelibrary.wiley.com/page/journal/16121880/homepage/forauthors.html>

Chapter 4: Summary and conclusion

ACKNOWLEDGEMENTS

My supervisor, **Dr. R.M. Beteck**. Thank you for the opportunity to conduct research in your lab and most of all your patience with me during the study.

My co-supervisor, **Prof. L.J. Legoabe**. Thank you for your motivation.

My assistant supervisor, **Dr. O.J. Jesumoroti**. Thank you for your laboratory expertise and your commitment to constantly offer a helping hand in teaching me the lab skills I know today. Thank you for all the laughs.

Drs. J. Jordaan and **D. Otto** for HRMS and NMR spectroscopy.

Audrey Jordaan and **Prof. D. Warner**, for performing antitubercular screening at the University of Cape Town in South Africa.

The **South African Research Council** for additional financial support towards the antitubercular screening.

The **Community for Open Antimicrobial Drug Discovery (CO-ADD)** for performing antimicrobial, antifungal, and cytotoxic screening, which was funded in part by the Wellcome Trust in the United Kingdom and the University of Queensland in Australia.

My **colleagues** at the Centre of Excellence for Pharmaceutical Sciences (Pharmacen – NWU), thank you for all your assistance.

My **parents** and my **brother**. Thank you for this lifetime opportunity, your love, and unconditional support in all aspects of my life.

Jennica Möller and **Heinrich de Beer**. Thank you for always believing in me and in the possibility of this achievement.

My friend, **Steven le Roux**. Thank you for your ongoing words of encouragement and moral support through some difficult journeys. You played a crucial part in this success, for which I will be eternally grateful. Net dankie!

In honour of my grandmother, **Susan Hart**, I will continue to strive to make you proud.

ABSTRACT

Tuberculosis (TB), caused by the bacterium *Mycobacterium tuberculosis* (*Mtb*), is one of the world's most fatal infectious diseases. Annually, 10 million people fall ill with TB and 1.5 million people die from it globally. TB control and management solely rely on the use of drugs, most of which were developed 40–60 years ago. The emergence and spread of drug-resistant *Mtb* strains, as well as toxicity associated with these drugs create an irrefutable demand for novel drugs with potent activity against active and latent TB infections. Treatment can take up to 4–9 or 18–24 months with a cocktail of first- and second-line antitubercular drugs, depending on *Mtb* drug susceptibility. This often results in patients not complying with their antitubercular treatments, which is the major cause of treatment failure or relapse. Novel oral drugs that may shorten treatment regimens while still achieving complete *Mtb* clearance would have a positive influence on patient compliance, slowing the onset of disease as well as the evolution of drug-resistant *Mtb* strains.

In addition to *Mtb*, other pathogenic bacteria commonly referred to as ESKAPE pathogens are also currently seen as a global public health threat. In the last decade, the prevalence of antimicrobial-resistant (AMR) bacteria in hospitals has increased, as has the challenge of hospital-acquired infections (HAIs). The majority of HAIs include central line-associated bloodstream infections, catheter-associated urinary tract infections, surgical site infections, and ventilator-associated pneumonia, all of which are linked to a high prevalence of multidrug-resistant pathogens known as ESKAPE (*Enterococcus faecium*, *Staphylococcus aureus*, *Klebsiella pneumoniae*, *Acinetobacter baumannii*, *Pseudomonas aeruginosa*, and *Enterobacter* spp.). In addition, ESKAPE pathogens are also wreaking havoc on many areas of individual patient healthcare, including increased direct health care expenses, increased length of hospitalisation, and higher fatality rates. The identification of new antimicrobial drugs with activity against drug-resistant ESKAPE pathogens is vital and urgent since treatment

options for them are rapidly becoming limited. Indeed, if no new antimicrobial is discovered promptly, it is predicted that no drug will be available to treat AMR bacteria by 2050.

Nitazoxanide (NTZ), an antimicrobial agent harbouring a 5-nitrothiazole moiety, has been demonstrated to have activity against both replicating and non-replicating *Mtb* through a novel mechanism of action. Thiazolidin-4-one is another well-known privilege scaffold with possible substitution sites at the second, third, and fifth positions of its heterocyclic ring system. With this in mind, the molecular hybridisation strategy has been employed in this study as a rational design strategy for generating novel ligands or prototypes in which the pharmacophoric subunits in the molecular structure of NTZ and the biologically active thiazolidin-4-ones were merged to produce novel hybrid compounds with a possible poly-pharmacological mechanism of action.

In this study, 17 novel nitrothiazole-thiazolidinone hybrids were synthesised and evaluated *in vitro* against *Mtb* and certain ESKAPE pathogens. Compounds were also screened for antifungal activity against *Candida albicans*. The hybrids were synthesised using a multi-step synthetic protocol that includes *N*-acylation, dehydrative cyclization (*S*-alkylation and intermolecular cyclization), and Knoevenagel condensation. The condensation of different electron withdrawing and electron donating benzylidene moieties in the fifth position (C5) of the thiazolidin-4-one scaffold was used to investigate the structure-activity relationship of the hybrids. After purification, the hybrid-target compounds were synthesised in yields ranging from 26% to 69%. However, the poor solubility of the hybrid-target compounds in standard solvents such as dichloromethane, ethanol, or methanol was recognised as a limitation in this work, emphasising the need for optimisation in future research. Nuclear magnetic resonance (¹H and ¹³C), high resolution mass spectrometry, and Fourier-transform infrared spectroscopy were used to characterise all synthesised hybrids, and the purity of the compounds was assessed using high performance liquid chromatography. Finally, the target compounds were

tested for overt cell toxicity against human embryonic kidney cells (HEK-293) and haemolysis against whole human red blood cells (RBCs).

All hybrid compounds displayed remarkable antitubercular activity of $< 0.24 - 2.00 \mu\text{M}$. Most compounds had low micromolar activity against *S. aureus* and *C. albicans*. Compound **3b**, in particular, demonstrated sub-micromolar activity against *Mtb* and *C. albicans* while also having superior activity against methicillin-resistant *Staphylococcus aureus* (MRSA) ($< 0.25 \mu\text{g/ml}$) as compared to the reference drug vancomycin ($1 \mu\text{g/ml}$). Compound **3g** had activity against *C. albicans* ($\leq 0.25 \mu\text{g/ml}$) comparable to that of the drug fluconazole ($0.12 \mu\text{g/ml}$). The antimicrobial SAR reveals that *ortho* substitution of the C5-benzylidene moiety favours activity against *S. aureus*.

Keywords: Antimicrobial; 5-nitrothiazoles; Thiazolidin-4-ones; Molecular hybridization; ESKAPE pathogens

TABLE OF CONTENT

PREFACE	i
ACKNOWLEDGEMENTS	ii
ABSTRACT	iii
LIST OF TABLES AND SCHEMES	ix
LIST OF FIGURES	x
LIST OF ABBREVIATIONS	xii
CHAPTER 1: INTRODUCTION AND PROBLEM STATEMENT	1
1.1. Background	1
1.2. Tuberculosis	2
1.3. The burden of treating tuberculosis	3
1.4. Advances in antitubercular treatment	4
1.5. Antimicrobial resistance	5
1.6. Hospital-acquired infections (HAIs)	6
1.7. Hypothesis	7
1.8. Rationale and strategy	7
1.9. Aims and objectives	9
REFERENCE LIST – CHAPTER 1	11
CHAPTER 2: LITERATURE REVIEW	16
PART ONE: TUBERCULOSIS (TB)	16
2.1. Background	16
2.2. Epidemiology of TB	17
2.3. Mtb cellular morphology	19
2.4. Pathophysiology of Mtb	19
2.5. Virulence factors of Mtb	23
2.6. Clinical manifestations of TB	25
2.6.1. Post-primary pulmonary TB (reactivation TB).....	25
2.6.2. Extrapulmonary TB	25
2.7. Detection and diagnosis of TB	26
2.7.1. Microbiological assays	27
2.7.2. Immunoassays.....	29
2.7.3. Nucleic Acid Amplification Tests (NAATs).....	31
2.8. Vaccination	33
2.9. Overview of TB Treatment	34
2.10. First-line drugs for the treatment of drug-susceptible TB (DS-TB)	35

2.10.1.	Isoniazid (INH)	35
2.10.2.	Rifamycins.....	37
2.10.3.	Ethambutol (ETH).....	40
2.10.4.	Pyrazinamide (PZA)	41
2.11.	Drug-resistant tuberculosis	43
2.12.	Second-line drugs for the treatment of drug-resistant TB (DR-TB).....	44
2.12.1.	Quinolones.....	45
2.12.1.1.	Discovery of fluoroquinolones (FQNs).....	45
2.12.1.2.	Classification and structural modifications of fluoroquinolones	47
2.12.1.3.	Mechanism of action of fluoroquinolones.....	49
2.12.1.4.	Fluoroquinolones for the treatment of drug-resistant TB.....	50
2.12.2.	Aminoglycosides: streptomycin (SM) and amikacin (AM)	52
2.12.3.	Thioamides: ethionamide (ETO) and prothionamide (PTO)	54
2.12.4.	Cycloserine (CS) or terizidone (TRD)	56
2.12.5.	<i>para</i> -Aminosalicylic acid (PAS).....	57
2.12.6.	Linezolid (LZD).....	59
2.12.8.	Clofazimine (CFZ)	63
2.12.9.	Nitroazoles: delamanid (DLM) and pretomanid (PTM).....	65
PART TWO:	HOSPITAL-ACQUIRED INFECTIONS (HAIs)	68
2.13.	Background.....	68
2.14.	Call for antimicrobial drug development.....	70
2.15.	The ESKAPE pathogens.....	71
2.15.1.	<i>Enterococcus faecium</i>	71
2.15.2.	<i>Staphylococcus aureus</i>	72
2.15.3.	<i>Klebsiella pneumoniae</i>	74
2.15.4.	<i>Acinetobacter baumannii</i>	75
2.15.5.	<i>Pseudomonas aeruginosa</i>	75
2.15.6.	<i>Enterobacter</i> spp.	76
2.16.	Common ESKAPE-associated hospital-acquired infections	77
2.16.1.	Central line-associated bloodstream infections (CLABSIs)	77
2.16.2.	Catheter-associated urinary tract infections (CAUTIs)	78
2.16.3.	Surgical Site Infections (SSIs)	79
2.16.4.	Ventilator-associated pneumonia (VAP)	80
2.17.	Compound classes of interest in this study	81
2.17.1.	Nitroazole: Nitazoxanide (NTZ)	81
2.17.1.1.	Antimicrobial activity of nitazoxanide	82
2.17.1.2.	Antitubercular activity of nitazoxanide.....	83

2.17.2.	Thiazolidin-4-ones	84
2.17.3.	Mechanism for <i>N</i> -acylation reaction (intermediate 1)	85
2.17.4.	Mechanism for dehydrative cyclization reaction (intermediate 2)	87
2.17.5.	Mechanism for Knoevenagel condensation reaction (target compounds) ...	88
2.18.	Summary and rational design of target compounds	90
REFERENCE LIST – CHAPTER 2		92
CHAPTER 3: ARTICLE FOR SUBMISSION		131
NITROTHIAZOLE-THIAZOLIDINONE HYBRIDS: SYNTHESIS AND <i>IN VITRO</i>		
ANTIMICROBIAL EVALUATION		132
GRAPHICAL ABSTRACT		133
ABSTRACT		134
3.1.	Introduction	135
3.2.	Results and discussion	139
3.2.1.	Chemistry and structure characterisation	139
3.2.2.	Antitubercular activity	141
3.2.3.	Antibacterial and antifungal activities	143
3.2.4.	Cytotoxicity and haemolytic studies	145
3.2.5.	<i>In silico</i> drug-like prediction	145
3.3.	Materials and methods	147
3.3.1.	General methods	147
3.3.2.	Synthesis (Experimental)	148
3.3.2.1.	<i>N</i> -Acylation (1)	148
3.3.2.2.	Dehydrative cyclization (2)	148
3.3.2.3.	Knoevenagel condensation (3a – 3q)	149
3.3.3.	<i>In vitro</i> antitubercular evaluation	155
3.3.4.	<i>In vitro</i> antibacterial and antifungal evaluation	155
3.3.5.	<i>In vitro</i> cytotoxicity evaluation: resazurin assay	156
3.3.6.	<i>In vitro</i> haemolytic evaluation	156
3.4.	Conclusion	157
3.5.	Acknowledgements	157
3.6.	Conflict of interest	158
3.7.	Data availability statement	158
REFERENCE LIST – CHAPTER 3		159
CHAPTER 4: SUMMARY AND CONCLUSION		164
REFERENCE LIST – CHAPTER 4		169
ANNEXURE A: SUPPLEMENTARY MATERIAL FOR CHAPTER 3		172
ANNEXURE B: PERMISSIONS AND LICENSES		228

LIST OF TABLES AND SCHEMES

Table 2.1	Second-line drugs for the treatment of drug-resistant tuberculosis.....	45
Table 2.2	Classification and structural modification-associated activities of FQNs.....	47
Table 2.3	WHO priority pathogens list.	70
Table 3.1	Antimicrobial and cytotoxic activities of compounds 2 and 3a – 3j	142
Table 3.2	Physiochemical properties of compounds 2 and 3a – 3j	146
Table 4.1	Target compounds with the best MIC values against evaluated pathogens	168
Scheme 1	Synthesis of conceptualised target compounds.....	139

LIST OF FIGURES

Figure 1.1	First-line antitubercular drugs.....	4
Figure 1.2	Delamanid (DLM) and pretomanid (PTM)	5
Figure 1.3	Nitazoxanide (NTZ) and thiazolidin-4-one antimicrobial agent.	8
Figure 1.4	Design of hybrid-target compounds	9
Figure 2.1	Tuberculosis incidence rates in 2020.	18
Figure 2.2	The formation and progression of granulomas.	21
Figure 2.3	Pathophysiology of tuberculosis.....	23
Figure 2.4	Isoniazid (1)	37
Figure 2.5	Rifampicin (2), rifapentine (3), rifabutin (4), and rifaximin (5).....	39
Figure 2.6	Ethambutol (6)	41
Figure 2.7	Pyrazinamide (7).....	43
Figure 2.8	Nalidixic acid (8) and the fluoroquinolone scaffold (9)	46
Figure 2.9	Norfloxacin (10), ciprofloxacin (11), levofloxacin (12), and moxifloxacin (13).	48
Figure 2.10	Levofloxacin (12) and moxifloxacin (13).....	52
Figure 2.11	Streptomycin (14) and amikacin (15)	54
Figure 2.12	Ethionamide (16), prothionamide (17), and ethionamide <i>S-oxide</i> (18)	55
Figure 2.13	Cycloserine (19), terizidone (20), and D-alanine (21).....	57
Figure 2.14	<i>para</i> -Aminosalicylic acid (22) and <i>para</i> -Aminobenzoic acid (23)	59
Figure 2.15	Linezolid (24)	60
Figure 2.16	Bedaquiline (25)	63
Figure 2.17	Clofazimine (26)	64
Figure 2.18	Delamanid (27) and pretomanid (28)	67
Figure 2.19	Nitroazoles: nitazoxanide (29), metronidazole (30), and tizoxanide (31)	82
Figure 2.20	Thiazolidin-4-one (32) and structure-activity relationship	85

Figure 3.1	Structures of biological active nitroazole drugs	137
Figure 3.2	Molecular hybridization strategy	138
Figure 4.1	General structure of target compounds (3a – 3j).....	166

LIST OF ABBREVIATIONS

μM	Micromolar
^1H NMR	Proton nuclear magnetic resonance
^{13}C NMR	Carbon nuclear magnetic resonance
ACP	Acyl carrier protein
AFB	Acid-fast bacilli
AM	Amikacin
AMB	Antimicrobial-resistant bacteria
APCI	Atmospheric pressure chemical ionization
ATP	Adenosine 5'-triphosphate
BBB	Blood-brain barrier
BCG	Bacillus Calmette-Guérin
BDQ	Bedaquiline
BSIs	Bloodstream infections
CAS	Casitone
CAMHB	Cation-Adjusted Mueller Hinton Broth
CAUTIs	Catheter-associated urinary tract infections
CC ₅₀	Cytotoxic concentration (50%)
CDC	Centre for Disease Prevention and Control
CFU	Colony-forming units
CFZ	Clofazimine

CLABSIs	Central line-associated bloodstream infections
CNS	Central nervous system
Coa	Coagulase
CS	Cycloserine
CSF	Cerebrospinal fluid
CYP450	Cytochrome P450
(D ₆)DMSO	Deuterated dimethyl sulfoxide
Da	Daltons
Ddn	Deazaflavin-dependent nitroreductase
DHFR	Dihydrofolate reductase
DHFS	Dihydrofolate synthase
DHPS	Dihydropteroate synthase
DLM	Delamanid
DLS	Damped least-squares
DMEM	Dulbecco's Modified Eagle Medium
DMF	Dimethylformamide
DNA	Deoxyribonucleic acid
DR-TB	Drug-resistant tuberculosis
DS-TB	Drug-susceptible tuberculosis
EDG	Electron donating group
ESBLs	Extended spectrum β -lactamases

ESKAPE	<i>Enterococcus faecium</i> , <i>Staphylococcus aureus</i> , <i>Klebsiella pneumoniae</i> , <i>Acinetobacter baumannii</i> , <i>Pseudomonas aeruginosa</i> , <i>Enterobacter</i> spp.
ESX	Type VII secretion system
ETH	Ethambutol
ETO	Ethionamide
EWG	Electron withdrawing group
FAS II	Fatty acid synthase II
FBP	Folate biosynthesis pathway
FBS	Foetal bovine serum
FDA	Food and drug administration
FLDs	First-line drugs
FQNs	Fluoroquinolones
FTIR	Fourier-transform infrared spectroscopy
GI	Gastrointestinal
HAIs	Hospital-acquired infections
HBA	Hydrogen bond acceptors
HBD	Hydrogen bond donors
HBHA	Heparin-binding hemagglutinin
HC ₁₀	Haemolysis concentration (10%)
HEK-293	Human embryonic kidney cells
HIV	Human immunodeficiency virus

HPLC	High-performance liquid chromatography
HRMS	High-resolution mass spectrometry
Hz	Hertz
ICU	Intensive care unit
IFN- γ	Interferon gamma
IGRAs	Interferon- γ -release assay
INH	Isoniazid
LAM	Lipoarabinomannan
LFX	Levofloxacin
LPAs	Line probe assays
LZD	Linezolid
mAGP	Mycolyl arabinogalactan–peptidoglycan
MDR-TB	Multidrug-resistant tuberculosis
MXF	Moxifloxacin
MH	Molecular hybridisation
MIC	Minimum inhibitory concentration
MOA	Mechanism of action
m.p.	Melting point
mRNA	Messenger ribonucleic acid
MRSA	Methicillin-resistant <i>Staphylococcus aureus</i>
Mtb	<i>Mycobacterium tuberculosis</i>

MTZ	Metronidazole
MW	Molecular weight
NA	Nalidixic acid
NAATs	Nucleic acid amplification tests
NADH	Nicotinamide adenine dinucleotide
NO	Nitric oxide
NTZ	Nitazoxanide
PA	Pyrazinoic acid
PABA	<i>para</i> -Aminobenzoic acid
PAS	<i>para</i> -Aminosalicylic acid
PBP	Penicillin-binding protein
PCR	Polymerase chain reaction
PFOR	Pyruvate-ferredoxin oxidoreductase
PPD	Purified protein derivative
ppm	Parts per million
PTM	Pretomanid
PTO	Prothionamide
PZA	Pyrazinamide
RBCs	Red blood cells
RIF	Rifampicin
RNA	Ribonucleic acid

RoB	Rotatable bonds
rRNA	Ribosomal ribonucleic acid
r.t.	Room temperature
SAR	Structure-activity relationship
SLDs	Second-line drugs
SM	Streptomycin
SSIs	Surgical site infections
$T_{1/2}$	Half-life
TB	Tuberculosis
TDR-TB	Total drug-resistant tuberculosis
TEA	Triethylamine
TIZ	Tizoxanide
TLC	Thin-layer chromatography
TNF- α	Tumour necrotic factor
<i>t</i> PSA	Topological polar surface area
TRD	Terizidone
tRNA	Transfer ribonucleic acid
TST	Tuberculin skin test
UTIs	Urinary tract infections
VAP	Ventilator-associated pneumonia
VISA	Vancomycin-intermediate <i>Staphylococcus aureus</i>

VRE	Vancomycin-resistant enterococci
VRSA	Vancomycin-resistant <i>Staphylococcus aureus</i>
vWbp	von Willebrand factor-binding protein
WHO	World Health Organisation
XDR-TB	Extensively drug-resistant tuberculosis
YEPD	Yeast Extract Peptone Dextrose
ZN	Ziehl-Neelsen

CHAPTER 1: INTRODUCTION AND PROBLEM STATEMENT

1.1. Background

Before COVID-19, tuberculosis (TB) was the world's foremost infectious disease caused by a single pathogen. The COVID-19 pandemic seems to be erasing the advances made in the past 20 years toward eradicating TB (Togun *et al.*, 2020).

The COVID-19 pandemic has also increased awareness regarding the threat posed by infectious diseases, highlighting the silent epidemic of antimicrobial-resistant (AMR) bacteria. Antibiotics' diminishing efficacy against bacteria is jeopardising the practice of modern medicine. This is especially evident in infections caused by a group of pathogens collectively referred to as ESKAPE. ESKAPE pathogens are the major cause of hospital-acquired infections (HAIs) (infections acquired while receiving treatment in a healthcare facility) globally. In fact, antimicrobial resistance among these pathogens is wreaking havoc on global public health (Ayobami *et al.*, 2022).

Therefore, there is a continuous demand for effective antimicrobial drugs for the prevention and treatment of infections such as TB and HAIs. This project intends to address this need by discovering and evaluating a novel antimicrobial drug having activity against ESKAPE pathogens as well as Mtb, as described in this report.

First, this chapter will provide introductory information on TB and HAIs, followed by a hypothesis, the rationale and strategy for the study, as well as its aims and objectives.

Chapter two provides a literature review of current research relevant to the study topic, while chapter three presents the results of the study in article format. The fourth chapter is a summary and conclusion.

1.2. Tuberculosis

The second leading cause of mortality worldwide from a single infectious pathogen is tuberculosis (TB), a clinically progressive chronic disease. *Mycobacterium tuberculosis* (Mtb), a pathogenic mycobacterium of the *Mycobacteriaceae* family that is thought to have originated in the ancient African human ancestors some three million years ago, is the culprit behind TB (Ernst *et al.*, 2007:1738). Despite the fact that TB can be prevented and treated for many of the most vulnerable populations, such as children, pregnant women, people living with human immunodeficiency virus (HIV), miners and medical professionals, the year 2020 witnessed little progress toward the elimination of TB. Public health services – notably TB prevention and control - were severely impacted by the COVID-19 pandemic. The worldwide decline in the number of TB diagnoses is the most obvious consequence. Evidence of such a significant decline includes limited access to healthcare, decreased desire and availability to seek treatment during lockdowns and activity restrictions, and the stigma associated with symptoms shared by TB and COVID-19 (WHO, 2021).

Latent TB and active TB need to be distinguished from one another in order to contextualise the transmission of TB. Latent TB is an asymptomatic stage of immune sensitisation to Mtb. Conversely, Mtb infections that progress to various life-threatening pulmonary or extrapulmonary clinical symptoms are what are known as "active TB" (CDC, 2014; Laycock *et al.*, 2021:2). One-third of the world's population, or over 2.3 billion people, have latent TB and act as a reservoir for reactivation into active TB at any given time (Houben & Dodd, 2016:3). It is unlikely that people with latent TB who do not progress to active TB would transmit Mtb to others. However, their lifetime chance of acquiring active TB is 10% (CDC, 2014). When people with active TB cough, sneeze or engage in other strong expiratory behaviours, they create Mtb-containing droplet nuclei (airborne particles) which can be transmitted and subsequently infect healthy people (Churchyard *et al.*, 2017:S630-S631). TB is the top risk factor for mortality among people who are HIV-positive. It is responsible for an estimated 26% of all HIV-related deaths, 99% of which occur in developing nations. Furthermore, in high-

burden countries like those in Africa, co-infection with HIV multiplies the chance of latent TB reactivation by 20. In fact, the two conditions amplify one another in the host, accelerating the loss of host immune functionalities and, if untreated, bringing about untimely death (Bruchfeld *et al.*, 2015:2; Pawlowski *et al.*, 2012:1).

1.3. The burden of treating tuberculosis

The first-line drugs (FLDs) used to treat drug-susceptible TB (DS-TB) include isoniazid (INH), rifampicin (RIF), ethambutol (ETH) and pyrazinamide (PZA) (see **Fig. 1.1**). Drug-resistant TB (DR-TB) is more challenging to treat despite the availability of these treatments due to *Mtb*'s immense ability to develop resistance to them (Mehari *et al.*, 2019:2). DR-TB prevalence has exponentially increased and reached epidemic levels in recent years, killing more people than malaria and HIV combined (Moreira *et al.*, 2020:1). TB that is resistant to or does not react to at least two of the most potent antitubercular drugs, INH and RIF, is known as multidrug-resistant TB (MDR-TB). Extensively drug-resistant TB (XDR-TB), a subtype of MDR-TB, is sporadic and responds to even fewer treatment regimens. XDR-TB has evolved resistance to other antitubercular drugs known as second-line drugs (SLDs) in addition to FLDs (WHO, 2018).

A two-month intensive phase of INH, RIF, PZA, and ETH, followed by a four-month continuation phase of INH and RIF, continues to be the recommended treatment plan for TB infections. However, even following culture conversion, treatment for those with DR-TB on prolonged regimens may take up to 20 months with additional SLDs (Mabhula & Singh, 2019:1345-1346; Migliori *et al.*, 2020:S20). Patient compliance to antitubercular drugs is crucial for achieving successful treatment outcomes, limiting the spread and minimizing the emergence of DR-TB. Several variables are known to influence compliance with TB drugs, including socioeconomic considerations, complexity of regimens, and extended treatment duration (Bea *et al.*, 2021:2). Poor compliance with TB drugs is generally recognized as a source of increased morbidity, mortality, and financial burden. According to a worldwide meta-

analysis, patient non-compliance with antitubercular drugs is shown to be a major risk factor for MDR-TB. Moreover, MDR-TB patients usually have worse treatment outcomes than drug-susceptible patients (Pradipta *et al.*, 2020:1).

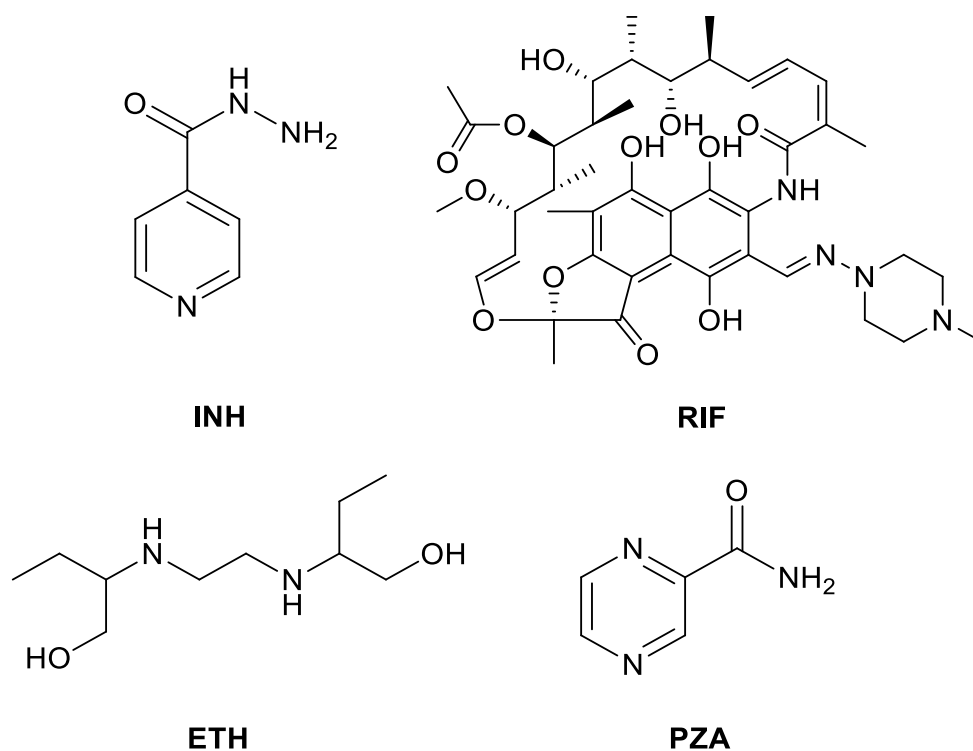


Figure 1.1 First-line antitubercular drugs

1.4. Advances in antitubercular treatment

After more than four decades of rigorous study, bedaquiline (BDQ) and delamanid (DLM) have received accelerated or conditional regulatory approval based on the outcomes of their Phase II clinical trials against *Mtb* strains. The first innovative antitubercular drug with a novel mechanism of action (MOA) approved in 2012 to treat DR-TB was BDQ (Rodriguez *et al.*, 2019:32). Additionally, two novel nitroazole families of antibiotics have been approved for the treatment of DR-TB, including DLM and its structural analogue, pretomanid (PTM) (see **Fig. 1.2**). Recently, these two 5-nitroimidazole-based compounds have shown potent *in vivo* and *in vitro* activity against *Mtb*, particularly MDR- and XDR-TB (Wen *et al.*, 2019:1293). Furthermore, they have the potential to considerably shorten the course of extended MDR-

and XDR-TB regimens while also promoting patient treatment outcomes. However, mutations related to Mtb resistance to both DLM and PTM were soon discovered (Kadura *et al.*, 2020:2031).

Linezolid (LZD), an oxazolidinone that has been repurposed owing to its antimycobacterial properties, has also earned its position in the World Health Organization's (WHO) consolidated guidelines as a group A antitubercular drug for the treatment of MDR-TB and XDR-TB. However, a major drawback of adopting LZD as a treatment is the frequency of treatment discontinuation and serious adverse effects that study participants often experience (Padayatchi *et al.*, 2020:1024).

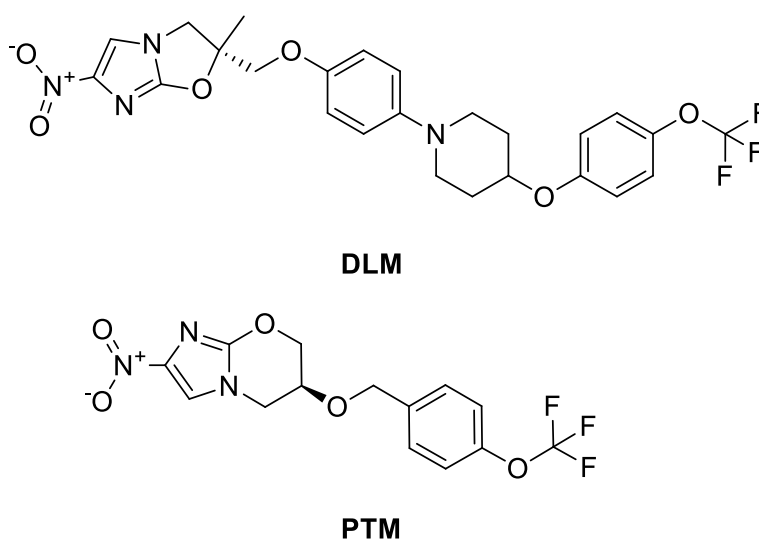


Figure 1.2 Delamanid (DLM) and pretomanid (PTM)

1.5. Antimicrobial resistance

The emergence and spread of AMR bacteria are a serious global public health problem. AMR bacteria, sometimes known as "superbugs," can thrive in the presence of antimicrobials, creating countless treatment problems as well as elevated morbidity and mortality rates in both hospitals and the community (Allcock *et al.*, 2017). AMR bacteria cause over two million infections and at least 23,000 deaths in the United States each year. This statistic is expected to rise by a factor of ten every year, with mortality estimates by 2050 varying by region (Ma *et*

al., 2020:1). Globally, antimicrobial resistance is now expected to cause over 700,000 deaths each year. Unless the resistance trend is reversed, this number may rise to 10 million by 2050, with more than 4 million deaths occurring each year in Africa and Asia alone (Xu *et al.*, 2019:3209).

The relationship between antibiotic use and antimicrobial resistance establishment complicates antimicrobial resistance even more and has long been linked to its development in individual patients. Antimicrobial resistance is primarily driven by selective pressures exerted on these pathogens due to long-term exposure to antimicrobials such as β -lactams, aminoglycosides, fluoroquinolones (FQNs) and macrolides. Bacteria can, however, adapt and become resistant to antimicrobials through a variety of other mechanisms, such as enzyme production and drug target site modification. Thus, resistant bacteria may possess one or more of these resistance mechanisms, resulting in antimicrobial resistance to more than one class of antibiotics (Allcock *et al.*, 2017; Cristino, 1999:199-202). Today, existing antibiotics are rendered ineffective as a result of these resistant infections.

1.6. Hospital-acquired infections (HAIs)

Infections that are not present or incubating at the time of hospitalisation but manifest at least 48 hours later in addition to the main reason for hospitalisation are referred to as HAIs (Viderman *et al.*, 2019:35). HAIs include respiratory tract infections, urinary tract infections (UTIs), infections related to the use of surgical equipment, as well as intravascular cannulas and catheters (Spelman, 2002:286-288). *Enterococcus faecium*, *Staphylococcus aureus*, *Klebsiella pneumoniae*, *Acinetobacter baumannii*, *Pseudomonas aeruginosa* and *Enterobacter spp.* are among a group of potentially fatal hospital-acquired bacteria known as ESKAPE pathogens that have the ability to "escape" the biocidal activity of currently used antimicrobial drugs. The greatest clinical threat currently comes from drug-resistant ESKAPE pathogens like methicillin-resistant *S. aureus* (MRSA), vancomycin-resistant *enterococci* (VRE), and other β -lactam resistant pathogens. These bacteria usually show novel

pathogenesis, transmission and resistance mechanisms, resulting in difficult-to-treat diseases (Navidinia *et al.*, 2017:779; Pandey *et al.*, 2021:2202). Treatment options for infections caused by these bacteria may become more problematic to manage in the future as long as the resistance patterns for these pathogens persist. As a result, it is critical to discover novel antimicrobials with activity against ESKAPE pathogens (De Oliveira *et al.*, 2020:2).

1.7. Hypothesis

HAIs are increasingly being associated with ESKAPE pathogens, which have developed several mechanisms to nullify the activity of all antimicrobials now in clinical use and are therefore resistant or not susceptible to routinely prescribed antibiotics such as FQNs and β -lactams. Furthermore, despite progress in reducing the global incidence of TB via DOTS (Directly Observed Treatment Shortcourse) (WHO, 1999) or antitubercular prevalence-and-surveillance studies, the rise of MDR- and XDR-TB during the past decade threatens to undo these gains (Zignol *et al.*, 2016:1086-1087). As a result, and considering the poor success rates of DR-TB, novel and innovative TB drugs to treat both drug-susceptible TB (DS-TB) and drug-resistant TB (DR-TB) are urgently required.

Herein, it is hypothesized that synthesizing poly-pharmacophoric ligands as potential drug leads for the treatment of both drug-susceptible and drug-resistant pathogens, such as Mtb and ESKAPE pathogens, will slow the global onset of drug resistance development. On the other hand, poly-pharmacophoric ligands act simultaneously on several microbiological targets, which should limit resistance development since concurrent mutation of multiple sites in bacteria is associated with a fitness cost.

1.8. Rationale and strategy

The 5-nitroimidazole-based drugs DLM and PTM, both of which are used to treat MDR-TB, were discovered and given the green light in recent years. The availability of these drugs has rekindled interest in nitroazole scaffolds as a source of potent antimicrobials. While the focus

is still primarily on nitrofurans and nitroimidazoles, such as metronidazole (MTZ), which are well-known as bio-reductive pro-drugs, other 5-membered nitroazole compounds with a 5-nitrothiazole moiety, such as nitazoxanide (NTZ) (see **Fig. 1.3**), have also been reported (Rice *et al.*, 2021:2). NTZ exhibits promising antitubercular and antimicrobial activity in addition to having a MOA that differs from the conventional reductive activation of the 5-nitro group (like for MTZ), while simultaneously avoiding resistance from bacteria (De Carvalho *et al.*, 2009:5789–5792). In addition, NTZ has the potential to shorten current TB regimens (Iacobino *et al.*, 2019:1-4).

Another well-known class of heterocycles that are thought to offer promising structures as preferred scaffolds for the development of novel drugs are the thiazolidin-4-ones. Thiazolidin-4-one-based compounds exhibit a wide range of biological activities, and this class contains many known lead compounds, potential drug candidates, and commercially available drugs (Kaminsky *et al.*, 2017:543; Mech *et al.*, 2021:1; Skóra *et al.*, 2022:1-2). Due to their immense chemical significance at their potential substitution sites, thiazolidin-4-ones are widely and successfully used in many drug development methodologies. For instance, among all thiazolidin-4-one subtypes, C5 substituted thiazolidin-4-ones, specifically C5-benzylidene derivatives (see **Fig. 1.3**), are of particular interest in terms of their chemical properties and antimicrobial activities (Kaminsky *et al.*, 2017:554; Vicini *et al.*, 2006:3859; Vicini *et al.*, 2008:3714).

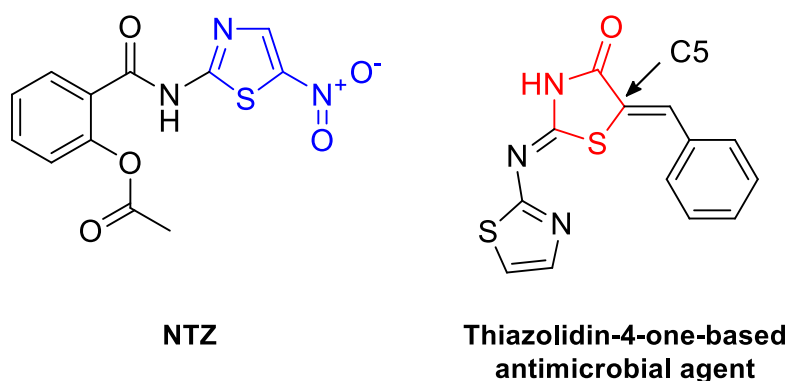
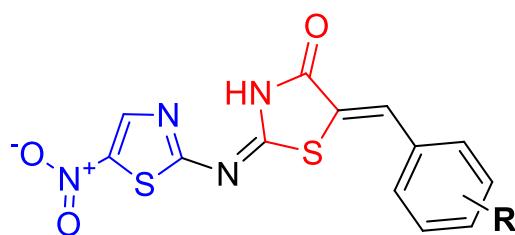


Figure 1.3 Nitazoxanide (NTZ) and thiazolidin-4-one antimicrobial agent.

The molecular hybridisation (MH) approach has produced chemical libraries based on privileged structures, with heterocyclic moieties receiving special attention due to their proven utility in medicinal chemistry. It is clear, for example, that nitrogen-containing heterocyclic moieties are present in more than 75% of drugs approved by the American Food and Drug Administration (FDA) and now available on the market. The presence of non-carbon atoms in heterocycles is responsible for the unique properties of this scaffold (Kerru *et al.*, 2020:1). As a result, we believe that drugs containing the 2-amino-5-nitrothiazole (5-nitrothiazole) head group from NTZ and the thiazolidin-4-one scaffold will be active against microorganisms via a poly-pharmacophoric mechanism. Given these considerations, and especially in light of the therapeutic potential of 5-nitrothiazoles and thiazolidin-4-ones, an attempt was made to integrate these moieties to generate novel hybrid compounds (see **Fig 1.4**) that are potentially active against Mtb as well as a number of Gram-positive and Gram-negative ESKAPE pathogens.



Hybrid compound

R = F, Cl, Br, NO₂, OH, Me, MeO

Figure 1.4 Design of hybrid-target compounds

1.9. Aims and objectives

This study aims to synthesise a series of a novel (2*E*,5*Z*)-5-benzylidene-2-((5-nitrothiazol-2-yl)imino)thiazolidin-4-one derivatives and investigate their antimicrobial potential against some ESKAPE pathogens, *Mycobacterium tuberculosis* and the fungus *Candida albicans*.

Objectives:

- Synthesis of conceptualised target compounds.
- Characterization of intermediates and target compounds using analytical methods such as Fourier-transform infrared spectroscopy (FTIR), proton nuclear magnetic resonance (^1H NMR) spectroscopy, carbon nuclear magnetic resonance (^{13}C NMR) spectroscopy, high-resolution mass spectrometry (HRMS), and high-performance liquid chromatography (HPLC) analysis.
- *In vitro* antimicrobial activity evaluation of hybrid-target compounds.
- *In vitro* cytotoxic activity evaluation of hybrid-target compounds.
- Analyse the structure-activity relationship (SAR) of antimicrobial inhibition by various derivatives synthesized in this study.
- *In silico* drug-like and ADME predictions of hybrid-target compounds.

REFERENCE LIST – CHAPTER 1

Allcock, S., Young, E.H., Holmes, M., Gurdasani, D., Dougan, G., Sandhu, M.S., ... Torok, M.E. 2017. Antimicrobial resistance in human populations: challenges and opportunities. *Global Health Epidemiology Genomics*, 2, art. #e4. <https://doi.org/10.1017/gheg.2017.4>

Ayobami, O., Brinkwirth, S., Eckmanns, T & Markwart, R. 2022. Antibiotic resistance in hospital-acquired ESKAPE-E infections in low-and lower-middle-income countries: a systematic review and meta-analysis. *Emerging Microbes & Infections*, 11(1): 443-451. <https://doi.org/10.1080/22221751.2022.2030196>

Bea, S., Lee, H., Kim, J.H., Jang, S.H., Son, H., Kwon, J.W. & Shin, J.Y. 2021. Adherence and associated factors of treatment regimen in drug-susceptible tuberculosis patients. *Frontiers in Pharmacology*, 12, art. #625078. <https://doi.org/10.3389/fphar.2021.625078>

Bruchfeld, J., Correia-Neves, M. & Källenius, G. 2015. Tuberculosis and HIV coinfection, *Cold Spring Harbor Perspectives in Medicine*. 5(7), art. #a017871. doi:10.1101/cshperspect.a017871

CDC (Centre for Disease Control and Prevention). 2014. *The Difference Between Latent TB Infection and TB Disease*. <https://www.cdc.gov/tb/publications/factsheets/general/ltbiandactivetb.htm> Date of access: 08 May. 2022.

Churchyard, G., Kim, P., Shah, N.S., Rustomjee, R., Gandhi, N., Mathema, B., ... Cardenas, V. 2017. What we know about tuberculosis transmission: an overview. *The Journal of Infectious Diseases*, 216(suppl_6): S629-S635. <https://doi.org/10.1093/infdis/jix362>

Cristino, J.M. 1999. Correlation between consumption of antimicrobials in humans and development of resistance in bacteria. *International Journal of Antimicrobial Agents*, 12(3): 199-202. doi:10.1016/S0924-8579(99)00052-7

De Carvalho, L.P.S., Lin, G., Jiang, X. & Nathan, C. 2009. Nitazoxanide kills replicating and nonreplicating *Mycobacterium tuberculosis* and evades resistance. *Journal of Medicinal Chemistry*, 52(19): 5789-5792. <https://doi.org/10.1021/jm9010719>

De Oliveira, D.M., Forde, B.M., Kidd, T.J., Harris, P.N., Schembri, M.A., Beatson, S.A., ... Walker, M.J. 2020. Antimicrobial resistance in ESKAPE pathogens. *Clinical Microbiology Reviews*, 33(3), e00181-19. <https://doi.org/10.1128/CMR.00181-19>

Ernst, J.D., Trevejo-Nuñez, G. & Banaiee, N. 2007. Genomics and the evolution, pathogenesis, and diagnosis of tuberculosis. *The Journal of Clinical Investigation*, 117(7): 1738-1745. <https://doi.org/10.1172/JCI31810>

Houben, R.M.G.J. & Dodd, P.J. 2016. The global burden of latent tuberculosis infection: a re-estimation using mathematical modelling. *PloS Medicine*, 13(10), e1002152. doi:10.1371/journal.pmed.1002152

Iacobino, A., Giannoni, F., Pardini, M., Piccaro, G. & Fattorini, L. 2019. The Combination Rifampin-Nitazoxanide, but Not Rifampin-Isoniazid-Pyrazinamide-Ethambutol, Kills Dormant *Mycobacterium tuberculosis* in Hypoxia at Neutral Ph. *Antimicrobial Agents and Chemotherapy*, 63(7), e00273-19. doi:10.1128/AAC.00273-19

Kadura, S., King, N., Nakhoul, M., Zhu, H., Theron, G., Köser, C.U. & Farhat, M. 2020. Systematic review of mutations associated with resistance to the new and repurposed *Mycobacterium tuberculosis* drugs bedaquiline, clofazimine, linezolid, delamanid and pretomanid. *The Journal of Antimicrobial Chemotherapy*, 75(8): 2031-2043. doi:10.12659/MSM.913510

Kaminsky, D., Kryshchshyn, A. & Lesyk, R. 2017. 5-Ene-4-thiazolidinones – an efficient tool in medicinal chemistry. *European Journal of Medicinal Chemistry*, 140: 542-594. <https://doi.org/10.1016/j.ejmech.2017.09.031>

Kerru, N., Gummidi, L., Maddila, S., Gangu, K.K. & Jonnalagadda, S.B. 2020. A review on recent advances in nitrogen-containing molecules and their biological applications. *Molecules*, 25(8), art. #1909. <https://doi.org/10.3390/molecules25081909>

Laycock, K.M., Enane, L.A. & Steenhoff, A.P. 2021. Tuberculosis in adolescents and young adults: emerging data on TB transmission and prevention among vulnerable young people. *Tropical Medicine and Infectious Disease*, 6(3), art. #148. <https://doi.org/10.3390/tropicalmed6030148>

- Ma, Y.X., Wang, C.Y., Li, Y.Y., Li, J., Wan, Q.Q., Chen, J.H., ... Niu, L.N. 2020. Considerations and caveats in combating ESKAPE pathogens against nosocomial infections. *Advanced Science*, 7, art. #1901872. doi:10.1002/adv.201901872
- Mabhula, A. & Singh, V. 2019. Drug-resistance in *Mycobacterium tuberculosis*: where we stand. *MedChemComm*, 10(8): 1342-1360. doi:10.1039/c9md00057g
- Mech, D., Kurowska, A. & Trotsko, N. 2021. The bioactivity of thiazolidin-4-ones: a short review of the most recent studies. *International Journal of Molecular Sciences*, 22(21), art. #11533. <https://doi.org/10.3390/ijms222111533>
- Mehari, K., Asmelash, T., Hailekiros, H., Wubayehu, T., Godefay, H., Araya, T. & Saravanan, M. 2019. Prevalence and factors associated with multidrug-resistant tuberculosis (MDR-TB) among presumptive MDR-TB patients in Tigray region, northern Ethiopia. *Canadian Journal of Infectious Diseases and Medical Microbiology*, 2019, art. #2923549. <https://doi.org/10.1155/2019/2923549>
- Migliori, G.B., Tiberi, S., Zumla, A., Petersen, E., Chakaya, J.M. Wejse, C., ... Zellweger, J.P. 2020. MDR/XDR-TB management of patients and contacts: Challenges facing the new decade. The 2020 clinical update by the Global Tuberculosis Network. *International Journal of Infectious Diseases*, 92(Supplement): S15–S25. <https://doi.org/10.1016/j.ijid.2020.01.042>
- Moreira, J.D., Silva, H.R., De Toledo, V.D.C.P. & Guimaraes, T.M.P.D. 2020. Microparticles in the pathogenesis of TB: novel perspectives for diagnostic and therapy management of *Mycobacterium tuberculosis* infection. *Microbial Pathogenesis*, 144, art. #104176. <https://doi.org/10.1016/j.micpath.2020.104176>
- Navidinia, M., Goudarzi, M., Rameshe, S.M., Farajollahi, Z., Asl, P.E., Khosravi, S.Z. & Mounesi, M.R. 2017. Molecular characterization of resistance genes in MDR-ESKAPE pathogens. *Journal of Pure and Applied Microbiology*, 11(2): 779-792. <https://dx.doi.org/10.22207/JPAM.11.2.17>
- Padayatchi, N., Bionghi, N., Osman, F., Naidu, N., Ndjeka, N., Master, I., ... O'Donnell, M. 2020. Treatment outcomes in patients with drug-resistant TB-HIV co-infection treated with bedaquiline and linezolid. *The International Journal of Tuberculosis and Lung Disease*, 24(10): 1024-1031. <https://doi.org/10.5588/ijtld.20.0048>

Pandey, R., Mishra, S.K. & Shrestha, A. 2021. Characterisation of ESKAPE pathogens with special reference to multidrug resistance and biofilm production in a Nepalese hospital. *Infection and Drug Resistance*, 14: 2201-2212. doi:10.2147/IDR.S306688

Pawlowski, A., Jansson, M., Sköld, M., Rottenberg, M.E. & Källenius, G. 2012. Tuberculosis and HIV co-infection. *PLoS Pathogens*, 8(2), e1002464.
<https://doi.org/10.1371/journal.ppat.1002464>

Pradipta, I.S., Houtsma, D., van Boven, J.F., Alffenaar, J.W.C. & Hak, E. 2020. Interventions to improve medication adherence in tuberculosis patients: a systematic review of randomized controlled studies. *NPJ Primary Care Respiratory Medicine*, 30(1), art. #21.
<https://doi.org/10.1038/s41533-020-0179-x>

Rodriguez, C.A., Brooks, M.B., Guglielmetti, L., Hewison, C., Jachym, M.F., Lessem, E., ... Mitnick, C.D. 2019. Barriers and facilitators to early access of bedaquiline and delamanid for MDR-TB: a mixed-methods study. *Public Health Action*, 9(1): 32-41.
<https://doi.org/10.5588/pha.18.0078>

Rice, A.M., Long, Y. & King, S.B. 2021. Nitroaromatic antibiotics as nitrogen oxide sources. *Biomolecules*, 11(2), art. #267. <https://doi.org/10.3390/biom11020267>

Skóra, B., Lewińska, A., Kryshchyn-Dylevych, A., Kaminsky, D., Lesyk, R. & Szychowski, K.A. 2022. Evaluation of anticancer and antibacterial activity of four 4-thiazolidinone-based derivatives. *Molecules*, 27(3), art. #894.
<https://doi.org/10.3390/molecules27030894>

Spelman, D.W. 2002. 2: Hospital-acquired infections. *Medical Journal of Australia*, 176(6): 286-291. <https://doi.org/10.5694/j.1326-5377.2002.tb04412.x>

Togun, T., Kampmann, B., Stoker, N.G. & Lipman, M. 2020. Anticipating the impact of the COVID-19 pandemic on TB patients and TB control programmes, *Annals of Clinical Microbiology and Antimicrobials*, 19, art. #21. <https://doi.org/10.1186/s12941-020-00363-1>

Vicini, P., Geronikaki, A., Anastasia, K., Incerti, M. & Zani, F. 2006. Synthesis and antimicrobial activity of novel 2-thiazolylimino-5-arylidene-4-thiazolidinones. *Bioorganic & Medicinal Chemistry*, 14(11): 3859-3864. <https://doi.org/10.1016/j.bmc.2006.01.043>

Vicini, P., Geronikaki, A., Anastasia, K., Incerti, M. & Zani, F., Dearden, J. & Hewitt, M. 2008. 2-Heteroarylrimino-5-benzylidene-4-thiazolidinones analogues of 2-thiazolyrimino-5-benzylidene-4-thiazolidinones with antimicrobial activity: synthesis and structure–activity relationship. *Bioorganic & Medicinal Chemistry*, 16(7): 3714-3724.

<https://doi.org/10.1016/j.bmc.2008.02.001>

Viderman, D., Brotfain, E., Khamzina, Y., Kapanova, G., Zhumadilov, A. & Poddighe, D. 2019. Bacterial resistance in the intensive care unit of developing countries: report from a tertiary hospital in Kazakhstan. *Journal of Global Antimicrobial Resistance*, 17: 35-38.

<https://doi.org/10.1016/j.jgar.2018.11.010>

Wen, S.A., Jing, W., Zhang, T., Zong, Z., Xue, Y., Shang, Y., ... Pang, Y. 2019. Comparison of *in vitro* activity of the nitroimidazoles delamanid and pretomanid against multidrug-resistant and extensively drug-resistant tuberculosis. *European Journal of Clinical Microbiology & Infectious Diseases*, 38(7): 1293-1296. <https://doi.org/10.1007/s10096-019-03551-w>

WHO (World Health Organization). 2021. *Global tuberculosis report 2021*.

<https://www.who.int/teams/global-tuberculosis-programme/tb-reports/global-tuberculosis-report-2021> Date of access: 09 Mar. 2022.

WHO (World Health Organization). 2018. *Tuberculosis*.

<https://www.afro.who.int/news/tuberculosis> Date of access: 08 May. 2022.

WHO (World Health Organization). 1999. *What is DOTS? : a guide to understanding the WHO-recommended TB control strategy known as DOTS*.

<https://apps.who.int/iris/handle/10665/65979> Date of access: 12 Mar. 2022.

Xu, W.C., Silverman, M.H., Yu, X.Y., Wright, G. & Brown, N. 2019. Discovery and development of DNA polymerase III C inhibitors to treat Gram-positive infections. *Bioorganic and Medicinal Chemistry*, 27(15): 3209-3217. <https://doi.org/10.1016/j.bmc.2019.06.017>

Zignol, M., Dean, A.S., Falzon, D., van Gemert, W., Wright, A., van Deun, A., ... Raviglione, M.C. 2016. Twenty years of global surveillance of antituberculosis-drug resistance. *New England Journal of Medicine*, 375(11): 1081-1089. doi:10.1056/NEJMSr1512438

CHAPTER 2: LITERATURE REVIEW

The literature review will be divided into two parts, with the first concentrating on tuberculosis (TB) and the second on hospital-acquired infections (HAIs), in order to gain a more in-depth understanding of current research relevant to the study topic.

PART ONE: TUBERCULOSIS (TB)

2.1. Background

The bacterium *Mycobacterium tuberculosis*, or Mtb, causes tuberculosis (TB), one of the oldest known human diseases that has co-evolved alongside human populations for many centuries. For example, evidence of skeletal TB (Pott's lesions) was discovered in ancient Egyptian mummy's spinal cord segments dated to 2400 B.C., indicating a definite pathological sign of TB deterioration up to this point (Barberis *et al.*, 2017:E9).

In 1679, Sylvius de la Boe, a Dutch researcher from Amsterdam, published the earliest anatomical and pathological descriptions of TB by recognising tubercles as a typical clinical manifestation in the lungs of Mtb-infected individuals. The first to identify TB as an infectious disease was Benjamin Martin. He also postulated that prolonged contact with a Mtb-infected individual was needed to acquire TB (Herzog, 1998:6-7). However, a French military physician named Jean-Antoine Villemin physically demonstrated the infectious nature of Mtb for the first time in 1865 and learned that it could be transmitted from animals to humans. At the time, the mode of transmission was unknown (Schluger, 2005:251). Later, in 1882, Robert Koch presented a unique staining method for visualizing and isolating the *Mycobacterium* responsible for TB. Subsequently, he also established the airborne method of transmission of Mtb. These key developments paved the way for scientists to conduct extensive research on Mtb in an attempt to eradicate the bacterium responsible for TB (Cambau & Drancourt, 2014:197-199).

Selman Waksman's discovery of streptomycin (SM) in the early 1940s set the groundwork for effective TB treatment, leading many healthcare experts to assume that TB would soon be eradicated (Zumla & Grange, 1999:104). However, its usage in extended treatment regimens proved challenging owing to the difficulties of administering SM orally and its toxicity profile. Additionally, it was also discovered that TB could not be treated with a single drug, due to the emergence of Mtb resistance as a result of ribosomal target site mutations (Prabhu & Singh, 2019:936).

TB has been known by multiple names throughout the years. Hippocrates, the father of medicine, who was fully aware of TB and its clinical manifestations, introduced the term "phthisis", which means "consumption" in Greek. The phrase "consumption," points to how TB seems to "devour or consume" the host through significant weight loss and "wasting away", primarily striking adults between the ages of 18 and 35 (Daniel, 2006:1863; Moonan, 2018:592). In the late 18th and early 19th centuries, TB spread over Europe and the United States, labelled as "The Great White Plague." It was dubbed "white" because of the extreme anaemia-related paleness of those affected. The World Health Organization (WHO) declared TB a global emergency because every year during this time, the mortality rate fluctuated from 800 to 1,000 per 100,000 Mtb infected individuals (Frith, 2014:32; Zumla *et al.*, 2009:197).

TB remains a public health concern even today, despite the production of newer antitubercular drugs, making it one of the leading causes of death among people in developing countries, especially those co-infected with the human immunodeficiency virus (HIV) (WHO, 2017a).

2.2. Epidemiology of TB

According to the WHO (2021a), approximately 10 million people worldwide contracted TB in 2020. Males accounted for 56% (5.6 million) of all TB infections, women bore 33% (3.3 million) of the TB burden, and children 11% (1.1 million). Africa, Southeast Asia and the Western Pacific had the most TB cases, followed by the Eastern Mediterranean, Europe and the

Americas. High-prevalence countries accounted for 86% of all TB cases. Eight countries accounted for two-thirds of the global TB burden: the Philippines (6%), India (26%), Pakistan (5.8%), China (8.5%), Bangladesh (3.6%), Indonesia (8.4%), Nigeria (4.6%) and South Africa (3.3%).

The COVID-19 pandemic has resulted in the first annual increase in TB deaths since 2005, mainly due to the limited access to TB diagnosis and treatment. The number of fatalities has increased from 1.2 million to 1.3 million, including 240,000 HIV-related deaths in 2020. The prevalence of multidrug-resistant TB (MDR-TB) is steadily increasing with the number of people treated for MDR-TB declining from 177,100 to 150,359 in 2020. It seems that just one in three people in need of MDR-TB therapy sought medical care. This 2020 results render TB a public health emergency and a global threat, making it the second most infectious killer after COVID-19 (WHO, 2021a).

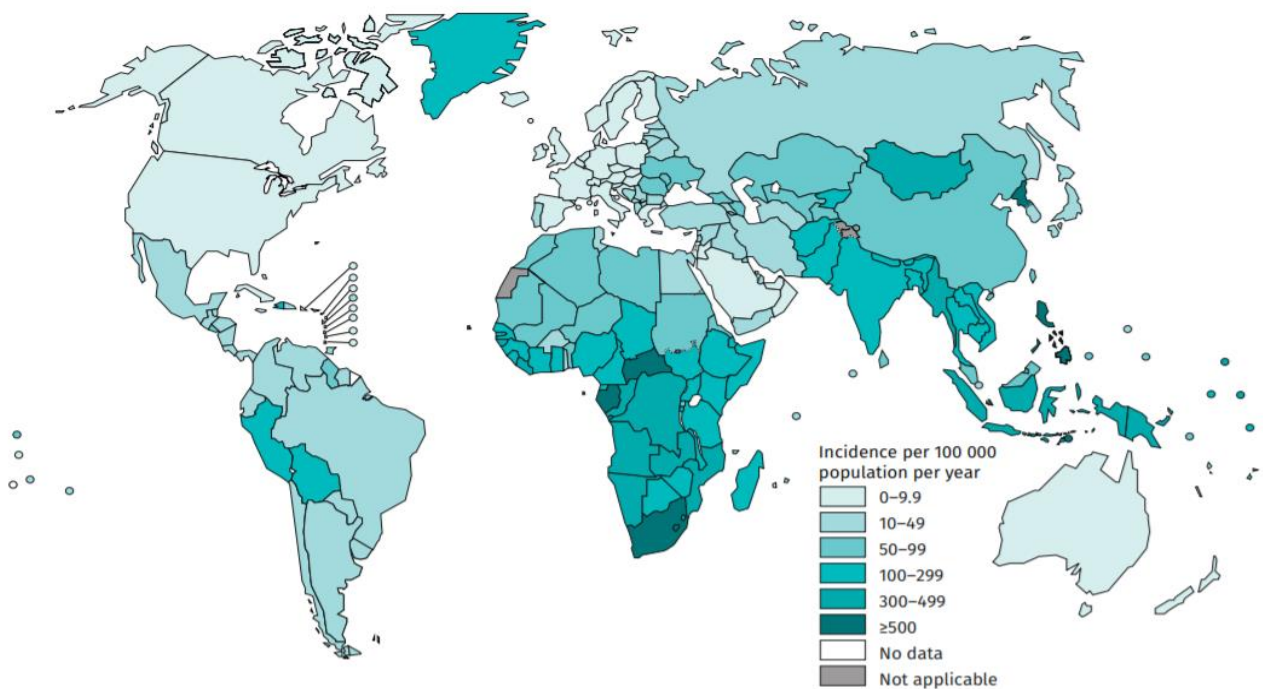


Figure 2.1 Tuberculosis incidence rates in 2020 (WHO, 2021a).

2.3. Mtb cellular morphology

Depending on the environmental circumstances, Mtb develops as long, straight or slightly thin, curved rods (1.0–10 µm long and 0.2–0.7 µm wide). Mtb does not produce spores and is normally aerobic to microaerophilic. Mtb grows slowly and create observable colonies in 2–60 days at ideal conditions (Ahamad *et al.*, 2022:3). Furthermore, it replicates at a far slower rate (16–20 hours) than other bacteria, which often divide in less than an hour (Sharma *et al.*, 2011:244).

Microscopy reveals that the cell wall of Mtb consists of an outer membrane similar to Gram-negative bacteria, packed in an asymmetrical lipid bilayer composed of glycolipids and waxy materials on the outside and long fatty acid chains on the inside (mycolic acids). The periplasmic space is made up of the inner and outer membranes. It is formed by peptidoglycan that is covalently bound to arabinogalactan and lipoarabinomannan (LAM), which are subsequently covalently bonded to mycolic acids. This forms the mycolyl arabinogalactan-peptidoglycan (mAGP) complex, or commonly termed, the cell wall nuclei (Alderwick *et al.*, 2015:1; Delogu *et al.*, 2013). The cell wall of Mtb is additionally surrounded by a mycobacterial capsule. The capsule contains a high concentration of neutral polysaccharides, lipids and proteins, which, along with glycolipids and inert waxes, form an impenetrable barrier against noxious TB drugs and compounds (Shaku *et al.*, 2020:2). Mtb is resistant to Gram staining due to its overall lipid-rich cell wall composition. This is because, when stained with Gram stain dyes, the cell wall is resistant to the hydrophilic acid alcohol decolorizing agent, hence they are classified as "acid-fast" bacilli (Vilchèze & Kremer, 2017:1).

2.4. Pathophysiology of Mtb

The risk of contracting TB is solely dependent on the probability of inhaling an infectious dosage or quantity of Mtb and the development thereof into an established active infection (assuming total susceptibility). Individuals with pulmonary TB produce Mtb-contaminated dehydrated residua droplet nuclei, or larger aerosols generated through sneezing, coughing,

laughing or shouting (Nardell, 2015:1-2). These physical acts pave the way for Mtb to enter the respiratory system and be caught by goblet cells, which release mucus. However, after slipping past the body's first mucociliary defensive barrier, the bacilli infiltrate the oxygenated alveoli of the lungs, triggering the host's innate immunological response. After activation of the latter, alveolar macrophages engulf Mtb by primary phagocytosis (Chai *et al.*, 2020:1860; Luies & Du Preez, 2020:2). Phago-lysosomal fusion is responsible for the early elimination of Mtb. However, while in the phagosome, Mtb may produce the phosphatase *SapM* and the serine/threonine kinase *PknG*, which prevents such fusion, and subsequently promote the survival and multiplication of Mtb within macrophages (Pieters, 2008:402).

During this phase, which lasts approximately two to three weeks, the human body mounts a complex cell-mediated immunity to combat Mtb. Monocytes, dendritic cells and neutrophils begin to surround the site of the infection. The infected dendritic cells become activated and migrate to a nearby draining lymph node, where they present antigens to T lymphocytes, allowing for a host T cell response. The infected macrophages, on the other hand, release pro-inflammatory cytokines (Silva Miranda *et al.*, 2012:2; Welin, 2011:11). The excreted cytokines activate natural killer cells, which then produce interferon gamma (IFN- γ) and subsequently activate macrophages to release tumour necrosis factor (TNF- α) as well as bactericidal chemicals in an attempt to destroy Mtb. Additional immune cells and macrophages are recruited from the blood circulation through cytokine and chemokine signaling, which aggregate into cell clusters at the primary site of infection called the granuloma (Welin, 2011:11) (see **Fig. 2.2**).

The formation of such granulomas, which contain both uninfected and infected cells covered by a lymphocytic cuff is the hallmark of TB infection. Granulomas are the main site of the host-pathogen interaction and functions by limiting Mtb dissemination from the lungs to other places in the body (Kotze *et al.*, 2021:2; Sia & Rengarajan, 2019:1). However, research using the zebrafish TB model has recently indicated that granulomas may potentially offer a niche for

the survival of Mtb and may also facilitate the dissemination of the bacilli inside the host (Ravimohan *et al.*, 2018:10; Volkman *et al.*, 2010:466). Some infected granulomas may heal entirely (sterilising cure) over time or stay in a balanced, compact form, restricting Mtb at their centres as a result of the host's reaction to infection (Kotze *et al.*, 2021:2; Russell *et al.*, 2009:3).

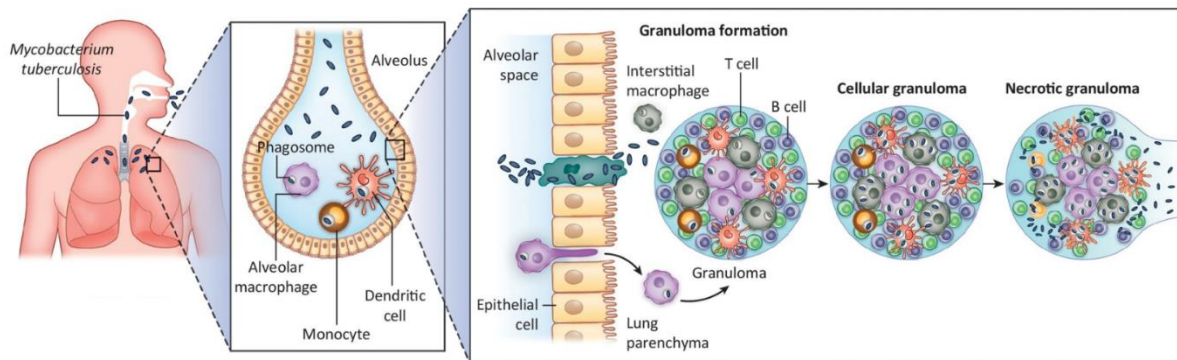


Figure 2.2 The formation and progression of granulomas (Koch & Mizrahi, 2018).

The healing process requires the macrophages within the granulomas to undergo necrotic destruction through a process called caseous necrosis. The necrotic tissue is now known as a ghon focus (Ani Fatonah *et al.*, 2019). Mtb may additionally spread via lymphatic vessels to regional lymph nodes as a direct extension of the ghon focus. At this point, the ghon focus and its accompanying lymph nodes are referred to as the ghon complex (Pillay *et al.*, 2020:66). The tissue contained by the ghon complex gradually undergoes fibrosis and calcification, generating scar tissue or lesions that may be seen on a chest X-ray. The radiological appearance of the calcified ghon complex on a chest X-ray is referred to as a ranke complex (Hicks *et al.*, 2014:129). At this stage, the progression of the infection has been halted. However, some Mtb bacilli that are capable of surviving under the stressful conditions executed by the host escape death by avoiding elimination by the immune response and entering a state of dormancy (Ahmad, 2011:4).

During the dormancy period, the disease is usually asymptomatic and not contagious because the Mtb bacilli cannot enter the airways to be exhaled and transmitted, leaving the patient with a latent TB infection (Sharma *et al.*, 2021:4362). It is believed that viable Mtb bacilli may stay dormant and reactivate days, months or even years later (Ai *et al.*, 2016:1). Of all people latently infected with TB, 5–15% will develop active TB over their lifetime (Dutta & Karakousis, 2014:344).

Reactivation of latent TB occurs when the patient's immune system weakens, as with HIV co-infection which is the most significant single risk factor for disease escalation to active TB in adults (Ahmad, 2011:9). The immune system is incapable of controlling the infection, enabling the dormant Mtb bacilli to reactivate by replicating at a high density and increasing their concentration within granulomas (Fattorini *et al.*, 2013:2). As a result, the caseous necrotic core of the granuloma liquefies and cavitates, spewing hundreds of reactivated Mtb into the airways (as seen in **Fig. 2.2**) (Ndlovu & Marakalala, 2016:3). The reactivated bacilli may rapidly disseminate from the initial infection, and Mtb can be found in lymph nodes near the lungs and subsequently in other organs within two weeks, known as extrapulmonary TB (Moule & Cirillo, 2020:5).

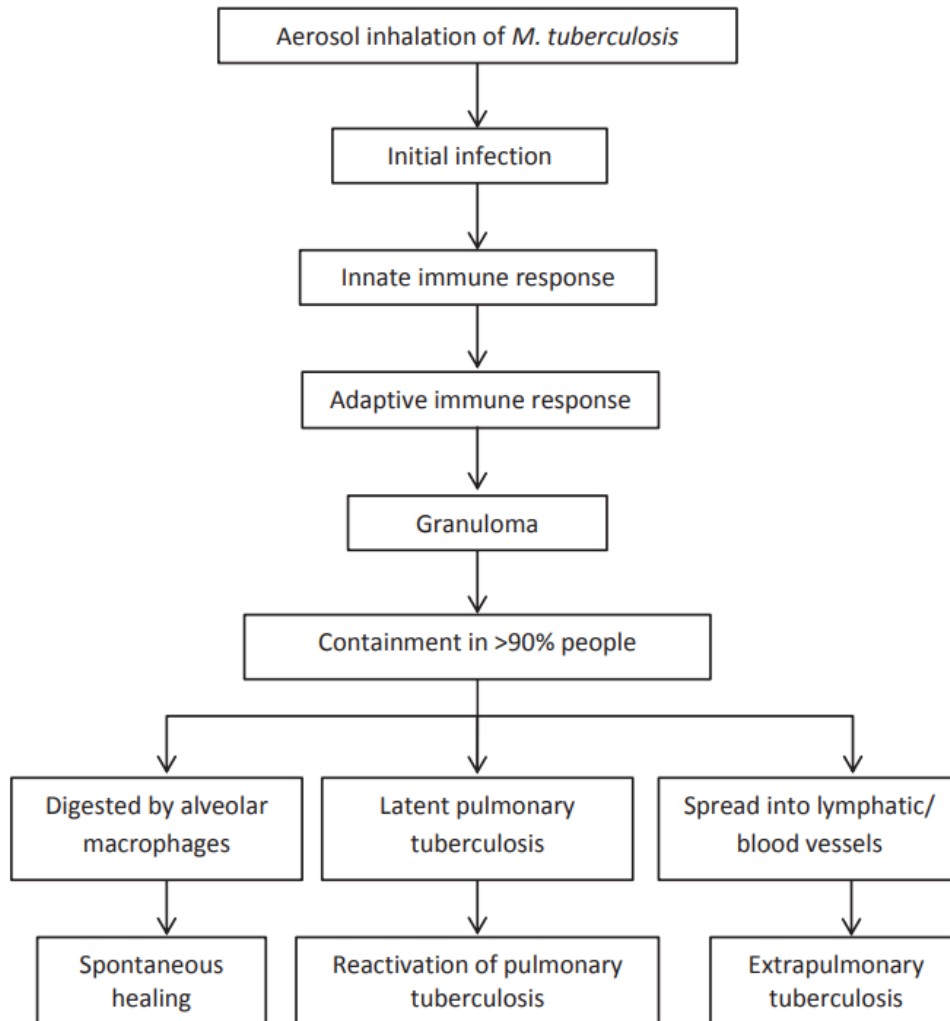


Figure 2.3 Pathophysiology of tuberculosis (Susilawati & Larasati, 2019).

2.5. Virulence factors of Mtb

The pathophysiology of Mtb clearly shows that mycobacteria can withstand host immunity. Mtb lacks the typical virulence factors that are generated by the majority of other bacteria, such as endotoxins to poison host cells, capsules to avoid phagocytosis, flagella for mobility, and other adhesins for attachment to host tissues (Cambier *et al.*, 2014:1497; Smith, 2003:468). Mtb, on the other hand, employs a number of additional characteristics that are critical for the progression of TB in order to subvert and/or evade the host's immune system (Sundararajan & Muniyan, 2021:6182) and subsequently promote mycobacterial replication and survival within the host:

- **Mycolic acids** are β -hydroxy fatty acids with a long α -alkyl side chain. They appear as a homologous sequence of C₅₄ to C₆₃ fatty acids with C₂₂ to C₂₄ α side chains. Mtb specifically contains α -, methoxy-, and keto-mycolic acids (Takayama *et al.*, 2005:82) that create a lipid shell surrounding Mtb and alter cell permeability. They are also known to protect mycobacteria against lysozyme, oxygen radicals and cationic proteins (Rao & Meena, 2011a:2).
- **Trehalose 6,6'-dimycolate** (cord factor) is the most abundant extractable lipid on the surface of Mtb (Harland *et al.*, 2008:4718). The cord factor is toxic to mammalian cells and is known to inhibit neutrophil migration during host cell-mediated immune response. It also promotes the Mtb infected macrophages to form granulomas by inducing cytokine (INF- γ) production (Rao & Meena, 2011b: 3-4). In addition, the cord factor inhibits phago-lysosomal fusion as well as the migration of Mtb to acidic compartments in macrophages (Harland *et al.*, 2008:4718).
- **Lipoarabinomannan (LAM)** is a complicated cell wall glycolipid comprised of phosphatidylinositol and a mannose nucleus, branched with arabinofuranosyl side chains (Maiti *et al.*, 2001:329). LAM inhibits INF- γ mediated macrophage activation. In addition, LAM may scavenge toxic oxygen free radicals, inhibit protein kinase C activity, and prevent the transcriptional activation of INF- γ inducible genes in macrophages (Joshi *et al.*, 2020:252).
- **Type VII secretion system (T7SS; ESX):** The ESX protein secretion system exports intracellular virulence-promoting proteins over Mtb's cell envelope. Mtb encodes five unique type VII secretion proteins, ESX-1 through ESX-5 (Bunduc *et al.*, 2020:316). ESX-1 enables Mtb to escape phagosome vesicles to avoid destruction (Rao & Meena, 2011a:3) and secretes antigens that cause the membrane of phagosomes to rupture. ESX-2 ensures survival of Mtb, while ESX-3 regulates iron and zinc influx and hinders phagosome maturation. ESX-4 is needed for conjugation, whereas ESX-5 releases immunomodulatory proteins (Roy *et al.*, 2020:203).

2.6. Clinical manifestations of TB

2.6.1. Post-primary pulmonary TB (reactivation TB)

Reactivation of primary Mtb infection or a new infection from an external source, for example an infected individual, can result in post-primary TB. Post-primary TB may be misdiagnosed and possibly be contagious for up to three years or more, with symptoms only manifesting late in the disease's progression (Pozniak, 2019). It normally affects just the uppermost lobes of the lungs, with no involvement of lymph nodes or other organs. It accounts for about 80% of all confirmed TB cases and almost 100% of infection transmission (Hunter, 2011:498). Patients may manifest symptoms such as chest discomfort, shortness of breath, low grade fever and a slight, non-productive cough. As the infection worsens, cough may become more productive with bloody-greenish sputum. Anorexia, weight loss, muscular atrophy and wasting ("consumption") may be seen in extreme cases (Alzayer & Al Nasser, 2021:4; Pozniak, 2019).

2.6.2. Extrapulmonary TB

TB can affect every organ system in the human body, despite the fact that TB in the pulmonary system is the most common form. Extrapulmonary TB is a kind of TB disease that involves organs other than the lungs and represents 10–50% of confirmed TB cases (Shivakumar *et al.*, 2022:341). Extrapulmonary TB is more prevalent in individuals with weaker immune systems, particularly those who are also HIV-infected. The most likely affected extrapulmonary TB sites are the lymphatic system, the bones and joints, the genito-urinary system and the central nervous system (CNS), followed by peritoneal and other abdominal organs (De Backer *et al.*, 2006:248-249).

Extrapulmonary TB clinical manifestations include typical post-primary pulmonary TB symptoms such as fever, weight loss, night sweats or malaise, as well as various systemic symptoms related to the affected organ (Gopaldaswamy *et al.*, 2021:141). The most prevalent manifestation of extrapulmonary TB, for example, is lymphadenitis, or inflammation of the

cervical lymph nodes. Lymphadenitis may cause significant swelling in the neck that mimics a growth or tumour in extreme instances (Moule & Cirillo, 2020:2). The renal system is commonly affected, It is, however, typically asymptomatic. Mtb may enter the glomerular system and get caught in the Henle loop, causing new focal points of infection to develop in the renal pyramids. Peritoneal TB is often associated with other types of abdominal TB. Necrotic lymph node rupture induces peritoneal TB, with ascites being the most common manifestation (Rodriguez-Takeuchi *et al.*, 2019:2028-2032).

The most severe form of extrapulmonary TB with CNS involvement is TB meningitis (5–10% of all TB cases). Fatigue, nausea, fever, headaches and disorientation are all symptoms of TB meningitis. Convulsions, comas and stupor may also occur (Azad & Chowdhury, 2022:132). Miliary TB develops via hematogenous spread of the primary infection. If not treated properly, this is the most lethal type of extrapulmonary TB, accounting for 15–20% of teenage and 25–30% of adult TB fatalities (Vohra & Dhaliwal, 2022:9). Miliary TB most often affects the lymph nodes, liver, meninges, adrenal glands, spleen, lung and bone marrow. Septicaemia with fever, lethargy, anorexia, weight loss, and coughing are all common manifestations of miliary TB (Azad & Chowdhury, 2022).

2.7. Detection and diagnosis of TB

Rapid and accurate diagnostic tests for TB, with the management of latent TB are vital to Mtb eradication attempts. The diagnosis of primary pulmonary TB and latent TB incorporates culture development, immunological tests and molecular assays to identify the presence of Mtb. Extrapulmonary TB is detected similarly to post-primary and latent TB, albeit invasive biopsies are typically used. The diagnostic tests are less effective in HIV-positive patients, those with latent TB, and adolescents unable to produce Mtb-containing sputum. Furthermore, they require expensive, sophisticated laboratory equipment and highly qualified staff, both of which are uncommon or inaccessible in low- and middle-income countries (MacGregor-Fairlie *et al.*, 2020:436).

2.7.1. Microbiological assays

A. TB Culture

The ultimate gold standard diagnostic test for TB is incubating a sputum sample for Mtb culture growth, which may also provide evidence of drug susceptibility or resistance, including emerging mutations (Oommen & Banaji, 2017:325). Culture has a 99% specificity for diagnosing TB. However, owing to Mtb's slow growth, it may take a long time to develop a suitable culture. This, in turn, delays treatment initiation in the absence of a confirmed diagnosis (Acharya *et al.*, 2020:4069).

There are three types of culture media: Löwenstein-Jensen (egg-based), Middlebrook 7H10 or 7H11 (agar-based), and Middlebrook 7H12 (liquid-based). Mycobacterial growth is more conducive to egg-based media than agar-based media, and growth in liquid media is often more rapid than growth in solid media. A further benefit of using agar medium is that it enables researchers to examine the morphology of Mtb colonies and distinguish between diversified mycobacterial cultures (Sia & Wieland, 2011:354). To diagnose TB, sputum isolates are inoculated onto various media containing increasing doses of antibiotics to determine the lowest concentration at which 99% of growth is inhibited. To determine resistance and susceptibility, two media are prepared, one with antibiotics and one without, and the percentage of Mtb colonies growing in the presence of antibiotics is compared to those growing in the absence of antibiotics. The isolate is classified as sensitive or resistant based on predetermined ranges (Cudahy & Shenoj, 2016:191).

Traditional solid culture growth is time-consuming, difficult, and have little therapeutic benefit. Automated liquid culture methods have essentially supplanted solid culture, with around 10% greater yields and a shorter time to diagnosis. However, automated liquid cultures are costly, prone to contamination, and need a significant amount of laboratory equipment and experience (Peter *et al.*, 2012:128). Growth requires 4 to 8 weeks on a typical egg-based

medium, with an additional 4 weeks for drug sensitivity testing. As a result, diagnosing MDR-TB takes an average of 70 days (Oommen & Banaji, 2017:325).

B. Acid-Fast Bacilli (AFB) smear microscopy

Mtb can be detected through AFB smear microscopy using the Ziehl-Neelsen (ZN) staining technique. Staining for AFB has been the foundation of TB diagnosis since its discovery by Koch in 1882. The effectiveness of AFB smear microscopy lies in its ability to detect the most infectious patients. However, there are a number of variables that might alter the yield of a smear, including collection time and sputum processing (Cudahy & Shenoi, 2016:190).

The procedure includes carbolfuchsin staining of the sputum-smear slides by submerging the smear in carbolfuchsin and subsequently heating the slide until steam rises without boiling the dye. This allows the stain to be fixed into the cell wall of Mtb and the whole smear will become red at this stage. The second step after stain fixation is to cover the slide with acid alcohol for 2–3 minutes. Acid alcohol decolourises all non-acid-fast organisms, leaving behind only the red stained acid-fast Mtb. Finally, the slides are then counterstained with methylene blue, which enhances the visual contrast of the red acid-fast Mtb against a blue background during microscopy (Bayot *et al.*, 2019). The benefits of the ZN include low-cost rapid testing for Mtb. However, results are often hampered due to low sensitivity, which may range from 20–80%. The smear needs high bacilli count from sputum to be successful and its sensitivity is further significantly reduced in HIV-coinfected individuals (Ojha *et al.*, 2020:1431–1432). Other limitations of smear microscopy include the test's inability to differentiate between viable and non-viable organisms, Mtb and non-tuberculous mycobacteria, and drug-susceptible and drug-resistant strains of Mtb (Harries & Kumar, 2018:3-4).

2.7.2. Immunoassays

A. Mantoux Tuberculin Skin Test (TST)

A TST is an intradermal injection of tuberculin purified protein derivative (PPD) extracted from *Mtb* cultures. The test detects a type IV delayed-type hypersensitivity response in *Mtb*-exposed people based on immunological recognition of the PPD antigen (Pahal & Sharma, 2021). This reaction is delayed since it takes time to recruit immune cells and activated macrophages to the injection site. Intradermal injection of 0.1 ml of five test unit PPD stimulates antigen-specific lymphocyte influx and the release of inflammatory cytokines. The subsequent inflammatory reaction causes an indurated zone at the injection site, which is needed for diagnosis. After 48–72 hours, a healthcare professional palpates the injection site for induration and measures it. Depending on a patient's comorbidities or history of TB exposure, 5–15 mm of induration indicates a positive result (Kestler & Tyler, 2022:L415).

The TST is not always reliable – it often delivers false-positive and false-negative results. False-positive results are due to its inability to differentiate between *Mtb* and either non-tuberculosis mycobacteria or the Bacille Calmett-Guérin (BCG) vaccine (*Mycobacterium bovis*). These false-positive results are often ascribed to an immunological response generated by homologous antigens from environmental mycobacteria or *M. bovis* (Yang *et al.*, 2012:276). In addition, HIV infection, severe acute diseases, cancer, ageing and immunosuppressive drugs might decrease the immune system's capacity to react to the TST, causing false-negative results (Almeida Santos *et al.*, 2020:542). Finally, a positive TST solely indicates *Mtb* infection. It does not tell whether someone has latent TB or active TB. A chest X-ray and sputum analysis are, therefore, required for a complete diagnosis after a TST (CDC, 2022).

B. Interferon- γ Release Assays (IGRAs)

IGRAs are Mtb antigen-specific IFN- γ release assays designed to measure *in vitro* IFN- γ concentration after incubation of whole blood or peripheral blood mononuclear cells with antigens (ESAT-6 and CFP10), encoded within the region of difference-1 locus of Mtb. These antigens are absent in the vast majority of non-TB mycobacteria and BCG strains, making the IGRAs more selective than the TST (Kestler & Tyler, 2022:L416; Pourakbari *et al.*, 2019:437). Two IGRAs are available: the QuantiFERON-TB Gold In-Tube Plus test, which measures the amount of IFN- γ in culture supernatant using an enzyme-linked immunosorbent assay (ELISA), and the T-SPOT.TB assay which recognises the amount of IFN- γ producing T cells using an enzyme-linked immunospot (ELISPOT) assay (Zhou *et al.*, 2015:2).

For the QuantiFERON-TB Gold In-Tube Plus test, blood samples are incubated with Mtb-specific antigens and controlled at $37^{\circ}\text{C} \pm 1^{\circ}\text{C}$ for 16 to 24 hours. After incubation, tubes are centrifuged, plasma is extracted, and ELISA measures the amount of IFN- γ produced by T cells (Lee *et al.*, 2021:1695). However, for the T-SPOT.TB, the procedure is more complex and carried out in microtiter wells pre-coated with Mtb-specific capture antigens (IFN- γ -specific). Sample preparation involves separating, quantifying and diluting peripheral blood mononuclear cells from whole blood, after which it is incubated at 37°C with 5% CO_2 for 16 to 20 hours. The pre-coated antibodies capture the released IFN- γ at the bottom of each well. After adding a second antigen and a soluble substrate, an insoluble precipitate forms on the membrane at the bottom of each well. Finally, using an ELISPOT plate reader, spots are counted. Each spot represents an individual cytokine-secreting T cell, and the number of spots observed indicates the abundance of Mtb-sensitive effector T cells in peripheral blood compared to the control (ECDP, 2018).

The sensitivity of IGRAs is lowered in immunocompromised individuals, similar to the TST. In addition, it cannot discriminate between latent and active TB (Sotgiu *et al.*, 2019:444). Recent evidence indicates, however, that the combination of IGRAs and mycobacterial heparin-

binding hemagglutinin (HBHA) is a potential test for differentiating between latent and active TB. This is because HBHA is a typical Mtb antigen linked with latency (Tang *et al.*, 2021:1-2). The specificity of IGRAs is believed to exceed 95%, whereas the sensitivity ranges between 80% and 90%. IGRAs are substantially more expensive than TSTs and require phlebotomy, scientific equipment, and technical competence for sample collection, processing, and assessment (Kestler & Tyler, 2022:L416).

2.7.3. Nucleic Acid Amplification Tests (NAATs)

A. Molecular Line Probe Assays (LPAs)

Numerous molecular strategies and technologies have been developed to enable a rapid turnaround time of one day for NAATs, as opposed to two weeks or more for culture development (Teo *et al.*, 2011:3659). The GenoType® MTBDR*plus* v1.0 and GenoType® MTBDR*s/* v2.0 tests are both LPAs based on genotype rather than phenotype. They rely on gene mutations associated with antitubercular drug resistance to detect Mtb complex (Stephen *et al.*, 2019:84). GenoType® MTBDR*plus* v1.0 detects resistance to rifampicin (RIF) and isoniazid (INH), while GenoType® MTBDR*s/* v2.0 detects resistance to fluoroquinolones (FQNs) and other second-line injectables (Chen *et al.*, 2019:2). Although LPAs aid in the rapid detection of MDR-TB, deoxyribonucleic acid (DNA) extraction, amplification, hybridization and the result interpretation are manual, laborious operations that necessitate error-prone multistep processes and at least three different rooms to avoid contamination, which makes them labour-intensive (David *et al.*, 2020:3302).

The procedure for LPAs includes the extraction of DNA, the preparation and addition of master samples, multiplexed nucleic acid amplification using biotinylated primers through polymerase chain reaction (PCR), detection of the amplicons by reverse hybridization with oligonucleotide probes attached on a nitrocellulose strip in parallel lines, and finally colorimetric development that enables lines to be seen where the probes are situated on the strip (Eddabra & Ait Benhassou, 2018:5; Javed *et al.*, 2018:2; Meaza *et al.*, 2017:2). The GenoType® MTBDR*plus*

v1.0 test has a sensitivity of 95.8% and a specificity of 98.4% for detecting RIF resistance, and 94.5% sensitivity and 99.3% specificity for detecting INH resistance. The GenoType® MTBDRs/ v2.0 test, on the other hand, has a sensitivity of 86.2% and a specificity of 98.6% for detecting FQN resistance, and 87.0% sensitivity and 99.5% specificity for detecting second-line injectable drug resistance (WHO, 2022a).

B. Xpert MTB/RIF assay

The Xpert MTB/RIF assay (a novel NAAT) was authorized by the WHO in 2010 as a primary diagnostic test for MDR-TB or HIV-associated TB, and it may be used as a follow-up test to AFB smear microscopy in countries where MDR-TB or HIV are less of a problem (WHO, 2011). The Xpert MTB/RIF assay has revolutionised TB control by further improving the turnaround time for NAATs. Results can now be delivered in less than two hours, either directly from a sputum sample or after decontamination and concentration of the sputum (CDC, 2016a; Steingart *et al.*, 2013:6-7). It helps TB patients commence treatment much sooner (as opposed to have them wait for other drug susceptibility tests). A retrospective cohort study in South Africa, where MDR-TB and HIV rates are extremely high, confirms this. The Xpert MTB/RIF test reduced treatment delays by 50% between 2011 (after deployment of Xpert MTB/RIF) and 2013 (Cox *et al.*, 2017:3).

Xpert MTB/RIF uses hemi-nested real-time PCR and molecular beacon technology to simultaneously detect Mtb and RIF resistance by recognising mutations in the normal, RIF-susceptible "wild-type" sequence of Mtb's ribonucleic acid (RNA) polymerase gene, *rpoB*. Five distinct coloured beacons are applied, each covering a specific nucleic acid sequence in the amplified *rpoB* gene (Rufai *et al.*, 2014:1846; Steingart *et al.*, 2013:6-7). The Xpert MTB/RIF assay, unlike other standard NAATs (like LPAs), integrates sputum processing, DNA extraction, PCR amplification and Mtb detection into a single self-contained cartridge. After inserting the sample, the assay is completely automated and confined inside the cartridge, which reduces the possibility of errors related to other NAATs (WHO, 2013). The cartridge-

based device benefits from convenience of use and a sealed amplification system that prevents cross-contamination between specimens (Caulfield & Wengenack, 2016:40).

In an attempt to boost the sensitivity of the Xpert MTB/RIF, the WHO (2017b) suggested and employed the use of Xpert MTB/RIF Ultra as an alternative to Xpert MTB/RIF in 2017. The same analyser as in the Xpert MTB/RIF assay is used, but with an upgraded specimen cartridge and operating system. This implies that the Xpert MTB/RIF Ultra test detects Mtb and RIF resistance in the same way as the Xpert MTB/RIF assay. However, it seems to be substantially more sensitive than Xpert MTB/RIF for detecting Mtb in smear-negative, culture-positive, paediatric, extrapulmonary and HIV-infected samples (WHO, 2017b). Unlike LPAs, the Xpert MTB/RIF and Xpert MTB/RIF Ultra cannot detect INH resistance. Hence, RIF resistance coexists with INH resistance in 85–90% of TB patients and the two assays combined may thus be used to predict MDR-TB cases (Liu *et al.*, 2020:6).

2.8. Vaccination

The only WHO-approved TB vaccine is a live-attenuated Bacille Calmett-Guérin vaccine derived from *M. bovis*, which shares > 90% of its genetic makeup with Mtb. Over four billion people worldwide have received the BCG vaccine, making it the most common and oldest vaccine in use (Li *et al.*, 2021:1). The BCG vaccine has a 90-year safety record. Its effectiveness, though, is disputed and only lasts for 10 to 20 years after inoculation (Escobar *et al.*, 2020:7720; Fatima *et al.*, 2020:1-2). The controversial aspect of BCG is how inconsistently well it works to prevent TB. It provides adequate protection for children against meningitis TB and other extrapulmonary TB, such as miliary TB, however, protection against adult pulmonary TB fluctuates between 0% and 80%. Hence, some countries, like the USA, do not routinely administer the BCG vaccine due to the vaccine's questionable effectiveness against pulmonary TB and the need to preserve the TST as a diagnostic tool. Furthermore, the BCG vaccine does not prevent or protect against reactivation of latent TB (Teo & Shingadia, 2006:530; WHO, 2008).

A single dose of BCG is administered to new-borns in TB-prone areas where BCG is included in the national childhood immunisation program, within hours or days of birth. Only children at risk of contracting TB and healthcare workers at risk of exposure to drug-resistant TB (DR-TB) receive BCG in countries with low TB incidence (WHO, 2008). BCG is contraindicated for people with compromised immune systems (such as those who are HIV-positive or have had organ transplantation), pregnant woman, and those who have already had TB (CDC, 2016b). According to the last scenario, the host has already acquired some sort of immunity to TB as a result of prior mycobacterial exposure. The "blocking hypothesis" describes how this immunity causes a response to antigens that are cross-reactive with BCG antigens, preventing the dissemination and replication of BCG within the host, and subsequently depleting its effectiveness. Thus, receiving the vaccine in such case could result in unwanted side effects (Andersen & Doherty, 2005:659).

2.9. Overview of TB Treatment

The standard treatment for drug-susceptible TB (DS-TB) consists of giving four antitubercular drugs over a minimum period of six months (two months for the intensive phase, followed by four or seven months for the continuation phase) (CDC, 2016c). This regimen has an overall success rate of 85%. First-line drugs (FLDs) are a feasible therapeutic option, but they are not always successful in treating TB. One of the reasons is that the vast majority of *Mtb* strains are resistant to two or more of the most potent FLDs which can only be cured by using an intricate cocktail of additional drugs referred to as second-line drugs (SLDs) (CDC, 2017). Increased drug resistance has been brought on by a variety of factors, including inadequate healthcare facilities, the wrong treatment being prescribed (either the incorrect dosage or the incorrect duration), poor quality drugs, drug shortages or *Mtb* re-infection, among others (Allué-Guardia *et al.*, 2021:2).

The primary reasons for TB treatment failure are patient negligence and non-compliance with antitubercular drug regimens, making TB treatment seemingly virtually impossible. Patient

non-compliance compromises treatment outcomes, increases the risk of TB transmission and reactivation, causes the rapid emergence of DR-TB, and elevates TB mortality rates (Fang *et al.*, 2019:1929). One of the main reasons patients do not complete taking their prescribed antitubercular drugs is the prolonged period of treatment that must continue even after clinical improvement (Woimo *et al.*, 2017:2). Patients do not follow suggested treatments for a number of additional reasons, such as apprehension about side effects, stigma, a lack of information, the price of medicines and a lack of awareness on the part of patients and their families about the possible repercussions of TB (AlSahafi *et al.*, 2019:2). As a result, the End TB Strategy's goal of lowering TB infections by 90% by 2035 is under threat due to the rapid rise of DR-TB, especially in places where TB is endemic (WHO, 2015a).

2.10. First-line drugs for the treatment of drug-susceptible TB (DS-TB)

2.10.1. Isoniazid (INH)

INH (**1**), also known as iso-nicotinic hydrazide, is a small, freely soluble molecule used to treat DS-TB since 1952 and continues to serve as the cornerstone of TB treatment together with RIF. INH is effective against extracellular and intracellular metabolically active Mtb bacilli owing to its ability to penetrate macrophages (Deck & Winston, 2012a:840; Palomino & Martin, 2014:318-319). The structure of INH is simply a hydrazine-and-carbonyl (CONHNH₂) group joined to the *para* position of a pyridine ring containing nitrogen (Fernandes *et al.*, 2017:299). The structure-activity relationship (SAR) of INH demonstrates that the pyridine heterocycle is optimum, but substitution with alternative heterocycles results in a significant potency decrease. The CONHNH₂ moiety is, however, required for activity. The activity is furthermore diminished by even seemingly minor alterations, including adding a methyl group to the pyridine ring or isomerising the nitrogen atom to a different position on the pyridine ring (Hegde *et al.*, 2021:2).

INH is a prodrug that enters Mtb by passive diffusion and must first be activated by *KatG*, the catalase-peroxidase produced by mycobacteria, in order to have any effect. Mycolic acid

production depends on the Mtb nicotinamide adenine dinucleotide (NADH)-dependent enoyl-acyl carrier protein (ACP) reductase of fatty acid synthase II (FAS II), which is encoded by *inhA* and targeted by INH (Marrakchi *et al.*, 2014:77). INH inhibits mycolic acid biosynthesis by forming a covalent complex with *AcpM*, an ACP, and *KasA*, a β -keto-ACP synthase, which ends up killing Mtb cells. INH resistance has been linked to mutations that increase the expression of *inhA*, which encodes NADH-dependent enoyl-ACP, *KatG* mutations or deletions that prevent INH prodrug activation, promoter mutations that cause overexpression of *ahpC* (which shields Mtb from oxidative stress), and *KasA* mutations (Deck & Winston, 2012a:840). *KasA* mutations are uncommon but have been noted in isolates that are INH susceptible. Low levels of INH resistance are caused by *inhA* mutations, but high levels of resistance by *KatG* mutations (Jaiswal *et al.*, 2017:144).

INH is readily absorbed from the gastro-intestinal (GI) tract after a single 300 mg oral dose, and it diffuses rapidly throughout body tissues, including the cerebrospinal fluid (CSF) (Deck & Winston, 2012a:840). However, food and antacids impede INH from being absorbed. It is therefore recommended to consume INH on an empty stomach (Rossiter, 2020:331). The peak plasma concentration reaches 3–5 $\mu\text{g/ml}$ in one to two hours after administration of the drug (Deck & Winston, 2012a:840). Metabolism of INH occurs in the liver through acetylators, including *N*-acetylation by *N*-acetyltransferase–2 to form *N*-acetyl-INH and hydrolysis by amidase to produce iso-nicotinic acid and hydrazine. Metabolites are mainly excreted in urine (Wang *et al.*, 2016:385).

INH causes unfavourable side effects. Rashes and fever are two occasional, dose-dependent side effects. INH-induced hepatitis (hepatotoxicity) occurs in 10–20% of individuals receiving INH treatment. Clinical signs of INH-induced hepatotoxicity include lack of appetite, nausea, jaundice, vomiting and right upper quadrant pain (Deck & Winston, 2012a:841; Rossiter, 2020:332). INH-induced neurotoxicity is dose-dependent and most typically presents as seizures in pyridoxine (Vitamin B6) deficient people due to first-pass metabolism (Badrinath &

John, 2018). Less common CNS complications include seizures, memory loss and psychosis. Other adverse effects include haematological abnormalities, anaemia (from pyridoxine deficiency), hearing impairment and GI irritation. Drug-induced systemic lupus erythematosus has been reported, but it is rare (Deck & Winston, 2012a:841).

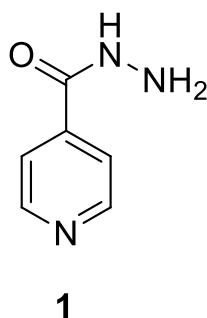


Figure 2.4 Isoniazid (1)

2.10.2. Rifamycins

Rifamycins are macrocyclic antibiotics that belong to the ansamycin family. They are made up of a naphthoquinone core with two ends connected by a poly-hydroxylated ansa-chain (long-chain) (Aristoff *et al.*, 2010:96). Rifamycins were discovered as natural products from the soil actinomycete *Amycolatopsis mediterranei*, with the first compound of rifamycin B being found to have relatively weak antimicrobial activity (Qi *et al.*, 2016:3803). However, researchers have improved their activities and developed new effective commercial rifamycins through hemi-synthesis (Dey & Chatterji, 2012:88).

The most well-known member of the rifamycin family, RIF (**2**), is a semi-synthetic derivative of rifamycin that was first made available in 1968 (Qi *et al.*, 2016:3803). It is quite effective against both replicating and non-replicating Mtb bacilli. Its activity against the latter is believed to be responsible for shortening the length of TB treatment regimens from 12 or 18 months to 9 months when RIF is included. One of RIF's most salient characteristics is that it is the most effective "sterilising" antitubercular drug. This means that the bacillary population can be

adequately reduced to avoid infection relapse (Peloquin & Davies, 2021:1459). Additional rifamycin derivatives have been developed over time, such as rifapentine (**3**), which has a longer half-life ($T_{1/2}$) and greater activity than RIF but is inactive against RIF-resistant Mtb strains (Zhang, 2005:537). Rifabutin (**4**) is used for the treatment of *Mycobacterium avium* complex in HIV patients and rifaximin (**5**), a non-oral rifamycin, is used for the treatment of enteropathogenic *E. coli*, which causes traveller's diarrhoea (Aristoff *et al.*, 2010:94).

RIF inhibits the Mtb RNA transcription process by restricting elongation of the RNA chain by binding to the DNA-dependent RNA polymerase of Mtb in its β -subunit (encoded by *rpoB*) (Khawbung *et al.*, 2021:2). When RIF is bound, it prevents the synthesis of RNAs larger than dinucleotides, sterically blocking the route of nascent RNA at the beginning of the transcription process (Dey & Chatterji, 2012:88). When the RNA reaches a length of 3–4 nucleotides, the RNA and RIF collide, releasing the RNA from the promoter complex as an interrupted transcript and eventually causing Mtb cell death (Mosaei *et al.*, 2018:263). Resistance to RIF may develop as a consequence of any *rpoB* gene mutation. Over 95% of Mtb clinical isolates seem to have a mutation in its RIF resistance-determining region, an 81-base pair hotspot region of the *rpoB* gene (Rando-Segura *et al.*, 2021:2; Xu *et al.*, 2018:2).

Following oral administration, RIF is well absorbed and widely disseminated throughout body fluids and tissues (Deck & Winston, 2012a:841). However, RIF is highly protein bound (80–90%) making CSF penetration (10–20%) limited (Cresswell *et al.*, 2018:3; Rossiter, 2020:323). RIF is eliminated *via* the liver into the biliary system. It then undergoes enterohepatic recirculation followed by deacetylation by Cytochrome P450 (CYP450) iso-enzymes to generate the metabolites 25-O-desacetyl-RIF and 3-formyl-RIF SV. Deacetylated metabolites are mostly excreted in the faeces and a fraction is also excreted in the urine (Deck & Winston, 2012a:841; Pacifici, 2019:1).

RIF turns tears, urine and body fluids orange to reddish brown. Patients on RIF should know that it may permanently stain contact lenses. GI problems include nausea, vomiting, diarrhoea and mild abdominal pain, which may be reduced by taking RIF with meals. However, an empty stomach is best for optimum absorption (Rossiter, 2020:333). Hypersensitivity symptoms include fever, chills, myalgias, anaemia and thrombocytopenia. Hepatotoxicity is uncommon, yet fatal. The risk of hepatotoxicity is increased when RIF is co-administrated with INH, PZA or other drugs metabolised in the same manner, such as contraceptives, protease inhibitors, anticoagulants, methadone, cyclosporine, anticonvulsants and other non-nucleoside reverse transcriptase inhibitors. This is because RIF induces most CYP450 iso-enzymes, which cause overexpression of multiple drug metabolising enzymes and transporters, accelerating the elimination of these drugs. This ultimately results in decreased serum concentrations, which necessitates larger drug dosages and in effect promote hepatotoxicity (Deck & Winston, 2012a:842; Rossiter, 2020:333).

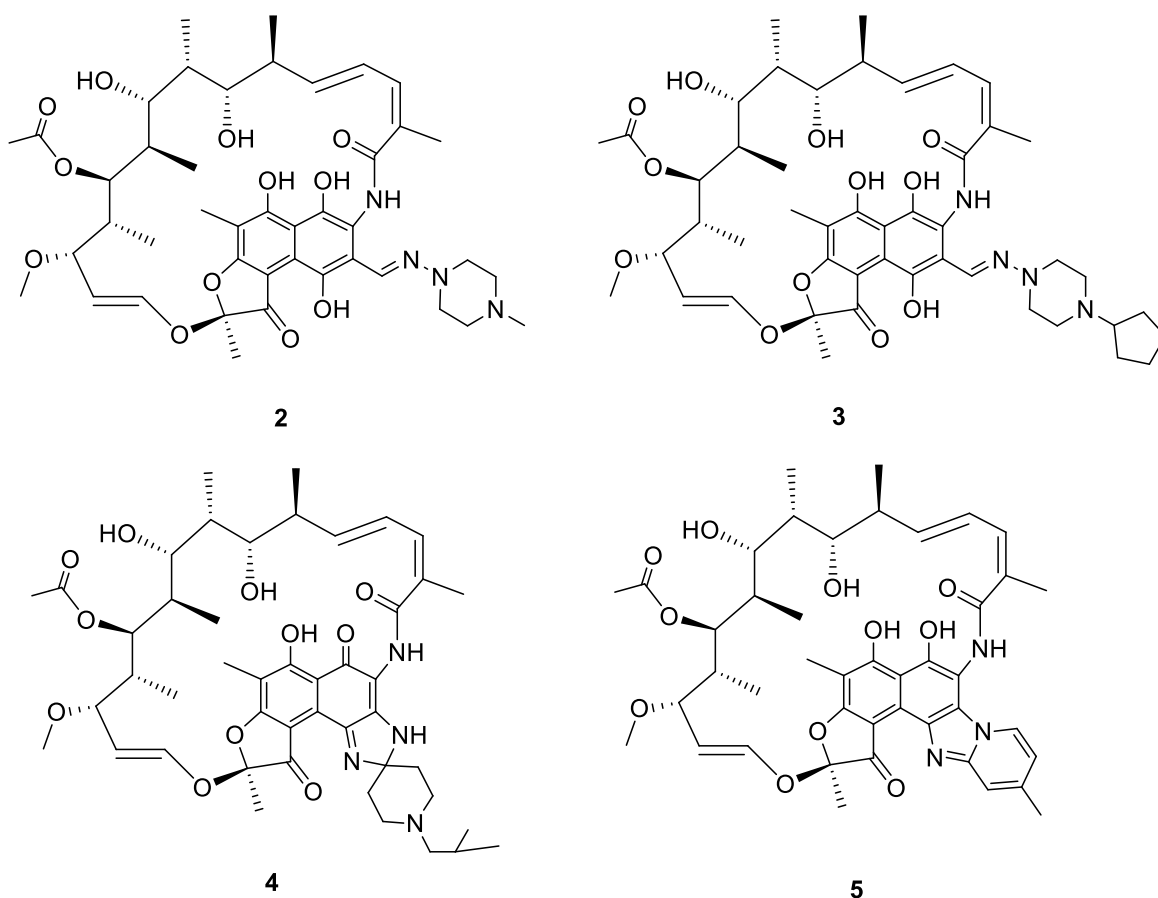


Figure 2.5 Rifampicin (2), rifapentine (3), rifabutin (4), and rifaximin (5)

2.10.3. Ethambutol (ETH)

ETH (6) is a synthetic, heat-stable, water-soluble molecule that is administered as a dihydrochloric salt. It is bacteriostatic, although higher dosages of ETH are bactericidal (Deck & Winston, 2012a:842; Rossiter, 2020:331). ETH acts on rapidly replicating Mtb bacilli that are both intracellular and extracellular in nature (Arbex *et al.*, 2010:635). It was recently discovered that *EtbR*, a *TetR* transcriptional regulator in Mtb, is a novel ETH-binding protein involved in a synergistic effect between INH and ETH. As a repressor, *EtbR* inhibits the expression of *inhA*, the target gene of INH. Thus, when both drugs are taken at the same time, a non-lethal dose of ETH may increase Mtb's susceptibility to INH, which in turn promotes INH's activity (Lee & Nguyen, 2021; Zhu *et al.*, 2018:16741).

As its primary MOA, ETH disrupts the synthesis and integrity of Mtb's cell wall. It is believed that it does this by inhibiting the mycobacterial arabinosyl transferases, which are encoded by Mtb's *embCAB* operon. Thus, it inhibits the polymerisation phase of arabinogalactan (encoded by the *embB* gene) and the formation of LAM, which are required for the integrity of the Mtb cell wall (Deck & Winston, 2012a:842). Three genes with a 65% similarity make up the *emb* operon: *embA*, *embB*, and *embC*. Mutations in the *embA* and *embC* genes are rarely observed and may be a factor in ETH resistance. However, the majority of the time, mutations in the *embB* gene, particularly at codon 306, are associated with ETH resistance. Mutations in *embB306* are present in between 50–70% of Mtb strains that are resistant to ETH (Mohammadi *et al.*, 2020:1-2). It is interesting to note that *embB306* mutations were only found in ETH-resistant strains by Plinke *et al.* (2006:1900). However, Hazbón *et al.* (2005:3796-3798) studied 1,020 clinical isolates of Mtb from over the globe and found that *embB306* mutations also confer resistance to other drugs, not only ETH.

Similar to RIF, ETH is rapidly absorbed via the GI tract after oral administration (plasma concentration of 2–5 µg/ml after 2–4 hours), diffuses widely across body fluids and tissues (Deck & Winston, 2012a:842), and has little CSF penetration (10–50% penetrates only

inflamed meninges) (Rossiter, 2020:331). Alcohol dehydrogenase initially oxidises ETH to an aldehyde in the liver before aldehyde dehydrogenase converts it into a dicarboxylic acid (Arbex *et al.*, 2010:635-636). About 20% of unaltered ETH is eliminated in faeces and 50% is excreted in urine (Deck & Winston, 2012a:842).

Chronic ETH usage often causes severe toxicity to appear at doses of 25 mg/kg/day. Dose-dependent retrobulbar optic neuritis (Deck & Winston 2012a:842), which may result in red-green colour blindness and varying degrees of vision impairment, is the most serious side effect of ETH. Blue-yellow visual abnormalities can also exist. Additionally, it has been noted that contrast sensitivity can be reduced (Saxena *et al.*, 2021). Due to this adverse effect on the eyes, ETH should not be used in children who cannot yet complete visual acuity and red-green colour discrimination tests (WHO, 2006). ETH ocular toxicity may typically be reversed if identified and managed early (Saxena *et al.*, 2021:3734). However, nerve damage to the eye is irreversible (Rossiter, 2020:331).

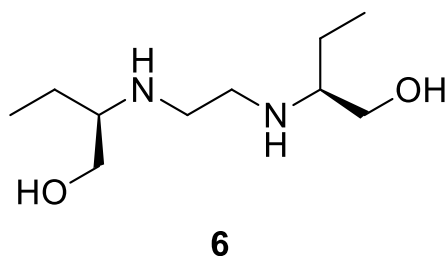


Figure 2.6 Ethambutol (6)

2.10.4. Pyrazinamide (PZA)

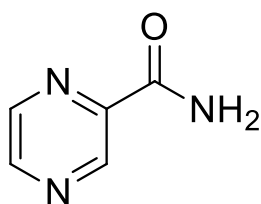
PZA (7) is a nicotinamide relative that is stable but only moderately water soluble, having a chemical structure similar to INH (Deck & Winston, 2012a:842). Under typical *in vitro* conditions at neutral pH, PZA is not active against Mtb. However, it was discovered that it is only active at an acidic pH of 5.5. It has an exceptional *in vivo* sterilising effect, and when included in regimens containing RIF, it is mostly responsible for the eradication of persistent

Mtb bacilli during the intensive phase of treatment, enabling the duration of treatment to be shortened from 12 months to 6 months (Zhang & Mitchison, 2003:6).

The MOA of PZA is not widely understood and the precise pharmacological target is unclear (Deck & Winston, 2012a:843). However, a pH-dependent model is still regarded as an accepted mechanism. PZA is a prodrug like INH, and for it to have an effect, it needs to be in its active form. The *pncA* gene, which encodes mycobacterial pyrazinamidase, mediates PZA activation. Mycobacterial pyrazinamidase converts PZA into pyrazinoic acid (PA), which is released extracellularly after administration of the drug. PA becomes protonated in an acidic environment and permeates Mtb where it accumulates. Following that, the protonated PA reduces inter-mycobacterial pH and subsequently de-energises the membrane potential by compressing the proton gradient and interfering with membrane transport, which eventually results in Mtb cell death. However, the activity of PZA has also been shown to be pH-independent, and additional MOAs have been proposed. For instance, PZA inhibits the aspartate decarboxylase *PanD* from functioning and promotes its degradation via the *Clp* protease system, thus preventing the synthesis of coenzyme-A (Santucci *et al.*, 2021:2; Zhang & Mitchison, 2003:10). Resistance to PZA has been documented and is attributed to mutations in the *pncA* gene, which prevents PZA from being converted to its active form. Additional resistance mechanisms are known but have not been adequately investigated. Among these is the lack of absorption of PZA and mutations in *PanD*, preventing coenzyme-A depletion (Gopal *et al.*, 2016:623; Raynaud *et al.*, 1999:1359). Mtb develops resistance to PZA rapidly but does not demonstrate cross-resistance to INH or other antitubercular drugs (Deck & Winston, 2012a:843).

PZA is well absorbed and widely distributed throughout body tissues, with a maximum plasma concentration of 30–50 µg/ml achieved after 2 hours of administration (Arbex *et al.*, 2010:633). It is extensively metabolised in the liver by CYP2E1 and CYP3A4 to PA and 5-hydroxy-PA, which may cause hepatotoxicity – the most significant adverse effect of PZA. The mechanism

of PZA hepatotoxicity is unknown. However, it might be caused by either PA (the drug itself) or its metabolites (Rawat *et al.*, 2018:374). Hepatotoxicity may range from a reversible increase in blood transaminases to an overt toxic hepatitis (Rossiter, 2020:332). Hyperuricemia with non-gouty joint pain is a common side effect of PZA owing to decreased uric acid clearance. However, it is often self-limiting and may only rarely necessitate the discontinuation of PZA (Deck & Winston, 2012a:843; Rossiter, 2020:332).



7

Figure 2.7 Pyrazinamide (7)

2.11. Drug-resistant tuberculosis

Drug-resistant Mtb isolates are emerging despite the effectiveness of antitubercular drugs. It further complicates TB treatment and threatens global public health. Several mechanisms, including compensated evolution, epistasis, clonal interference, cellular membrane permeability, efflux pumps, drug modification and degradation, drug target site mimicking, and phenotypic drug tolerance, among others, facilitate antitubercular drug resistance in Mtb isolates. The main culprit, however, is that prolonged TB treatment regimens often result in patient non-compliance, resulting in the rapid evolution of Mtb from mono-to-multi-to extensively drug-resistant (Singh *et al.*, 2019:1554).

Charles Darwin's theory of evolution (survival of the fittest) and the emergence of drug-resistant Mtb isolates are closely related because, like any unique characteristic that arises during the process of selective evolution, Mtb-resistant strains can only propagate among Mtb populations if their resistance phenotypes (like virulence factors) offer the mutants a greater

chance of survival than their susceptible counterparts. As a result of ongoing drug use in response to an increase in DR-TB cases, Mtb strains that are more resistant to available antitubercular drugs are constantly evolving (Khawbung *et al.*, 2021:1; Smith *et al.*, 2013:54).

Multi-drug resistant TB (MDR-TB) and extensively drug-resistant TB (XDR-TB) are the two main subtypes of DR-TB. MDR-TB occurs when Mtb strains are resistant to the FLDs INH and RIF, two of the most potent antitubercular drugs. MDR-TB progresses to XDR-TB as Mtb strains become resistant to additional SLDs (WHO, 2020). The WHO recently amended the definition of XDR-TB, which should have gone into effect globally in January 2021: "XDR-TB is a kind of DR-TB in which Mtb strains are resistant to RIF, INH, at least one FQN, and either bedaquiline (BDQ) or linezolid (LZD) (or both)" (WHO, 2019b). Furthermore, some studies have identified Mtb strains that are completely resistant to all currently available antitubercular drugs, resulting in a TB condition known as total drug-resistant TB (TDR-TB) (Migliori *et al.*, 2013:169-179; Velayati *et al.*, 2009:420-425). However, due to a scarcity of drug susceptibility testing and the difficulties in defining such a highly resistant pathogen, the WHO has yet to recognise TDR-TB and continues to refer to it as XDR-TB (Cegielski *et al.*, 2012; WHO, 2015b; WHO, 2021a).

2.12. Second-line drugs for the treatment of drug-resistant TB (DR-TB)

The WHO published consolidated guidelines in 2019 on SLDs to be used in the treatment of DR-TB, and the MDR-/XDR-TB treatment paradigm has significantly changed since then. The recommendations include both longer and shorter treatment regimens and divide the drugs used in the longer regimens into three categories – groups A, B and C (**Table 2.1**). Additionally, it emphasises that for the great majority of DR-TB patients, oral treatment should be their first option (WHO, 2019b). This is a significant improvement since it minimises the need for injectable drugs (group C aminoglycosides) when developing a longer regimen for treating DR-TB patients (Mase & Chorba, 2019:776). However, a personalised "rescue regimen" including injectable drugs is still advised for treating TB cases resistant to RIF who are

suspected or confirmed to be resistant to BDQ or LZD from group A, and/or clofazimine (CFZ) from group B, in TB-endemic areas like South Africa (DOH, 2019).

SLDs are less effective than FLDs, more costly, and have a greater toxicity profile, making tolerance and treatment adherence a problem. Furthermore, since SLDs have limited sterilising activity, DR-TB treatment often takes 18–24 months (Seung *et al.*, 2015:5). The cost of treatment with SLDs alone is anticipated to be 50–200 times higher for DR-TB patients when compared to treating individuals with DS-TB (Pinto & Menzies, 2011:130).

Table 2.1 Second-line drugs for the treatment of drug-resistant tuberculosis

GROUP A	GROUP B	GROUP C
Levofloxacin (LFX) OR Moxifloxacin (MFX)	Clofazime (CFZ)	Ethambutol (ETH)
Bedaquiline (BDQ)	Cycloserine (CS) OR Terizidone (TRD)	Delamanid (DLM)
Linezolid (LZD)		Pyrazinamide (PZA)
		Imipenem-cilastatin (IPM-CLN) OR Meropenem (MPM)
		Amikacin (AM) OR Streptomycin (SM)
		Ethionamide (ETO) OR Prothionamide (PTO)
		<i>para</i> -Aminosalicylic acid (PAS)

2.12.1. Quinolones

2.12.1.1. Discovery of fluoroquinolones (FQNs)

Nalidixic acid (NA) (**8**) was discovered in the 1960s during the analogue synthesis of a lead structure, which was found as an impurity in the synthesis of the antimalarial drug chloroquine. NA stood out for its moderate antimicrobial activity against Gram-negative pathogens, including *E. coli*, with the exception of *Pseudomonas aeruginosa* (Bush *et al.*, 2020:2). NA has a rapid renal elimination rate and a significant risk of neurological, dermatological and GI

adverse effects. As a result, one may conclude that NA was never an appropriate drug for treating systemic infections. However, because of its urinary antiseptic properties, NA was eventually approved for the treatment of uncomplicated urinary tract infections (UTIs). Notwithstanding, NA provided the chemical groundwork for the synthesis of NA analogues with the aim of maximising its activity (Sharma *et al.*, 2017:2). However, in terms of activity and plasma concentration levels, these analogues demonstrated minimal improvement over NA. The NA analogues, together with NA (which, according to its structure, is a 1,8-naphthyridone and not a genuine quinolone) were dubbed first-generation quinolones (Bush *et al.*, 2020:2).

It was not until the 1980s that the structure of NA was modified to increase absorption and bioavailability and hence broaden its activity against Gram-positive pathogens. Fluorination of the quinolone scaffold at position C6 was one of these modifications, which resulted in the discovery of FQNs (9) (Pallo-Zimmerman *et al.*, 2010:E1). Norfloxacin, the first novel clinically accessible second-generation quinolone with broad antimicrobial activity, was far more used than NA. Following the success of this drug, numerous other FQNs were synthesised over the following three years, several of which are still routinely used to treat infections (Telfer, 2011:14).

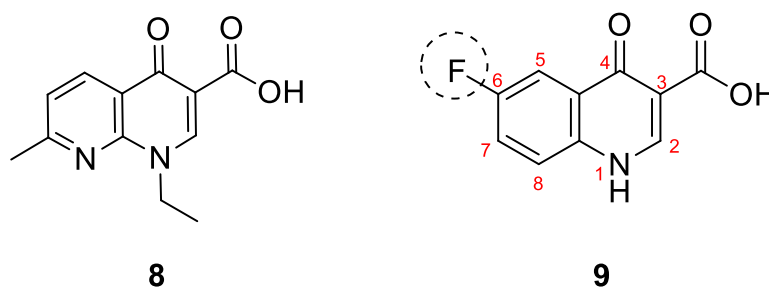


Figure 2.8 Nalidixic acid (8) and the fluoroquinolone scaffold (9)

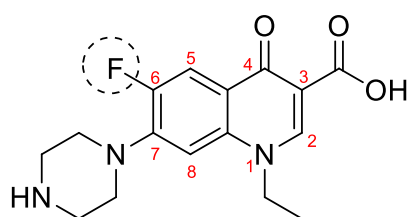
2.12.1.2. Classification and structural modifications of fluoroquinolones

The different generations of FQNs have been classified based on their increasing antimicrobial activity against Gram-negative and Gram-positive strains of bacteria, with the first-generation (NA and its analogues) having the narrowest pharmacological spectrum and the later generations having greater structural complexity and increased antimicrobial activity. The addition of carefully chosen substituents to critical sites of the quinolone nucleus (N1, C6, C7, and C8) (see **Fig. 2.8**) enables the quinolone to target certain groups of pathogens. **Table 2.2** summarizes the classification and structural modifications associated with the common antimicrobial activities of major FLQs (information adapted and tabulated from Ball, 2000; Mohammed *et al.*, 2019; Pham *et al.*, 2019; Rusu *et al.*, 2021).

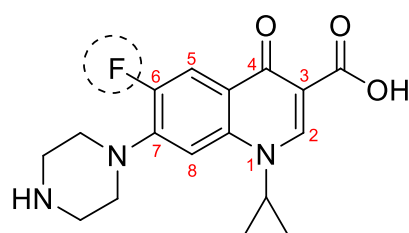
Table 2.2 Classification and structural modification-associated activities of FQNs.

Classification of quinolones	Drug	Structural modifications	Activity
1st generation	Nalidixic acid	<ul style="list-style-type: none"> - Nitrogen atom (C8) - Methyl group (C7) - Ethyl group (N1) 	<p>Limited to Gram-negative <i>Enterobacteriaceae</i>.</p> <p>No activity for Gram-negative <i>pseudomonas spp.</i></p> <p>No Gram-positive pathogen activity.</p>
2nd generation (See Fig. 2.9)	Norfloxacin (10) Ciprofloxacin (11) Ofloxacin	<ul style="list-style-type: none"> - Fluorine atom (C6) - Piperazine ring (C7) - Cyclopropyl (11) and ethyl groups (10) (N1) 	<p>Predominant Gram-negative activity (including <i>pseudomonas spp.</i>)</p> <p>Improved Gram-positive activity to <i>S. aureus</i>.</p> <p>Atypical pathogens (<i>Mycoplasma pneumoniae</i> and <i>Chlamydia pneumoniae</i>).</p>
3rd generation (See Fig. 2.9)	Levofloxacin (12) (L-isomer of ofloxacin)	<ul style="list-style-type: none"> - Fluorine atom (C6) - Alkylated piperazine ring (C7) 	<p>Increased predominant Gram-negative activity.</p> <p>4-fold increased Gram-positive activity.</p>

Classification of quinolones	Drug	Structural modifications	Activity
		- Cyclic -OCH ₂ substituent (C8)	Increased atypical pathogen activity. Mycobacterial activity (Mtb).
4th generation (See Fig. 2.9)	Moxifloxacin (13)	- Fluorine atom (C6) - Azabicyclonyl side chain on pyrrolidine (C7) - Cyclopropyl group (N1) - -OCH ₃ (MeO) substituent (C8)	Superior potency against Gram-positive pathogens. Atypical pathogens. Anaerobic activity (nitrogen atom). Mycobacterial activity (Mtb).

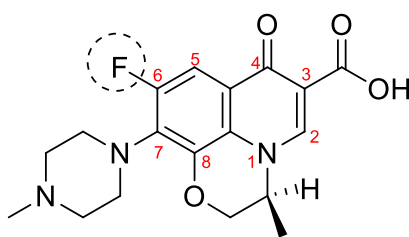


10



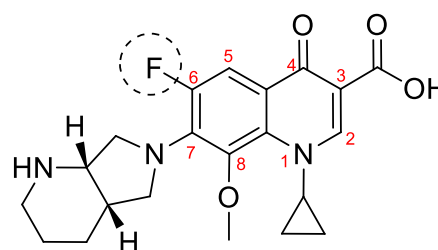
11

2nd generation



12

3rd generation



13

4th generation

Figure 2.9 Norfloxacin (**10**), ciprofloxacin (**11**), levofloxacin (**12**), and moxifloxacin (**13**)

2.12.1.3. Mechanism of action of fluoroquinolones

FQNs target DNA topoisomerase IV and DNA gyrase, two vital type II bacterial topoisomerase enzymes involved in DNA synthesis during bacterial replication and transcription (Hooper & Jacoby, 2016:2). Helicase enzymes uncoil the DNA double helix to initiate DNA replication, which results in excessive supercoiling of the remaining DNA double helix. In order for the process to continue, the tension building up in this remaining DNA double helix must be released (Ezalarab *et al.*, 2018:15). The only enzyme capable of inducing negative supercoiling at the remaining supercoiled DNA double helix is DNA gyrase. DNA gyrase is made up of two A subunits and two B subunits, which are encoded by the genes *gyrA* and *gyrB*, respectively. The FQNs bind to the DNA gyrase subunits and inhibit negative supercoiling, preventing the supercoiled DNA double helix from relaxing and ultimately resulting in cell death. On the other hand, DNA topoisomerase IV acts to separate the daughter chromosomes following bacterial DNA replication, enabling segregation into daughter cells. FQNs inhibit DNA topoisomerase IV, which prevents Mtb cells from dividing and ultimately results in cell death (Hooper, 2000:S24).

DNA gyrase is situated ahead of the DNA replication complex of enzyme-binding sites on chromosomal DNA, while topoisomerase IV is positioned behind it. As a result, FQN interactions with DNA gyrase appear to lead to a more rapid inhibition of DNA replication than FQN interactions with topoisomerase IV (Hooper & Jacoby, 2016:2). In Gram-negative pathogens such as *E. coli*, FQNs interact with DNA gyrase as their main target and topoisomerase IV as their secondary target. The opposite is true for Gram-positive pathogens such as *S. aureus*. However, exceptions to this rule do occur. For example, it was revealed that DNA gyrase in *Streptococcus pneumoniae* (a Gram-positive bacterium) is more susceptible to FQNs than topoisomerase IV. In addition, Mtb lacks the topoisomerase IV enzyme. Thus, it was revealed that DNA gyrase is FQN's only target in its antitubercular activity against Mtb (Somasundaram & Manivannan, 2013:300).

2.12.1.4. Fluoroquinolones for the treatment of drug-resistant TB

According to current MDR-TB treatment guidelines, all patients should be treated with later-generation FQNs. The two most commonly prescribed second-line FQNs for the treatment of MDR-TB are Levofloxacin (LFX (**12**)) and Moxifloxacin (MFX (**13**)) (Kang *et al.*, 2016:364; WHO, 2019b). FQN resistance in Mtb emerges rapidly when an FQN is added to other SLDs or added alone to a failed regimen and basically serves as the only agent in a multidrug regimen. Since Mtb lacks topoisomerase IV, mutations in the quinolone resistance-determining region of *gyrA* (the target of FQNs in Mtb) are the most common source of FQN resistance. The most prevalent mutation in FQN-resistant Mtb isolates is a codon 94 substitution in the *gyrA* gene, which reduces the drug's affinity to the gyrase DNA complex (Ginsburg *et al.*, 2003). The widespread use of FQNs (for example, for lower respiratory tract infections) further complicates Mtb FQN resistance and may result in resistance in undetected TB patients. In light of this, especially in areas with a high incidence of TB, such as South Africa, newer FQNs (e.g., LFX and MFX) should not be used for respiratory tract infections unless the patient has an allergy to β -lactam antimicrobial drugs (Rossiter, 2020:309; Ziganshina *et al.*, 2005:4).

After oral treatment, FQNs are well absorbed, with peak plasma concentrations reached 1–3 hours later. FQN concentrations surpass blood levels in urine, kidney, lung and prostate tissue, as well as in faeces, bile, macrophages and neutrophils (MacDougall, 2017a:1016). However, the presence of multivalent cations in milk and antacids containing aluminium and magnesium reduces oral bioavailability. This reaction is the consequence of chelation between the metallic cations and the 4-oxo and adjacent carboxyl groups present on all FQNs, which leads to the formation of insoluble, non-absorbable complexes in the GI tract (Pitman *et al.*, 2019:2). Hence, it is advised to take FQNs two hours before and at least four hours after consuming products containing these cations. The majority of FQNs are eliminated via renal routes by tubular secretion or glomerular filtration. MFX is, however, eliminated via nonrenal

routes, negating the need for dosage adjustments in patients with renal impairment (Deck & Winston, 2012b:836).

In general, FQNs are well tolerated. However, GI problems are the side effects of newer generation FQNs like LFX and MFX that are often reported. Four to six percent of participants in preregistration clinical trials reported experiencing diarrhoea, while eight percent reported nausea as the most frequent side effect. Milder neurotoxic side effects, including fatigue, headaches and insomnia, are followed by more severe forms like psychosis, depression and hallucination (Stahlmann, 2002:271-272). The FQNs' ability to reduce the seizure threshold and increase the risk of an epileptic episode in individuals using non-steroidal anti-inflammatory drugs or those with a history of epilepsy, is a serious neurological symptom. There is debate regarding the precise mechanism through which FQNs cause seizures. However, a substantial correlation between the chemical structures of several substituents at position C7 of the quinolone nucleus and gamma-aminobutyric acid (the principal inhibitory neurotransmitter in the cerebral cortex) seems to exist (Owens & Ambrose, 2005:S146-S147).

Because MFX inhibits the human cardiac K⁺ channel hERG, it has been widely associated with electrocardiographic QT prolongation, and the risk rises significantly when used in conjunction with other SLDs like BDQ and DLM (Alexandrou *et al.*, 2006:904; Angula *et al.*, 2021:4). FQNs have also been associated with arthropathy (joint disease) and cartilage degeneration (tendonitis). As a result, these drugs are typically not advised for individuals under the age of 18. Contrarily, tendonitis is a very uncommon adult complication despite risk factors such as advanced age and concomitant steroid usage (Deck & Winston, 2012b:836).

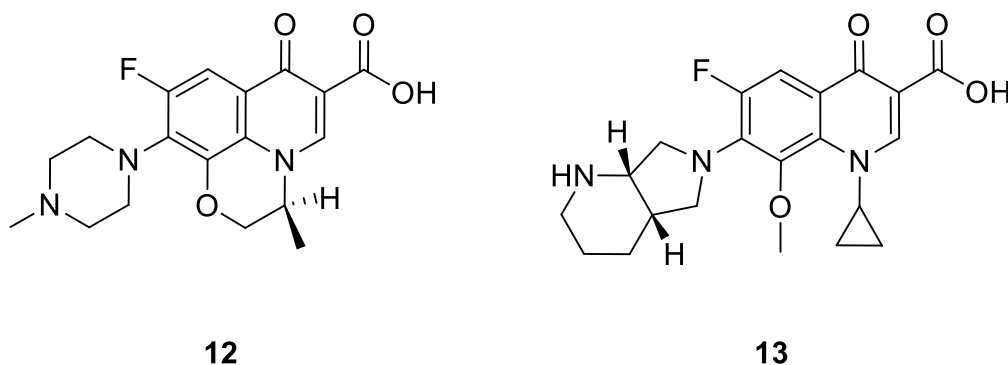


Figure 2.10 Levofloxacin (**12**) and moxifloxacin (**13**)

2.12.2. Aminoglycosides: streptomycin (SM) and amikacin (AM)

The structure of aminoglycosides consists of a hexose ring to which different amino sugars are joined through glycosidic bonds. Based on the aminocyclitol nucleus, aminoglycosides are divided into two major structural classes: streptidine (for SM) and deoxystrepatamine (for AM and others) (Childs-Kean *et al.*, 2019:2). The first antimicrobial drug with demonstrated activity against Mtb was SM (**14**). Its current therapeutic value is limited due to the early onset of SM resistance brought on by its initial widespread usage in the treatment of numerous diseases (Cohen *et al.*, 2020:1-2). Therefore, SM is often exclusively used to treat endocarditis when combined with a β -lactam as well as DR-TB. SM is also active against other nontuberculous diseases such as brucellosis, tularaemia and plague (*Y. pestis*) (Deck & Winston, 2012c:824). In contrast to SM, AM (**15**) exhibits activity against highly resistant Gram-negative pathogens such as *A. baumannii* and *P. aeruginosa*. It is also highly effective against the majority of aerobic Gram-negative pathogens belonging to the *Enterobacteriaceae* family, as well as *Nocardia* spp. and other mycobacteria (Sizar *et al.*, 2021).

All aminoglycosides exhibit concentration-dependent bactericidal activity via protein synthesis inhibition regardless of structural differences (Childs-Kean *et al.*, 2019:2). The 30S ribosomal subunit of mycobacterial pathogens is the major intracellular site of action of aminoglycosides. Aminoglycosides disrupt the protein synthesis initiation complex by binding to polysomes in

the 30S ribosomal subunit and causing mRNA (messenger ribonucleic acid) misinterpretation and premature termination. As a result, incorrect amino acids are added to growing polypeptide chains, creating a protein that is not functional. The resultant aberrant proteins may be introduced into the cell membrane of Mtb, altering its permeability and enhancing the transport of aminoglycosides into the pathogenic cell. The interference with the protein synthesis of Mtb caused by these events eventually results in cell death (MacDougall, 2017b:1039-1040). The 16S mRNA, which is encoded by the *rpsL* gene, makes up the 30S ribosomal subunit. To optimise the effectiveness of tRNA (transfer ribonucleic acid) binding and mRNA interpretation, the 16S mRNA binds to the ribosomal protein S12, which is encoded by the *rrs* gene. Mutations in the *rpsL* and *rrs* genes are often seen in mycobacteria that have developed high levels of aminoglycoside resistance. Additionally, low-level SM resistance is linked to *gidB* gene mutations. *GidB* functions as an rRNA (ribosomal ribonucleic acid) methyltransferase for 16S rRNA. In addition, clinical isolates of Mtb with low levels of SM resistance were shown to have efflux pump-mediated resistance (Gumbo, 2017:1075).

The oral pharmacokinetic properties of aminoglycosides are unsatisfactory because of their polarity. For example, none of them are absorbed well enough after oral administration, their concentrations in the CSF are low, and almost the entire oral dosage is eliminated in the faeces (MacDougall, 2017b:1039). Aminoglycoside has some potentially dangerous side effects, the severity of which is dose- and drug-dependent. Ototoxicity and nephrotoxicity are the characteristic features of aminoglycoside toxicity. These side effects typically manifest themselves within five days of treatment initiation, at high dosages, in patients who have renal insufficiency and in elderly patients (Deck & Winston, 2012c:824). In the most severe cases, ototoxicity can cause irreversible vestibular impairment in addition to deafness. Aminoglycosides can cause nephrotoxicity due to proximal tubule necrosis, which can range from small to large lesions. Manifestations of nephrotoxicity include mild proteinuria, an increase in cellular excretion and elevations in blood urea (Waters & Tadi, 2022).

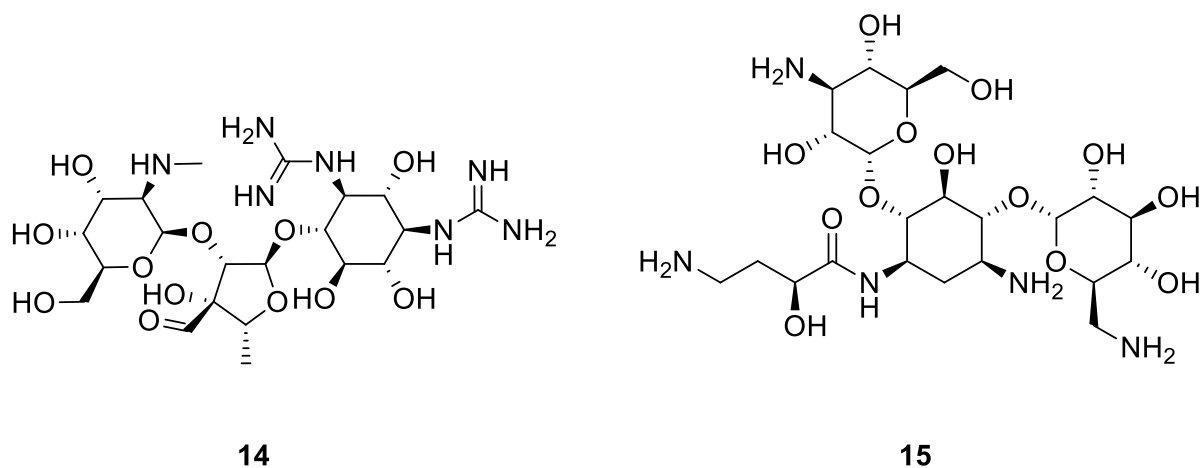


Figure 2.11 Streptomycin (**14**) and amikacin (**15**)

2.12.3. Thioamides: ethionamide (ETO) and prothionamide (PTO)

The nicotinamide derivatives ETO (**16**) and PTO (**17**), which is its propyl analogue, are structurally related to INH. The antitubercular activity of these drugs, like that of INH, requires enzyme activation, but thioamides are activated in a different manner by flavin-containing monooxygenase enzymes (encoded by *EthA*), leading to the oxygenation of thioamides to the corresponding sulfenic acid, sulfoxide metabolite (*S*-oxide) (**18**), and then to a highly reactive sulfonic acid that subsequently spontaneously decomposes to 2-ethyl-4-amidopyridine (Palmer *et al.*, 2012:1148).

The NADH-dependent-enoyl-ACP reductase of FAS II, which is the same target enzyme for INH, is inhibited by the *S*-oxide metabolite (active drug of thioamides). This inhibits the production of mycolic acid, which affects mycobacterial cell wall synthesis (Gumbo, 2017:1077; Nishida & Ortiz de Montellano, 2011:2). Thioamide resistance is brought on by mutations in the *inhA* gene (its target site), which is linked to INH resistance. Mutations in the genes encoding its activation (*ethA*) or the *ethA* regulator, *ethR*, may also contribute to Mtb resistance to ETO. Compared to *katG* mutants, which may be found in up to 94% of Mtb clinical isolates that are INH-resistant, no dominant *ethA* mutation is found in clinical isolates that are ETO-resistant (Vilchèze & Jacobs, 2014:13). Surprisingly, the absence of cross-

resistance is the main distinction between ETO and INH. INH is effective against the majority of ETO-resistant pathogens. Some INH-resistant pathogens do, however, only show slight susceptibility to ETO (Baulard *et al.*, 2000:28326-28327).

Food has no effect on the absorption of ETO from the GI tract, and the drug is freely distributed throughout the body, reaching the same concentration in both the plasma and the CSF. ETO can only be consumed orally. However, it is poorly tolerated due to severe neurologic side effects (e.g., seizures, anxiety, acute psychosis, depression and optic neuritis) and GI irritation (such as nausea, vomiting, metallic taste, abdominal pain, diarrhoea and weight loss). Thioamides should not be used in combination with other antitubercular drugs like INH because they may cause additive neurological adverse effects, or with cycloserine or terizidone because they raise the probability of neurological side effects. Pyridoxine may be used to treat ETO-related neurological symptoms (Deck & Winston, 2012a:843; Rossiter, 2020:337).

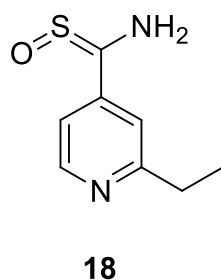
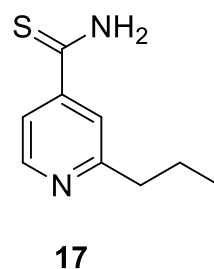
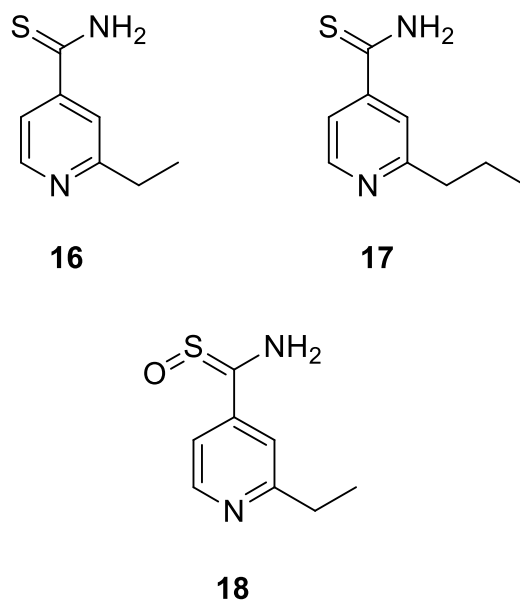


Figure 2.12 Ethionamide (**16**), prothionamide (**17**), and ethionamide *S*-oxide (**18**)

2.12.4. Cycloserine (CS) or terizidone (TRD)

Both CS (D-4-amino-3-isoxazolidone) (**19**) and TRD (**20**) are D-alanine analogues (**21**). It was found that *Streptococcus orchidaceus* produced the antimicrobial drug CS. TRD, a dimer of CS, is often more tolerated than CS, although its effectiveness is debatable. While these D-alanine analogues are almost exclusively used to treat DR-TB, they are also effective against a wide variety of Gram-positive and Gram-negative pathogens, including *Enterococci*, *E. coli*, *S. aureus*, *Nocardia spp.* and *chlamydia* (Deck & Winston, 2012d:805; Gumbo, 2017:1078; Hwang *et al.*, 2013:1257).

CS and TRD both inhibit alanine racemase, an enzyme that converts L-alanine to D-alanine used for the synthesis of the cell wall of Mtb, as well as D-alanine-D-alanine ligase, which is necessary for the adenosine 5'-triphosphate (ATP)-dependent synthesis of the D-alanine-D-alanine dipeptide bond. These two vital enzymes are also necessary for the synthesis of the cell wall of Mtb (Prosser & De Carvalho, 2013:7145). CS resistance has been seen in 10–80% of clinical isolates of Mtb and has been associated with mutations in alanine racemase and D-alanine-D-alanine ligase, despite the fact that the molecular basis of CS resistance among clinical isolates of Mtb is poorly known (Desjardins *et al.*, 2016:2-3; Gumbo, 2017:1078).

Compared to other SLDs, CS is very toxic and has a significant risk of neuropsychiatric disorders, hence the moniker of CS, psych-serine. Nevertheless, a meta-analysis revealed that CS was more effective than some of the most widely used antitubercular drugs, and the WHO has included CS or TZD as a group B drug for extended MDR-TB treatment regimens despite its known toxicity (Court *et al.*, 2021:688). One gram of CS per day causes psychiatric side effects in 50% of consumers, ranging from headaches and sleep disturbances to severe psychosis, convulsions and suicidal tendencies (Gumbo, 2017:1078). Thus, according to WHO recommendations, CS should not be used if a patient has a history of seizures or epilepsy or a serious current mental illness such as depression or psychosis (Hwang *et al.*, 2013:1257). Although CS is not registered in South Africa, it may be accessed with the South

African Health Products Regulatory Authority approval on a named-patient basis. However, TZD is accessible and pyridoxine supplementation is advised to address neuropsychiatric side effects when used to treat DR-TB (Rossiter, 2020:337-338).

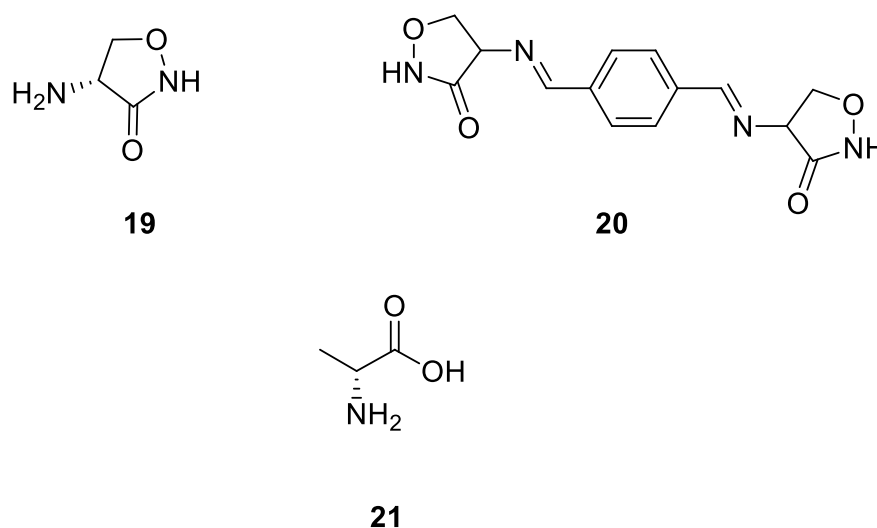


Figure 2.13 Cycloserine (19), terizidone (20), and D-alanine (21)

2.12.5. *para*-Aminosalicylic acid (PAS)

PAS (22) is an antagonist of folate synthesis that was rediscovered as an antitubercular drug in the 1940s. It is structurally related to *para*-Aminobenzoic acid (PABA) (23) and is virtually active only against Mtb (Deck & Winston, 2012a:844). PAS is often reserved for the treatment of XDR-TB and the management of complicated MDR-TB cases (De Kock *et al.*, 2014:6242). Zhang *et al.* (2019:827) reported on *in vitro* data revealing that an INH–PAS drug combination had synergistic activity against the majority of Mtb isolates in their study. In other words, the presence of PAS significantly elevates the Mtb isolates' susceptibility to INH. This discovery may be beneficial in shortening the extensive duration of MDR-TB treatment regimens that are currently required.

PABA participates in the Mtb *de novo* folate biosynthesis pathway (FBP) of Mtb. In the upper stream region of the FBP, dihydropteroate synthase (DHPS), which is encoded by *FoIC*,

catalyses the conversion of PABA to dihydropteroate. Meanwhile, dihydrofolate synthase (DHFS) catalyses the ATP-dependent addition of L-glutamate to dihydropteroate (converted PABA) to produce dihydrofolic acid (Minato *et al.*, 2015:5099).

The precise sites of PAS activity on the Mtb FBP are yet unknown. However, it is thought that when PAS is administered, its structural resemblance to PABA enables it to act as a deceptive substrate for DHPS via its conversion through *FoIC*. As a result, the incorporation of PAS instead of PABA culminates in the formation of hydroxyl (OH)-containing dihydrofolate antimetabolites (the active form of PAS), which further inhibits the dihydrofolate reductase (DHFR) enzyme down the line of the FBP. This ultimately results in Mtb's growth being inhibited since it is unable to synthesize purines and DNA (Chakraborty *et al.*, 2013:1; Heo *et al.*, 2022). *ThyA*, *FoIC*, *DfrA*, and *RibD* gene mutations may be responsible for PAS resistance. Cells receive DHFR activity from *DfrA* and *RibD*, which is necessary for the conversion of dihydrofolate to tetrahydrofolate downstream of the FBP. Therefore, mutations that result in enhanced *DfrA* or *RibD* gene expression would shield Mtb against PAS inhibition. Decreased *FoIC* expression or DHFS enzymatic activity, result in PAS not being converted to its active form. Regarding *ThyA*, it is not quite known why mutations in this gene promote PAS resistance (Nguyen, 2016:1589).

PAS is easily absorbed in the GI tract and reaches a plasma concentration of at least 50 µg/ml (Deck & Winston, 2012a:844). It undergoes *N*-acylation in the liver, where it may generate hepatotoxins (*N*-acetyl PAS). The advantages of PAS are very constrained due to the predominance of GI problems, which often impair patient compliance. The likelihood of undesirable GI symptoms linked to PAS use ranges from 10% to 30% (Gumbo 2017:1077). In severe cases, peptic ulcers and haemorrhage might occur. Increased body temperature, joint pain, skin rashes, hepatitis, hepatosplenomegaly, adenopathy and granulocytopenia are all common signs of PAS hypersensitivity. Very high PAS levels discharged in the urine have also been linked to crystalluria (Deck & Winston, 2012a:844).

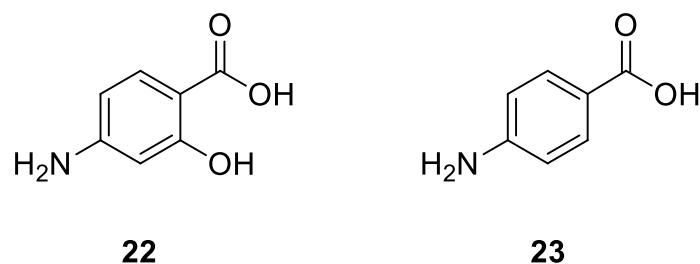


Figure 2.14 *para*-Aminosalicylic acid (**22**) and *para*-Aminobenzoic acid (**23**)

2.12.6. Linezolid (LZD)

LZD (**24**) is a member of the oxazolidinone class of drugs. Oxazolidinones are novel synthetic antimicrobial drugs used to treat pneumonia acquired in a hospital or community setting as well as complicated and minor skin and soft tissue infections caused by Gram-positive pathogens. *Nocardia* infections are one of the off-label indications of LZD (Deck & Winston, 2012e:817). The WHO recently repurposed LZD as a group A antitubercular drug and added it to the list of SLDs to treat MDR-TB due to its activity against resistant Mtb isolates (WHO, 2021b).

Unlike other protein synthesis inhibitors, LZD has a distinct MOA. The four primary stages of bacterial protein synthesis are initiation, elongation, termination and recycling. While LZD inhibits the initiation phase of protein synthesis, other protein synthesis inhibitors such as chloramphenicol, macrolides, lincosamides and tetracyclines interfere with the elongation (polypeptide extension) phase (Ament *et al.*, 2002:664-665). LZD targets the 50S ribosomal subunit, which is present on the 23S rRNA of bacterial pathogens, impeding the assembly of its complex with the 30S subunit and, therefore, the formation of the 70S initiation complex, a crucial step in the translation process for bacterial pathogens (De Vriese *et al.*, 2006:1115). The binding of LZD to the 50S subunit delays the formyl methionyl-tRNA recognition, ultimately slowing the initiation of translation (Angula *et al.*, 2021:12). As for its activity against Mtb, a team of researchers used commercial oligonucleotide microarrays to examine transcriptional mutations throughout the whole genome. They discovered that a number of vital genes,

including those involved in protein synthesis, the metabolism of sulphite, the cell envelope and virulence of Mtb, were significantly altered (Jadhavar *et al.*, 2015:4384).

The co-administration of antacids has no effect on the oral absorption of LZD and results in 100% bioavailability, requiring no dose adjustments when switching to intravenous administration. Approximately 30% of LZD is eliminated in the urine – the remaining is metabolised *via* renal and non-renal pathways, where it is oxidised to two major inactive metabolites (Ager & Gould, 2012:88-97). LZD tolerance and safety, on the other hand, are dose – and duration dependent. A metallic taste, headaches, moniliasis, cramps and GI symptoms such as nausea, vomiting, diarrhoea and cramps, are all common adverse effects of LZD (Rossiter, 2020:316). Long-term treatment has been associated with ocular and peripheral neuropathy, as well as lactic acidosis. The inhibition of mitochondrial protein synthesis by LZD is likely to be the source of these adverse effects. Serotonin syndrome may occur when LZD is combined with serotonergic drugs, most often antidepressants such as serotonin reuptake inhibitors (Deck & Winston, 2012e:817).

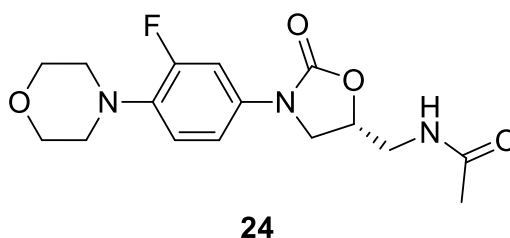


Figure 2.15 Linezolid (**24**)

2.12.7. Bedaquiline (BDQ)

Andries *et al.* (2005:223) discovered the diarylquinoline BDQ (**25**) as having a unique range of potent and selective *in vitro* activity against Mtb (0.030 to 0.120 µg/ml, compared to 0.500 µg/ml for RIF and 0.120 µg/ml for INH). The American Food and Drug Administration (FDA)

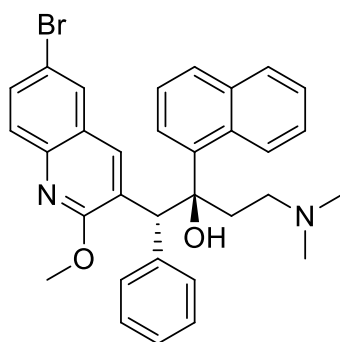
has authorized BDQ as the first drug approved for the treatment of TB in almost four decades. The approval was based on the findings of two Phase IIb trials that demonstrated improved efficacy in the clinical context of DR-TB, with cure rates of 62% and 44% in patients treated with BDQ and a placebo, respectively (Cholo *et al.*, 2017:334). This potent activity is reflected through *in vivo* reductions in treatment duration where it has been proven that the addition of BDQ for 6 months to an MDR-TB treatment regimen considerably enhanced short-term treatment results with sputum culture conversion to negative just after 2 months of treatment (Svensson *et al.*, 2015:1106). Importantly, BDQ has bactericidal activity against non-replicating Mtb at therapeutically achievable doses (Sarathy *et al.*, 2019:2). This is often accomplished by combining BDQ with other bactericidal drugs such as third-generation FQNs (like LFX), PTO or PZA (Li *et al.*, 2019:99).

BDQ is the first of a new class of antitubercular drugs with a novel MOA. It inhibits mycobacterial F₁F_o-ATP synthase, an important membrane-bound enzyme, interfering with energy synthesis and altering intracellular metabolism in both replicating and non-replicating Mtb (Field, 2015:173). BDQ exerts its MOA by binding to the membrane-bound c-ring rotor of the F_o component of ATP synthase. This binding inhibits c-subunit rotation (a required conformational change for the flow of protons) and proton transfer. Concurrently, ATP production is hindered, and intracellular ATP levels decrease, ultimately leading to Mtb cell death (Hards *et al.*, 2018:7326; Worley & Estrada, 2014:1189). Surprisingly, BDQ's bactericidal activity is delayed, i.e., cell death does not occur immediately after ATP depletion (Sarathy *et al.*, 2019:2).

Unlike in many other bacteria, ATP synthase is required for Mtb survival, and any mutation in the c-subunit may result in BDQ resistance (Chahine *et al.*, 2014:108). The *atpE* gene, which encodes the ATP synthase c-subunit, may contain a variety of point mutations that confer high-level resistance, all of which impact amino acid residues adjacent to the BDQ binding site (Worley & Estrada, 2014:1189). Mutations in *Rv0678*, a transcriptional regulator of the genes

encoding the *MmpS5–MmpL5* efflux pump, indicate non-target-based resistance to BDQ (Nguyen *et al.*, 2017:1626). According to Hartkoorn *et al.* (2014:2980), resistance to azoles and CFZ is caused by the active efflux of these compounds by these multi-substrate transporter pumps. Thus, even before BDQ was extensively used, cross-resistance between BDQ and CFZ had been established. In rare situations, *Rv0678* mutations co-occur with genetic polymorphism in other genes encoding the unknown transporter *Rv1979c* and the cytoplasmic peptidase *PepQ* (*Rv2535c*), both of which are linked to CFZ resistance (Degiacomi *et al.*, 2020:1).

There is a significant lag period between oral intake and BDQ absorption after which the drug is extensively distributed throughout the body tissues (Gumbo, 2017:1076). BDQ is further distinguished by a very long terminal $T_{1/2}$ of about 5.5 months, which is mostly due to the delayed redistribution from the tissues where it is stored (Gumbo, 2017:1076). In the liver, CYP450 iso-enzyme 3A4 predominantly converts BDQ to the *N*-mono-desmethyl metabolite M2. M2 is effective against *Mtb*, although about 5 times less effective than BDQ (Van Heeswijk *et al.*, 2014:2312). M2 has been observed to prolong the QT interval, creating safety concerns for torsades de pointes, particularly when taken with other QT-prolonging drugs such as FQNs, DLM and CFZ (Koele *et al.*, 2022:1-2). BDQ was also related to an unexplained increase in late mortality in one randomized Phase II study. Patients who were given BDQ died at a higher rate than those who were given a placebo (Diacon *et al.*, 2014:723). Other commonly reported BDQ side effects include joint pain, nausea, headaches, haemoptysis (coughing up blood), chest pain, skin rashes and elevated liver enzymes (Gumbo, 2017:1077; Rossiter, 2020:335).



25

Figure 2.16 Bedaquiline (25)

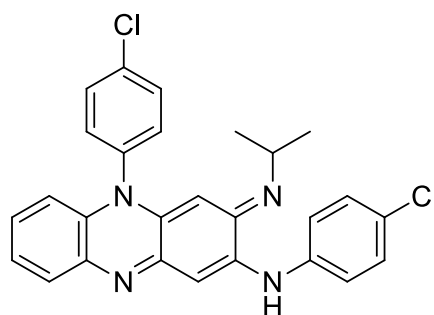
2.12.8. Clofazimine (CFZ)

CFZ (26) is a fat-soluble riminophenazine dye with antibacterial activity against a wide range of Gram-positive pathogens, including *S. aureus*, coagulase-negative *staphylococci*, *Streptococcus pyogenes* and *Listeria monocytogenes*. CFZ is also used to treat *Mycobacterium ulcerans*-caused chronic skin ulcers (Buruli ulcers) (Gumbo, 2017:1075-1076). In general, CFZ is thought to be unsuccessful in the treatment of pulmonary TB. This disagreement stems from early research that revealed inconsistencies in CFZ's therapeutic effect in diverse animal models (Cholo *et al.*, 2011:290). As a consequence, CFZ was abandoned as a treatment for TB in humans, most likely because INH and other TB drugs introduced at the same time were superior to CFZ (Deck & Winston, 2012a:846; Murray *et al.*, 2015:1755).

The antitubercular activity of CFZ was re-evaluated as the global incidence of DR-TB rose. A pivotal trial conducted in Bangladesh in 2010 found that a treatment regimen combining CFZ with additional antitubercular drugs was especially beneficial for reducing the treatment duration of MDR-TB, which may have aided the achievement of a 9-month TB treatment regimen (Gopal *et al.*, 2013:1006). As a result, the WHO now considers CFZ to be a key component of the new short-course MDR-TB regimen (WHO, 2019b).

The CFZ MOA is not well understood. However, it has been proposed that the principal site of action is Mtb's outer membrane. CFZ inhibits two potential targets: the mycobacterial respiratory chain and ion transporters. Phenazine dyes, such as CFZ, are auto-oxidizable compounds that generate reactive oxygen species when re-oxidized in air. As a result, CFZ serves as an artificial electron acceptor, and Mtb's respiratory system oxidizes CFZ rather than NADH, resulting in a decrease in the amount of ATP available for all cellular functions (Mirnejad *et al.*, 2018:1354; Yano *et al.*, 2011:10276). *Rv0678* modulates the expression of the *MmpS5-MmpL5* efflux pump, and its overexpression or mutation increases CFZ MIC by two- to four-fold. Mutations in *Rv1979c*, which encodes a possible amino acid membrane transporter with permease activity, have also been linked to CFZ resistance. Mutations in the proline aminopeptidase gene *pepQ* have additionally been demonstrated to confer low-level cross-resistance between CFZ and BDQ *in vitro* (Park *et al.*, 2022:2).

The oral bioavailability of CFZ is 45–60%. High-fat meals increase it two-fold while antacids reduce it by 30%. CFZ is extremely lipophilic and forms crystal-like deposits within the tissues of the mononuclear phagocyte system. The $T_{1/2}$ of these crystalline deposits is at least 2–3 months (Baik *et al.*, 2013:1218; Gumbo, 2017:1076). This might provide a rationale for the shortened CFZ-based antitubercular regimens. On the one hand, tissue accumulation and the resulting long $T_{1/2}$ provide a benefit in reducing treatment duration, while crystal deposition of the drug in tissues, on the other hand, is at the root of the most common undesired side effects of reddish-brown skin and conjunctival discoloration (Rossiter, 2020:336).



26

Figure 2.17 Clofazimine (26)

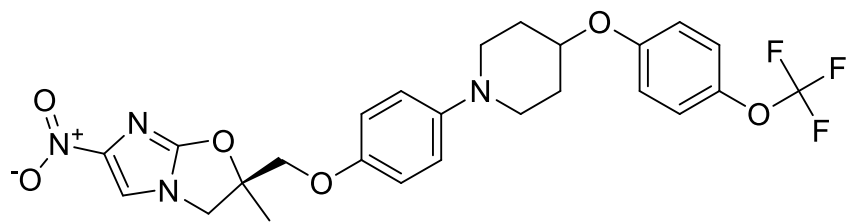
2.12.9. Nitroazoles: delamanid (DLM) and pretomanid (PTM)

Nitroazole-based drugs have long been used to treat bacterial and parasitic infections. Both DLM (a nitroimidazooxazole) (**27**) and PTM (a nitroimidazooxazine) (**28**) are two newer nitroimidazole-containing drugs that inhibit both replicating and non-replicating Mtb. Both DLM and PTM are lipophilic, which may aid penetration through the highly lipophilic cell wall of Mtb and account for their significant efficacy. They are, however, poorly water soluble and tend to bind to human plasma proteins (Showalter, 2020:2-3). The European Medicines Agency authorized DLM in 2014 as the second novel antitubercular drug after BDQ, based on a Phase 2 study that showed that a higher percentage of MDR-/XDR-TB patients taking DLM compared to a placebo achieved sputum culture conversion after just 8 weeks of therapy. The FDA authorised PTM in 2019 and the EMA approved it in 2020 as part of a six-month regimen (called BPaL) that also included LZD and BDQ. The Phase 3 Nix-TB study was the pivotal trial for PTM approval. Six months following therapy, 90% of patients who received the BPaL regimen had a favourable result. Thus, for the first time in history, there is evidence that effective chemotherapy for at least sub-categories of DR-TB may be accomplished in the same time period as DS-TB treatment utilising the nitroimidazole based drugs DLM and PTM (Black & Buchwald, 2021:7).

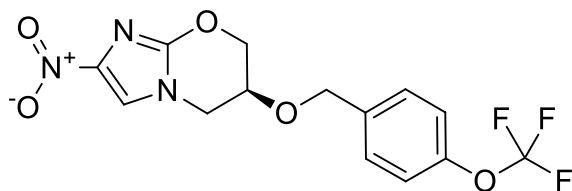
Following bio-activation through the denitrification process, these pro-drugs seem to have a multi-target MOA. In the redox cycling of cofactor F_{420} , the enzyme deazaflavin-dependent nitro-reductase (Ddn) converts DLM and PTM to their des-nitroimidazole metabolites, which yield reactive nitrogen species such as nitric oxide (NO). The release of NO during drug metabolism under anaerobic conditions is thought to facilitate Mtb respiratory poisoning. However, under aerobic conditions, the major MOA of these nitroazoles is the inhibition of mycolic acid biosynthesis, which is required for the synthesis of Mtb's outer lipid membrane (Grzelak *et al.*, 2019:721; Mudde *et al.*, 2022:882). Interestingly, human nitro-reductases were shown to be incapable of activating DLM, perhaps due to the fact that humans use nicotinamide adenine dinucleotide phosphate as an electron donor, which has a higher redox

potential than cofactor F₄₂₀. The fact that pro-drug activation of these drugs is specific to mycobacterial Ddn may represent some of the selective activity against Mtb while remaining non-mutagenic to humans (Mudde *et al.*, 2022:882). Mtb resistance to DLM and PTM is induced by mutations in the genes *fgd1*, *fbiA*, *fbiB* and *fbiC*, which are responsible for the production and reactivation of cofactor F₄₂₀, preventing DLM and PTM pro-drug activation by Ddn (Kadura *et al.*, 2020:2035-2040). Recently, a novel mechanism of resistance was revealed in Mtb strains with mutations in *Rv2983 (fbiD)*, a gene that had not previously been linked to nitroimidazole resistance but was shown to be a guanylyl-transferase necessary for the production of cofactor F₄₂₀ (Rifat *et al.*, 2020:1).

The oral bioavailability of DLM varies between 35% and 60%. DLM is highly protein-bound (> 97%), and its metabolism is predominantly controlled by plasma albumin. DLM had no adverse effects on the CNS or respiratory systems in animal studies at concentrations 18.5 or 3.2 times greater than the highest blood concentrations predicted in humans at a dosage of 100 mg twice a day. However, QT interval prolongation is one of the adverse side effects of DLM usage (Lewis & Sloan, 2015:781). PTM has a more favourable pharmacokinetic profile than DLM. It is easily absorbed, well tolerated and has good bioavailability (Bahuguna & Rawat, 2019:271). Some of the most commonly reported side effects of PTM usage in various research include vomiting, acne, nausea, migraines, musculoskeletal discomfort and headaches. Optic problems, hepatic enzyme imbalances, dermatitis, GI upset and severe cutaneous side effects are more likely to be induced by PTM (as seen in patients taking the BPAL regimen in the Nix-TB trial) (Fekadu *et al.*, 2022:179).



27



28

Figure 2.18 Delamanid (**27**) and pretomanid (**28**)

PART TWO: HOSPITAL-ACQUIRED INFECTIONS (HAIs)

2.13. Background

An HAI is defined as an infection that is neither present nor incubating when a patient is admitted to a healthcare facility. The time for diagnosing an HAI will therefore be reliant on the incubation period of the infection, which is commonly suspected to be 48 to 72 hours after admission. Although these infections are mainly associated with hospitalisation (hence the phrase "hospital-acquired infections"), they may develop at any given time after admission to any healthcare facility (Vincent, 2003:2068). HAIs are widespread in the intensive care unit (ICU), where acute life-threatening conditions are assessed and treated (WHO, 2022b). ICU patients have a five to ten times higher risk of acquiring HAIs owing to intrinsic factors such as their clinical state, weakened immune systems and external factors such as the requirement for advanced surgical procedures or the administration of medical devices (Alves *et al.*, 2021:1744; Dadi, 2021:1).

The most prevalent HAIs include central line-associated bloodstream infections (CLABSIs), catheter-associated urinary tract infections (CAUTIs), surgical site infections (SSIs) and ventilator-associated pneumonia (VAP) (CDC, 2014). Hospitalised patients acquire such infections through pathogenic organisms that organise themselves into biofilms and colonize on medical equipment. The type of pathogen causing an HAI differs based on the type of medical intervention and medical device used as well as where and how a procedure was given to a patient (Dadi *et al.*, 2021:2).

The ESKAPE pathogens are responsible for the majority of HAIs. The acronym ESKAPE refers to six hypervirulent and antibiotic resistant pathogens, including *Enterococcus faecium*, *Staphylococcus aureus*, *Klebsiella pneumoniae*, *Acinetobacter baumannii*, *Pseudomonas aeruginosa*, and other *Enterobacter* spp. These pathogens display significant degrees of antimicrobial resistance because they frequently exhibit novel pathophysiology, modes of

transmission and resistance patterns that makes HAIs caused by them nearly untreatable (Navidinia *et al.*, 2017:779; Orosz *et al.*, 2022:27).

Currently, the ESKAPE pathogens are resistant to the majority of existing antimicrobial drugs, including FQNs, tetracyclines, lipopeptides, β -lactams, β -lactam- β -lactamase inhibitor drug combinations, macrolides, oxazolidinones and last-line antibiotics such as carbapenems, glycopeptides and polymyxins (De Oliveira *et al.*, 2020:2). These pathogens are very effective in up-regulating or adopting genes that code for antimicrobial resistance mechanisms, particularly in the presence of antibiotic drug selection pressure, as observed in most healthcare settings. With a plethora of antimicrobial resistance mechanisms at their disposal, they have the capacity to deploy several of these mechanisms against the same antimicrobial drug or a single mechanism against multiple drugs, representing a new paradigm in contemporary medicine (De Oliveira *et al.*, 2020:2; Peleg & Hooper, 2010:1).

The morbidity and mortality rates associated with HAIs are quite high, and as a consequence, the healthcare system loses billions of dollars. The expenditures associated with the abovementioned HAIs total around \$9.8 billion per year, with SSIs being the most expensive of the bunch. In addition to this, an increase in the number of days spent in the hospital is almost always connected to the presence of these infections (Monegro *et al.*, 2020). Marturano and Lowery (2019:1) investigated whether ESKAPE pathogens were associated with worse hospital outcomes than non-ESKAPE pathogens in a data set of more than 1.1 million patient encounters in the United States and reported that ESKAPE pathogens accounted for 42.2% of species isolated from bloodstream infections (BSIs) and were additionally related to a 3.3–day increase in hospital stay, a \$5,500 increase in healthcare expenditure per case, and a 2.1% increase in mortality.

2.14. Call for antimicrobial drug development

According to the WHO 2022 global report on infection prevention and control, seven patients in high-income countries and 15 patients in low-and middle-income countries are expected to acquire at least one HAI for every 100 hospitalised patients (WHO, 2022b). It is also predicted that if new drugs and means to address this global menace are not discovered by 2050, drug-resistant pathogens will kill 10 million individuals globally each year. In fact, if left unchecked, the rapid spread of antimicrobial resistance might make many pathogens much more fatal than they are now (Murray *et al.*, 2022:630).

The WHO (2017c) published a global priority pathogen list (GPPL) in 2017 to identify pathogens for which new antimicrobial development is urgently needed. The GPPL prioritises bacterial pathogens into three categories: critical, high and medium, with the ESKAPE pathogens receiving critical and high priority rank. The critical priority category includes carbapenem-resistant *A. baumannii*, *P. aeruginosa*, and *Enterobacteriaceae* spp., including *K. pneumoniae*. This category of multidrug-resistant organisms poses a significant threat in hospitals, especially among patients who need ventilators and catheters for treatment and management. Methicillin-resistant and vancomycin-intermediate/resistant *S. aureus*, as well as *E. faecium*, are classified as high priority (WHO, 2017c). This clearly illustrates the global need for antimicrobial drugs with novel molecular targets against ESKAPE pathogens, as well as to alleviate the burden of HAIs.

Table 2.3 WHO priority pathogens list (tabulated from WHO, 2017c).

PRIORITY	RESISTANT PATHOGENS	DRUGS TO WHICH IT IS RESISTANT
Priority 1: CRITICAL*	- <i>Acinetobacter baumannii</i>	Carbapenem-resistant
	- <i>Pseudomonas aeruginosa</i>	Carbapenem-resistant
	- <i>Enterobacteriaceae</i> [#]	Carbapenem-resistant, ESBL-producing
Priority 2:	- <i>Enterococcus faecium</i>	Vancomycin-resistant

PRIORITY	RESISTANT PATHOGENS	DRUGS TO WHICH IT IS RESISTANT
HIGH	<ul style="list-style-type: none"> - <i>Staphylococcus aureus</i> - <i>Helicobacter pylori</i> - <i>Campylobacter spp.</i> - <i>Salmonellae</i> - <i>Neisseria gonorrhoeae</i> 	<p>Methicillin-resistant, vancomycin-intermediate and resistant</p> <p>Clarithromycin-resistant</p> <p>Fluoroquinolone-resistant</p> <p>Fluoroquinolone-resistant</p> <p>Fluoroquinolone-resistant, cephalosporin-resistant</p>
Priority 3: MEDIUM	<ul style="list-style-type: none"> - <i>Streptococcus pneumoniae</i> - <i>Haemophilus influenzae</i> - <i>Shigella spp.</i> 	<p>Penicillin-non-susceptible</p> <p>Ampicillin-resistant</p> <p>Fluoroquinolone-resistant</p>
<p>*Mtb is not included in the priority list since the need for drug development is already established.</p> <p>#<i>Enterobacteriaceae</i> include <i>E. coli</i>, <i>K. pneumoniae</i>, <i>Enterobacter spp.</i>, <i>Citrobacter spp.</i>, <i>Morganella spp.</i>, <i>Providencia spp.</i>, <i>Proteus spp.</i>, <i>Serratia spp.</i></p>		

2.15. The ESKAPE pathogens

2.15.1. *Enterococcus faecium*

Enterococcus spp. are Gram-positive, facultative anaerobes that generally colonise the intestines of healthy individuals. They are members of the lactic acid bacteria group, which produces bacteriocins (Fischer & Phillips, 2009:1749-1751). The majority of *enterococci* are employed in the manufacture of pharmaceutical probiotics and have an important role in the maintenance of human intestinal homeostasis. Furthermore, they serve as the initiating culture in the fermentation of meats and cheeses, and are commonly used during food preservation (Krawczyk *et al.*, 2021:1).

However, *enterococci* are opportunistic pathogens that, outside of their normal commensal habitats, propagate themselves as life-threatening pathogens. Among the *enterococci*, *E. faecalis* and *E. faecium* are the most common pathogens that cause infections in humans,

and they have aggressively expanded as global hospital-acquired pathogens by successfully adapting to circumstances in a healthcare facility (Zhou, 2020:1). They are often associated with HAIs such as BSIs, UTIs, endocarditis (endocardium inflammation) and sepsis. In addition, catheter-related infections that may cause meningitis have also been recorded in new-borns and babies (Krawczyk *et al.*, 2021:6).

Enterococci resistance to penicillin/ampicillin, aminoglycosides (high level resistance) and glycopeptides is emerging in a growing number of isolates, indicating a limited treatment spectrum in the future (Orsi & Ciorba, 2013:485). Ampicillin resistance is explained by penicillin binding protein (PBP) mutations and/or overexpression, or by mutations in the β -subunit of this protein. Ampicillin resistance is uncommon in *E. faecalis*, but it is found in 90% of *E. faecium* isolates (Gagetti *et al.*, 2019:180). Vancomycin (a glycopeptide) resistance is found in about 35.5% of *enterococci* and is caused by the production of a mutated cell wall precursor that is unable to attach to glycopeptides. *VanA*, *VanB*, *VanD*, *VanN*, and *VanM* mutations are often found in vancomycin-resistant *enterococci* (VRE) isolates, with *VanA* and *VanB* being the most prevalent and abundant (Darvishi *et al.*, 2020:165). As a consequence, the available antimicrobials for treating VRE infections are limited to bacteriostatic drugs such as LZD, tigecycline and quinupristin-dalfopristin (inactive against *E. faecalis*) (Orsi & Ciorba, 2013:489).

2.15.2. *Staphylococcus aureus*

S. aureus is a Gram-positive coccus that colonises the cutaneous microbiota of the nose and perineum of humans, and their cells are typically organised in unique grape-like clusters. Transmission of *S. aureus* may occur *via* direct contact or by airborne vectors (Santajit & Indrawattana, 2016:5). *Staphylococci* are classified as either coagulase (Coa)-positive or coagulase (Coa)-negative depending on their ability to induce plasma clotting (Pickering *et al.*, 2021:1). *S. aureus*, for example, stimulates the human coagulation cascade by secreting two coagulases, staphylo-Coa and von Willebrand factor-binding protein (vWbp), which binds to

prothrombin in the blood. The interaction of any of these enzymes with prothrombin causes a morphological shift in the thrombin's active site, converting plasma-soluble fibrinogen into insoluble fibrin segments – initiating clot formation (Vanassche *et al.*, 2013:93).

The propensity of *S. aureus* to clot host plasma has been used to identify it. In this dimension, staphylo-Coa is crucial for distinguishing the virulent pathogen from less virulent Coa-negative *S. aureus* spp., and may be identified using a tube test or a slide test. The former is often employed to detect free extracellular Coa, while the latter detects bound Coa (Kateete *et al.*, 2010:3). *S. aureus* infections are effectively treated with β -lactam antibiotics such as penicillin, cephalosporins and carbapenems. Overuse of these drugs, however, led to the emergence of β -lactamase-producing *S. aureus* spp., including the well-known MRSA strain, which is resistant to all β -lactam antimicrobials. This resulted in a more than 80% increase in *S. aureus* related infections in both communities and hospitals over the course of two decades (Santajit & Indrawattana, 2016:5).

MRSA is a major cause of life-threatening HAIs. Vancomycin, a glycopeptide cell wall synthesis inhibitor that has been in use for more than 50 years, remains the FLD for MRSA infections and the majority of *S. aureus* infections. However, there are substantial concerns since *S. aureus* susceptibility to this drug has decreased and total resistance has increased during the last 20 years (Choo & Chambers, 2016:267; McGuinness *et al.*, 2017:270). For example, MRSA exposure to high vancomycin concentrations resulted in a predicted rise in vancomycin-intermediate *S. aureus* (VISA) and vancomycin-resistant *S. aureus* (VRSA). VISA and VRSA originated as a response to modifications in bacterial cell wall thickness and composition, which restricted drug penetration through the cell wall to the site of action (Conly & Johnston, 2002:283).

S. aureus's key virulence factors include the capacity to form a biofilm on implanted medical devices or damaged host tissue, providing a niche for survival. This is particularly noticeable

in hospital settings where antibiotics are extensively used. This matrix encourages antimicrobial resistance, which contributes to the pathogen's role as a prevalent cause of chronic and recurrent infections (McCarthy *et al.*, 2015:1). Furthermore, staphylo-Coa and vWbp are well-known *S. aureus* pathogenesis attributes for catheter-related biofilm production and survival during BSIs (Pickering *et al.*, 2021:8-9).

2.15.3. *Klebsiella pneumoniae*

K. pneumoniae is a Gram-negative bacillus from the *Enterobacteriaceae* family. It colonises human mucosal surfaces such as the nasal cavity (up to 19%) and the GI tract (up to 77%). *K. pneumoniae* causes major HAIs such as pneumonia, UTIs (the most prevalent) and BSIs. However, *Klebsiella spp.* is the most common cause of VAP in ICU patients. Environmental strains of *K. pneumoniae* are much more sensitive to antimicrobial drugs than clinically isolated *K. pneumoniae*, indicating that drug resistance is often driven by selective antimicrobial drug pressure (Martin & Bachman, 2018:2-3). *K. pneumoniae* infections are often treated with β -lactam antibiotics such as penicillin, cephalosporins and carbapenems. However, they develop a range of β -lactamase enzymes that confer resistance to all β -lactams (Babic *et al.*, 2006:143-144). An example is the production of extended spectrum β -lactamases (ESBLs), which hydrolyse the oxyimino group contained in the structure of third-generation cephalosporins, rendering them ineffective before they reach the PBP target (Ashurst & Dawson, 2022).

The genes encoding ESBLs are located on the same plasmids as those encoding resistance to aminoglycosides and sulphonamides. This implies that ESBL-producing *Enterobacteriaceae* are often multidrug resistant, posing a significant challenge for the treatment of HAIs (Paterson, 2006:S21). As a result, carbapenems became one of the few drugs available to treat infections caused by ESBL *K. pneumoniae*. However, it has been shown that carbapenem-resistant *K. pneumoniae* causes over 80% of *Enterobacteriaceae*

related infections, thus limiting the therapeutic choices available for this family (Ashurst & Dawson, 2022).

2.15.4. *Acinetobacter baumannii*

A. baumannii is a Gram-negative opportunistic pathogen that spreads rapidly, causing HAIs such as septicaemia, UTIs, kidney infections, meningitis, bone infections and pneumoniae, particularly in ICU patients. Given their capacity to resist severe environmental conditions, *Acinetobacter* spp. are very adaptive and resilient. It can, for example, multiply at temperatures ranging from 150°C to 440°C (Hassani, 2014:80-81). Furthermore, *A. baumannii* seems to remain viable for relatively long periods on inanimate objects and surfaces, such as catheters, ventilators and tubes, and may withstand regular disinfecting attempts (Mohammed *et al.*, 2022:2).

The spread of *A. baumannii* in a healthcare setting is aided by both resistance to desiccation and the establishment of antimicrobial resistance by antimicrobial selection pressure (Navidinia, 2016:46). MDR *A. baumannii* is resistant to three or more antimicrobials, including β -lactams, aminoglycosides, FQNs and third-generation cephalosporins. As a consequence, colistin and tigecycline are the only active antimicrobial drugs available and have become the last lines of treatment against MDR *A. baumannii* (Cai *et al.*, 2012:1607).

2.15.5. *Pseudomonas aeruginosa*

P. aeruginosa is an anaerobic bacterium that can grow in the presence of oxygen. Human colonisation takes place in the GI tract and spreads to moist cutaneous areas, including the perineum and axilla (Pachori *et al.*, 2019:110). It can, however, be isolated from a variety of sources, including several life-threatening infections in cystic fibrosis patients, wounds, UTIs and pulmonary infections, as well as medical equipment such as inhalers, dialysis machinery, ventilators, anaesthetic equipment, toilets and sinks (Azam & Khan, 2019:350). *P. aeruginosa* is the fourth most prevalent pathogen identified in hospitals, accounting for 10% of all HAIs,

the second most common cause of VAP, and the third most common Gram-negative cause of BSIs. It can survive for 6 hours to 6 months due to its adaptability and excellent resilience (Pachori *et al.*, 2019:111).

P. aeruginosa can thrive at a wide range of temperatures. Their cells proliferate rapidly on water delivery systems' surfaces to produce a biofilm. Some investigations show that hospital plumbing reservoirs can be contaminated with *P. aeruginosa* and cause patient colonisation and infection. The use of tap water, that contaminates hospital staff hands have been identified as a transmission vehicle. Furthermore, the discharge of wash water and ventilator traps is thought to be a possible way for *P. aeruginosa* to be transported from patient to plumbing (Loveday *et al.*, 2014:8-9).

P. aeruginosa resists most antimicrobials by preventing them from penetrating its outer membrane. However, some FLQs (e.g., CFX and LFX), aminoglycosides (e.g., gentamicin, tobramycin and AM), β -lactams (e.g., piperacillin-tazobactam, ceftazidime, cefepime, ceftolozane-tazobactam, ceftazidime-avibactam, imipenem, meropenem and doripenem), and polymyxins remain active against a hand full of *P. aeruginosa* isolates. *P. aeruginosa* may furthermore generate resistance to these agents via modified pharmacological targets, active efflux, decreased permeability and degradation enzymes (Spagnolo *et al.*, 2021:171).

2.15.6. *Enterobacter* spp.

The *Enterobacter* genus comprises 22 species of opportunistic Gram-negative pathogens that colonize the normal commensals of the human GI microbiota. However, only a few pathogens within this species including *E. aerogenes*, *E. cloacae*, and *E. hormaechei* have been linked to HAIs (Davin-Regli *et al.*, 2019:2). Transmission occurs via hand carriage and fomites. It is also known that aspiration of colonised pharyngeal *Enterobacteriaceae* causes hospital-acquired pneumonia, while cutaneous organisms introduced into sterile areas may cause UITs, SSIs and CLABSIs (Mehrad *et al.*, 2015:1414).

An inducible, chromosomally encoded beta-lactamase known as *AmpC*, which confers resistance to penicillins, second- and third-generation cephalosporins, and aztreonam, is present in all *Enterobacter* species (Lim & Webb, 2005:895). In addition, β -lactamase inhibitors such as clavulanate have little effect on *Enterobacter* species (Lim & Webb, 2005:895). ESBLs and carbapenemases are used by a large number of *Enterobacter* organisms to confer resistance to almost all available antimicrobial drugs, except tigecycline and colistin. These include the Verona integron-borne metallo- β -lactamase, oxacillin hydrolysing enzymes, metallo- β -lactamase-1, and *K. pneumoniae* carbapenemase (Santajit & Indrawattana, 2016:6). However, with the discovery of the polymyxin-resistant gene *MCR-1*, which is responsible for plasmid-mediated colistin resistance in *Enterobacter* isolates, there have been a great number of studies pointing to the rapidly spreading nature of this transmissible mechanism conferring resistance to these last line drugs (Ma *et al.*, 2020:1).

2.16. Common ESKAPE-associated hospital-acquired infections

2.16.1. Central line-associated bloodstream infections (CLABSIs)

A central line is an intravenous catheter that originates at or near the heart or from one of the major arteries. It is used for intravenous drug infusion, the withdrawal of blood or hemodynamic monitoring. CLABSIs may occur within 48 hours of central line placement due to sterility breaches at the time of central line insertion or during the maintenance of the catheter, which is unrelated to any previous infection or condition (Clover *et al.*, 2022:15; Lobdell *et al.*, 2012:66). The rates of CLABSIs are mostly determined by two factors related to exposure risk: the (i) length and (ii) frequency of central line catheterisation. Other risk factors, in addition to this exposure, include the kind of catheter, the site at which it is inserted, and infection control measures (Blot *et al.*, 2022:1). The rate of CLABSIs was determined to be 5.05 cases per one thousand central line days, as stated in a study that was compiled by the International Nosocomial Infection Control Consortium and carried out in 45 different countries between 2012 and 2017 (Clover *et al.*, 2022:15).

Between 40% and 80% of all CLABSIs are caused by Gram-positive pathogens. These pathogens include *enterococci*, coagulase-negative *staphylococci*, and *S. aureus*. Gram-negative pathogens are responsible for 20% to 30% of CLABSIs and MRSA-related CLABSIs are rather common (Farrington & Allon, 2019:612). A meta-analysis of approximately 4000 publications indicated that the estimated additional healthcare costs associated with CLABSIs are \$48,108 per annum, with excess mortality estimated at 0.15 per HAI case, implying that there are 150 excess fatalities for every 1,000 in-hospital CLABSI cases (AHRQ, 2017).

2.16.2. Catheter-associated urinary tract infections (CAUTIs)

A CAUTI is an infection associated with the use of indwelling urinary catheters. Approximately 1 million CAUTIs are diagnosed yearly, accounting for over 40% of all HAIs, thus making CAUTIs the most common type of HAI (Jacobsen *et al.*, 2008:26). Indwelling urinary catheters cause up to 80% of hospital-acquired UTIs. Fever is the most common indicator of a UTI in patients with indwelling catheters (Tenke *et al.*, 2017:138-140). 60–80% of hospitalised patients with a catheter receive antimicrobials, mainly for non-UTI indications. This extensive antimicrobial exposure implies that resistant pathogens are often detected in the urine of catheterised patients (Nicolle, 2014:1-2). *E. coli* (21.4%) and *Candida* spp. (21.0%) are the most prevalent pathogens associated with CAUTIs, followed by *Enterococcus* spp. (14.9%), *P. aeruginosa* (10.0%), *K. pneumoniae* (7.7%), and *Enterobacter* spp. (4.1%), amongst others less prevalent (CDC, 2009).

More than 100,000 colony-forming units (CFU)/ml of urine is generally regarded to be diagnostic of a UTI. However, lesser numbers of organisms might become troublesome in a catheterised patient if not adequately treated. Thus, having more than 1000 to 10,000 CFU/mL of urine are often characterised as a CAUTI (Lobdell *et al.*, 2012:71). CAUTIs pose a major morbidity and mortality risk to the general hospital inpatient population. This risk, however, is almost five to ten times higher among patients admitted to the ICU. Every year, over 13,000 people die as a result of CAUTIs, and it is estimated that each CAUTI case costs almost \$600

to diagnose and treat, resulting in nearly \$131 million in annual national medical costs. Younger people and females have been identified as risk factors for CAUTIs (Podkovik *et al.*, 2019:5).

2.16.3. Surgical Site Infections (SSIs)

SSIs are the third most prevalent HAI, accounting for 10 to 40% of all HAIs (Legesse Laloto *et al.*, 2017:2). About 1% to 3% of surgical operations result in SSIs. SSIs are defined as infections that develop within 30 days following operative procedures due to microbial pathogens infiltrating the wound at the time of surgery, or within a year if an implant is left in place and the infection is believed to be attributable to surgery. The frequency of SSIs after abdominal surgery is 15–25%, depending on the extent of contamination, which is much greater than other types of surgery (Alkaaki *et al.*, 2019:112). *S. aureus* is one of the most prevalent SSI causative pathogens in 2% to 5% of patients receiving extra-abdominal surgery and up to 20% of patients receiving intra-abdominal surgery. The global prevalence of SSIs ranges from 2.5% to 41.9%, with South Africa's incidence rate of 5.6 SSIs per 100 surgeries being much higher than published rates in developed countries (Legesse Laloto *et al.*, 2017:2). SSIs involving the subcutaneous tissues, organs or implanted material may be more severe than superficial skin infections around the epidermis (WHO, 2018).

SSIs continue to be a burden to post-operative patients despite the use of prophylactic antimicrobials before and after surgery, as well as other preventative measures like upgraded ventilation in the operating room, better disinfection techniques and surgical skills (Hope, 2019:1). Patients who acquire SSIs have a fivefold increase in death and a fivefold increase in readmissions to hospital (Nel, 2014:33). In addition, SSIs, on average, lengthen hospital stays by 7–10 days (Isik *et al.*, 2015:458). Furthermore, it has been stated that the extra healthcare expenses ascribed to SSIs vary from \$11,778 to \$42,177 per case, and the mortality rates of SSIs are estimated to be 26 excess deaths per 1,000 cases (AHRQ, 2017).

2.16.4. Ventilator-associated pneumonia (VAP)

VAP is the second most prevalent HAI, affecting 5–40% of patients receiving invasive mechanical ventilation for more than 2 days (Papazian *et al.*, 2020:888). Mechanical ventilation entails supplying oxygen *via* a nasopharyngeal tube placed in a patient's mouth or nose or through a tracheostomy (a hole in the front of the neck) (CDC, 2014). Mechanical ventilation is associated with 86% of hospital-acquired pneumonias, and VAP is often diagnosed when a patient acquires a new or progressive infiltrate on a chest radiograph, leucocytosis, and purulent tracheobronchial secretions (Koenig & Truwit, 2006:637).

Gram-negative bacilli such as *P. aeruginosa*, *E. coli*, *K pneumoniae*, and *Acinetobacter* are frequent pathogens of VAP, as are Gram-positive cocci such as *S. aureus*. The most prevalent pathogen of VAP is *P. aeruginosa* (Wu *et al.*, 2019:4). The length of mechanical ventilation prior to the onset of VAP is a significant predictor of the pathogen most likely to cause VAP. Within four days after endotracheal intubation, VAP infections caused by antimicrobial susceptible pathogens are more prevalent, but later VAP infections are more typically caused by multidrug resistant pathogens such as *P. aeruginosa*, *Acinetobacter spp.* and MRSA (Hunter, 2012:3). Fungi such as *Candida spp.* can also be a causative pathogen of VAP. A lung biopsy containing yeast or pseudo-hyphae, on the other hand, is diagnostic of *Candida*-associated VAP (Lobdell *et al.*, 2012:69).

When compared to patients without VAP, it is projected that VAP elongates mechanical ventilation by 7.6 to 11.5 days and hospital stay by 11.5 to 13.1 days (Klompas, 2018). In 2017, the average additional medical expenses associated with VAP were estimated to range from \$19,325 to over \$80,013 per case (AHRQ, 2017). The risk of mortality from VAP is one of the highest. The reported death rate for VAP varies from 24 to 50%, and in extreme circumstances, it may reach as high as 76% (Chastre & Fagon, 2002:867).

2.17. Compound classes of interest in this study

2.17.1. Nitroazole: Nitazoxanide (NTZ)

NTZ (**29**) is a thiazolyl-salicylamide containing a 5-nitrothiazole head group attached to a salicylamide via an amide bond. Nitrothiazole unit is structurally analogous to nitroimidazole – a moiety present in drugs such as metronidazole (MTZ) (**30**). Following oral administration, NTZ is rapidly metabolised to its desacetyl derivative tizoxanide (TIZ) (**31**), which is the active metabolite *in vivo* (Hemphill *et al.*, 2006:954).

NTZ was primarily used as an anthelmintic and parasiticide in 1975 (Rossignol & Cavier, 1976:1–8). Human trials conducted in the 1980s, however, discovered that it was beneficial in treating infections caused by *Hymenolepis nana* and *Taenia saginata* (Rossignol & Maisonneuve, 1984). Later, *in vitro* evaluations of NTZ demonstrated a very broad activity range, thus expanding its therapeutic use. Today, NTZ is often used as a single agent to treat mixed intestinal infections caused by protozoa and helminths, as an antibacterial agent primarily for *Clostridium difficile* and *Helicobacter pylori* infections, rotavirus diarrhoea in children, and chronic Hepatitis B and C infections (Singh & Narayan, 2011:67-68).

NTZ's antiviral properties were unintentionally discovered while treating cryptosporidium diarrhoea in HIV-positive patients co-infected with hepatitis B or C. Since then, scientists have investigated NTZ's potential as an antiviral agent. For instance, it has been claimed that NTZ can inhibit the most recent outbreak of SARS-CoV-2 at a low micromolar concentration of 2.12, following infection in Vero E6 cells (Mahmoud *et al.*, 2020:2-3).

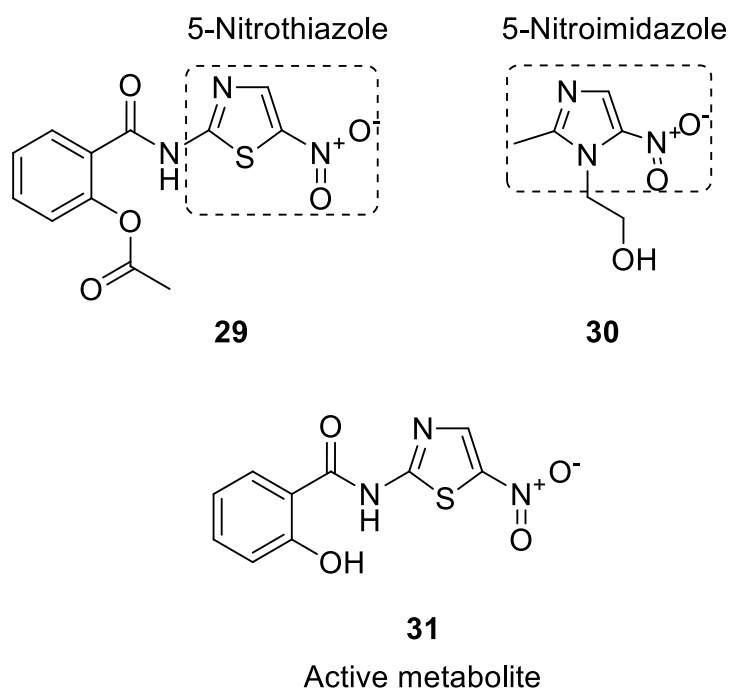


Figure 2.19 Nitroazoles: nitazoxanide (**29**), metronidazole (**30**), and tizoxanide (**31**)

2.17.1.1. Antimicrobial activity of nitazoxanide

The antimicrobial MOA of NTZ has been found to be selective inhibition of pyruvate-ferredoxin oxidoreductase (PFOR), which is required for protozoan and anaerobic bacterial energy metabolism (Singh & Narayan, 2011:67). In contrast to its anaerobic activity, NTZ is almost completely inactive against aerobically cultured *Staphylococcus*, *Enterococcus*, *Pseudomonas* and *Enterobacteriaceae* (De Carvalho *et al.*, 2009:5789). NTZ inhibition occurs independently of reduced ferredoxin and acetyl-coenzyme-A, unlike other drugs that target PFOR – such as MTZ. This is since inhibition of NTZ occurs earlier in the catalytic cycle (Hoffman *et al.*, 2007:869; Soria-Arteche *et al.*, 2013:6839). In other words, unlike MTZ, which interacts with the catalytic sites during PFOR metabolism, NTZ interferes with the binding of pyruvate to the thiamine pyrophosphate cofactor during the first phase of the PFOR cycle. This differential MOA may aid in avoiding cross resistance between NTZ and MTZ derivatives. Other possible NTZ MOAs remain unclear since some species lack the PFOR target (Anderson & Curran, 2007:1950).

2.17.1.2. Antitubercular activity of nitazoxanide

During a drug repurpose study, De Carvalho *et al.* (2009:5789) discovered that *in vitro* evaluation of NTZ and its active metabolite, TIZ, exhibited activity against replicating and non-replicating Mtb strains at low inhibitory concentrations, as well as that these compounds avoided resistance development. NTZ was shown to be effective against clinical isolates of drug-susceptible and drug-resistant Mtb strains, with a median MIC of 16 µg/ml. No resistance was identified when 10¹² CFU of Mtb were exposed to NTZ (Walsh *et al.*, 2020:1). Furthermore, it was recently observed during a RIF–NTZ conjunctive study that RIF co-administered with NTZ eliminated latent Mtb cells in 28–35 days vs. the six months required therapy by other first-line TB combinatory regimens. This clearly indicates that NTZ has significant TB treatment shortening potential and could be useful in the development of novel antitubercular drugs (Iacobino *et al.*, 2019:1-4). In addition, NTZ exhibited antimycobacterial activity at 25 mg/kg when administered by gavage to *Mycobacterium leprae* infected mice, which implies that NTZ could also be considered for the treatment of leprosy. This was demonstrated in a study that was carried out by Bailey and colleagues (2017:1-9) in 2017.

NTZ's MOA against Mtb was unexpected since Mtb lacks a homologue for the anaerobic bacterial target, PFOR, which NTZ is known to target. Furthermore, Mtb-NTZ susceptibility is irrespective of whether the environment is microaerophilic or anaerobic. However, NTZ has a distinct MOA that may encompass numerous targets in Mtb. NTZ functions as an uncoupler, interfering with oxidative phosphorylation and thereby affecting membrane potential and intra-organism pH homeostasis, both of which are required for Mtb survival (De Carvalho *et al.*, 2011:850). Plasma protein interactions seem to limit the potential of NTZ for the treatment of TB in humans, despite the promising outcomes of NTZ studies against MDR Mtb (Umumararungu *et al.*, 2020:550).

2.17.2. Thiazolidin-4-ones

Thiazolidinones are heterocyclic ring structures containing a sulphur atom (S) in the first position, a nitrogen atom (N) in the third position, and a carbonyl (C=O) functional group in the second, fourth or fifth position, yielding the derivatives thiazolidin-2-one, thiazolidin-4-one, and thiazolidin-5-one (Nirwan *et al.*, 2019:1239). The thiazolidin-4-one derivative (**32**) is regarded as a "wonder nucleus" due to its wide array of biological activities, including anti-inflammatory, antiproliferative, antiviral, anticonvulsant, antidiabetic, antihyperlipidemic, cardiovascular, anti-tubercular, antidiarrheal, antiarthritic, antiparasitic and antibacterial (Kulkarni *et al.*, 2022:2031). This extensive library of activity can be ascribed to its broad and non-specific inhibition of several pathogenic molecular targets, including peroxisome proliferator activated receptor, aldose reductase, cyclooxygenase, phosphoinositide 3-kinase or mitogen activated protein kinase, pim kinase, protein tyrosine phosphatase-1B, UDP-N-acetylmuramoylalanine D-glutamate ligase, amongst others (Kaur Manjal *et al.*, 2017:1; Trotsko, 2021:2-3).

The thiazolidin-4-one core is a well-known privileged scaffold in pharmaceutical chemistry and a valuable resource for designing novel drug-like compounds, particularly in rational privileged substructure-based diversity-oriented synthesis (Lesyk, 2020:33). For example, ralitoline, etozoline, pioglitazone and thiazolidomycin are just a few drugs based on this pharmacophore available on the market for the treatment of epilepsy, high blood pressure, hyperglycaemia and *streptomyces* spp. infections (Tripathi *et al.*, 2014:52). The physicochemical properties of thiazolidin-4-one are significantly affected by its numerous possible ring system modifications. However, it has been established that modifications to the C2 and C5 positions often result in compounds with optimised biological activity (Molina *et al.*, 2021:130).

Vicini *et al.* (2006:3863) demonstrated that C5-benzylidene substituted thiazolidin-4-one derivatives have significantly greater antibacterial activity compared to analogues wherein the C5 position is unsubstituted. Due to the potential Michael addition of nucleophilic protein

residues to the exocyclic double bond complex, the conjugation of the C5-benzylidene fragment to the C4 carbonyl functional group to form an α,β -unsaturated carbonyl group make such compounds electrophilic and possibly reactive (Kaminsky *et al.*, 2017:552; Lesyk, 2020:34). Thus, these compounds may be regarded as Michael acceptors and covalent binders, which function similarly to β -lactams in their antimicrobial activity (Hammad *et al.*, 2020:2).

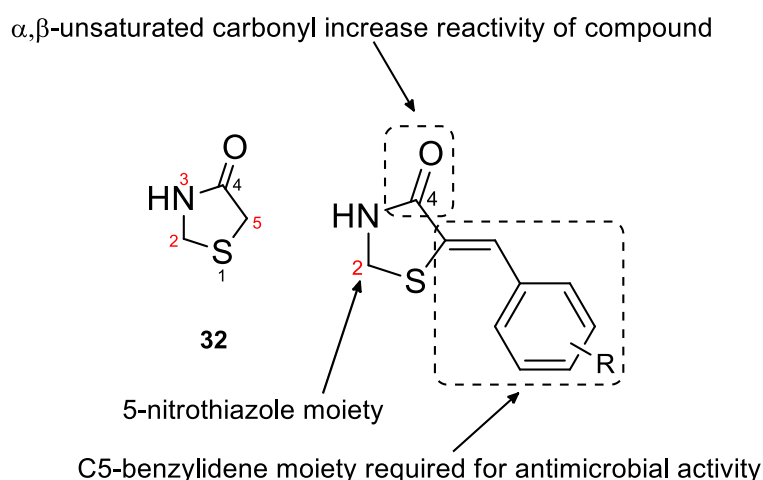
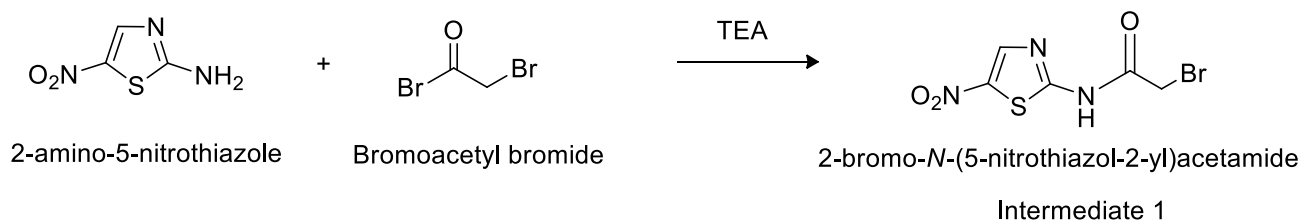


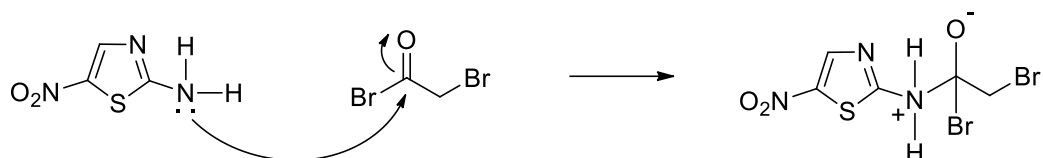
Figure 2.20 Thiazolidin-4-one (**32**) and structure-activity relationship

2.17.3. Mechanism for *N*-acylation reaction (intermediate 1)

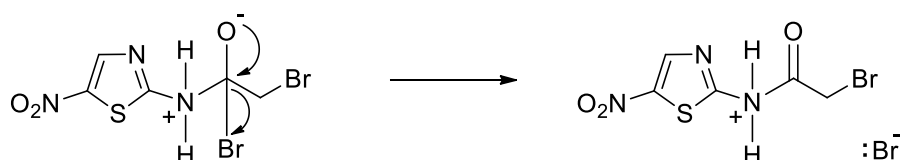


One of the most often utilised reactions in the synthesis of secondary and tertiary amides is the *N*-acylation reaction of amines (Taylor & Bull, 2014). It's interesting to note that varied regioselectivity for acylation agents may be seen in *N*-acylated products. However, the products are often *N*-acylation products with the reaction sites on the primary amine (NH_2) when it is treated with acylation reagents under alkaline conditions at room temperature or

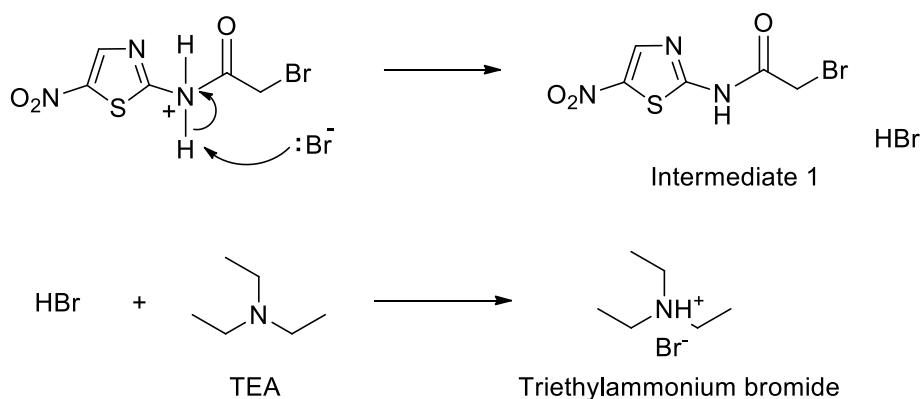
below (Cui *et al.*, 2022:1). In the presence of triethylamine (TEA), the reaction between 2-amino-5-nitrothiazole and bromoacetyl bromide proceeds in two stages: an addition stage and an elimination stage. The amine's (NH₂) lone pair on the nitrogen atom engages in a nucleophilic attack on the carbonyl carbon (C=O) of bromoacetyl bromide during the addition stage. This mechanism totally repels the two electrons from one of the C=O double bonds onto the oxygen, leaving it negatively charged (Clark, 2000).



The elimination stage is divided into two stages. The C=O double bond reforms in the first stage, and a bromide ion is driven off.



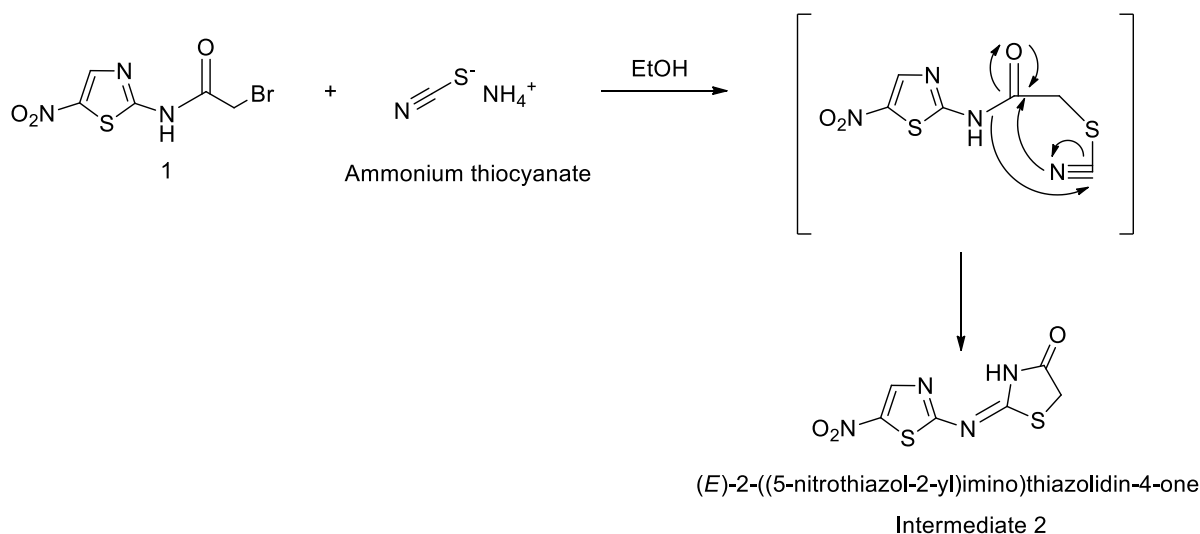
Finally, one of the hydrogen ions attached to the nitrogen is eliminated to afford the desired product (intermediate 1). The hydrogen is eliminated by the free bromide ion, generating HBr, which would instantly react with the TEA (an acid acceptor) in the process to produce insoluble triethylammonium bromide, the hydrobromide salt of triethylamine (Clark, 2000).



2.17.4. Mechanism for dehydrative cyclization reaction (intermediate 2)

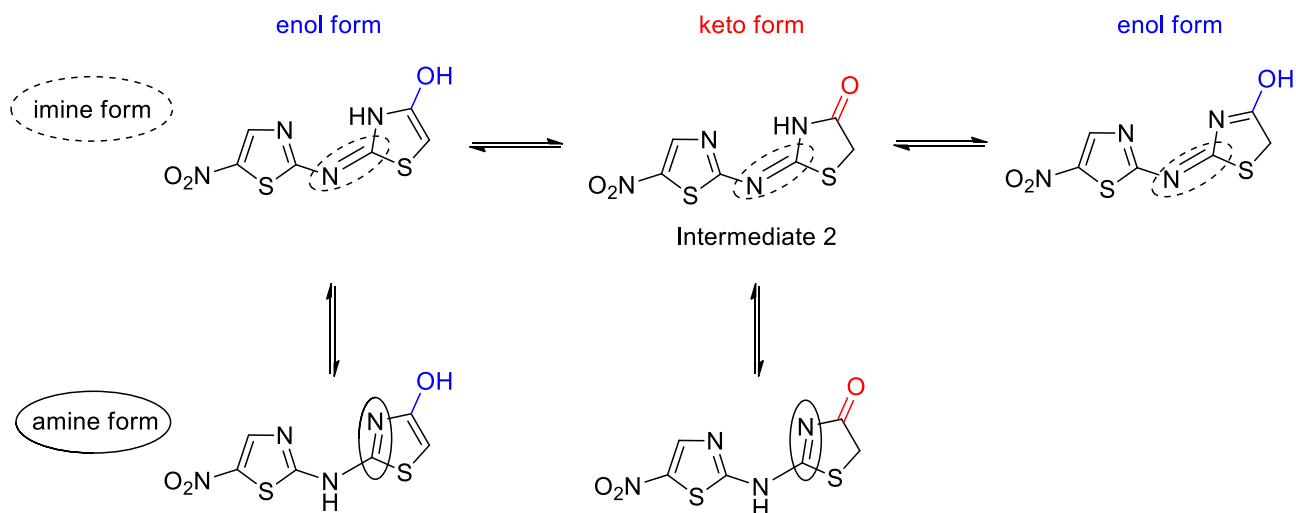
Numerous approaches may be used to synthesize the 4-thiazolidinone ring system. One of these reactions is the cyclization of halogen-containing acetamide compounds in the presence of potassium thiocyanate (Baboo *et al.*, 2017:247; Liu *et al.*, 2000:1056) or ammonium thiocyanate (Çakır *et al.*, 2015:3; Kulabaş *et al.*, 2010:372; Küçükgülzel *et al.*, 2013:9).

In this study, the product (intermediate 1) from the *N*-acylation reaction will be treated with ammonium thiocyanate in refluxing ethanol (EtOH) to attain the desired intermediate 2. It is well known that the reaction does not terminate at the nucleophilic substitution step. Following the removal of water, the reaction proceeds by spontaneous intramolecular cyclization of the α -thiocyanatoamide intermediate and Dimroth-like rearrangements (Abu-Melha, 2018:3–4; Gzella *et al.*, 2014:813; Tripathi *et al.*, 2014:53). The reaction's most probable mechanism is shown here.

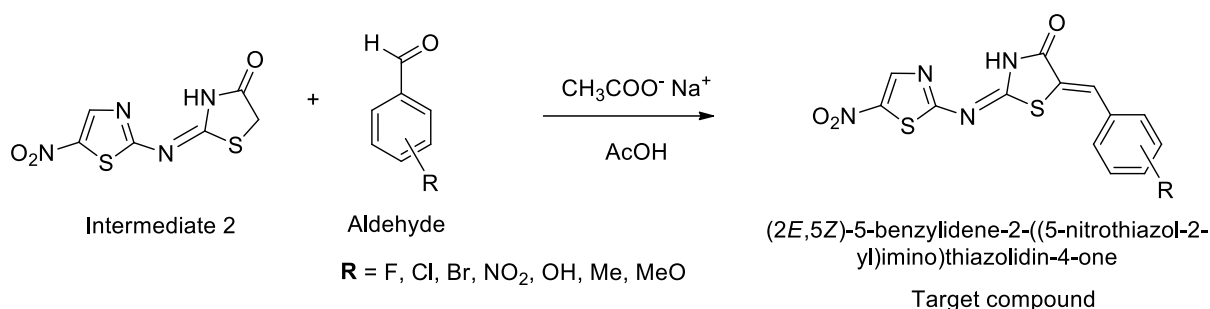


The synthesis of intermediate 2 comprises a tautomeric mixture of keto/enol and amino/imino forms. The structure below is an example of a probable tautomeric equilibrium for the synthesis of intermediate 2 (adapted from Türe *et al.*, 2021:1029). The lack of hydroxylic (OH) functional groups in intermediate 2's FTIR and ^1H NMR spectra will rule out tautomerism involving an enol form (Chawla *et al.*, 2012:3268; Nowaczyk *et al.*, 2014:2). 2-imino-4-thiazolidinones (exocyclic C=N bond) and 2-amino-4-thiazolidinones (endocyclic C=N bond)

are two more tautomeric forms of intermediate 2. (Mishchenko *et al.*, 2020:7). A ^1H NMR resonance of a $-\text{NH}-$ proton peaking at roughly 12-13 ppm (downfield) indicates the presence of a $-\text{NH}-$ lactam proton. These downfield $-\text{NH}-$ lactam signals will confirm intermediate 2's keto-imine (exocyclic $\text{C}=\text{N}$) tautomeric structure. This is also significant evidence for ring closure (Vicini *et al.*, 2008:3715; Geronikaki *et al.*, 2008:5222).



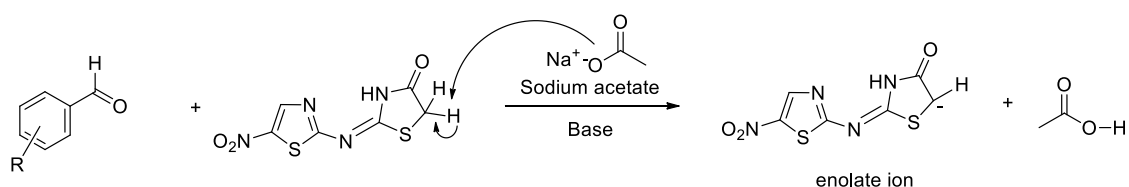
2.17.5. Mechanism for Knoevenagel condensation reaction (target compounds)



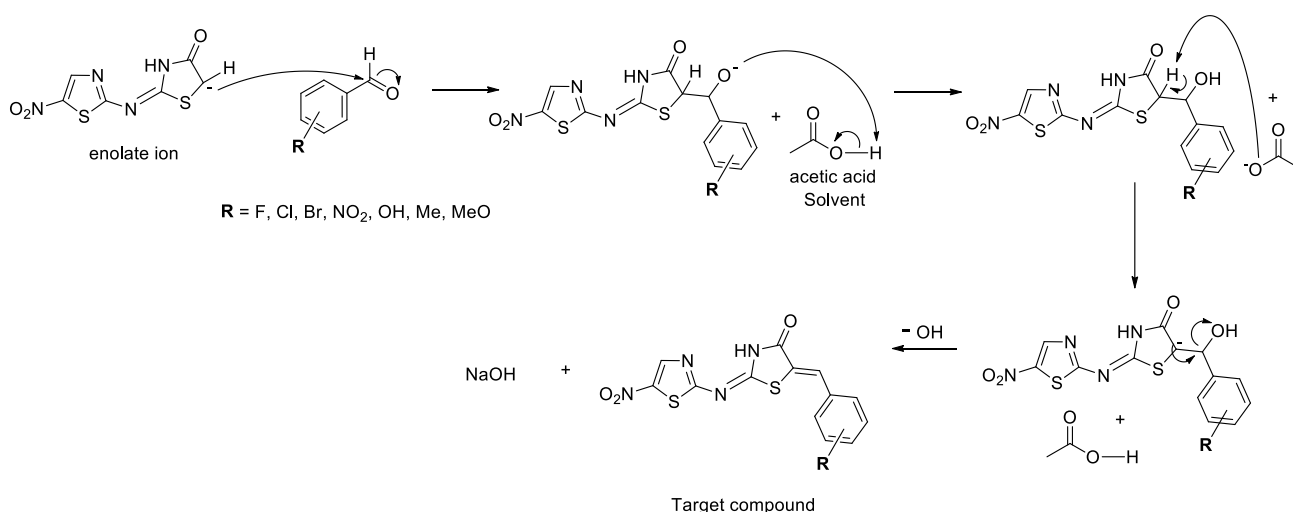
The Knoevenagel condensation reaction is a modified Aldol condensation in which an aldehyde or ketone is added to an active methylene (CH_2) compound in the presence of a basic catalyst, followed by dehydration to yield a conjugated enone product. The reaction is known as nucleophilic addition and the product is often referred to as an α, β -unsaturated ketone (Heravi *et al.*, 2020:439; Lin *et al.*, 2017:10).

In the instance of intermediate 2, the active methylene compounds are those flanked by two electron withdrawing groups, namely a carbonyl carbon (C=O) and a sulphur atom (S). These electron-withdrawing groups render the methylene group's hydrogen atoms acidic, which may be readily removed with a suitable base. As a result, these hydrogen atoms are known as "active hydrogen atoms," since they are ionisable owing to the electron withdrawing effect of the surrounding groups (Bakhshi *et al.*, 2013).

Thus, the mechanism of Knoevenagel condensation necessitates the formation of a carbanion, which attacks the electrophilic center of the other molecule as a nucleophile. So, deprotonation of the activated methylene by the base (sodium acetate) generates a carbanion, which is stabilized by resonance with an enolate ion (Rupainwar & Pandey, 2019:424).

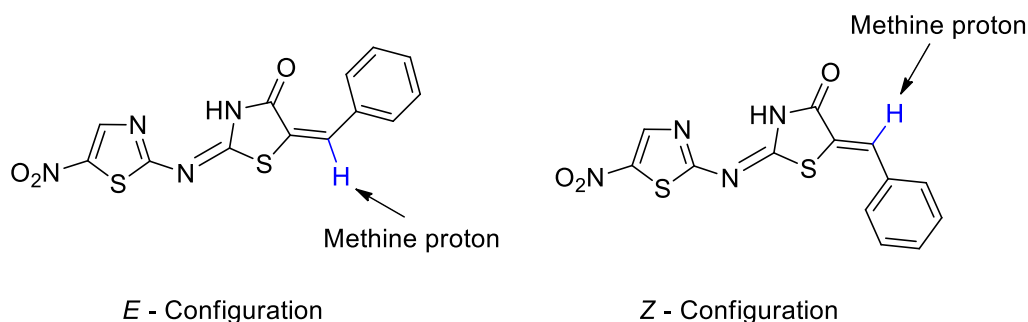


Furthermore, according to the mechanistic considerations, this enolate ion attacks as a nucleophile on the carbonyl carbon (C=O) of the aldehyde. The resulting intermediate further undergoes base-induced elimination to afford the target compounds (Bakhshi *et al.*, 2013).



With regard to the exocyclic C=C bond, the target compounds may exist as possible *E* and *Z* geometrical isomers (see structure below). ¹H NMR spectral analysis will be used to validate the *Z* configuration of the exocyclic C=C bond in the target compounds. Because of the

deshielding effect of the adjacent C=O group, the methine proton resonates at higher chemical shift values (7.7-7.8 ppm as a single peak of one proton) in the *Z* isomer, whereas it resonates at lower chemical shifts in the *E* isomer due to the comparatively less deshielding effect of the sulphur atom (Abdellatif *et al.*, 2015:153; Çakır *et al.*, 2015:4; Chawla *et al.*, 2012:3268).



2.18. Summary and rational design of target compounds

The literature review pertaining to this study focused on providing more insight into existing literature and information on infectious diseases caused by various bacteria, that are difficult to treat due to a global increase in antimicrobial drug resistance.

Part one focused on tuberculosis (TB), and amongst others, how it presents in terms of epidemiology, cellular morphology, pathophysiology, virulence factors and clinical manifestation thereof. The detection and diagnosis of TB were also discussed, followed by an overview of the available treatment options, and the effectiveness of these drugs for both drug-susceptible and drug-resistant TB cases.

Part two focused on hospital-acquired infections (HAIs) and the so-called ESKAPE pathogens which are responsible for most of these infections, secondary to the initial reason for hospital admission. As with the TB-section, different treatment options were also discussed. However, it has been established that most bacteria are resistant or not susceptible to routinely prescribed antibiotics now in clinical use.

Literature reveals that the MOA of NTZ largely depends on the reduction of the 5-nitrothiazole moiety through PFOR. However, it has been shown that NTZ exhibit a unique and interesting MOA against Mtb as well as a low frequency of resistance. Lastly, Thiazolidin-4-one derivatives have been reported to exhibit broad pharmacological activities. Their MOA, although not precisely known, is unlikely akin to that presented by 5-nitrothiazole derivatives in general. Based on this assumption, we do believe that generating molecules that contain a 5-nitrothiazole moiety appended to thiazolidin-4-one might lead to novel compounds with a novel MOA and/or poly-pharmacology against a variety of resistant microbial pathogens.

The next chapter contains the crux of the study in the form of the published research article on the topic, and will focus more on the synthesis of novel compounds screened for antimicrobial activity against the bacterium that causes TB as well as the ESKAPE pathogens.

REFERENCE LIST – CHAPTER 2

- Abdellatif, K.R., Abdelall, E.K., Abdelgawad, M.A., Abdelhakeem, M.M. & Omar, H.A. 2015. Design and synthesis of certain novel arylidene thiazolidinone derivatives as anticancer agents. *Der Pharma Chemica*, 7(8): 149-161. Date of access: 15 Dec. 2022.
- Abu-Melha, S. 2018. Synthesis, modeling study and antioxidants activity of new heterocycles derived from 4-antipyrinyl-2-chloroacetamidothiazoles. *Applied Sciences*, 8(11), art. #2128. <https://doi.org/10.3390/app8112128>
- Acharya, B., Acharya, A., Gautam, S., Ghimire, S.P., Mishra, G., Parajuli, N. & Sapkota, B. 2020. Advances in diagnosis of tuberculosis: an update into molecular diagnosis of *Mycobacterium tuberculosis*. *Molecular Biology Reports*, 47(5): 4065-4075. <https://doi-org.nwulib.nwu.ac.za/10.1007/s11033-020-05413-7>
- Ager, S. & Gould, K. 2012. Clinical update on linezolid in the treatment of Gram-positive bacterial infections. *Infection and Drug Resistance*, 5: 87-102. doi:10.2147/IDR.S25890
- Ahamad, N., Gupta, S. & Parashar, D. 2022. Using omics to study leprosy, tuberculosis, and other mycobacterial diseases. *Frontiers in Cellular and Infection Microbiology*, 12, art. #792617. <https://doi.org/10.3389/fcimb.2022.792617>
- Ahmad, S. 2011. Pathogenesis, immunology, and diagnosis of latent *Mycobacterium tuberculosis* infection. *Clinical and Developmental Immunology*, 2011, art. #814943. doi:10.1155/2011/814943
- AHRQ (Agency for Healthcare Research and Quality). 2017. *Estimating the Additional Hospital Inpatient Cost and Mortality Associated With Selected Hospital-Acquired Conditions*. <https://www.ahrq.gov/hai/pfp/haccost2017-results.html> Date of access: 07 May. 2022.
- Ai, J.-W., Ruan, Q.-L., Liu, Q.-H. & Zhang, W.-H. 2016. Updates on the risk factors for latent tuberculosis reactivation and their managements. *Emerging Microbes and Infections*, 5(1): 1-8. doi:10.1038/emi.2016.10

Alderwick, L.J., Harrison, J., Lloyd, G.S. & Birch, H.L. 2015. The mycobacterial cell wall–peptidoglycan and arabinogalactan. *Cold Spring Harbor Perspectives in Medicine*, 5(8), a021113. doi:10.1101/cshperspect.a021113

Alexandrou, A.J., Duncan, R.S., Sullivan, A., Hancox, J.C., Leishman, D.J., Witchel, H.J. & Leaney, J.L. 2006. Mechanism of Herg K⁺ channel blockade by the fluoroquinolone antibiotic moxifloxacin. *British Journal of Pharmacology*, 147(8): 905-916.
<https://doi.org/10.1038/sj.bjp.0706678>

Alkaaki, A., Al-Radi, O.O., Khoja, A., Alnawawi, A., Alnawawi, A., Maghrabi, A., ... Aljiffry, M. 2019. Surgical site infection following abdominal surgery: a prospective cohort study. *Canadian Journal of Surgery*, 62(2): 111-117. doi:10.1503/cjs.004818

Allué-Guardia, A., García, J.I. & Torrelles, J.B. 2021. Evolution of drug-resistant *Mycobacterium tuberculosis* strains and their adaptation to the human lung environment. *Frontiers in Microbiology*, 12, art. #612675 <https://doi.org/10.3389/fmicb.2021.612675>

Almeida Santos, J., Duarte, R. & Nunes, C. 2020. Tuberculin skin test and predictive host factors for false-negative results in patients with pulmonary and extrapulmonary tuberculosis. *The Clinical Respiratory Journal*, 14(6): 541-548. doi:10.1111/crj.13166

Alsaifi, A.J., Shah, H.B.U., Alsayali, M.M., Mandoura, N., Assiri, M., Almohammadi, E.L., ... Algarni, F. 2019. High non-compliance rate with anti-tuberculosis treatment: a need to shift facility-based directly observed therapy short course (DOTS) to community mobile outreach team supervision in Saudi Arabia. *BMC Public Health*, 19(1), art. #1168.
<https://doi.org/10.1186/s12889-019-7520-8>

Alves, S.B., Guimarães, E.E.R., Braga, J.R., Neves, H.C.C., Dos Santos, S.D.L.V. & Moreira, M.A.C. 2021. Central line-associated bloodstream infection trend in Brazilian adult intensive care units: an ecological study. *The Journal of Infection in Developing Countries*, 15(11): 1744-1749. doi:10.3855/jidc.14730

Alzayer, Z. & Al Nasser, Y. 2021. *Primary Lung Tuberculosis*. Available from StatPearls: <https://www.ncbi.nlm.nih.gov/books/NBK567737/?report=classic> Date of access: 05 Feb. 2022.

Ament, P.W., Jamshed, N. & Horne, J.P. 2002. Linezolid: its role in the treatment of Gram-positive, drug-resistant bacterial infections. *American Family Physician*, 65(4): 663-671. Date of access: 30 Mar. 2022.

Andersen, P. & Doherty, T.M. 2005. The success and failure of BCG—implications for a novel tuberculosis vaccine. *Nature Reviews Microbiology*, 3(8): 656-662.
<https://doi.org/10.1038/nrmicro1211>

Anderson, V.R. & Curran, M.P. 2007. Nitazoxanide. *Drugs*, 67(13): 1947-1967.
<https://doi.org/10.2165/00003495-200767130-00015>

Andries, K., Verhasselt, P., Guillemont, J., Göhlmann, H.W.H., Neefs, J.-M., Winkler, H., ... Jarlier, V. 2005. A diarylquinoline drug active on the ATP synthase of *Mycobacterium tuberculosis*. *Science*, 307(5707): 223-227. doi:10.1126/science.1106753

Angula, K.T., Legoabe, L.J. & Beteck, R.M. 2021. Chemical classes presenting novel antituberculosis agents currently in different phases of drug development: a 2010–2020 review. *Pharmaceuticals*, 14(5), art. #461. <https://doi.org/10.3390/ph14050461>

Ani Fatonah, I., Wicaksono, S. & Tambunan, U.S.F. 2019. Strategies of tuberculosis–hiv vaccines design using immunoinformatic approach. *Journal of Biological Sciences*, 19(2): 110-116. doi:10.3844/ojbsci.2019.110.116

Arbex, M.A., Varella, M.D.C.L., Siqueira, H.R.D. & Mello, F.A.F.D. 2010. Antituberculosis drugs: drug interactions, adverse effects, and use in special situations-part 1: first-line drugs. *Jornal Brasileiro de Pneumologia*, 36(5): 626-640. <https://doi.org/10.1590/S1806-37132010000500016>

Aristoff, P.A., Garcia, G.A., Kirchhoff, P.D. & Hollis Showalter, H.D. 2010. Rifamycins – Obstacles and opportunities. *Tuberculosis*, 90(2): 94-118.
<https://doi.org/10.1016/j.tube.2010.02.001>

Ashurst, J.V. & Dawson, A. 2022. *Klebsiella Pneumonia*. Available from StatPearls:
<https://www.ncbi.nlm.nih.gov/books/NBK519004/> Date of access: 14 Jun. 2022.

Azad, K.A.K. & Chowdhury, T. 2022. Extrapulmonary tuberculosis (Eptb): an overview. *Bangladesh Journal of Medicine*, 33(2): 130-137. <https://doi.org/10.3329/bjm.v33i2.59285>

Azam, M.W. & Khan, A.U. 2019. Updates on the pathogenicity status of *Pseudomonas aeruginosa*. *Drug Discovery Today*, 24(1): 350-359.

<https://doi.org/10.1016/j.drudis.2018.07.003>

Babic, M., Hujer, A.M. & Bonomo, R.A. 2006. What's new in antibiotic resistance? Focus on beta-lactamases. *Drug Resistance Updates*, 9(3): 142-156.

<https://doi.org/10.1016/j.drug.2006.05.005>

Baboo, P., Gautam, G. & Gupta, S.K. 2017. Strategies for the synthesis and biological screening of thiazolidinone derivatives. *Asian Journal of Research in Chemistry*, 10(2): 240-248. doi:10.5958/0974-4150.2017.00039.6

Badrinath, M. & John, S. 2018. *Isoniazid toxicity*. Available from StatPearls:

<https://www.ncbi.nlm.nih.gov/books/NBK531488/> Date of access: 07 Mar. 2022.

Bahuguna, A. & Rawat, D.S. 2019. An overview of new antitubercular drugs, drug candidates, and their targets. *Medicinal Research Reviews*, 40(1): 263-292.

<https://doi.org/10.1002/med.21602>

Baik, J., Stringer, K.A., Mane, G. & Rosania, G.R. 2013. Multiscale distribution and bioaccumulation analysis of clofazimine reveals a massive immune system-mediated xenobiotic sequestration response. *Antimicrobial Agents and Chemotherapy*, 57(3): 1218-1230. doi:10.1128/AAC.01731-12

Bakhshi, A.K., Rarh, V., Rawat, D.S., Milhotra, A. & Krishnamurty, H.G. 2013. *Organic Chemistry- III (Reaction Mechanism-II): Perkin and Knoevenagel condensation*. Available from e-PGPathshala:

<https://epgp.inflibnet.ac.in/Home/ViewSubject?catid=13G8VouhmrFfuhs6rkiyTA==> Date of access: 17 Dec. 2022.

Ball, P. 2000a. Quinolone generations: natural history or natural selection? *Journal of Antimicrobial Chemotherapy*, 46(suppl_3): 17-24.

<https://doi.org/10.1093/oxfordjournals.jac.a020889>

Bailey, M.A., Na, H., Duthie, M.S., Gillis, T.P., Lahiri, R. & Parish, T. 2017. Nitazoxanide is active against *Mycobacterium leprae*. *PloS One*, 12(8), e0184107.

<https://doi.org/10.1371/journal.pone.0184107>

Barberis, I., Bragazzi, N.L., Galluzzo, L. & Martini, M. 2017. The history of tuberculosis: from the first historical records to the isolation of Koch's bacillus. *Journal of Preventive Medicine and Hygiene*, 58(1): E9-E12. Date of access: 26 Jan. 2022.

Baulard, A.R., Betts, J.C., Engohang-Ndong, J., Quan, S., Mcadam, R.A., Brennan, P.J., ... Besra, G.S. 2000. Activation of the Pro-drug Ethionamide Is Regulated in Mycobacteria*. *Journal of Biological Chemistry*, 275(36): 28326-28331.
<https://doi.org/10.1074/jbc.M003744200>

Bayot, M.L., Mirza, T.M. & Sharma, S. 2019. *Acid Fast Bacteria*. Available from StatPearls: <https://www.ncbi.nlm.nih.gov/books/NBK537121/> Date of access: 06 Mar. 2022.

Black, T.A. & Buchwald, U.K. 2021. The pipeline of new molecules and regimens against drug-resistant tuberculosis. *Mycobacterial Diseases*, 25, art. #100285.
<https://doi.org/10.1016/j.ictube.2021.100285>

Blot, K., Hammami, N., Blot, S., Vogelaers, D. & Lambert, M.L. 2022. Gram-negative central line-associated bloodstream infection incidence peak during the summer: a national seasonality cohort study. *Scientific Reports*, 12(1): art. #5202
<https://doi.org/10.1038/s41598-022-08973-9>

Bunduc, C.M., Bitter, W. & Houben, E.N.G. 2020. Structure and function of the mycobacterial type VII secretion systems. *Annual Review of Microbiology*, 74, 315-335.
<https://doi.org/10.1146/annurev-micro-012420-081657>

Bush, N.G., Diez-Santos, I., Abbott, L.R. & Maxwell, A. 2020. Quinolones: mechanism, lethality and their contributions to antibiotic resistance. *Molecules*, 25(23), art. #5662.
doi:10.3390/molecules25235662

Cai, Y., Chai, D., Wang, R., Liang, B. & Bai, N. 2012. Colistin resistance of *Acinetobacter baumannii*: clinical reports, mechanisms and antimicrobial strategies. *Journal of Antimicrobial Chemotherapy*, 67(7): 1607-1615. <https://doi.org/10.1093/jac/dks084>

Çakır, G., Küçükgülzel, İ., Guhamazumder, R., Tatar, E., Manvar, D., Basu, A., ... Kaushik-Basu, N. 2015. Novel 4-thiazolidinones as non-nucleoside inhibitors of hepatitis C virus NS5B RNA-dependent RNA polymerase. *Archiv der Pharmazie*, 348(1): 10-22.
<https://doi.org/10.1002/ardp.201400247>

Cambau, E. & Drancourt, M. 2014. Steps towards the discovery of *Mycobacterium tuberculosis* by Robert Koch, 1882. *Clinical Microbiology and Infection*, 20(3): 196-201.
<https://doi.org/10.1111/1469-0691.12555>

Cambier, C.J., Falkow, S. & Ramakrishnan, L. 2014. Host evasion and exploitation schemes of *Mycobacterium tuberculosis*. *Cell*, 159(7): 1497-1509.
<https://doi.org/10.1016/j.cell.2014.11.024>

Caulfield, A.J. & Wengenack, N.L. 2016. Diagnosis of active tuberculosis disease: from microscopy to molecular techniques. *Journal of Clinical Tuberculosis and Other Mycobacterial Diseases*, 4: 33-43. <https://doi.org/10.1016/j.ictube.2016.05.005>

CDC (Centre for Disease Prevention and Control). 2009. *Guideline for Prevention of Catheter-Associated Urinary Tract Infections*.
<https://www.cdc.gov/infectioncontrol/guidelines/cauti/background.html> Date of access: 07 May. 2022.

CDC (Centre for Disease Prevention and Control). 2014. *Types of Healthcare-associated Infections*. <https://www.cdc.gov/hai/infectiontypes.html> Date of access: 07 May. 2022.

CDC (Centre for Disease Prevention and Control). 2016a. *A New Tool to Diagnose Tuberculosis: The Xpert MTB/RIF Assay*.
https://www.cdc.gov/tb/publications/factsheets/testing/xpert_mtb-rif.htm Date of access: 23 Apr. 2022.

CDC (Centre for Disease Prevention and Control). 2016b. *BCG Vaccine*.
<https://www.cdc.gov/tb/publications/factsheets/prevention/bcg.htm> Date of access: 04 Mar. 2022.

CDC (Centre for Disease Prevention and Control). 2016c. *Highlights from the 2016 Treatment of Drug-Susceptible Tuberculosis Guidelines*.
<https://www.cdc.gov/tb/topic/treatment/guidelinehighlights.htm> Date of access: 07 Mar. 2022.

CDC (Centre for Disease Prevention and Control). 2017. *Drug-Resistant TB*.
[https://www.cdc.gov/tb/topic/drtb/default.htm#:~:text=Multidrug%2Dresistant%20TB%20\(MDR%20TB\)%20is%20caused%20by%20TB,all%20persons%20with%20TB%20disease](https://www.cdc.gov/tb/topic/drtb/default.htm#:~:text=Multidrug%2Dresistant%20TB%20(MDR%20TB)%20is%20caused%20by%20TB,all%20persons%20with%20TB%20disease) Date of access: 07 Mar. 2022.

CDC (Centre for Disease Prevention and Control). 2022. *TB testing & diagnosis*.
<https://www.cdc.gov/tb/topic/testing/default.htm> Date of access: 15 Aug. 2022.

Cegielski, P., Nunn, P., Kurbatova, E.V., Weyer, K., Dalton, T.L., Wares, D.F., ... Raviglione, M. 2012. Challenges and controversies in defining totally drug-resistant tuberculosis. *Emerging Infectious Diseases*, 18(11), e2. doi:10.3201/eid1811.120526

Chahine, E.B., Karaoui, L.R. & Mansour, H. 2014. Bedaquiline: a novel diarylquinoline for multidrug-resistant tuberculosis. *Annals of Pharmacotherapy*, 48(1): 107-115.
<https://doi.org/10.1177/1060028013504087>

Chai, Q., Lu, Z. & Liu, C.H. 2020. Host defense mechanisms against *Mycobacterium tuberculosis*. *Cellular and Molecular Life Sciences*, 77(10): 1859-1878.
<https://doi.org/10.1007/s00018-019-03353-5>

Chakraborty, S., Gruber, T., Barry, C.E., III, Boshoff, H.I. & Rhee, K.Y. 2013. Para-aminosalicylic acid acts as an alternative substrate of folate metabolism in *Mycobacterium tuberculosis*. *Science*, 339(6115): 88-91. doi:10.1126/science.1228980

Chawla, P., Singh, R. & Saraf, S.K. 2012. Effect of chloro and fluoro groups on the antimicrobial activity of 2, 5-disubstituted 4-thiazolidinones: a comparative study. *Medicinal Chemistry Research*, 21(10): 3263-3271. <https://doi.org/10.1007/s00044-011-9864-1>

Chastre, J. & Fagon, J.-Y. 2002. Ventilator-associated pneumonia. *American Journal of Respiratory and Critical Care Medicine*, 165(7): 867-903.
<https://doi.org/10.1164/ajrccm.165.7.2105078>

Chen, C.-Y., Weng, J.-Y., Huang, H.-H., Yen, W.-C., Tsai, Y.-H., Cheng, T.C. & Jou, R. 2019. A new oligonucleotide array for the detection of multidrug and extensively drug-resistance tuberculosis. *Scientific Reports*, 9(1), art. #4425. <https://doi.org/10.1038/s41598-019-39339-3>

Childs-Kean, L.M., Shaeer, K.M., Varghese Gupta, S. & Cho, J.C. 2019. Aminoglycoside allergic reactions. *Pharmacy*, 7(3), art. #124. <https://doi.org/10.3390/pharmacy7030124>

Cholo, M.C., Mothiba, M.T., Fourie, B. & Anderson, R. 2017. Mechanisms of action and therapeutic efficacies of the lipophilic antimycobacterial agents clofazimine and bedaquiline. *Journal of Antimicrobial Chemotherapy*, 72(2): 338-353. <https://doi.org/10.1093/jac/dkw426>

Cholo, M.C., Steel, H.C., Fourie, P.B., Germishuizen, W.A. & Anderson, R. 2011. Clofazimine: current status and future prospects. *Journal of Antimicrobial Chemotherapy*, 67(2): 290-298. <https://doi.org/10.1093/jac/dkr444>

Choo, E.J. & Chambers, H.F. 2016. Treatment of methicillin-resistant *Staphylococcus aureus* bacteremia. *Infection & Chemotherapy*, 48(4): 267-273. doi:10.3947/ic.2016.48.4.267

Clark, J. 2000. *Explaining nucleophilic addition / elimination in the reaction between acyl chlorides and amines*. <https://www.chemguide.co.uk/mechanisms/addelim/aminestt.html>

Date of access: 17 Dec. 2022.

Clover, E., Abrahamson, A., Adams, J., Poken, S.R., Hainsworth, S.L., Lamprecht, A., ... Maasdorp, S.D. 2022. Central line-associated bloodstream infections at the multidisciplinary intensive care unit of Universitas Academic Hospital, Bloemfontein, South Africa. *African Journal of Thoracic and Critical Care Medicine*, 28(1): 15-19. <https://doi.org/10.7196/AJTCCM.2022.v28i1.175>

Cohen, K.A., Stott, K.E., Munsamy, V., Manson, A.L., Earl, A.M. & Pym, A.S. 2020. Evidence for expanding the role of streptomycin in the management of drug-resistant *Mycobacterium tuberculosis*. *Antimicrobial Agents and Chemotherapy*, 64(9), e00860-20. <https://doi.org/10.1128/AAC.00860-20>

Conly, J.M. & Johnston, B.L. 2002. VISA, hetero-VISA and VRSA: the end of the vancomycin era? *The Canadian Journal of Infectious Diseases*, 13(5): 282-284. doi:10.1155/2002/245109

Court, R., Centner, C.M., Chirehwa, M., Wiesner, L., Denti, P., De Vries, N., ... Mcilleron, H. 2021. Neuropsychiatric toxicity and cycloserine concentrations during treatment for multidrug-resistant tuberculosis. *International Journal of Infectious Diseases*, 105(2021): 688-694. <https://doi.org/10.1016/j.ijid.2021.03.001>

Cox, H., Dickson-Hall, L., Ndjeka, N., Van't Hoog, A., Grant, A., Cobelens, F., ... Nicol, M. 2017. Delays and loss to follow-up before treatment of drug-resistant tuberculosis following

implementation of Xpert MTB/RIF in South Africa: a retrospective cohort study. *PloS Medicine*, 14(2), art. #e1002238. <https://doi.org/10.1371/journal.pmed.1002238>

Cresswell, F.V., Ssebambulidde, K., Grint, D., Te Brake, L., Musabire, A., Atherton, R.R., ... Elliott, A.M. 2018. High dose oral and intravenous rifampicin for improved survival from adult tuberculous meningitis: a phase II open-label randomised controlled trial (the RifT study). *Wellcome Open Research*, 3, art. #83. doi:10.12688/wellcomeopenres.14691.1

Cudahy, P. & Shenoi, S.V. 2016. Diagnostics for pulmonary tuberculosis. *Postgraduate Medical Journal*, 92(1086): 187-193. doi:10.1136/postgradmedj-2015-133278

Cui, J., Zhou, L., Zhang, X., Wei, X. & Yan, H. 2022. Revealing the regioselective *N*-acylation of 5-bromo-2-aminobenzimidazole using experiment and theoretical calculation. *Tetrahedron*, 120, art. #32905. <https://doi.org/10.1016/j.tet.2022.132905>

Dadi, N.C.T., Radochová, B., Vargová, J. & Bujdáková, H. 2021. Impact of healthcare-associated infections connected to medical devices—an update. *Microorganisms*, 9(11), art. #2332. <https://doi.org/10.3390/microorganisms9112332>

Daniel, T.M. 2006. The history of tuberculosis. *Respiratory Medicine*, 100(11): 1862-1870. doi:10.1016/j.rmed.2006.08.006

Darvishi, M., Forootan, M., Nazer, M.R., Karimi, E. & Noori, M. 2020. Nosocomial infections, challenges and threats: a review article. *Iranian Journal of Medical Microbiology*, 14(2): 162-181. doi:10.30699/ijmm.14.2.162

David, A., Singh, L., Da Silva, P., Scott, L. & Stevens, W. 2020. The performance of the Abbott real time MTB RIF/INH compared to the MTBDRplus V2 for the identification of MDR-TB among isolates. *Infection and Drug Resistance*, 13: 3301–3308. doi:10.2147/IDR.S247524

Davin-Regli, A., Lavigne, J.P. & Pagès, J.M. 2019. Enterobacter spp.: update on taxonomy, clinical aspects, and emerging antimicrobial resistance. *Clinical Microbiology Reviews*, 32(4), e00002-19. doi:10.1128/CMR.00002-19

De Backer, A., Mortelet, K., De Keulenaer, B. & Parizel, P. 2006. Tuberculosis: epidemiology, manifestations, and the value of medical imaging in diagnosis. *Journal of the Belgian Society of Radiology*, 89(5): 243-250. Date of access: 05 Feb. 2022.

De Carvalho, L.P.S., Darby, C.M., Rhee, K.Y. & Nathan, C. 2011. Nitazoxanide disrupts membrane potential and intrabacterial pH homeostasis of *Mycobacterium tuberculosis*. *ACS Medicinal Chemistry Letters*, 2(11): 849-854. <https://doi.org/10.1021/ml200157f>

De Carvalho, L.P.S., Lin, G., Jiang, X. & Nathan, C. 2009. Nitazoxanide kills replicating and nonreplicating *Mycobacterium tuberculosis* and evades resistance. *Journal of Medicinal Chemistry*, 52(19): 5789-5792. <https://doi.org/10.1021/jm9010719>

De Kock, L., Sy, S.K., Rosenkranz, B., Diacon, A.H., Prescott, K., Hernandez, K.R., ... Donald, P.R. 2014. Pharmacokinetics of *para*-aminosalicylic acid in HIV-uninfected and HIV-coinfected tuberculosis patients receiving antiretroviral therapy, managed for multidrug-resistant and extensively drug-resistant tuberculosis. *Antimicrobial Agents and Chemotherapy*, 58(10): 6242-6250. doi:10.1128/AAC.03073-14

De Oliveira, D.M., Forde, B.M., Kidd, T.J., Harris, P.N., Schembri, M.A., Beatson, S.A., ... Walker, M.J. 2020. Antimicrobial resistance in ESKAPE pathogens. *Clinical Microbiology Reviews*, 33(3), art. #e00181-19. <https://doi.org/10.1128/CMR.00181-19>

De Vriese, A.S., Van Coster, R., Smet, J., Seneca, S., Lovering, A., Van Haute, L.L., ... Boelaert, J.R. 2006. Linezolid-induced inhibition of mitochondrial protein synthesis. *Clinical Infectious Diseases*, 42(8): 1111-1117. <https://doi.org/10.1086/501356>

Deck, D.H. & Winston, L.G. 2012a. Antimycobacterial drugs. In: Katzung, B.G., Masters, S.B. & Trevor, A.J., eds. *Basic & Clinical Pharmacology*. NY: Lange Medical. pp. 839-847.

Deck, D.H. & Winston, L.G. 2012b. Sulfonamides, Trimethoprim & Quinolones. In: Katzung, B.G., Masters, S.B. & Trevor, A.J., eds. *Basic & clinical pharmacology*. NY: Lange Medical. pp. 831-838.

Deck, D.H. & Winston, L.G. 2012c. Aminoglycosides & Spectinomycin. In: Katzung, B.G., Masters, S.B. & Trevor, A.J., eds. *Basic & clinical pharmacology*. NY: Lange Medical. pp. 821-829.

Deck, D.H. & Winston, L.G. 2012d. Beta-Lactam & Other Cell Wall- & Membrane-Active Antibiotics. In: Katzung, B.G., Masters, S.B. & Trevor, A.J., eds. *Basic & clinical pharmacology*. NY: Lange Medical. pp. 790-808.

Deck, D.H. & Winston, L.G. 2012e. Tetracyclines, Macrolides, Clindamycin, Chloramphenicol, Streptogramins, & Oxazolidinones. In: Katzung, B.G., Masters, S.B. & Trevor, A.J., eds. *Basic & clinical pharmacology*. NY: Lange Medical. pp. 809-819.

Degiacomi, G., Sammartino, J.C., Sinigiani, V., Marra, P., Urbani, A. & Pasca, M.R. 2020. *In vitro* study of bedaquiline resistance in *Mycobacterium tuberculosis* multi-drug resistant clinical isolates. *Frontiers in Microbiology*, 11, art. #559469.

<https://doi.org/10.3389/fmicb.2020.559469>

Delogu, G., Sali, M. & Fadda, G. 2013. The biology of *Mycobacterium tuberculosis* infection. *Mediterranean Journal of Hematology and Infectious Diseases*, 5(1), e2013070.

doi:10.4084/MJHID.2013.070

Desjardins, C.A., Cohen, K.A., Munsamy, V., Abeel, T., Maharaj, K., Walker, B.J., ... Pym, A.S. 2016. Genomic and functional analyses of *Mycobacterium tuberculosis* strains implicate ald in D-cycloserine resistance. *Nature Genetics*, 48(5): 544-551. doi:10.1038/ng.3548

Dey, A. & Chatterji, D. 2012. Tracing the Variation in Physiological Response to Rifampicin Across the Microbial Spectrum. *Journal of Bacteriology and Virology*, 42(2): 87-100.

<https://doi.org/10.4167/jbv.2012.42.2.87>

Diacon, A.H., Pym, A., Grobusch, M.P., De Los Rios, J.M., Gotuzzo, E., Vasilyeva, I., Leimane, V., ... De Marez, T. 2014. Multidrug-resistant tuberculosis and culture conversion with bedaquiline. *New England Journal of Medicine*, 371(8): 723-732.

doi:10.1056/NEJMoa1313865

DOH (South Africa). 2019. *Management of rifampicin-resistant tuberculosis*.

<https://www.health.gov.za/wp-content/uploads/2020/11/management-of-rifampicin-resistant-tb-booklet-0220-v11.pdf> Date of access: 25 Mar. 2022.

Dutta, N.K. & Karakousis, P.C. 2014. Latent tuberculosis infection: myths, models, and molecular mechanisms. *Microbiology and Molecular Biology Reviews*, 78(3): 343-371.

doi:10.1128/MMBR.00010-14

ECDP (European Centre for Disease Prevention and Control). 2018. *Handbook on tuberculosis laboratory diagnostic methods in the European Union*.

<https://www.ecdc.europa.eu/en/publications-data/handbook-tuberculosis-laboratory-diagnostic-methods-european-union-updated-2018> Date of access: 17 Aug. 2022.

Eddabra, R. & Ait Benhassou, H. 2018. Rapid molecular assays for detection of tuberculosis. *Pneumonia*, 10(1), art. #4. <https://doi.org/10.1186/s41479-018-0049-2>

Escobar, L. E., Molina-Cruz, A. & Barillas-Mury, C. 2020. BCG vaccine protection from severe coronavirus disease 2019 (COVID-19). *Proceedings of the National Academy of Sciences*, 117(30): 17720-17726. <https://doi.org/10.1073/pnas.2008410117>

Ezelarab, H.A., Abbas, S.H., Hassan, H.A. & Abuo-Rahma, G.E.D.A. 2018. Recent updates of fluoroquinolones as antibacterial agents. *Archiv der Pharmazie*, 351(9), art. #1800141. doi:10.1002/ardp.201800141

Fang, X.-H., Shen, H.-H., Hu, W.-Q., Xu, Q.-Q., Jun, L., Zhang, Z.-P., ... Wu, G.-C. 2019. Prevalence of and factors influencing anti-tuberculosis treatment non-adherence among patients with pulmonary tuberculosis: a cross-sectional study in Anhui province, Eastern China. *International Medical Journal of Experimental and Clinical Research*, 25: 1928-1935. doi:10.12659/MSM.913510

Farrington, C.A. & Allon, M. 2019. Management of the hemodialysis patient with catheter-related bloodstream infection. *Clinical Journal of the American Society of Nephrology*, 14(4): 611-613. <https://doi.org/10.2215/CJN.13171118>

Fatima, S., Kumari, A., Das, G. & Dwivedi, V.P. 2020. Tuberculosis vaccine: A journey from BCG to present. *Life Sciences*, 252, art. #117594. <https://doi.org/10.1016/j.lfs.2020.117594>

Fattorini, L., Piccaro, G., Mustazzolu, A. & Giannoni, F. 2013. Targeting dormant bacilli to fight tuberculosis. *Mediterranean Journal of Hematology and Infectious Diseases*, 5(1), art. # e2013072. doi:10.4084/MJHID.2013.072

Fekadu, G., Tolossa, T., Turi, E., Bekele, F. & Fetensa, G. 2022. Pretomanid development and its clinical roles in treating tuberculosis. *Journal of Global Antimicrobial Resistance*, 31: 175-184

Fernandes, G.F.D.S., Salgado, H.R.N. & Santos, J.L.D. 2017. Isoniazid: a review of characteristics, properties and analytical methods. *Critical Reviews in Analytical Chemistry*, 47(4): 298-308. <https://doi.org/10.1080/10408347.2017.1281098>

Field, S.K. 2015. Bedaquiline for the treatment of multidrug-resistant tuberculosis: great promise or disappointment? *Therapeutic Advances in Chronic Disease*, 6(4): 170-184. <https://doi.org/10.1177/2040622315582325>

Fischer, K. & Phillips, C. 2009. The ecology, epidemiology and virulence of *Enterococcus*. *Microbiology*, 155(6): 1749–1757. doi:10.1099/mic.0.026385-0

Frith, J. 2014. History of tuberculosis. Part 1-phthisis, consumption and the white plague. *Journal of Military and Veterans Health*, 22(2): 29-35. <https://search.informit.org/doi/10.3316/informit.430338287813994>

Gagetti, P., Bonofiglio, L., Gabarrot, G.G., Kaufman, S., Mollerach, M, Vigliarolo L., ... Lopardo, H.A. 2019. Resistance to β -lactams in enterococci. *Revista Argent Ina De Microbiología*, 51(2): 179-183. <https://doi.org/10.1016/j.ram.2018.01.007>

Geronikaki, A., Eleftheriou, P., Vicini, P., Alam, I., Dixit, A. & Saxena, A.K. 2008. 2-Thiazolylimino/heteroarylimino-5-arylidene-4-thiazolidinones as new agents with SHP-2 inhibitory action. *Journal of Medicinal Chemistry*, 51(17): 5221-5228. <https://doi.org/10.1021/jm8004306>

Ginsburg, A.S., Grosset, J.H. & Bishai, W.R. 2003. Fluoroquinolones, tuberculosis, and resistance. *The Lancet Infectious Diseases*, 3(7): 432-442. [https://doi.org/10.1016/S1473-3099\(03\)00671-6](https://doi.org/10.1016/S1473-3099(03)00671-6)

Gopal, M., Padayatchi, N., Metcalfe, J.Z. & O'donnell, M.R. 2013. Systematic review of clofazimine for the treatment of drug-resistant tuberculosis. *The International Journal of Tuberculosis and Lung Disease*, 17(8): 1001-1007. doi:10.5588/ijtld.12.0144

Gopal, P., Yee, M., Sarathy, J., Low, J.L., Sarathy, J.P., Kaya, F., ... Dick, T., 2016. Pyrazinamide resistance is caused by two distinct mechanisms: prevention of coenzyme A depletion and loss of virulence factor synthesis. *ACS Infectious Diseases*, 2(9): 616-626. <https://doi.org/10.1021/acsinfecdis.6b00070>

Gopaldaswamy, R., Dusthacker, V.N.A., Kannayan, S. & Subbian, S. 2021. Extrapulmonary tuberculosis—an update on the diagnosis, treatment and drug resistance. *Journal of Respiration*, 1(2): 141-164. <https://doi.org/10.3390/jor1020015>

Grzelak, E.M., Choules, M.P., Gao, W., Cai, G., Wan, B., Wang, Y. ... Cho, S. 2019. Strategies in anti-*Mycobacterium tuberculosis* drug discovery based on phenotypic screening. *The Journal of Antibiotics*, 72(10): 719-728. <https://doi.org/10.1038/s41429-019-0205-9>

Gumbo, T. 2017. Chemotherapy of Tuberculosis, Mycobacterium avium Complex Disease, and Leprosy. In: Brunton, L.L., Hilal-Dandan, R. & Knollmann, B.C., eds. Goodman & Gilman's: *The Pharmacological Basics of Therapeutics*. 13 ed. NY: McGraw-Hill. pp 1067-1086.

Gzella, A.K., Kowiel, M., Suseł, A., Wojtyra, M.N. & Lesyk, R. 2014. Heterocyclic tautomerism: reassignment of two crystal structures of 2-amino-1, 3-thiazolidin-4-one derivatives. *Acta Crystallographica Section C: Structural Chemistry*, 70(8): 812-816. <https://doi.org/10.1107/S2053229614015162>

Hammad, S.G., El-Gazzar, M.G., Abutaleb, N.S., Li, D., Ramming, I., Shekhar, A., ... Abouzid, K.A. 2020. Synthesis and antimicrobial evaluation of new halogenated 1,3-Thiazolidin-4-ones. *Bioorganic Chemistry*, 95: art. #103517. <https://doi.org/10.1016/j.bioorg.2019.103517>

Hards, K., McMillan, D.G., Schurig-Briccio, L.A., Gennis, R.B., Lill, H., Bald, D. & Cook, G.M. 2018. Ionophoric effects of the antitubercular drug bedaquiline. *Proceedings of the National Academy of Sciences*, 115(28): 7326-7331. <https://doi.org/10.1073/pnas.1803723115>

Harland, C.W., Rabuka, D., Bertozzi, C.R. & Parthasarathy, R. 2008. The *Mycobacterium tuberculosis* virulence factor trehalose dimycolate imparts desiccation resistance to model mycobacterial membranes. *Biophysical Journal*, 94(12): 4718-4724.
doi:10.1529/biophysj.107.125542

Harries, A.D. & Kumar, A.M. 2018. Challenges and progress with diagnosing pulmonary tuberculosis in low-and middle-income countries. *Diagnostics*, 8(4), art. #78. <https://doi.org/10.3390/diagnostics8040078>

Hartkoorn, R.C., Uplekar, S. & Cole, S.T. 2014. Cross-resistance between clofazimine and bedaquiline through upregulation of MmpL5 in *Mycobacterium tuberculosis*. *Antimicrobial Agents and Chemotherapy*, 58(5): 2979-2981. doi:10.1128/AAC.00037-14

Hassani, M. 2014. The crisis of resistant Gram-negative bacterial infections: Is there any hope for ESKAPE. *Clinical Research in Infectious Diseases*, 1(1), art. #1005. Date of access: 11 May. 2022.

Hazbón, M.H., Valle, M.B.D., Guerrero, M.I., Varma-Basil, M., Filliol, I., Cavatore, M., ... Alland, D. 2005. Role of *embB* Codon 306 Mutations in *Mycobacterium tuberculosis* Revisited: a Novel Association with Broad Drug Resistance and IS6110 Clustering Rather than Ethambutol Resistance. *Antimicrobial Agents and Chemotherapy*, 49(9): 3794-3802. doi:10.1128/AAC.49.9.3794-3802.2005

Hegde, P., Boshoff, H.I.M., Rusman, Y., Aragaw, W.W., Salomon, C.E., Dick, T. & Aldrich, C.C. 2021. Reinvestigation of the structure-activity relationships of isoniazid. *Tuberculosis*, 129, art. #102100. <https://doi.org/10.1016/j.tube.2021.102100>

Hemphill, A., Mueller, J. & Esposito, M. 2006. Nitazoxanide, a broad-spectrum thiazolide anti-infective agent for the treatment of gastrointestinal infections. *Expert Opinion on Pharmacotherapy*, 7(7): 953-964. <https://doi.org/10.1517/14656566.7.7.953>

Heo, J., Koh, D., Woo, M., Kwon, D., De Almeida Falcão, V.C., Wood, C., Lee, H., ... Delorme, V. 2022. A combination screening to identify enhancers of *para*-aminosalicylic acid against *Mycobacterium tuberculosis*. *Scientific Reports*, 12(1), art. #5635. <https://doi.org/10.1038/s41598-022-08209-w>

Heravi, M.M., Janati, F. & Zadsirjan, V. 2020. Applications of Knoevenagel condensation reaction in the total synthesis of natural products. *Monatshefte für Chemie*, 151(4): 439-482. <https://doi.org/10.1007/s00706-020-02586-6>

Herzog, H. 1998. History of tuberculosis. *Respiration*, 65(1): 5-15. Date of access: 26 Jan. 2022.

Hicks, A., Muthukumarasamy, S., Maxwell, D. & Howlett, D. 2014. Chronic inactive pulmonary tuberculosis and treatment sequelae: chest radiographic features. *The*

International Journal of Tuberculosis and Lung Disease, 18(2): 128-133.

<https://doi.org/10.5588/ijtld.13.0360>

Hoffman, P.S., Sisson, G., Croxen, M.A., Welch, K., Harman, W.D., Cremades, N. & Morash, M.G. 2007. Antiparasitic drug nitazoxanide inhibits the pyruvate oxidoreductases of *Helicobacter pylori*, selected anaerobic bacteria and parasites, and *Campylobacter jejuni*. *Antimicrobial Agents and Chemotherapy*, 51(3): 868-876. doi:10.1128/AAC.01159-06

Hooper, D.C. 2000. Mechanisms of action and resistance of older and newer fluoroquinolones. *Clinical Infectious Diseases*, 31(suppl_2): S24-S28.

<https://doi.org/10.1086/314056>

Hooper, D.C. & Jacoby, G.A., 2016. Topoisomerase inhibitors: fluoroquinolone mechanisms of action and resistance. *Cold Spring Harbor Perspectives in Medicine*, 6(9), a025320. doi:10.1101/cshperspect.a025320

Hope, D., Ampaire, L., Oyet, C., Muwanguzi, E., Twizerimana, H. & Apecu, R.O. 2019. Antimicrobial resistance in pathogenic aerobic bacteria causing surgical site infections in Mbarara regional referral hospital, Southwestern Uganda. *Scientific Reports*, 9(1), art. #17299. <https://doi.org/10.1038/s41598-019-53712-2>

Hunter, J.D. 2012. Ventilator associated pneumonia. *The British Medical Journal*, 344, art. #e3325. doi:10.1136/bmj.e3325

Hunter, R.L. 2011. Pathology of post primary tuberculosis of the lung: an illustrated critical review. *Tuberculosis*, 91(6): 497-509. <https://doi.org/10.1016/j.tube.2011.03.007>

Hwang, T., Wares, D., Jafarov, A., Jakubowiak, W., Nunn, P. & Keshavjee, S. 2013. Safety of cycloserine and terizidone for the treatment of drug-resistant tuberculosis: a meta-analysis. *The International Journal of Tuberculosis and Lung Disease*, 17(10): 1257-1266. <https://doi.org/10.5588/ijtld.12.0863>

Iacobino, A., Giannoni, F., Pardini, M., Piccaro, G. & Fattorini, L. 2019. The Combination Rifampin-Nitazoxanide, but Not Rifampin-Isoniazid-Pyrazinamide-Ethambutol, Kills Dormant *Mycobacterium tuberculosis* in Hypoxia at Neutral Ph. *Antimicrobial Agents and Chemotherapy*, 63(7), e00273-19. doi:10.1128/AAC.00273-19

Isik, O., Kaya, E., Dundar, H.Z. & Sarkut, P. 2015. Surgical site infection: re-assessment of the risk factors. *Chirurgia*, 110(5): 457-461. Date of access: 02 Oct. 2022.

Jacobsen, S.M., Stickler, D.J., Mobley, H.L.T. & Shirliff, M.E. 2008. Complicated catheter-associated urinary tract infections due to *Escherichia coli* and *Proteus mirabilis*. *Clinical Microbiology Reviews*, 21(1): 26-59. doi:10.1128/CMR.00019-07

Jaiswal, I., Jain, A., Singh, P., Verma, S., Prakash, S., Dixit, P. & Singh, M. 2017. Mutations in *katG* and *inhA* genes of isoniazid-resistant and-sensitive clinical isolates of *Mycobacterium tuberculosis* from cases of pulmonary tuberculosis and their association with minimum inhibitory concentration of isoniazid. *Clinical Epidemiology and Global Health*, 5(3): 143-147. <https://doi.org/10.1016/j.cegh.2016.08.008>

Javed, H., Bakula, Z., Pleń, M., Hashmi, H.J., Tahir, Z., ... Jagielski, T. 2018. Evaluation of genotype MTBDR plus and MTBDR sl assays for rapid detection of drug resistance in extensively drug-resistant *Mycobacterium tuberculosis* isolates in Pakistan. *Frontiers in Microbiology*, 9, art. #2265. <https://doi.org/10.3389/fmicb.2018.02265>

Joshi, Y.N., Kasam, A., Raccha, G.A. & Vinod, P.S. 2020. Screening and identification potent inhibitors of lam protein involved in *Mycobacterium tuberculosis*. *International Journal of Scientific Research in Science and Technology*, 7(2): 251-258. <https://doi.org/10.32628/IJSRST>

Kadura, S., King, N., Nakhoul, M., Zhu, H., Theron, G., Köser, C.U. & Farhat, M. 2020. Systematic review of mutations associated with resistance to the new and repurposed *Mycobacterium tuberculosis* drugs bedaquiline, clofazimine, linezolid, delamanid and pretomanid. *The Journal of Antimicrobial Chemotherapy*, 75(8): 2031-2043.

doi:10.12659/MSM.913510Kaminsky, D., Kryshchyn, A. & Lesyk, R. 2017. 5-Ene-4-thiazolidinones – An efficient tool in medicinal chemistry. *European Journal of Medicinal Chemistry*, 140(2017): 542-594. <https://doi.org/10.1016/j.ejmech.2017.09.031>

Kang, Y.A., Shim, T.S., Koh, W.-J., Lee, S.H., Lee, C.-H., Choi, J.C., ... Jung, K.H. 2016. Choice between levofloxacin and moxifloxacin and multidrug-resistant tuberculosis treatment outcomes. *Annals of the American Thoracic Society*, 13(3): 364-370. <https://doi.org/10.1513/AnnalsATS.201510-690BC>

Kateete, D.P., Kimani, C.N., Katabazi, F.A., Okeng, A., Okee, M.S., Nanteza, A., ... Najjuka, F.C. 2010. Identification of *Staphylococcus aureus*: Dnase and Mannitol salt agar improve the efficiency of the tube coagulase test. *Annals of Clinical Microbiology and Antimicrobials*, 9, art. #23 <https://doi.org/10.1186/1476-0711-9-23>

Kaur Manjal, S., Kaur, R., Bhatia, R., Kumar, K., Singh, V., Shankar, R., ... Rawal, R.K. 2017. Synthetic and medicinal perspective of thiazolidinones: A review. *Bioorganic Chemistry*, 75(2017): 406-423. <https://doi.org/10.1016/j.bioorg.2017.10.014>

Kestler, B. & Tyler, S.K. 2022. Latent tuberculosis testing through the ages: the search for a sleeping killer. *American Journal of Physiology-Lung Cellular and Molecular Physiology*, 322(3): L412-L419.

Khawbung, J.L., Nath, D. & Chakraborty, S. 2021. Drug resistant Tuberculosis: A review. *Comparative Immunology, Microbiology and Infectious Diseases*, 74(2021), art. #101574. <https://doi.org/10.1016/j.cimid.2020.101574>

Klompas, M. 2018. *Epidemiology, pathogenesis, microbiology, and diagnosis of hospital-acquired and ventilator-associated pneumonia in adults*. Available from UpToDate: <https://www.medilib.ir/uptodate/show/7020> Date of access: 02 Oct. 2022.

Koch, A. & Mizrahi, V. 2018. *Mycobacterium tuberculosis*. *Trends in Microbiology*, 26(6): 555-556. <https://doi.org/10.1016/j.tim.2018.02.012>

Koele, S.E., Van Beek, S.W., Maartens, G., Brust, J.C. & Svensson, E.M. 2022. Optimized loading dose strategies for bedaquiline when restarting interrupted drug-resistant tuberculosis treatment. *Antimicrobial Agents and Chemotherapy*, 66(3), e01749-21. <https://doi.org/10.1128/aac.01749-21>

Koenig, S.M. and Truitt, J.D. 2006. Ventilator-associated pneumonia: diagnosis, treatment, and prevention. *Clinical Microbiology Reviews*, 19(4): 637-657. doi:10.1128/CMR.00051-05

Kotze, L.A., Beltran, C.G., Lang, D., Loxton, A.G., Cooper, S., Meiring, M., ... Glanzmann, B. 2021. Establishment of a patient-derived, magnetic levitation-based, three-dimensional spheroid granuloma model for human tuberculosis. *mSphere*, 6(4), e00552-21. <https://doi.org/10.1128/mSphere.00552-21>

Krawczyk, B., Wityk, P., Gałęcka, M. & Michalik, M. 2021. The many faces of *Enterococcus* spp.—commensal, probiotic and opportunistic pathogen, *Microorganisms*, 9, art. #1900 <https://doi.org/10.3390/microorganisms9091900>

Küçükgülzel, İ., Satılmış, G., Gurukumar, K.R., Basu, A., Tatar, E., Nichols, D.B., ... Kaushik-Basu, N. 2013. 2-Heteroarylimino-5-arylidene-4-thiazolidinones as a new class of non-nucleoside inhibitors of HCV NS5B polymerase. *European Journal of Medicinal Chemistry*, 69, 931-941. <https://doi.org/10.1016/j.ejmech.2013.08.043>

Kulabaş, N., Özakpınar, Ö.B., Özsavcı, D., Leyssen, P., Neyts, J. & Küçükgülzel, İ. 2017. Synthesis, characterization and biological evaluation of thioureas, acylthioureas and 4-thiazolidinones as anticancer and antiviral agents. *Marmara Pharmaceutical Journal*, 21(2): 371-384. <https://doi.org/10.12991/marupj.300913>

Kulkarni, P.S., Karale, S.N., Khandebharad, A.U., Agrawal, B.R. & Sarda, S.R. 2022. Design, synthesis, and biological evaluation of newer arylidene incorporated 4-thiazolidinones derivatives as potential antimicrobial agents. *Polycyclic Aromatic Compounds*, 42(5): 2031-2044. <https://doi.org/10.1080/10406638.2020.1823861>

Lee, J.-K., Lee, H.W., Heo, E.Y., Yim, J.-J. & Kim, D.K. 2021. Comparison of QuantiFERON-TB Gold Plus and QuantiFERON-TB Gold In-Tube tests for patients with active and latent tuberculosis: A prospective cohort study. *Journal of Infection and Chemotherapy*, 27(12): 1694-1699.

Lee, N. & Nguyen, H. 2021. *Ethambutol*. Available from StatPearls: <https://www.ncbi.nlm.nih.gov/books/NBK559050/> Date of access: 17 Mar. 2022.

Legesse Laloto, T., Hiko Gemed, D. & Abdella, S.H. 2017. Incidence and predictors of surgical site infection in Ethiopia: prospective cohort. *BMC Infectious Diseases*, 17(1), art. #119. doi:10.1186/s12879-016-2167-x

Lesyk, R., 2020. Drug design: 4-thiazolidinones applications. Part 1. Synthetic routes to the drug-like molecules. *Journal of Medical Science*, 89(1): 33-49. <https://doi.org/10.20883/medical.406>

Lewis, J.M. & Sloan, D.J. 2015. The role of delamanid in the treatment of drug-resistant tuberculosis. *Therapeutics and Clinical Risk Management*, 11: 779–791. doi:10.2147/TCRM.S71076

Li, J., Zhan, L. & Qin, C. 2021. The double-sided effects of *Mycobacterium Bovis* bacillus Calmette–Guérin vaccine. *NPJ Vaccines*, 6, art. #14. <https://doi.org/10.1038/s41541-020-00278-0>

Li, Y., Sun, F. & Zhang, W. 2019. Bedaquiline and delamanid in the treatment of multidrug-resistant tuberculosis: Promising but challenging. *Drug Development Research*, 80(1): 98-105. doi:10.1002/ddr.21498

Lim, S.M. & Webb, S.A.R. 2005. Nosocomial bacterial infections in Intensive Care Units. I: Organisms and mechanisms of antibiotic resistance. *Anaesthesia*, 60(9): 887-902. <https://doi.org/10.1111/j.1365-2044.2005.04220.x>

Lin, C.I., McCarty, R.M. & Liu, H.W. 2017. The enzymology of organic transformations: a survey of name reactions in biological systems. *Angewandte Chemie International Edition*, 56(13): 3446-3489. doi:10.1002/anie.201603291

Liu, H.L., Li, Z. & Anthonsen, T. 2000. Synthesis and fungicidal activity of 2-imino-3-(4-arylthiazol-2-yl)-thiazolidin-4-ones and their 5-arylidene derivatives. *Molecules*, 5(9): 1055-1061. <https://doi.org/10.3390/50901055>

Liu, Z., Zhang, M., Wang, J., Chen, S., Wu, B., Zhou, L., ... Wang, X. 2020. Longitudinal analysis of prevalence and risk factors of rifampicin-resistant tuberculosis in Zhejiang, China. *BioMed Research International*, 2020, art. #3159482. <https://doi.org/10.1155/2020/3159482>

Lobdell, K.W., Stamou, S. & Sanchez, J.A. 2012. Hospital-acquired infections. *Surgical Clinics*, 92(1): 65-77. doi:10.1016/j.suc.2011.11.003

Loveday, H.P., Wilson, J.A., Kerr, K., Pitchers, R., Walker, J.T. & Browne, J., 2014. Association between healthcare water systems and *Pseudomonas aeruginosa* infections: a rapid systematic review. *Journal of Hospital Infection*, 86(1): 7-15. <https://doi.org/10.1016/j.jhin.2013.09.010>

Luijckx, L. & Du Preez, I. 2020. The echo of pulmonary tuberculosis: mechanisms of clinical symptoms and other disease-induced systemic complications. *Clinical Microbiology Reviews*, 33(4), e00036-20. doi:10.1128/CMR.00036-20

- Ma, Y.X., Wang, C.Y., Li, Y.Y., Li, J., Wan, Q.Q., Chen, J.H., ... Niu, L.N. 2020. Considerations and caveats in combating ESKAPE pathogens against nosocomial infections. *Advanced Science*, 7, art. #1901872. doi:10.1002/advs.201901872
- MacDougall, C. 2017a. Sulfonamides, Trimethoprim- Sulfamethoxazole, Quinolones, and Agents for Urinary Tract Infections. In: Brunton, L.L., Hilal-Dandan, R. & Knollmann, B.C., eds. Goodman & Gilman's: *The Pharmacological Basics of Therapeutics*. 13 ed. NY: McGraw-Hill. pp 1012-1021.
- MacDougall, C. 2017b. Aminoglycosides. In: Brunton, L.L., Hilal-Dandan, R. & Knollmann, B.C., eds. Goodman & Gilman's: *The Pharmacological Basics of Therapeutics*. 13 ed. NY: McGraw-Hill. pp 1039-1047.
- MacGregor-Fairlie, M., Wilkinson, S., Besra, G.S. & Goldberg Oppenheimer, P. 2020. Tuberculosis diagnostics: overcoming ancient challenges with modern solutions. *Emerging Topics in Life Sciences*, 4(4): 435-448. <https://doi.org/10.1042/ETLS20200335>
- Mahmoud, D.B., Shitu, Z. & Mostafa, A. 2020. Drug repurposing of nitazoxanide: can it be an effective therapy for COVID-19? *Journal of Genetic Engineering and Biotechnology*, 18(1), art. #35. <https://doi.org/10.1186/s43141-020-00055-5>
- Maiti, D., Bhattacharyya, A. & Basu, J. 2001. Lipoarabinomannan from *Mycobacterium tuberculosis* promotes macrophage survival by phosphorylating bad through a phosphatidylinositol 3-kinase/Akt pathway. *Journal of Biological Chemistry*, 276(1): 329-333.
- Marrakchi, H., Lanéelle, M.A. & Daffé, M. 2014. Mycolic acids: structures, biosynthesis, and beyond. *Chemistry & Biology*, 21(1): 67-85. <https://doi.org/10.1016/j.chembiol.2013.11.011>
- Martin, R.M. & Bachman, M.A. 2018. Colonization, infection, and the accessory genome of *Klebsiella pneumoniae*. *Frontiers in Cellular and Infection Microbiology*, 8, art. #4 <https://doi.org/10.3389/fcimb.2018.00004>
- Marturano, J.E. & Lowery, T.J. 2019. ESKAPE pathogens in bloodstream infections are associated with higher cost and mortality but can be predicted using diagnoses upon admission. *Open Forum Infectious Diseases*, 6(12), art. #ofz503. <https://doi.org/10.1093/ofid/ofz503>

Mase, S.R. & Chorba, T. 2019. Treatment of Drug-Resistant Tuberculosis. *Clinics in Chest Medicine*, 40(4): 775-795. doi:10.1016/j.ccm.2019.08.002

McCarthy, H., Rudkin, J.K., Black, N.S., Gallagher, L., O'Neill, E. & O'gara, J.P. 2015. Methicillin resistance and the biofilm phenotype in *Staphylococcus aureus*. *Frontiers in Cellular and Infection Microbiology*, 5, art. #1. <https://doi.org/10.3389/fcimb.2015.00001>

McGuinness, W.A., Malachowa, N. & Deleo, F.R. 2017. Vancomycin resistance in *Staphylococcus aureus*. *The Yale Journal of Biology and Medicine*, 90(2): 269-281. Date of access: 09 May, 2022.

Meaza, A., Kebede, A., Yaregal, Z., Dagne, Z., Moga, S., Yenew, B., ... Getahun, M. 2017. Evaluation of genotype MTBDRplus VER 2.0 line probe assay for the detection of MDR-TB in smear positive and negative sputum samples. *BMC Infectious Diseases*, 17(1), art. #280. <https://doi.org/10.1186/s12879-017-2389-6>

Mehrad, B., Clark, N.M., Zhanel, G.G. & Lynch, J.P., III. 2015. Antimicrobial resistance in hospital-acquired Gram-negative bacterial infections. *Chest*, 147(5): 1413-1421. doi:10.1378/chest.14-2171

Migliori, G.B., Sotgiu, G., Gandhi, N.R., Falzon, D., Deriemer, K., Centis, R., ... Vargas, M.H. 2013. Drug resistance beyond extensively drug-resistant tuberculosis: individual patient data meta-analysis. *European Respiratory Journal*, 42(1): 169-179. doi:10.1183/09031936.00136312

Minato, Y., Thiede, J.M., Kordus, S.L., Mcklveen, E.J., Turman, B.J. & Baughn, A.D. 2015. *Mycobacterium tuberculosis* folate metabolism and the mechanistic basis for para-aminosalicylic acid susceptibility and resistance. *Antimicrobial Agents and Chemotherapy*, 59(9): 5097-5106. doi:10.1128/AAC.00647-15

Mirnejad, R., Asadi, A., Khoshnood, S., Mirzaei, H., Heidary, M., Fattorini, L., ... Darban-Sarokhalil, D. 2018. Clofazimine: A useful antibiotic for drug-resistant tuberculosis. *Biomedicine & Pharmacotherapy*, 105: 1353-1359. <https://doi.org/10.1016/j.biopha.2018.06.023>

- Mishchenko, M., Shtrygol, S., Kaminsky, D. & Lesyk, R. 2020. Thiazole-bearing 4-thiazolidinones as new anticonvulsant agents. *Scientia Pharmaceutica*, 88(1), art. #16. <https://doi.org/10.3390/scipharm88010016>
- Mohammadi, B., Ramazanzadeh, R., Nouri, B. & Rouhi, S. 2020. Frequency of codon 306 mutations in *embB* gene of *Mycobacterium tuberculosis* resistant to ethambutol: a systematic review and meta-analysis. *International Journal of Preventive Medicine*, 11, art. #112. doi:10.4103/ijpvm.IJPVM_114_19
- Mohammed, H.H., Abuo-Rahma, G.E.-D.A., Abbas, S.H. & Abdelhafez, E.-S. 2019. Current trends and future directions of fluoroquinolones. *Current Medicinal Chemistry*, 26(17): 3132-3149. doi:10.2174/0929867325666180214122944
- Mohammed, O.S., Noaman., A.A. & Jalil, S.S. 2022. Epidemiological review of nosocomial infections caused by *Acinetobacter baumannii*. *Science Archives*, 3(1): 80-83. <http://dx.doi.org/10.47587/SA.2022.3110>
- Molina, D.A., Ramos, G.A., Zamora-Vélez, A., Gallego-López, G.M., Rocha-Roa, C., Gómez-Marin, J.E. & Cortes, E. 2021. *In vitro* evaluation of new 4-thiazolidinones on invasion and growth of *Toxoplasma gondii*. *International Journal for Parasitology: Drugs and Drug Resistance*, 16: 129-139. <https://doi.org/10.1016/j.ijpddr.2021.05.004>
- Monegro, A.F., Muppidi, V. & Regunath, H. 2020. *Hospital acquired infections*. Available from StatPearls: <https://www.ncbi.nlm.nih.gov/books/NBK441857/> Date of access: 07 May. 2022.
- Moonan, P.K. 2018. Tuberculosis—the face of struggles, the struggles we face, and the dreams that lie within. *Emerging Infectious Diseases*, 24(3): 592-593. doi:10.3201/eid2403.170128
- Mosaei, H., Molodtsov, V., Keplinger, B., Harbottle, J., Moon, C.W., Jeeves, R.E., ... Wills, C. 2018. Mode of action of kanglemycin A, an ansamycin natural product that is active against rifampicin-resistant *Mycobacterium tuberculosis*. *Molecular Cell*, 72(2): 263-274. <https://doi.org/10.1016/j.molcel.2018.08.028>

Moule, M.G. & Cirillo, J.D. 2020. *Mycobacterium tuberculosis* Dissemination Plays a Critical Role in Pathogenesis. *Frontiers in Cellular and Infection Microbiology*, 10, art. #65.

<https://doi.org/10.3389/fcimb.2020.00065>

Mudde, S.E., Upton, A.M., Lenaerts, A., Bax, H.I. & De Steenwinkel, J.E.M. 2022. Delamanid or pretomanid? A Solomonian judgement! *Journal of Antimicrobial Chemotherapy*, 77(4): 880-902. <https://doi.org/10.1093/jac/dkab505>

Murray, C.J., Ikuta, K.S., Sharara, F., Swetschinski, L., Aguilar, G.R., Gray, A., ... Wool, E. 2022. Global burden of bacterial antimicrobial resistance in 2019: a systematic analysis. *The Lancet*, 399(10325): 629-655. [https://doi.org/10.1016/S0140-6736\(21\)02724-0](https://doi.org/10.1016/S0140-6736(21)02724-0)

Murray, J.F., Schraufnagel, D.E. & Hopewell, P.C. 2015. Treatment of tuberculosis. A historical perspective. *Annals of the American Thoracic Society*, 12(12): 1749-1759.

<https://doi.org/10.1513/AnnalsATS.201509-632PS>

Nardell, E.A. 2015. Transmission and institutional infection control of tuberculosis. *Cold Spring Harbor Perspectives in Medicine*, 6(2), a018192. doi:10.1101/cshperspect.a018192

Navidinia, M. 2016. The clinical importance of emerging ESKAPE pathogens in nosocomial infections. *Journal of Paramedical Sciences*, 7(3): 43-57. Date of access: 11 May. 2022.

Navidinia, M., Goudarzi, M., Rameshe, S.M., Farajollahi, Z., Asl, P.E., Khosravi, S.Z. & Mounesi, M.R. 2017. Molecular characterization of resistance genes in MDR-ESKAPE pathogens. *Journal of Pure and Applied Microbiology*, 11(2): 779-792.

<https://dx.doi.org/10.22207/JPAM.11.2.17>

Ndlovu, H. & Marakalala, M.J. 2016. Granulomas and inflammation: host-directed therapies for tuberculosis. *Frontiers in Immunology*, 7, art. #434.

<https://doi.org/10.3389/fimmu.2016.00434>

Nel, D.C. 2014. Surgical site infections. *South African Family Practice*, 56(5): 33-37. Date of access: 02 Oct. 2022.

Nguyen, L. 2016. Antibiotic resistance mechanisms in *M. tuberculosis*: an update. *Archives of Toxicology*, 90(7): 1585-1604. <https://doi.org/10.1007/s00204-016-1727-6>

Nguyen, T.V.A., Anthony, R.M., Bañuls, A.-L., Nguyen, T.V.A., Vu, D.H. & Alffenaar, J.-W.C. 2017. Bedaquiline resistance: its emergence, mechanism, and prevention. *Clinical Infectious Diseases*, 66(10): 1625-1630. <https://doi.org/10.1093/cid/cix992>

Nicolle, L.E. 2014. Catheter associated urinary tract infections. *Antimicrobial Resistance and Infection Control*, 3(1), art. #23. <https://doi.org/10.1186/2047-2994-3-23>

Niemz, A. & Boyle, D.S. 2012. Nucleic acid testing for tuberculosis at the point-of-care in high-burden countries. *Expert Review of Molecular Diagnostics*, 12(7): 687-701.

doi:10.1586/erm.12.71 Nirwan, S., Chahal, V. & Kakkar, R. 2019. Thiazolidinones: Synthesis, Reactivity, and Their Biological Applications. *Journal of Heterocyclic Chemistry*, 56(4): 1239-1253. <https://doi.org/10.1002/jhet.3514>

Nishida, C.R. & Ortiz De Montellano, P.R. 2011. Bioactivation of antituberculosis thioamide and thiourea prodrugs by bacterial and mammalian flavin monooxygenases. *Chemico-Biological Interactions*, 192(1-2): 21-25. <https://doi.org/10.1016/j.cbi.2010.09.015>

Nowaczyk, A., Kowiel, M., Gzella, A., Fijałkowski, Ł., Horishny, V. & Lesyk, R. 2014. Conformational space and vibrational spectra of 2-[(2, 4-dimethoxyphenyl) amino]-1, 3-thiazolidin-4-one. *Journal of Molecular Modeling*, 20(8), art. #2366. <https://doi.org/10.1007/s00894-014-2366-6>

Ojha, A., Banik, S., Melanthota, S.K. & Mazumder, N. 2020. Light emitting diode (LED) based fluorescence microscopy for tuberculosis detection: a review. *Lasers in Medical Science*, 35(6): 1431-1437. <https://doi.org/10.1007/s10103-019-02947-6>

Oommen, S. & Banaji, N. 2017. Laboratory diagnosis of tuberculosis: advances in technology and drug susceptibility testing. *Indian Journal of Medical Microbiology*, 35(3): 323-331. https://doi.org/10.4103/ijmm.IJMM_16_204

Orosz, L., Lengyel, G., Ánosi, N., Lakatos, L. & Burián, K. 2022. Changes in resistance pattern of ESKAPE pathogens between 2010 and 2020 in the clinical center of University of Szeged, Hungary. *Acta Microbiologica et Immunologica Hungarica*, 69(1): 27-34. doi:10.1556/030.2022.01640

Orsi, G.B. & Ciorba, V. 2013. Vancomycin resistant enterococci healthcare associated infections. *Annali di Igiene*, 25(6): 485-492. doi:10.7416/ai.2013.1948

Owens Jr, R.C. & Ambrose, P.G., 2005. Antimicrobial safety: focus on fluoroquinolones. *Clinical Infectious Diseases*, 41(Supplement_2): S144-S157.

Pachori, P., Gothwal, R. & Gandhi, P. 2019. Emergence of antibiotic resistance *Pseudomonas aeruginosa* in intensive care unit; a critical review. *Genes & Diseases*, 6(2): 109-119. <https://doi.org/10.1016/j.gendis.2019.04.001>

Pacifici, G. 2019. Clinical Pharmacology of Rifampin in Infants and Children. *Journal of Targeted Drug Delivery*, 3(1): 1-17. Date of access: 15 Mar. 2022.

Pahal, P. & Sharma, S. 2021. *PPD skin test*. Available from StatPearls: <https://www.ncbi.nlm.nih.gov/books/NBK556037/> Date of access: 15 Aug. 2022.

Pallo-Zimmerman, L.M., Byron, J.K. & Graves, T.K. 2010. Fluoroquinolones: then and now. *Compendium: Continuing Education for Veterinarians*, 32(7): E1-E9. Date of access: 26 Mar. 2022.

Palmer, A.L., Leykam, V.L., Larkin, A., Krueger, S.K., Phillips, I.R., Shephard, E.A. & Williams, D.E. 2012. Metabolism and pharmacokinetics of the anti-tuberculosis drug ethionamide in a flavin-containing monooxygenase null mouse. *Pharmaceuticals*, 5(11): 1147-1159. doi:10.3390/ph5111147

Palomino, J.C. & Martin, A. 2014. Drug resistance mechanisms in *Mycobacterium tuberculosis*. *Antibiotics*, 3(3): 317-340. <https://doi.org/10.3390/antibiotics3030317>

Pandey, R., Mishra, S.K. & Shrestha, A. 2021. Characterisation of ESKAPE Pathogens with Special Reference to Multidrug Resistance and Biofilm Production in a Nepalese Hospital. *Infection and Drug Resistance*, 14: 2201-2212. doi:10.2147/IDR.S306688

Papazian, L., Klompas, M. & Luyt, C.E. 2020. Ventilator-associated pneumonia in adults: a narrative review. *Intensive Care Medicine*, 46(5): 888-906. <https://doi.org/10.1007/s00134-020-05980-0>

Park, S., Jung, J., Kim, J., Han, S.B. & Ryoo, S. 2022. Investigation of clofazimine resistance and genetic mutations in drug-resistant *Mycobacterium tuberculosis* isolates. *Journal of Clinical Medicine*, 11(7), art. #1927. <https://doi.org/10.3390/jcm11071927>

Paterson, D.L. 2006. Resistance in Gram-negative bacteria: Enterobacteriaceae. *American Journal of Infection Control*, 34(5): S20-S28. doi:10.1016/j.ajic.2006.05.238

Peleg, A.Y. & Hooper, D.C. 2010. Current concepts hospital-acquired infections due to Gram-negative bacteria. *New England Journal of Medicine*, 362(19): 1804-1813. doi:10.1056/NEJMra0904124

Peloquin, C.A. & Davies, G.R. 2021. The Treatment of Tuberculosis. *Clinical Pharmacology & Therapeutics*, 110(6): 1455-1466. <https://doi.org/10.1002/cpt.2261>

Peter, J.G., van Zyl-Smit, R.N., Denkinger, C.M. & Pai, M. 2012. Diagnosis of TB: state of the art. *European Respiratory Monograph*, 58, 124-143. Date of access: 10 Aug. 2022.

Pham, T.D.M., Ziora, Z.M. & Blaskovich, M.A.T. 2019. Quinolone antibiotics. *MedChemComm*, 10(10): 1719-1739. doi:10.1039/C9MD00120D

Pickering, A.C., Yebra, G., Gong, X., Goncheva, M.I., Wee, B.A., Macfadyen, A.C., ... Fey, P.D. 2021. Evolutionary and functional analysis of coagulase positivity among the *Staphylococci*. *mSphere*, 6(4), art. #e00381-21. <https://doi.org/10.1128/mSphere.00381-21>

Pieters, J. 2008. *Mycobacterium tuberculosis* and the macrophage: maintaining a balance. *Cell Host & Microbe*, 3(6): 399-407. <https://doi.org/10.1016/j.chom.2008.05.006>

Pillay, T., Andronikou, S. & Zar, H.J. 2020. Chest imaging in paediatric pulmonary TB. *Paediatric Respiratory Reviews*, 36: 65-72. <https://doi.org/10.1016/j.prrv.2020.10.002>

Pinto, L. & Menzies, D. 2011. Treatment of drug-resistant tuberculosis. *Infection and Drug Resistance*, 4, 129-135. doi:10.2147/IDR.S10332

Pitman, S.K., Hoang, U.T., Wi, C.H., Alsheikh, M., Hiner, D.A. & Percival, K.M. 2019. Revisiting oral fluoroquinolone and multivalent cation drug-drug interactions: are they still relevant? *Antibiotics*, 8(3): art. #108. <https://doi.org/10.3390/antibiotics8030108>

Plinke, C., Rüscher-Gerdes, S. & Niemann, S. 2006. Significance of Mutations in *embB* Codon 306 for Prediction of Ethambutol Resistance in Clinical *Mycobacterium tuberculosis* Isolates. *Antimicrobial Agents and Chemotherapy*, 50(5): 1900-1902. doi:10.1128/AAC.50.5.1900-1902.2006

Podkovik, S., Toor, H., Gattupalli, M., Kashyap, S., Brazdzionis, J., Patchana, T., ... Wang, S. 2019. Prevalence of Catheter-Associated Urinary Tract Infections in Neurosurgical Intensive Care Patients – The Overdiagnosis of Urinary Tract Infections. *Cureus*, 11(8), e5494. doi:10.7759/cureus.5494

Pourakbari, B., Mamishi, S., Benvari, S. & Mahmoudi, S. 2019. Comparison of the QuantiFERON-TB Gold Plus and QuantiFERON-TB Gold In-Tube interferon- γ release assays: a systematic review and meta-analysis. *Advances in Medical Sciences*, 64(2): 437-443. <https://doi.org/10.1016/j.advms.2019.09.001>

Pozniak, A. 2019. *Clinical manifestations and complications of pulmonary tuberculosis*. Available from UpToDate: <https://www.medilib.ir/uptodate/show/7026#rid12> Date of access: 23 Jul. 2022.

Prabhu, R. & Singh, V. 2019. The history of tuberculosis: past, present, and future. *Advances in Microbiology*, 9(11): 931-942. doi:10.4236/aim.2019.911059

Prosser, G.A. & De Carvalho, L.P.S. 2013. Reinterpreting the mechanism of inhibition of *Mycobacterium tuberculosis* D-alanine:D-alanine ligase by D-cycloserine. *Biochemistry*, 52(40): 7145-7149. <https://doi.org/10.1021/bi400839f>

Qi, X., Lin, W., Ma, M., Wang, C., He, Y., He, N., ... Zhang, P. 2016. Structural basis of rifampin inactivation by rifampin phosphotransferase. *Proceedings of the National Academy of Sciences*, 113(14): 3803-3808. <https://doi.org/10.1073/pnas.1523614113>

Rando-Segura, A., Aznar, M.L., Moreno, M.M., Espasa Soley, M., Sulleiro Igual, E., Bocanegra Garcia, C., ... Tórtola Fernández, M.T. 2021. Molecular characterization of *rpoB* gene mutations in isolates from tuberculosis patients in Cubal, Republic of Angola. *BMC Infectious Diseases*, 21(1), art. #1056. <https://doi.org/10.1186/s12879-021-06763-8>

Rao, N. & Meena, L.S. 2011b. Biosynthesis and virulent behavior of lipids produced by *Mycobacterium tuberculosis*: LAM and cord factor: an overview. *Biotechnology Research International*, 2011, art. #274693. doi:10.4061/2011/274693

Rao, N. & Meena, L.S., 2011a. Unique characteristic features of *Mycobacterium tuberculosis* in relation to immune system. *American Journal of Immunology*, 7(1): 1-8. Date of access: 15 Jul. 2022.

Ravimohan, S., Kornfeld, H., Weissman, D. & Bisson, G.P. 2018. Tuberculosis and lung damage: from epidemiology to pathophysiology. *European Respiratory Review*, 27(147), art. #170077. doi:10.1183/16000617.0077-2017

Rawat, A., Chaturvedi, S., Singh, A.K., Guleria, A., Dubey, D., Keshari, A.K., ... Saha, S. 2018. Metabolomics approach discriminates toxicity index of pyrazinamide and its metabolic products, pyrazinoic acid and 5-hydroxy pyrazinoic acid. *Human & Experimental Toxicology*, 37(4): 373-389. <https://doi.org/10.1177/0960327117705426>

Raynaud, C., Lan  elle, M.A., Senaratne, R.H., Draper, P., Lan  elle, G. & Daff  , M. 1999. Mechanisms of pyrazinamide resistance in mycobacteria: importance of lack of uptake in addition to lack of pyrazinamidase activity. *Microbiology*, 145(6): 1359-1367. <https://doi.org/10.1099/13500872-145-6-1359>

Rifat, D., Li, S.-I., Ioerger, T., Shah, K., Lanoix, J.-P., Lee, J. ... Nuermberger, E. 2020. Mutations in fbiD (Rv2983) as a novel determinant of resistance to pretomanid and delamanid in *Mycobacterium tuberculosis*. *Antimicrobial Agents and Chemotherapy*, 65(1), e01948-20. doi:10.1128/AAC.01948-20

Rodr  guez-Takeuchi, S.Y., Renjifo, M.E. & Medina, F.J., 2019. Extrapulmonary tuberculosis: pathophysiology and imaging findings. *Radiographics*, 39(7): 2023-2037. <https://doi.org/10.1148/rq.2019190109>

Rossignol, J. & Maisonneuve, H. 1984. Nitazoxanide in the treatment of *Taenia saginata* and *Hymenolepis nana* infections. *The American Journal of Tropical Medicine and Hygiene*, 33(3): 511-512. doi:10.4269/ajtmh.1984.33.511

Rossignol, J.-F. & Cavier, R. 1976. *New derivatives of 2-benzamido-5-nitro thiazoles*. (Patent: US 3950351A). <https://patents.google.com/patent/US3950351A/en> Date of access: 15 May. 2022.

Rossiter, D., ed. 2020. *South African Medicines Formulary*. 14th ed. Rondebosch, SA: Health and Medical Publishing Group.

Roy, S., Ghatak, D., Das, P. & BoseDasgupta, S. 2020. ESX secretion system: The gatekeepers of mycobacterial survivability and pathogenesis. *European Journal of Microbiology and Immunology*, 10(4): 202-209. <https://doi.org/10.1556/1886.2020.00028>

Rufai, S.B., Kumar, P., Singh, A., Prajapati, S., Balooni, V. & Singh, S. 2014. Comparison of Xpert MTB/RIF with line probe assay for detection of rifampin-mono-resistant *Mycobacterium tuberculosis*. *Journal of Clinical Microbiology*, 52(6): 1846-1852. doi:10.1128/JCM.03005-13

Rupainwar, R. & Pandey, J. 2019. The importance and applications of Knoevenagel reaction (brief review). *Oriental Journal of Chemistry*, 35(1): 423-429. doi:10.13005/ojc/350154

Russell, D.G., Cardona, P.-J., Kim, M.-J., Allain, S. & Altare, F. 2009. Foamy macrophages and the progression of the human tuberculosis granuloma. *Nature Immunology*, 10(9): 943-948. doi:10.1038/ni.1781

Rusu, A., Lungu, I.-A., Moldovan, O.-L., Tanase, C. & Hancu, G. 2021. Structural characterization of the millennial antibacterial (fluoro) quinolones—shaping the fifth generation. *Pharmaceutics*, 13(8), art. #1289.

<https://doi.org/10.3390/pharmaceutics13081289>

Jadhavar, P.S., Vaja, M.D., Dhameliya, T.M. & Chakraborti, A.K. 2015. Oxazolidinones as anti-tubercular agents: discovery, development and future perspectives. *Current Medicinal Chemistry*, 22(38): 4379-4397.

Santajit, S. & Indrawattana, N. 2016. Mechanisms of antimicrobial resistance in ESKAPE pathogens. *BioMed Research International*, 2016, art. #2475067.

<https://doi.org/10.1155/2016/2475067>

Santucci, P., Greenwood, D.J., Fearn, A., Chen, K., Jiang, H. & Gutierrez, M.G. 2021. Intracellular localisation of *Mycobacterium tuberculosis* affects efficacy of the antibiotic pyrazinamide. *Nature Communications*, 12(1): 1-15. <https://doi.org/10.1038/s41467-021-24127-3>

Sarathy, J.P., Gruber, G. & Dick, T. 2019. Re-Understanding the Mechanisms of Action of the Anti-Mycobacterial Drug Bedaquiline. *Antibiotics*, 8(4), art. #261.

<https://doi.org/10.3390/antibiotics8040261>

Saxena, R., Singh, D., Phuljhele, S., Kalaiselvan, V., Karna, S., Gandhi, R., Prakash, A., ... Garg, R. 2021. Ethambutol toxicity: Expert panel consensus for the primary prevention, diagnosis and management of ethambutol-induced optic neuropathy. *Indian Journal of Ophthalmology*, 69(12): 3734-3739. doi:10.4103/ijo.IJO_3746_20

Schluger, N.W. 2005. The pathogenesis of tuberculosis: the first one hundred (and twenty-three) years. *American Journal of Respiratory Cell and Molecular Biology*, 32(4): 251-256. <https://doi.org/10.1165/rcmb.F293>

Seung, K.J., Keshavjee, S. & Rich, M.L. 2015. Multidrug-resistant tuberculosis and extensively drug-resistant tuberculosis. *Cold Spring Harbor Perspectives in Medicine*, 5(9), a017863. doi:10.1101/cshperspect.a017863

Shaku, M., Ealand, C. & Kana, B.D. 2020. Cell surface biosynthesis and remodeling pathways in mycobacteria reveal new drug targets. *Frontiers in Cellular and Infection Microbiology*, 10, art. #603382. <https://doi.org/10.3389/fcimb.2020.603382>

Sharma, A., De Rosa, M., Singla, N., Singh, G., Barnwal, R.P. & Pandey, A. 2021. Tuberculosis: an overview of the immunogenic response, disease progression, and medicinal chemistry efforts in the last decade toward the development of potential drugs for extensively drug-resistant tuberculosis strains. *Journal of Medicinal Chemistry*, 64(8): 4359-4395. <https://doi.org/10.1021/acs.jmedchem.0c01833>

Sharma, D., Patel, R.P., Zaidi, S.T.R., Sarker, M.M.R., Lean, Q.Y. & Ming, L.C., 2017. Interplay of the quality of ciprofloxacin and antibiotic resistance in developing countries. *Frontiers in Pharmacology*, 8, art. #546. <https://doi.org/10.3389/fphar.2017.00546>

Sharma, S., Sharma, P.K., Kumar, N. & Dudhe, R. 2011. A review on various heterocyclic moieties and their antitubercular activity. *Biomedicine & Pharmacotherapy*, 65(4): 244-251. <https://doi.org/10.1016/j.biopha.2011.04.005>

Shivakumar, S.V.B.Y., Padmapriyadarsini, C., Chavan, A., Paradkar, M., Shrinivasa, B.M., Gupte, A., ... Selvaraju, S. 2022. Concomitant pulmonary disease is common among patients with extrapulmonary TB. *The International Journal of Tuberculosis and Lung Disease*, 26(4): 341-347. <https://doi.org/10.5588/ijtld.21.0501> doi:10.5588/ijtld.21.0501

Showalter, H.D. 2020. Recent progress in the discovery and development of 2-nitroimidazooxazines and 6-nitroimidazooxazoles to treat tuberculosis and neglected tropical diseases. *Molecules*, 25(18), art. #4137. doi:10.3390/molecules25184137

Sia, I.G. & Wieland, M.L. 2011. Current concepts in the management of tuberculosis. *In Mayo Clinic Proceedings*, 86(4): 348-361 doi:10.4065/mcp.2010.0820

Sia, J.K. & Rengarajan, J. 2019. Immunology of *Mycobacterium tuberculosis* infections. *Microbiology Spectrum*, 7(4), PMID: PMC6636855. doi:10.1128/microbiolspec.GPP3-0022-2018

Silva Miranda, M., Breiman, A., Allain, S., Deknuydt, F. & Altare, F. 2012. The tuberculous granuloma: an unsuccessful host defence mechanism providing a safety shelter for the bacteria? *Clinical and Developmental Immunology*, 2012, art. #139127. doi:10.1155/2012/139127

Singh, N. & Narayan, S. 2011. Nitazoxanide : a broad spectrum antimicrobial. *Medical Journal Armed Forces India*, 67(1): 67-68. doi:10.1016/S0377-1237(11)80020-1

Singh, R., Dwivedi, S.P., Gaharwar, U.S., Meena, R., Rajamani, P. & Prasad, T. 2019. Recent updates on drug resistance in *Mycobacterium tuberculosis*. *Journal of Applied Microbiology*, 128(6): 1547-1567. <https://doi.org/10.1111/jam.14478>

Sizar, O., Rahman, S. & Sundareshan, V. 2021. *Amikacin*. Available from StatPearls: <https://www.ncbi.nlm.nih.gov/books/NBK430908/> Date of access: 27 Mar. 2022.

Smith, I. 2003. *Mycobacterium tuberculosis* pathogenesis and molecular determinants of virulence. *Clinical Microbiology Reviews*, 16(3): 463-496. doi:10.1128/CMR.16.3.463-496.2003

Smith, T., Wolff, K. A. & Nguyen, L. 2013. Molecular biology of drug resistance in *Mycobacterium tuberculosis*. *Current Topics in Microbiology and Immunology*, 374(1): 53-80. doi:10.1007/82_2012_279

Somasundaram, S. & Manivannan, K. 2013. An overview of fluoroquinolones. *Annual Research & Review in Biology*, 3(3): 296-313. <https://journalarrb.com/index.php/ARRB/article/view/24701>

Soria-Arteche, O., Hernández-Campos, A., Yépez-Mulia, L., Trejo-Soto, P.J., Hernández-Luis, F., Gres-Molina, J., ... Castillo, R. 2013. Synthesis and antiprotozoal activity of nitazoxanide–N-methylbenzimidazole hybrids. *Bioorganic & Medicinal Chemistry Letters*, 23(24): 6838-6841. <https://doi.org/10.1016/j.bmcl.2013.10.011>

Sotgiu, G., Saderi, L., Petruccioli, E., Aliberti, S., Piana, A., Petrone, L. & Goletti, D. 2019. QuantiFERON TB Gold Plus for the diagnosis of tuberculosis: a systematic review and meta-analysis. *Journal of Infection*, 79(5): 444-453. <https://doi.org/10.1016/j.jinf.2019.08.018>

Spagnolo, A.M., Sartini, M. & Cristina, M.L. 2021. *Pseudomonas aeruginosa* in the healthcare facility setting. *Reviews in Medical Microbiology*, 32(3): 169-175.
doi:10.1097/MRM.0000000000000271

Stahlmann, R. 2002. Clinical toxicological aspects of fluoroquinolones. *Toxicology Letters*, 127(1-3): 269-277. [https://doi.org/10.1016/S0378-4274\(01\)00509-4](https://doi.org/10.1016/S0378-4274(01)00509-4)

Steingart, K.R., Sohn, H., Schiller, I., Kloda, L.A., Boehme, C.C., Pai, M. & Dendukuri, N. 2013. Xpert® MTB/RIF assay for pulmonary tuberculosis and rifampicin resistance in adults. *The Cochrane Database of Systematic Reviews*, (1), art. #CD009593.
doi:10.1002/14651858

Stephen, S., Muzhizhizhi, D., Dhibi, N., Chidemo, T., Samaneka, W., Matubu, T.A., ... Chirenje, Z.M. 2019. Validation of the GenoType® MTBDRplus Ver 2.0 assay for detection of rifampicin and isoniazid resistance in *Mycobacterium tuberculosis* complex isolates at UZCHS-CTRC TB research laboratory. *International Journal of Mycobacteriology*, 8(1): 83-88. doi:10.4103/ijmy.ijmy_170_18

Sundararajan, S. & Muniyan, R. 2021. Latent tuberculosis: interaction of virulence factors in *Mycobacterium tuberculosis*. *Molecular Biology Reports*, 48(8): 6181-6196.
<https://doi.org/10.1007/s11033-021-06611-7>

Susilawati, T.N. & Larasati, R. 2019. A recent update of the diagnostic methods for tuberculosis and their applicability in 124hiazolid: A narrative review. *Medical Journal of Indonesia*, 28(3): 284-291. <https://doi.org/10.13181/mji.v28i3.2589>

Svensson, E.M., Murray, S., Karlsson, M.O. & Dooley, K.E. 2015. Rifampicin and rifapentine significantly reduce concentrations of bedaquiline, a new anti-TB drug. *Journal of Antimicrobial Chemotherapy*, 70(4): 1106-1114. <https://doi.org/10.1093/jac/dku504>

Takayama, K., Wang, C. & Besra, G.S. 2005. Pathway to synthesis and processing of mycolic acids in *Mycobacterium tuberculosis*. *Clinical Microbiology Reviews*, 18(1): 81-101.
doi:10.1128/CMR.18.1.81-101.2005

Tang, J., Huang, Y., Cai, Z. & Ma, Y. 2021. Mycobacterial heparin-binding hemagglutinin (HBHA)-induced interferon- γ release assay (IGRA) for discrimination of latent and active tuberculosis: A systematic review and meta-analysis. *PloS one*, 16(7): art. #e0254571. <https://doi.org/10.1371/journal.pone.0254571>

Taylor, J.E. & Bull, S.D. 2014. [N-Acylation reactions of amines] [Abstract]. *Comprehensive Organic Synthesis*, 7(2): 427-478. doi:10.1016/B978-0-08-097742-3.00617-0

Telfer, A.J. 2011. *Ciprofloxacin Metal Complexes and Linked Dimers as Potential Antimicrobial Agents*. England: University of York. (Dissertation – MSc).

Tenke, P., Mezei, T., Bőde, I. & Köves, B. 2017. Catheter-associated Urinary Tract Infections. *European Urology Supplements*, 16(4): 138-143. <https://doi.org/10.1016/j.eursup.2016.10.001>

Teo, J., Jureen, R., Chiang, D., Chan, D. & Lin, R. 2011. Comparison of two nucleic acid amplification assays, the Xpert MTB/RIF assay and the Amplified *Mycobacterium tuberculosis* Direct assay, for detection of *Mycobacterium tuberculosis* in respiratory and nonrespiratory specimens. *Journal of Clinical Microbiology*, 49(10): 3659-3662. doi:10.1128/JCM.00211-11

Teo, S.S.S. & Shingadia, D.V. 2006. Does BCG have a role in tuberculosis control and prevention in the United Kingdom? *Archives of Disease in Childhood*, 91(6): 529-531. doi:10.1136/adc.2005.085043

Tripathi, A.C., Gupta, S.J., Fatima, G.N., Sonar, P.K., Verma, A. & Saraf, S.K., 2014. 4-Thiazolidinones: the advances continue. *European Journal of Medicinal Chemistry*, 72: 52-77. <http://dx.doi.org/10.1016/j.ejmech.2013.11.017>

Trotsko, N. 2021. Antitubercular properties of thiazolidin-4-ones – A review. *European Journal of Medicinal Chemistry*, 215, art. #113266. <https://doi.org/10.1016/j.ejmech.2021.113266>

Türe, A., Ergül, M., Ergül, M., Altun, A. & Küçükgülzel, İ. 2021. Design, synthesis, and anticancer activity of novel 4-thiazolidinone-phenylaminopyrimidine hybrids. *Molecular Diversity*, 25(2): 1025-1050. <https://doi.org/10.1007/s11030-020-10087-1>

Umumararungu, T., Mukazayire, M.J., Mpenda, M., Mukanyangezi, M.F., Nkuranga, J.B., Mukiza, J. & Olawode, E.O. 2020. A review of recent advances in anti-tubercular drug development. *Indian Journal of Tuberculosis*, 67(4): 539-559.

<https://doi.org/10.1016/j.ijtb.2020.07.017>

Van Heeswijk, R.P.G., Dannemann, B. & Hoetelmans, R.M.W. 2014. Bedaquiline: a review of human pharmacokinetics and drug–drug interactions. *Journal of Antimicrobial Chemotherapy*, 69(9): 2310-2318. <https://doi.org/10.1093/jac/dku171>

Vanassche, T., Peetermans, M., Van Aelst, L.N., Peetermans, W.E., Verhaegen, J., Missiakas, D.M., ... Verhamme, P. 2013. The role of staphylothrombin-mediated fibrin deposition in catheter-related *Staphylococcus aureus* infections. *Journal of Infectious Diseases*, 208(1): 92-100. <https://doi.org/10.1093/infdis/jit130>

Velayati, A.A., Masjedi, M.R., Farnia, P., Tabarsi, P., Ghanavi, J., Ziazarifi, A.H. & Hoffner, S. E. 2009. Emergence of new forms of totally drug-resistant tuberculosis bacilli: super extensively drug-resistant tuberculosis or totally drug-resistant strains in Iran. *Chest*, 136(2): 420-425. <https://doi.org/10.1378/chest.08-2427>

Vicini, P., Geronikaki, A., Anastasia, K., Incerti, M. & Zani, F. 2006. Synthesis and antimicrobial activity of novel 2-thiazolylimino-5-arylidene-4-thiazolidinones. *Bioorganic & Medicinal Chemistry*, 14(11): 3859-3864. <https://doi.org/10.1016/j.bmc.2006.01.043>

Vilchèze, C. & Jacobs, W.R. 2014. Resistance to isoniazid and ethionamide in *Mycobacterium tuberculosis*: genes, mutations, and causalities. *Microbiology Spectrum*, 2(4), MGM2–0014-2013. doi:10.1128/microbiolspec.MGM2-0014-2013

Vilchèze, C. & Kremer, L., 2017. Acid-fast positive and acid-fast negative *Mycobacterium tuberculosis*: the Koch paradox. *Microbiology Spectrum*, 5(2), art. #5.2.15. <https://doi.org/10.1128/microbiolspec.TBTB2-0003-2015>

Vincent, J.-L. 2003. Nosocomial infections in adult intensive-care units. *The Lancet*, 361(9374): 2068-2077. [https://doi.org/10.1016/S0140-6736\(03\)13644-6](https://doi.org/10.1016/S0140-6736(03)13644-6)

Vohra, S. & Dhaliwal, H.S. 2022. *Miliary Tuberculosis*. Treasure Island, FL: Available from bookshelf NCBI: <https://www.ncbi.nlm.nih.gov/books/NBK562300/?report=classic> Date of access: 03 Jul. 2022.

- Volkman, H.E., Pozos, T.C., Zheng, J., Davis, J.M., Rawls, J.F. & Ramakrishnan, L. 2010. Tuberculous granuloma induction via interaction of a bacterial secreted protein with host epithelium. *Science*, 327(5964): 466-469. doi:10.1126/science.1179663
- Walsh, K.F., McAulay, K., Lee, M.H., Vilbrun, S.C., Mathurin, L., Jean Francois, D., Zimmernan, M., ... Fitzgerald, D.W. 2020. Early bactericidal activity trial of nitazoxanide for pulmonary tuberculosis. *Antimicrobial Agents and Chemotherapy*, 54(5), e01956-19. doi:10.1128/AAC.01956-19
- Wang, P., Pradhan, K., Zhong, X.B. & Ma, X. 2016. Isoniazid metabolism and hepatotoxicity. *Acta Pharmaceutica Sinica B*, 6(5): 384-392. <https://doi.org/10.1016/j.apsb.2016.07.014>
- Waters, M & Tadi, P. 2022. *Streptomycin*. Available from StatPearls: <https://www.ncbi.nlm.nih.gov/books/NBK555886/> Date of access: 27 Mar. 2022.
- Welin, A. 2011. *Survival strategies of Mycobacterium tuberculosis inside the human macrophage*. ResearchGate, Sweden: Linköping University. (Thesis – PhD). <https://www.researchgate.net/publication/267974029>
- WHO (World Health Organization) 2011. *Rapid Implementation of the Xpert MTB/RIF diagnostic test*. <https://apps.who.int/iris/handle/10665/44593> Date of access: 23 Apr. 2022.
- WHO (World Health Organization) 2013. *Xpert MTB/RIF assay for the diagnosis of pulmonary and extrapulmonary TB in adults and children*. <https://www.who.int/publications/i/item/9789241506335> Date of access: 21 Mar. 2022
- WHO (World Health Organization). 2006. *Ethambutol efficacy and toxicity: literature review and recommendations for daily and intermittent dosage in children*. http://apps.who.int/iris/bitstream/handle/10665/69366/WHO_HTM_TB_2006.365_eng.pdf?sequence=1 Date of access: 12 Mar. 2022.
- WHO (World Health Organization). 2008. *Implementing the WHO Stop TB Strategy: a handbook for national tuberculosis control programmes*. <https://apps.who.int/iris/handle/10665/43792> Date of access: 09 Mar. 2022.

WHO (World Health Organization). 2015a. *The End TB Strategy*. <https://www.who.int/teams/global-tuberculosis-programme/the-end-tb-strategy> Date of access: 07 Mar. 2022.

WHO (World Health Organization). 2015b. *Tuberculosis: Totally drug-resistant TB*. <https://www.who.int/news-room/questions-and-answers/item/tuberculosis-totally-drug-resistant-tb> Date of access: 21 Mar. 2022.

WHO (World Health Organization). 2017a. *Ten years in public health, 2007–2017: report by Dr Margaret Chan, Director-General*. <https://apps.who.int/iris/handle/10665/255355> Date of access: 07 May. 2022.

WHO (World Health Organization). 2017b. *WHO meeting report of a technical expert consultation: non-inferiority analysis of Xpert MTB/RIF ultra compared to Xpert MTB/RIF* <https://www.who.int/publications/i/item/WHO-HTM-TB-2017.04> Date of access: 19 Aug. 2022.

WHO (World Health Organization). 2017c. *Prioritization of pathogens to guide discovery, research and development of new antibiotics for drug-resistant bacterial infections, including tuberculosis*. <https://www.who.int/publications/i/item/WHO-EMP-IAU-2017.12> Date of access: 10 Oct. 2022.

WHO (World Health Organization). 2018. *Global guidelines for the prevention of surgical site infection*. <https://www.who.int/publications/i/item/global-guidelines-for-the-prevention-of-surgical-site-infection-2nd-ed>. Date of access: 07 May. 2022.

WHO (World Health Organization). 2019b. *WHO consolidated guidelines on drug-resistant tuberculosis treatment*. <https://apps.who.int/iris/handle/10665/311389> Date of access: 25 Mar. 2022.

WHO (World Health Organization). 2020. *Tuberculosis*. <https://www.who.int/news-room/fact-sheets/detail/tuberculosis> Date of access: 22 Apr. 2022.

WHO (World Health Organization). 2021a. *Global tuberculosis report 2021*. <https://www.who.int/teams/global-tuberculosis-programme/tb-reports/global-tuberculosis-report-2021> Date of access: 09 Mar. 2022.

WHO (World Health Organization). 2021b. *Meeting report of the WHO expert consultation on the definition of extensively drug-resistant tuberculosis*.

<https://www.who.int/publications/i/item/meeting-report-of-the-who-expert-consultation-on-the-definition-of-extensively-drug-resistant-tuberculosis> Date of access: 22 Mar. 2022.

WHO (World Health Organization). 2022a. *Line probe assays for detection of drug-resistant tuberculosis: interpretation and reporting manual for laboratory staff and clinicians*.

<https://www.who.int/publications/i/item/9789240046665> Date of access: 18 Aug. 2022.

WHO (World Health Organization). 2022b. *Global report on infection prevention and control*.

<https://www.who.int/publications/i/item/9789240051164> Date of access: 07 May. 2022.

Woimo, T.T., Yimer, W.K., Bati, T. & Gesesew, H.A. 2017. The prevalence and factors associated for anti-tuberculosis treatment non-adherence among pulmonary tuberculosis patients in public health care facilities in South Ethiopia: a cross-sectional study. *BMC Public Health*, 17(1), art. #269. <https://doi.org/10.1186/s12889-017-4188-9>

Worley, M.V. & Estrada, S.J. 2014. Bedaquiline: a novel antitubercular agent for the treatment of multidrug-resistant tuberculosis. *Pharmacotherapy*, 34(11): 1187-1197.

<https://doi-org.nwulib.nwu.ac.za/10.1002/phar.1482>

Wu, D., Wu, C., Zhang, S. & Zhong, Y. 2019. Risk factors of ventilator-associated pneumonia in critically ill patients. *Frontiers in Pharmacology*, 10, art. #482.

<https://doi.org/10.3389/fphar.2019.00482>

Xu, Z., Zhou, A., Wu, J., Zhou, A., Li, J., Zhang, S., ... Yao, Y.-F. 2018. Transcriptional approach for decoding the mechanism of *rpoC* compensatory mutations for the fitness cost in rifampicin-resistant *Mycobacterium tuberculosis*. *Frontiers in Microbiology*, 9, art. #2895.

<https://doi.org/10.3389/fmicb.2018.02895>

Yang, H., Kruh-Garcia, N.A. & Dobos, K.M. 2012. Purified protein derivatives of tuberculin—past, present, and future. *FEMS Immunology & Medical Microbiology*, 66(3): 273-280.

Yano, T., Kassovska-Bratinova, S., I, J.S., Winkler, J., Sullivan, K., Isaacs, A., ... Rubin, H. 2011. Reduction of clofazimine by mycobacterial type 2 NADH: quinone oxidoreductase: a pathway for the generation of bactericidal levels of reactive oxygen species. *Journal of Biological Chemistry*, 286(12): 10276-10287. <https://doi.org/10.1074/jbc.M110.200501>

Zhang, T., Jiang, G., Wen, S.A., Huo, F., Wang, F., Huang, H. & Pang, Y. 2019. Para-aminosalicylic acid increases the susceptibility to isoniazid in clinical isolates of *Mycobacterium tuberculosis*. *Infection and Drug Resistance*, 12: 825-829.
doi:10.2147/IDR.S200697

Zhang, Y. & Mitchison, D. 2003. The curious characteristics of pyrazinamide: a review. *The International Journal of Tuberculosis and Lung Disease*, 7(1): 6-21. Date of access: 13 Mar. 2022.

Zhang, Y. 2005. The magic bullets and tuberculosis drug targets. *Annual Review of Pharmacology and Toxicology*, 45(2005): 529-564.
doi:10.1146/annurev.pharmtox.45.120403.100120

Zhou, X., Willems, R.J., Friedrich, A.W., Rossen, J.W. & Bathoorn, E. 2020. *Enterococcus faecium*: from microbiological insights to practical recommendations for infection control and diagnostics. *Antimicrobial Resistance & Infection Control*, 9(1): art #130.
<https://doi.org/10.1186/s13756-020-00770-1>

Zhou, X.X., Liu, Y.L., Zhai, K., Shi, H.Z. & Tong, Z.H. 2015. Body fluid interferon- γ release assay for diagnosis of extrapulmonary tuberculosis in adults: a systematic review and meta-analysis. *Scientific Reports*, 5(1): art. #15284. doi:10.1038/srep15284

Zhu, C., Liu, Y., Hu, L., Yang, M. & He, Z.G. 2018. Molecular mechanism of the synergistic activity of ethambutol and isoniazid against *Mycobacterium tuberculosis*. *Journal of Biological Chemistry*, 293(43): 16741-16750. <https://doi.org/10.1074/jbc.RA118.002693>

Ziganshina, L.E., Vigel, A.A. & Squire, S.B. 2005. Fluoroquinolones for treating tuberculosis. *The Cochrane Database of Systematic Reviews*, 2005(3), art. #CD004795
doi:10.1002/14651858.CD004795.pub2.

Zumla, A. & Grange, J.M. 1999. The 'global emergency' of tuberculosis. *Journal of The Royal College of Physicians of Edinburgh*, 29(2): 104-115.
<https://doi.org/10.1177/147827159902900204>

Zumla, A., Mwaba, P., Huggett, J., Kapata, N., Chanda, D. & Grange, J. 2009. Reflections on the white plague. *The Lancet Infectious Diseases*, 9(3): 197-202.
[https://doi.org/10.1016/S1473-3099\(09\)70045-3](https://doi.org/10.1016/S1473-3099(09)70045-3)

CHAPTER 3: ARTICLE FOR SUBMISSION

Chapter 3 contains a manuscript that was accepted for publication in Chemistry & Biodiversity. This article is divided into an introduction, materials and methods (including an experimental section), results and discussion, and a conclusion section. It also includes *in vitro* biological and cytotoxic assessments, as well as *in silico* drug-like prediction. Additionally, it has an abstract and a graphic abstract.

This paper was written in accordance with the author's guidelines, which are accessible on the journal's webpage:

<https://onlinelibrary.wiley.com/page/journal/16121880/homepage/forauthors.html>

NITROTHIAZOLE-THIAZOLIDINONE HYBRIDS: SYNTHESIS AND *IN VITRO* ANTIMICROBIAL EVALUATION

Dylan Hart^a, Lesetja J. Legoabe^a, Omobolanle J. Jesumoroti^a, Audrey Jordaan^b, Digby F.

Warner^{b,c,d} Rebecca Steventon^e, and Richard M. Beteck^{a*}

^a *Centre of Excellence for Pharmaceutical Sciences, North-West University, Private Bag X6001, Potchefstroom 2520, South Africa.*

^b *SAMRC/NHLS/UCT Molecular Mycobacteriology Research Unit, Department of Pathology, University of Cape Town, Observatory, 7925, South Africa.*

^c *Institute of Infectious Disease and Molecular Medicine, University of Cape Town, Rondebosch, 7701, South Africa.*

^d *Wellcome Centre for Infectious Diseases Research in Africa (CIDRI-Africa), Faculty of Health Sciences, University of Cape Town, Rondebosch, 7701, South Africa.*

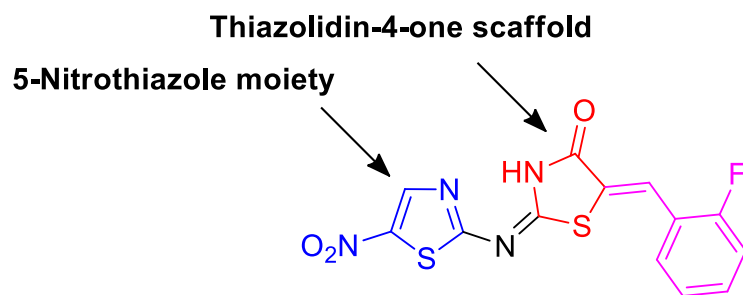
^e *School of life sciences, University of Warwick, United Kingdom.*

*** Correspondence:**

Centre of Excellence for Pharmaceutical Sciences, North-West University, Private Bag X6001, Potchefstroom, 2520, South Africa

* Corresponding author: e-mail: 25159194@nwu.ac.za OR richmbi1@yahoo.com; Tel.: +27 18 299 2249

GRAPHICAL ABSTRACT



Hybrid compound 3b

(2*E*,5*Z*)-5-(2-fluorobenzylidene)-2-((5-nitrothiazol-2-yl)imino)thiazolidin-4-one

Mtb gfp MIC₉₀ 0.45 μM
S. aureus MIC₈₀ 2 μg/ml
MRSA MIC < 0.25 μg/ml
C. albicans MIC ≤ 0.25 μg/ml
EKAP MIC > 32 μg/ml
HEK-293 CC₅₀ > 32 μg/ml
RBC HC₁₀ > 32 μg/ml
cLogP 2.53

ABSTRACT

Herein we report the synthesis of novel compounds inspired by the antimicrobial activities of nitroazole and thiazolidin-4-one based compounds reported in the literature. Target compounds were evaluated *in vitro* for antitubercular, antibacterial, antifungal, and overt cell toxicity properties. All compounds exhibited potent antitubercular activity. Most compounds exhibited low micromolar activity against *S. aureus* and *C. albicans* with no overt cell toxicity against HEK-293 cells nor haemolysis against human red blood cells. Notably, compound **3b** exhibited low to sub-micromolar activities against *Mycobacterium tuberculosis* (Mtb), methicillin-resistant *Staphylococcus aureus* (MRSA), and *Candida albicans*. Compound **3b** showed superior activity (< 0.25 µg/ml) against MRSA compared to vancomycin (1 µg/ml).

Keywords: Antimicrobial; 5-nitrothiazoles; Thiazolidin-4-ones; Molecular hybridisation; ESKAPE pathogens.

3.1. Introduction

Before COVID-19, tuberculosis (TB) was the world's foremost infectious disease caused by a single pathogen. TB is caused by a bacterium called *Mycobacterium tuberculosis* (Mtb). The COVID-19 pandemic is erasing the laborious advances made in the past 20 years toward eradicating TB [1]. Without concrete actions, the global 10 million estimated TB cases (including 815, 000 HIV-positive individuals) and more than 1.4 million TB deaths (including 208, 000 HIV-positive individuals) that occur annually will increase, and low-to-middle income countries will be the most affected [2]. The currently available first-line antitubercular treatment regimen is a 6-month course of rifampicin (RIF), isoniazid (INH), ethambutol (ETH), and pyrazinamide (PZA). This regimen presents adverse side effects, a prolonged treatment period, and non-compliance from TB patients, which ultimately leads to the emergence of drug-resistant strains of Mtb [3]. There is apparently a need for the discovery of efficacious chemotherapeutics with minimal toxicity and a novel mechanism of action (MOA) to address Mtb, with particular relevance to multidrug-resistant TB (MDR-TB) and extensively drug-resistant TB (XDR-TB) [4,5]. After approximately forty years of no novel antitubercular drugs entering the market, bedaquiline (BDQ) and nitro-containing drugs (delamanid (DLM) and pretomanid (PTM)) achieved conditional regulatory approval as novel antitubercular drugs to treat MDR-TB [6-8]. The approval of these three drugs is a great achievement in the fight against TB but does not suffice to completely eradicate TB, hence the need to continuously search for novel antitubercular agents.

The COVID-19 pandemic has also increased awareness regarding the threat posed by infectious diseases, and it has served as a major catalyst for reviving efforts to tackle the silent epidemic of antimicrobial-resistant (AMR) bacteria [9]. Antibiotics' diminishing efficacy against bacteria is jeopardising the practice of modern medicine. This is especially evident in infections caused by *Enterococcus* spp., *Staphylococcus aureus*, *Klebsiella pneumoniae*, *Acinetobacter baumannii*, *Pseudomonas aeruginosa*, *Enterobacter* spp. (ESKAPE-pathogens), and *Escherichia coli*. ESKAPE pathogens are the major cause of hospital-acquired infections

(HAIs) (an infection acquired while receiving treatment in a healthcare facility) globally. In fact, antimicrobial resistance among these pathogens is wreaking havoc on global public health [10].

ESKAPE pathogens are responsible for approximately 80% of HAIs — which include pneumonia, bloodstream infections, urinary tract infections, or surgical site infections [11]. These pathogens represent the top bacterial isolates in a hospital setting, possessing significant intrinsic drug resistance. Data from Centre for Disease Control and Prevention (CDC), suggests that 1 in 31 hospitalised patients develops a HAI every day, and approximately 99 000 deaths due to HAIs occur each year in the United States alone [12, 13]. These infections are anticipated to increase the cost of patient treatment by 4.5 to 5.7 billion dollars annually [14]. The increased burden of drug-resistant ESKAPE pathogens has prompted the WHO to classify ESKAPE pathogens into critical and high priority groups, which indicates an urgent need for the identification and development of new antibiotics against these pathogens [15].

Newly approved antitubercular drugs, DLM and PTM (see **Fig. 3.1**), belong to the nitroazole class of compounds. They have been identified as a novel and potent chemical class, exhibiting a MOA not seen with currently available antitubercular drugs [8]. Other notable nitroazole compounds are nitazoxanide (NTZ) and its hydrolysed active metabolite, tizoxanide (TIZ) (see **Fig. 3.1**). NTZ and TIZ are antiprotozoal 5-nitrothiazole-based agents that have been repurposed owing to their efficacy against *Mtb*. Targets perturbed by NTZ include pyruvate-ferredoxin oxidoreductase (PFOR) in anaerobic bacteria and protozoans [16], pyruvate dehydrogenase in *E. coli* [17], membrane potential, and pH homeostasis of *Mtb* [18], bacteria's chaperone/usher (CU) pathway [19], macrophage autophagy and *mTORC1* signalling [20]. At low concentrations, NTZ and TIZ eradicate both replicating and non-replicating (slow growing) *Mtb* while also appearing to evade resistance formation [21]. NTZ

is therefore a suitable template to inspire the identification and development of novel broad-spectrum anti-infective agents.

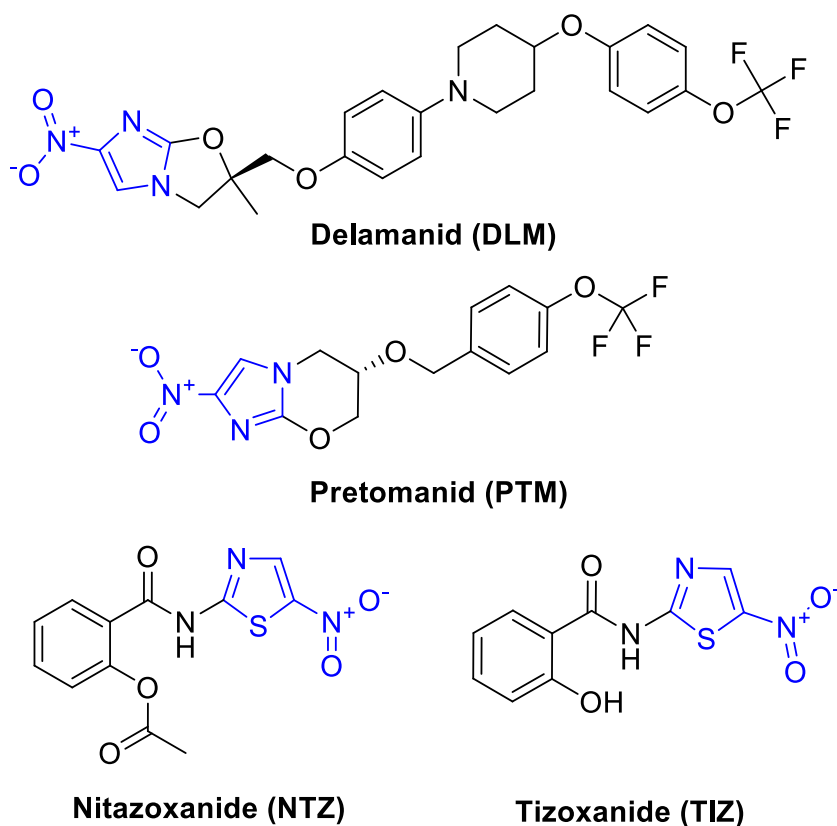


Figure 3.1 Structures of biological active nitroazole drugs

Thiazolidinone is a saturated heterocyclic thiazole bearing a carbonyl (C=O) functional group, a sulphur (S) atom and a nitrogen (N) atom [22]. There are predominantly three types of thiazolidinones: thiazolidin-2-one, thiazolidin-4-one, and thiazolidin-5-one [23]. The thiazolidin-4-one scaffold (see **Fig. 3.2**) has long been regarded as a magical structure (“wonder nucleus”) capable of almost any biological activity [24], including antibacterial (against Gram-positive and Gram-negative bacteria) [25-27], antimycobacterial [28], antifungal [27,29], anti-HIV [30,31], anticancer [32] and anticonvulsant [33] properties. Although the MOA of thiazolidin-4-one is unknown, Vicini *et al.* (2006) demonstrated that substituting a benzylidene moiety in the fifth position (fifth carbon-C5) of the thiazolidin-4-one heterocyclic core enhances its antibacterial properties [34].

The molecular hybridisation (MH) approach has been widely employed to develop novel molecules with potential poly-pharmacophoric characteristics. The MH strategy commonly employed involves the use of linkers to join two or more compounds with well-characterized biological activities [35]. This practice often leads to the synthesis of new compounds with an excessive molecular weight (> 500 Da) beyond Lipinski's recommendation. In this study, we employ the concept of MH (see **Fig. 3.2**) to generate novel compounds incorporating the 2-amino-5-nitrothiazole moiety (present in NTZ) and thiazolidin-4-one. C5 of the thiazolidin-4-one was used to explore SARs for this library. The target compounds (**3a – 3j**) were evaluated *in vitro* against Mtb, some ESKAPE pathogens, MRSA, and the fungus *C. albicans*. Additionally, these compounds were evaluated against human embryonic kidney and red blood cells for overt cell toxicity and haemolysis, respectively.

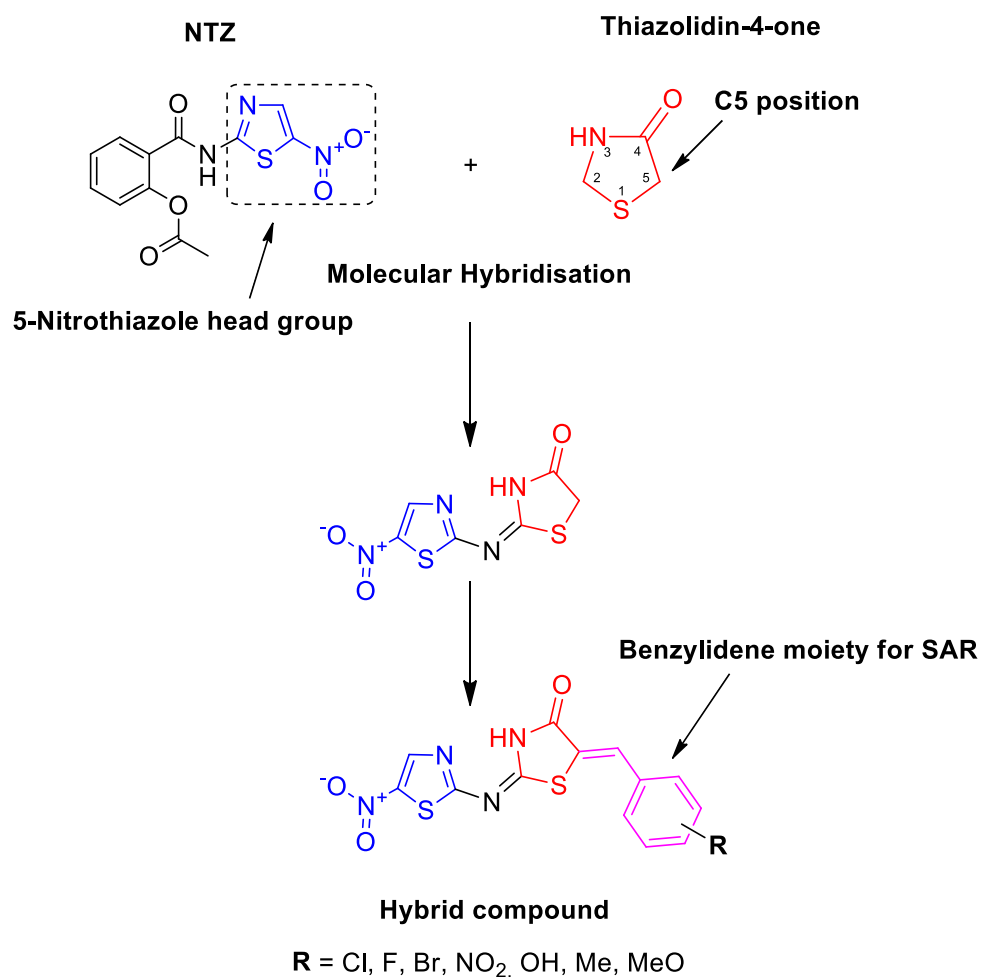
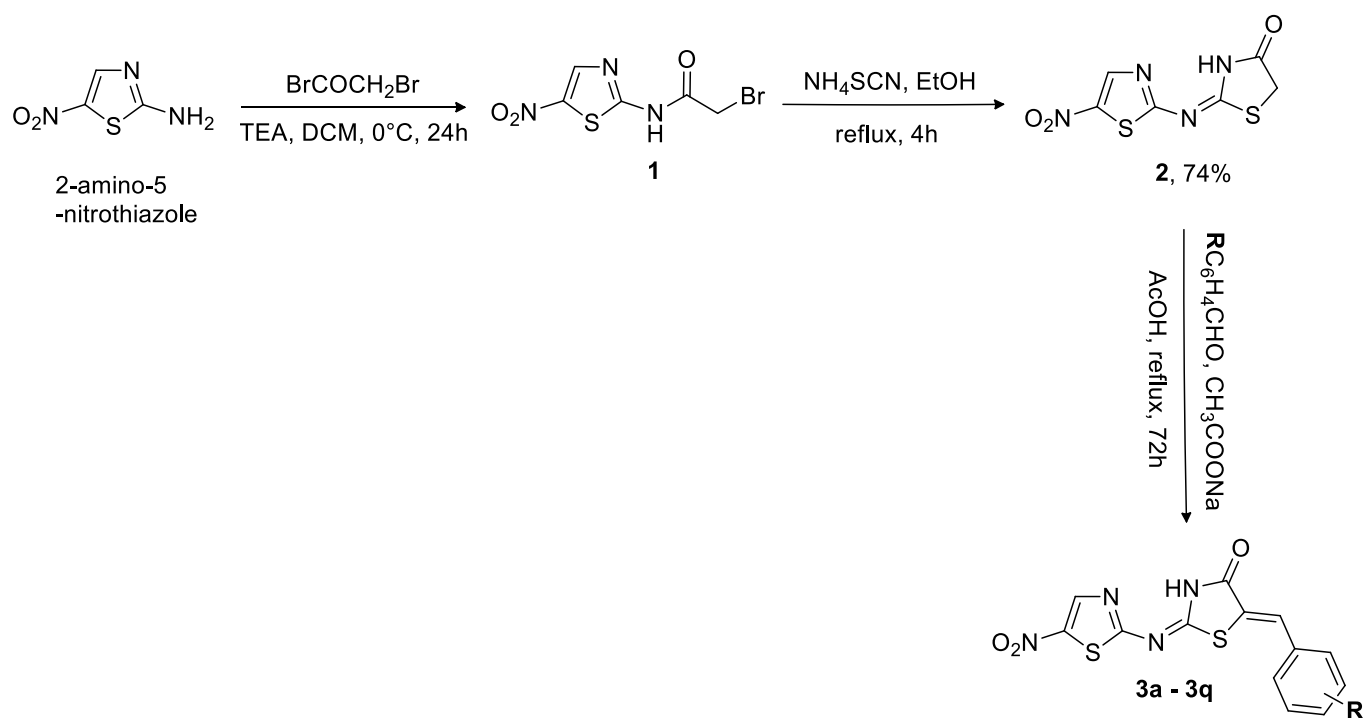


Figure 3.2 Molecular hybridization strategy

3.2. Results and discussion

3.2.1. Chemistry and structure characterisation

The target compounds were synthesized following a multi-step synthetic protocol presented in **Scheme 1**. *N*-acylation of the 2-amino-5-nitrothiazole with bromoacetyl bromide afforded intermediate **1** in 80% yield. Refluxing **1**, and ammonium thiocyanate in ethanol led to successive *S*-alkylation and intramolecular cyclization to provide the thiazolidine-4-one based heterocycle, intermediate **2** in 74% yield [26,34]. Target compounds (**3a – 3q**) were synthesized in 26–69% yield using the standard Knoevenagel condensation procedure by treating intermediate **2** with commercially available aldehydes.



* Percentage yield

R

3a : H, 52%*	3e : 3-F, 45%	3h : 4-F, 42%	3l : 2-Me, 38%	3n : 2,4-MeO, 51%	3q : 3,4-Cl, 35%
3b : 2-F, 26%	3f : 3-Cl, 46%	3i : 4-Cl, 40%	3m : 4-Me, 43%	3o : 2,4,6-MeO, 42%	
3c : 2-Cl, 52%	3g : 3-Br, 69%	3j : 4-NO ₂ , 31%		3p : 3-MeO, 54%	
3d : 2-NO ₂ , 36%		3k : 4-OH, 32%			

Scheme 1 Synthesis of conceptualised target compounds

The structures of intermediate **2** and target compounds **3a – 3q** were determined using FTIR, ^1H and ^{13}C -NMR and HRMS. The observable diagnostic peaks are stated below:

The FTIR spectra of intermediate **2** and all the target compounds **3a – 3q** showed absorbance at different wavelengths indicative of the functional groups present. For example, the 5- NO_2 group present on the fifth position of the thiazole moiety can be observed in all compounds as an intense broad stretch between 1521.91–1582.33 cm^{-1} (N–O) and 1294.77–1351.42 cm^{-1} (N–O). The –NH– stretch appeared around 3067.70–3144.49 cm^{-1} and the stretch around 1676.96–1729.23 cm^{-1} can be attributed to the amide carbonyl (C=O) functional group. In the FTIR spectra of compound **3k**, the broad stretching at 3260.80 cm^{-1} is indicative of the presence of an OH group.

The broad singlet at *ca.* 12.56–13.26 ppm in the ^1H NMR spectra of intermediate **2** and target compounds indicates the presence of a lactam –NH– group; this signal is however absent in compounds **3i**, **3j**, **3o**, **3q**, probably due to exchange with H_2O in deuterated (D_6)DMSO. In the ^1H NMR of **2**, the active methylene protons appear as a singlet, integrating to 2 protons at *ca.* 4 ppm. The disappearance of this singlet in the ^1H NMR of compounds **3a – 3q** suggests that the Knoevenagel condensation step was successful. In the ^1H NMR spectra of all compounds, the singlet peak, integrating to one proton at approximately 8.66 ppm, is assignable to the thiazolyl proton. Compound **3o** can be identified as an outlier due to the thiazolyl proton appearing at 7.40 ppm. The substituted methyl (R- CH_3) or methoxy (R- OCH_3) groups at the benzylidene moiety of compounds **3l – 3p**, are observed in the ^1H NMR spectra in the range of 2.36–3.91 ppm as three or more protons, depending on the structure. This series of compounds suffers from poor solubility in deuterated (D_6)DMSO and, as a result, all carbon peaks could not be accounted for.

The molecular mass for each compound was confirmed using HRMS. All compounds (except **3e**, **3n**, and **3o**) were confirmed to be > 96% pure using HPLC. Compounds **3e**, **3n**, and **3o**

displayed a purity of 79.04%, 88.02%, and 85.47%, respectively. Trace solvent impurities (1,4-dioxane, DMF, toluene, and ethanol) are present in the NMR spectra of some of the target compounds. Prior to biological evaluation, the target compounds were vacuum-dried for 72 h at 150°C and 200 Pa to remove solvent impurities.

3.2.2. Antitubercular activity

All compounds, **2**, **3a – 3q**, were screened *in vitro* for their antitubercular activity in CAS medium versus the gfp strain of Mtb. The first-line antitubercular drug, RIF, was used as a reference. Following incubation, the minimum inhibitory concentration (MIC₉₀) needed to inhibit 90% of mycobacterial growth was determined on day 14. The antitubercular activity results for the tested compounds are summarized in **Table 3.1**. Astoundingly, compounds **3a – 3q** were presented with excellent antitubercular activity, ranging from < 0.24–2.00 μM. Compounds **3c**, **3g – 3i**, **3l**, **3n**, and **3q** are the most potent against Mtb, showing MIC₉₀ values of < 0.24 μM. Compound **3k**, having a hydroxy (OH) group at the *para*-position of the benzylidene moiety, presented the least antitubercular activity of 2 μM. Comparing the MIC₉₀ value of intermediate **2** (31.25 μM) against the values of compound **3a – 3q**, suggests that appending on to **2** a benzylidene moiety bearing electron withdrawing– (EWG) or electron donating groups (EDG) is essential for antitubercular activity.

Table 3.1 Antimicrobial and cytotoxic activities of compounds **2** and **3a – 3j**

ID	R	Mtb ^a (CAS)	Sa ^b	MRSA ^c	Ca ^d	EKAP ^e	HEK-293 ^f	RBCs ^g
		Day 14 MIC ₉₀ µM	MIC (µg/ml)	MIC (µg/ml)	MIC (µg/ml)	MIC (µg/ml)	CC ₅₀ (µg/ml)	HC ₁₀ (µg/ml)
2	-	31.25	>32	>32	>32	>32	>32	>32
3a	H	0.48	8	>32	4	>32	>32	>32
3b	2-F	0.45	2	<0.25	4	>32	>32	>32
3c	2-Cl	<0.24	4	>32	>32	>32	>32	>32
3d	2-NO₂	0.72	2	>32	>32	>32	>32	>32
3e	3-F	0.52	4	>32	16	>32	>32	>32
3f	3-Cl	0.29	>32	>32	>32	>32	>32	>32
3g	3-Br	<0.24	2	>32	≤0.25	>32	>32	>32
3h	4-F	<0.24	>32	>32	32	>32	>32	>32
3i	4-Cl	<0.24	4	>32	>32	>32	>32	>32
3j	4-NO₂	0.92	>32	>32	>32	>32	>32	>32
3k	4-OH	2.00	>32	>32	>32	>32	>32	>32
3l	2-Me	<0.24	2	>32	>32	>32	>32	>32
3m	4-Me	0.48	2	>32	>32	>32	>32	>32
3n	2,4-MeO	<0.24	>32	>32	>32	>32	>32	>32
3o	2,4,6-MeO	0.48	>32	>32	>32	>32	>32	>32
3p	3-MeO	0.50	8	>32	>32	>32	>32	>32
3q	3,4-Cl	<0.24	>32	>32	32	>32	>32	>32
RIF		0.018	-	-	-	-	-	-
AMP		-	0.5	-	-	-	-	-
CPF		-	0.5	-	-	-	-	-
VM		-	-	1	-	-	-	-
FZ		-	-	-	0.12	-	-	-
CL		-	-	-	-	0.25	-	-
TF		-	-	-	-	-	9	-
MT		-	-	-	-	-	-	2.7

^a*M. tuberculosis* strain (Mtb pMSp12: gfp) in Middlebrook 7H9 CAS: 0.03% casitone, 0.4% glucose, and 0.05% tyloxapol; ^b*S. aureus*; ^c*Methicillin-resistant S. aureus*; ^d*C. albicans*; ^e*E. coli*, *K. pneumoniae*, *A. baumannii*, *P. aeruginosa*; ^fHuman embryonic kidney cells; ^gRed blood cells; **Reference drugs:** Rifampicin (RIF); Ampicillin (AMP) Ciprofloxacin (CPF), Colistin (CL), Vancomycin (VM), Fluconazole (FZ), Tamoxifen (TF), Mellitin (MT)

3.2.3. Antibacterial and antifungal activities

In addition to the antitubercular assay, the antibacterial activity of **2** and **3a – 3q** was determined against *Escherichia coli* (ATCC25922), *Klebsiella Pneumoniae* (ATCC700603), *Acinetobacter baumannii* (ATCC19606), *Pseudomonas aeruginosa* (ATCC27853), *Staphylococcus aureus* and *methicillin-resistant Staphylococcus aureus* (MRSA) (ATCC43300). Approved antibacterial drugs, ampicillin, colistin, vancomycin, and ciprofloxacin, were used as reference drugs, and the screening results are tabulated in **Table 3.1**. Hits were classified as any compound exhibiting an MIC value of ≤ 16 $\mu\text{g/ml}$. Generally, these compounds were not active against MRSA and Gram-negative bacteria (*E. coli*, *K. pneumoniae*, *A. baumannii*, *P. aeruginosa*, *Enterobacter* spp.), but exhibited varying degrees of activity (MIC: 2 – > 32 $\mu\text{g/ml}$) against *S. aureus*, a Gram-positive bacterium. This disparity in activity could be due to the cell wall of Gram-negative bacteria, which act as a barrier, preventing molecules from entering these bacteria.

Ten of the eighteen compounds tested were active against *S. aureus*. Compounds **3a**, **3b**, **3c**, **3d**, **3e**, **3g**, **3i**, **3l**, **3m**, and **3p** all exhibited potent antibacterial activity in the range of 2–8 $\mu\text{g/ml}$ against *S. aureus*. Among the active compounds, the fluoro-, nitro-, bromo-, and methyl substituted compounds, **3b**, **3d**, **3g**, **3l–3m**, respectively, had the highest and equipotent antibacterial activity (MIC: 2 $\mu\text{g/ml}$), whereas chloro- (**3c** and **3i**) and 3-fluoro-substituted (**3e**) compounds showed a two-fold increase in MIC values from 2 to 4 $\mu\text{g/ml}$. Compound **3a**, having an unsubstituted benzylidene moiety, and **3p**, harbouring a methoxy group, exhibited the lowest activity (MIC: 8 $\mu\text{g/ml}$).

In general, activity against *S. aureus* increases with substitution of the benzylidene moiety with EWG and EDG. For example, compounds **3b** and **3l**, bearing EWG and EDG, respectively, have equipotent activity (MIC: 2 $\mu\text{g/ml}$), which is a fourfold increase in activity when compared to compound **3a** (MIC: 8 $\mu\text{g/ml}$) bearing an un-substituted benzylidene moiety. No change in MIC values could be found between compounds **3c** and **3i** (4 $\mu\text{g/ml}$) having a chloro

substituent in the *ortho*- and *para*-positions, suggesting that both positions are preferred. Having said that, it is worth noting that compound **3f**, with a chloro substituent in the *meta*-position, exhibited no antibacterial activity against *S. aureus* (MIC > 32 µg/ml). Compounds **3b** and **3e** with a fluoro atom in the *ortho* and *meta*-positions, respectively, exhibited activity, while compound **3h**, with a fluoro atom in the *para*-position, showed no activity. Furthermore, the findings demonstrated that compound **3j** with a nitro substituent in the *para*-position is inactive against *S. aureus*, but the activity was restored to 2 µg/ml when the nitro atom was present in the *ortho*-position (**3d**). All these suggest that substitution at the *ortho* position of the benzylidene moiety favours activity against *S. aureus*.

It is noteworthy to note that compounds **3n** and **3o** bearing multiple methoxy substituents on the benzylidene moiety are inactive against *S. aureus*, but compound **3p** bearing a single methoxy substituent in the *meta*-position is active (MIC: 8 µg/ml). Finally, unlike the compounds with a single chloro-substituted atom (**3c** and **3i**), compound **3q** with disubstituted chlorine atoms in the *meta*- and *para*-positions exhibits no activity. This suggests that poly-substitution of the benzylidene moiety does not favour activity. Compound **3k**, with a hydroxy substituent in the *para*-position, showed no activity.

Except for compound **3b**, all compounds showing activity against *S. aureus* were inactive against MRSA. This suggests penicillin-binding protein (PBP) as the likely target for these compounds. **3b**, however, exhibited sub-micromolar activity (< 0.25 µg/ml) against MRSA, suggesting a different target from PBP and/or binding to a different pocket within PBP.

Compounds were also evaluated for antifungal activity against *Candida albicans* (ATCC90028). Only six compounds showed activity against *C. albicans*, and they include **3a** (4 µg/ml), **3b** (4 µg/ml), **3e** (16 µg/ml), **3g** (≤ 0.25 µg/ml), **3h** (32 µg/ml) and **3q** (32 µg/ml). Notably, compound **3g** exhibited comparable activity to the reference drug fluconazole (MIC: 0.12 µg/ml).

3.2.4. Cytotoxicity and haemolytic studies

Overt cell toxicity was determined against human embryonic kidney cells (HEK-293) and human red blood cells (RBCs), which are reported in **Table 3.1**. These cells were treated with test compounds at 32 µg/ml and their viability was assessed. No compound in this study reduced cells viability to below 80%, and as such, these compounds are assigned a CC₅₀ and HC₁₀ value of > 32 µg/ml.

3.2.5. *In silico* drug-like prediction

In silico physicochemical prediction of novel compounds is an integral part of drug discovery since it provides insight into a molecule's drug-like properties and safety. Using the SwissADME online web tool (<http://www.swissadme.ch>), we calculated and tabulated the consensus logarithm of the partition coefficient (cLogP), the molecular weight (MW), the number of hydrogen bond acceptors (HBA), the number of hydrogen bond donors (HBD), the topological polar surface area (tPSA), and the number of rotatable bonds. The results in **Table 3.2** were compared to Lipinski's five-point rule, as described in his foundational work [36]. According to the Lipinski rule of five, a molecule with a MW of under 500 Da, an octanol–water partition coefficient (cLogP) of less than 5, an HBA of less than 10, and no more than 5 potential HBD is more likely to be an acceptable oral active drug [37]. In the results, it can be observed that compounds **2**, **3a – 3q** do not violate Lipinski's five-point rule.

While lipophilicity is a critical physicochemical criterion, it is not the only property that determines effective drug design, as shown from the findings of a GlaxoSmithKline-funded study of rat availability data for 1100 drug candidates, conducted by Veber *et al.* (2002). This finding suggests that additional physicochemical properties, for example, tPSA and molecular flexibility (RoB), should be investigated, as they affect the oral bioavailability of drugs [38]. To select drugs with expected oral bioavailability, two simple guidelines were confirmed by Veber *et al.* (2002). If a rat oral bioavailability of ≥ 20–40% is acceptable, then tPSA ≤ 140 Å² paired with RoB ≤ 10 appears to be an efficient and selective parameter [39]. Interestingly, the newly

synthesized target compounds showed one violation of Veber's parameters regarding their *t*PSA, which is above 140 Å² but presents with good molecular flexibility according to the RoB parameter.

Table 3.2 Physiochemical properties of compounds **2** and **3a – 3j**

ID	cLogP _{o/w} ^a	MW ^b (Da)	HBA ^c	HBD ^d	RoB ^e	<i>t</i> PSA ^f Å ²	LogS ^g mol/l	Lipinski Violations	Veber Violations
2	0.62	244.25	5	1	2	153.71	-2.38	0	1
3a	2.26	332.36	5	1	3	153.71	-4.32	0	1
3b	2.53	350.35	6	1	3	153.71	-4.47	0	1
3c	2.78	366.80	5	1	3	153.71	-4.91	0	1
3d	1.49	377.36	7	1	4	199.53	-4.38	0	1
3e	2.53	350.35	6	1	3	153.71	-4.47	0	1
3f	2.76	366.80	5	1	3	153.71	-4.91	0	1
3g	2.85	411.25	5	1	3	153.71	-5.22	0	1
3h	2.52	350.35	6	1	3	153.71	-4.47	0	1
3i	2.75	366.80	5	1	3	153.71	-4.91	0	1
3j	1.45	377.36	7	1	4	199.53	-4.38	0	1
3k	1.54	348.36	6	2	3	173.94	-4.18	0	1
3l	2.34	346.38	5	1	3	153.71	-4.61	0	1
3m	2.30	346.38	5	1	3	153.71	-4.61	0	1
3n	2.01	392.41	7	1	5	172.17	-4.46	0	1
3o	1.98	422.44	8	1	6	181.40	-4.54	0	1
3p	1.98	362.38	6	1	4	162.94	-4.39	0	1
3q	3.31	401.25	5	1	3	153.71	-5.51	0	1

^aConsensus octanol–water partition coefficient indicating lipophilicity; ^bMolecular weight of compounds; ^cNumber of hydrogen bond acceptors; ^dNumber of hydrogen bond donors; ^eNumber of rotatable bonds; ^fTopological polar surface area; ^gLogarithm of the solubility in water.

Furthermore, the cLogP for the target compounds correlate negatively with the water solubility potentials (LogS). Predictions of distribution and absorption properties (see **Annexure A – Table 1**) revealed that none of the examined compounds can penetrate the blood–brain barrier (BBB), and none of the compounds are estimated to be substrates of P-glycoprotein.

Additionally, the passive human gastrointestinal (GI) absorption predictions found that all generated compounds had a limited absorption potential and displayed reasonably high inhibition of many or all the important CYP450 iso-enzymes associated with drug metabolism: CYP1A2, CYP2C19, CYP2C9, CYP2D6, and CYP3A4

3.3. Materials and methods

3.3.1. General methods

Reagents and solvents were purchased from various chemical suppliers including, Ambeed, AK Scientific, Rochelle, Labchem and Merck. Reaction progress was monitored through thin-layer chromatography method using Merck 60F₂₅₄ silica gel sheet supported on aluminium. UV light (254 and 366 nm) or iodine vapor staining was used to visualise the developed sheets. Melting points (m.p.) were determined with a Buchi B-545 apparatus. Fourier-transform infrared spectroscopy (FTIR) was done using a Bruker ALPHA FTIR Routine spectrometer. ¹H and ¹³C nuclear magnetic resonance (NMR) spectra were acquired on a Bruker Avance III 600 spectrophotometer at 600 MHz and 151 MHz, respectively, in deuterated DMSO ((D₆)DMSO). Chemical shifts are reported in parts per million (ppm) and were referenced to the residual solvent peaks ((D₆)DMSO: 2.50 and 39.52 ppm for ¹H and ¹³C-NMR, respectively). Spin multiplicities are given as s (singlet), d (doublet), t (triplets), m (multiplet), dt (doublet of triplets), td (triplet of doublets), and dd (doublet of doublets). Coupling constants (*J*) are reported in Hz. A Bruker micrOTOF-Q II mass spectrometer was used to record high-resolution mass spectra (HRMS) utilising atmospheric pressure chemical ionisation (APCI) in positive ion mode. A full scan from 50 to 1600 *m/z* was carried out at a capillary voltage of 4500 V, an end plate offset of -500 V, 1.8 Bar nebulisers, and a collision cell RF voltage of 150 Vpp. Compound purity was determined by high performance liquid chromatography (HPLC) analysis using an Agilent 1200 series HPLC system equipped with a quaternary pump and an Agilent 1200 series diode array detector. A Venusil XBP C18 column (4.60 × 150 mm, 5 μm) was used for separation, and the mobile phase consisted initially of 10% methanol and

90% MilliQ water at a flow rate of 1 ml/min. The compounds were prepared in HPLC-grade acetonitrile and injected at a volume of 10 μ l. The flow rate was set to 1 ml/min, and the samples were analysed at 280 nm and 400 nm wavelengths. The equilibration period between runs was 5 minutes, and each HPLC run was 13 minutes in length.

3.3.2. Synthesis (Experimental)

3.3.2.1. N-Acylation (1)

A round-bottom flask was charged with 35 ml of anhydrous CH_2Cl_2 , 2.3 g of 2-amino-5-nitrothiazole (15.9 mmoles) and 2.7 ml (1.2 equiv., 18.7 mmoles) of TEA. The mixture was cooled to 0°C using an ice bath, and 3 ml (2.2 equiv., 34 mmoles) of bromoacetyl bromide was added dropwise, after which it was stirred for 24 h at room temperature (r.t.) The reaction was monitored with TLC, and upon completion, the insoluble triethylamine hydrobromide salt formed was filtered off and the product-containing filtrate was concentrated *in vacuo*, followed by the addition of deionised water (20 ml), and the mixture stirred vigorously at r.t for 15–20 min. The ensued precipitate was filtered, dried, and washed with hexane to furnish intermediate **1** in 80% yield.

3.3.2.2. Dehydrative cyclization (2)

In a round-bottom flask, 3 g (11.4 mmoles) of **1** (2-bromo-N-(5-nitrothiazol-2-yl)acetamide), 1.7 g (2 equiv., 22.7 mmoles) of ammonium thiocyanate (NH_4SCN) and 20 ml of ethanol were added and the mixture heated under reflux for 4 h. The reaction was monitored with TLC, and after completion, it was left overnight at r.t. to precipitate. The product was filtered, washed with a cold ethanol: water (50:50) mixture to afford parent intermediate **2** at a 74% yield.

(E)-2-((5-nitrothiazol-2-yl)imino)thiazolidin-4-one (**2**)

Black powder; 74% yield; m.p.: > 400°C; ^1H NMR (600 MHz, (D_6) DMSO) δ 12.56 (s, 1H, NH), 8.65 (s, 1H, thiazole-CH), 4.11 (s, 2H, methylene-CH₂); ^{13}C NMR (151 MHz, (D_6) DMSO) δ

143.53, 143.08, 35.94; IR V_{\max} cm^{-1} : 3083.04 (N–H lactam), 2988.08 (Ar–H), 1721.67 (C=O stretch), 1630.95 (C=N stretch), 1550.72 (N–O stretch), 1333.53 (N–O stretch). m/z HRMS (APCI) found 244.9790, calcd for $\text{C}_6\text{H}_5\text{N}_4\text{O}_3\text{S}_2$: 244.9798 $[\text{M} + \text{H}]^+$; Purity (HPLC): 100%.

3.3.2.3. Knoevenagel condensation (3a – 3q)

Into a round-bottom flask was added 0.3 g (1.2 mmoles) of **2**, 0.35 g (3.5 equiv., 4.2 mmoles) of anhydrous sodium acetate (CH_3COONa), 20 ml of glacial acetic acid (AcOH), and 1.2 equiv. of the appropriate aldehyde. The mixture was heated under reflux for 72 h. The reaction was monitored with TLC and, after completion, left to cool to r.t. to initiate precipitation of the target compounds. The resultant precipitate was filtered, washed with water, and recrystallised from 1,4-Dioxane (**3a**, **3d**, **3e**, **3g**, **3h**, **3i**, **3k**, **3m**, **3p**, **3q**) and DMF (**3j**, **3n**, **3o**). Compounds **3b**, **3c**, and **3f** were recrystallised from toluene through hot filtration. For **3l**, it was precipitated out of ice cooled water, and recrystallised from ethanol.

(2E,5Z)-5-benzylidene-2-((5-nitrothiazol-2-yl)imino)thiazolidin-4-one (3a)

Green powder; 52% yield; m.p.: 288–290°C; ^1H NMR (600 MHz, (D_6) DMSO) δ 13.20 (s, 1H, NH), 8.73 (s, 1H, thiazole-CH), 7.80 (s, 1H, CH), 7.64 (d, $J = 7.5$ Hz, 2H, Ar-CH), 7.56 (t, $J = 7.6$ Hz, 2H, Ar-CH), 7.50 (t, $J = 7.3$ Hz, 1H, Ar-CH); ^{13}C NMR (151 MHz, (D_6) DMSO) δ 144.06, 131.13, 130.66, 129.88; IR V_{\max} cm^{-1} : 3082.67 (N–H lactam), 2987.76 (C–H arom), 1707.34 (C=O stretch), 1602.63 (C=N stretch), 1561.62 (N–O stretch), 1328.90 (N–O stretch). m/z HRMS (APCI) found 333.0136, calcd for $\text{C}_{13}\text{H}_9\text{N}_4\text{O}_3\text{S}_2$ 333.0111 $[\text{M} + \text{H}]^+$; Purity: 97.9%.

(2E,5Z)-5-(2-fluorobenzylidene)-2-((5-nitrothiazol-2-yl)imino)thiazolidin-4-one (3b)

Dark-maroon crystals; 26% yield; m.p.: 262–263°C; ^1H NMR (600 MHz, (D_6) DMSO) δ 13.21 (s, 1H, NH), 8.69 (s, 1H, thiazole-CH), 7.78 (s, 1H, CH), 7.57 (dt, $J = 8.7, 6.8$ Hz, 2H, Ar-CH), 7.40 (dt, $J = 9.0, 8.0$ Hz, 2H, Ar-CH); ^{13}C NMR (151 MHz, (D_6) DMSO) δ 161.29, 159.62, 143.26, 132.83, 129.08, 125.35, 121.01, 120.94, 116.15; IR V_{\max} cm^{-1} : 3144.49 (N–H lactam), 2987.84 (C–H arom), 1701.86 (C=O stretch), 1606.48 (C=N stretch), 1548.74 (N–O stretch),

1330.56 (N–O stretch). *m/z* HRMS (APCI) found 351.0039, calcd for C₁₃H₈FN₄O₃S₂: 351.0016 [M + H]⁺; Purity (HPLC): 97%.

(2E,5Z)-5-(2-chlorobenzylidene)-2-((5-nitrothiazol-2-yl)imino)thiazolidin-4-one (3c)

Brown powder; 52% yield; m.p.: 290–292°C ; ¹H NMR (600 MHz, (D₆)DMSO) δ 13.21 (s, 1H, NH), 8.68 (s, 1H, thiazole-CH), 7.92 (s, 1H, CH), 7.66 – 7.61 (m, 2H, Ar-CH), 7.56 (t, *J* = 7.2 Hz, 1H, Ar-CH), 7.51 (td, *J* = 7.7, 1.5 Hz, 1H, Ar-CH); ¹³C NMR (151 MHz, (D₆)DMSO) δ 143.26, 134.45, 131.89, 131.12, 130.33, 129.05, 128.07; IR *V*_{max} cm⁻¹: 3093.36 (N–H lactam), 2987.81 (C–H arom), 1723.31 (C=O stretch), 1641.63 (C=N stretch), 1582.33 (N–O stretch), 1351.42 (N–O stretch); *m/z* HRMS (APCI) : 366.9749, calcd for C₁₃H₈ClN₄O₃S₂: 366.9721 [M + H]⁺; Purity (HPLC): 97.9%.

(2E,5Z)-5-(2-nitrobenzylidene)-2-((5-nitrothiazol-2-yl)imino)thiazolidin-4-one (3d)

Black crystals; 36% yield; m.p.: 281–282°C ; ¹H NMR (600 MHz, (D₆)DMSO) δ 13.26 (s, 1H, NH), 8.66 (s, 1H, thiazole-CH), 8.23 (dd, *J* = 8.2, 0.8 Hz, 1H, Ar-CH), 8.05 (s, 1H, CH), 7.94 (td, *J* = 7.6, 0.8 Hz, 1H, Ar-CH), 7.79 – 7.73 (m, 2H, Ar-CH); ¹³C NMR (151 MHz, (D₆)DMSO) δ 147.71, 143.22, 134.55, 131.07, 129.54, 129.04, 125.38; IR *V*_{max} cm⁻¹: 3109.15 (N–H lactam), 2994.28 (C–H arom), 1702.15 (C=O stretch), 1618.43 (C=N stretch), 1521.91 (N–O stretch), 1338.19 (N–O stretch); *m/z* HRMS (APCI) found 377.9994, calcd for C₁₃H₈N₅O₅S₂: 377.9961 [M + H]⁺; Purity (HPLC): 99%.

(2E,5Z)-5-(3-fluorobenzylidene)-2-((5-nitrothiazol-2-yl)imino)thiazolidin-4-one (3e)

Light-maroon powder; 45%; m.p.: 281–283°C ; ¹H NMR (600 MHz, (D₆)DMSO) δ 12.98 (s, 1H, NH), 8.72 (s, 1H, thiazole-CH), 7.81 (s, 1H, CH), 7.64 – 7.58 (m, 1H, Ar-CH), 7.34 (t, *J* = 8.2 Hz, 1H, Ar-CH), 7.24 (t, *J* = 7.5 Hz, 1H, Ar-CH), 7.19 – 7.12 (m, 1H, Ar-CH); ¹³C NMR (151 MHz, (D₆)DMSO) δ 163.03, 143.39, 131.37, 128.76, 128.06, 125.62; IR *V*_{max} cm⁻¹: 3108.69 (N–H lactam), 2987.67 (C–H arom), 1708.91 (C=O stretch), 1607.92 (C=N stretch), 1562.45

(N–O stretch), 1304.24 (N–O stretch); *m/z* HRMS (APCI) found 351.0039, calcd for C₁₃H₈FN₄O₃S₂ 351.0016 [M + H]⁺; Purity (HPLC): 76%.

(2E,5Z)-5-(3-chlorobenzylidene)-2-((5-nitrothiazol-2-yl)imino)thiazolidin-4-one (3f)

Yellow-mustard powder; 46% yield; m.p.: 262–264°C; ¹H NMR (600 MHz, (D₆)DMSO) δ 13.18 (s, 1H, NH), 8.69 (s, 1H, thiazole-CH), 7.76 (s, 1H, CH), 7.69 (s, 1H, Ar-CH), 7.61 – 7.50 (m, 3H, Ar-CH); ¹³C NMR (151 MHz, (D₆)DMSO) δ 143.27, 135.72, 133.93, 131.05, 130.01, 129.86, 128.78, 127.81; IR *V*_{max} cm⁻¹: 3091.14 (N–H lactam), 2987.72 (C–H arom), 1701.66 (C=O stretch), 1677.56 (C=N stretch), 1577.63 (N–O stretch), 1343.04 (N–O stretch); *m/z* HRMS (APCI) found 366.9746, calcd for C₁₃H₈ClN₄O₃S₂: 366.9721 [M + H]⁺; Purity (HPLC): 99%.

(2E,5Z)-5-(3-bromobenzylidene)-2-((5-nitrothiazol-2-yl)imino)thiazolidin-4-one (3g)

Green-mustard powder; 69% yield; m.p.: 220–282°C ; ¹H NMR (600 MHz, (D₆)DMSO) δ 13.21 (s, 1H, NH), 8.70 (s, 1H, thiazole-CH), 7.83 (d, *J* = 1.6 Hz, 1H, Ar-CH), 7.76 (s, 1H, CH), 7.67 (dd, *J* = 7.8, 1.6 Hz, 1H, Ar-CH), 7.60 (d, *J* = 7.8 Hz, 1H, Ar-CH), 7.52 (t, *J* = 7.9 Hz, 1H, Ar-CH); ¹³C NMR (151 MHz, (D₆)DMSO) δ 143.32, 135.50, 132.95, 132.87, 131.28, 128.11, 122.45; IR *V*_{max} cm⁻¹: 3069.42 (N–H lactam), 2988.11 (C–H arom), 1693.43 (C=O stretch), 1604.87 (C=N stretch), 1578.68 (N–O stretch), 1343.29 (N–O stretch); *m/z* HRMS (APCI) found 410.9241, calcd for C₁₃H₈BrN₄O₃S₂ 410.9216 [M + H]⁺; Purity (HPLC): 97%.

(2E,5Z)-5-(4-fluorobenzylidene)-2-((5-nitrothiazol-2-yl)imino)thiazolidin-4-one (3h)

Green off-white puffy powder; 42% yield; m.p.: 273–275°C ; ¹H NMR (600 MHz, (D₆)DMSO) δ 13.20 (s, 1H, NH), 8.72 (s, 1H, thiazole-CH), 7.82 (s, 1H, CH), 7.71 (dd, *J* = 8.7, 5.4 Hz, 2H, Ar-CH) 7.43 (t, *J* = 8.8 Hz, 2H, Ar-CH); ¹³C NMR (151 MHz, (D₆)DMSO) δ 163.04, 143.54, 132.71, 132.64, 129.76, 116.69, 116.55; IR *V*_{max} cm⁻¹: 3093.91 (N–H lactam), 2988.02 (C–H arom), 1721.96 (C=O stretch), 1610.31 (C=N stretch), 1580.26 (N–O stretch), 1343.87 (N–O

stretch); *m/z* HRMS (APCI) found 351.0039, calcd for C₁₃H₈FN₄O₃S₂ 351.0016 [M + H]⁺; Purity (HPLC): 96%.

(2E,5Z)-5-(4-chlorobenzylidene)-2-((5-nitrothiazol-2-yl)imino)thiazolidin-4-one (3i)

Yellow crystals; 40% yield; m.p.: 298–300°C; ¹H NMR (600 MHz, (D₆)DMSO) δ 8.65 (s, 1H, thiazole-CH), 7.78 (s, 1H, CH), 7.64 (d, *J* = 8.6 Hz, 2H, Ar-CH), 7.61 (d, *J* = 8.6 Hz, 2H, Ar-CH); ¹³C NMR (151 MHz, (D₆)DMSO) δ 142.94, 135.00, 131.88, 131.42, 129.18; IR *V*_{max} cm⁻¹: 3093.37 (N–H lactam), 2987.93 (C–H arom), 1729.23 (C=O stretch), 1690.96 (C=N stretch), 1573.42 (N–O stretch), 1342.30 (N–O stretch); *m/z* HRMS (APCI) found 366.9744, calcd for C₁₃H₈ClN₄O₃S₂ 366.9721 [M + H]⁺; Purity (HPLC): 96%.

(2E,5Z)-5-(4-nitrobenzylidene)-2-((5-nitrothiazol-2-yl)imino)thiazolidin-4-one (3j)

Fine golden crystals; 31% yield; m.p.: 326–327°C; ¹H NMR (600 MHz, (D₆)DMSO) δ 8.70 (s, 1H, thiazole-CH), 8.38 (s, 1H, CH), 8.36 (s, 1H, Ar-CH), 7.88 (d, *J* = 8.7 Hz, 3H, Ar-CH); ¹³C NMR (151 MHz, (D₆)DMSO) δ 143.44, 130.93, 124.37; IR *V*_{max} cm⁻¹: 3093.08 (N–H lactam), 2987.89 (C–H arom), 1720.21 (C=O stretch), 1596.96 (C=N stretch), 1571.73 (N–O stretch), 1332.92 (N–O stretch); *m/z* HRMS (APCI): found 377.9984, calcd for C₁₃H₈N₅O₅S₂ 377.9961 [M + H]⁺; Purity (HPLC): 96%.

(2E,5Z)-5-(4-hydroxybenzylidene)-2-((5-nitrothiazol-2-yl)imino)thiazolidin-4-one (3k)

Mustard powder; 32%; m.p.: > 400°C; ¹H NMR (600 MHz, (D₆)DMSO) δ 13.00 (s, 1H, NH), 10.35 (s, 1H, OH), 8.68 (s, 1H, thiazole-CH), 7.70 (s, 1H, CH), 7.52 – 7.47 (m, 2H, Ar-CH), 6.96 – 6.91 (m, 2H, Ar-CH); ¹³C NMR (151 MHz, (D₆)DMSO) δ 160.25, 143.46, 134.50, 132.67, 123.87, 116.38; IR *V*_{max} cm⁻¹: 3260.80 (O–H stretch), 3110.97 (N–H lactam), 2987.31 (C–H arom), 1676.96 (C=O stretch), 1590.67 (C=N stretch), 1555.18 (N–O stretch), 1294.77 (N–O stretch); *m/z* HRMS (APCI) found 349.0084, calcd for C₁₃H₉N₄O₄S₂ 349.0060 [M + H]⁺; Purity (HPLC): 99%.

(2E,5Z)-5-(2-methylbenzylidene)-2-((5-nitrothiazol-2-yl)imino)thiazolidin-4-one (3l)

Golden-brown crystals; 38% yield; m.p.: 268–269°C ; ¹H NMR (600 MHz, (D₆)DMSO) δ 13.19 (s, 1H, NH), 8.70 (s, 1H, thiazole-CH), 7.91 (s, 1H, CH), 7.49–7.46 (m, 1H, Ar-CH), 7.41 – 7.34 (m, 3H, Ar-CH), 2.40 (s, 3H, CH₃); ¹³C NMR (151 MHz, (D₆)DMSO) δ 143.58, 138.84, 132.21, 131.05, 130.55, 127.46, 126.73, 19.42; IR V_{max} cm⁻¹: 3067.70 (N–H lactam), 2987.58 (C–H arom), 1689.15 (C=O stretch), 1605.42 (C=N stretch), 1562.61 (N–O stretch), 1341.91 (N–O stretch); *m/z* HRMS (APCI) found 347.0297, calcd for C₁₄H₁₁N₄O₃S₂ 347.0267 [M + H]⁺; Purity (HPLC): 99%.

(2E,5Z)-5-(4-methylbenzylidene)-2-((5-nitrothiazol-2-yl)imino)thiazolidin-4-one (3m)

Light-green puffy powder; 43% yield; m.p.: 268–269°C ; ¹H NMR (600 MHz, (D₆)DMSO) δ 13.09 (s, 1H, NH), 8.70 (s, 1H, thiazole-CH), 7.75 (s, 1H, CH), 7.51 (d, *J* = 8.0 Hz, 2H, Ar-CH), 7.36 (d, *J* = 8.0 Hz, 2H, Ar-CH), 2.36 (s, 3H, CH₃); ¹³C NMR (151 MHz, (D₆)DMSO) δ 143.47, 141.02, 130.19, 129.93, 21.04; IR V_{max} cm⁻¹: 3080.21 (N–H lactam), 3007.85 (C–H arom), 2880.37 (C–H methyl), 2798.27 (C–H methyl) 1719.61 (C=O stretch), 1690.79 (C=N stretch), 1577.20 (N–O stretch), 1343.38 (N–O stretch); *m/z* HRMS (APCI) found 347.0288, calcd for C₁₄H₁₁N₄O₃S₂: 347.0267 [M + H]⁺; Purity (HPLC): 98%.

(2E,5Z)-5-(2,4-dimethoxybenzylidene)-2-((5-nitrothiazol-2-yl)imino)thiazolidin-4-one (3n)

Bright-red powder; 51% yield; m.p.: 281°C ; ¹H NMR (600 MHz, (D₆)DMSO) δ 12.98 (s, 1H, NH), 8.68 (s, 1H, thiazole-CH), 7.94 (s, 1H, CH), 7.42 (d, *J* = 8.7 Hz, 1H, Ar-CH), 6.75 (dd, *J* = 8.7, 2.4 Hz, 1H, Ar-CH), 6.69 (d, *J* = 2.4 Hz, 1H, Ar-CH), 3.91 (s, 3H, CH₃), 3.86 (s, 3H, CH₃); ¹³C NMR (151 MHz, (D₆)DMSO) δ 163.42, 160.04, 143.53, 130.44, 114.33, 106.77, 98.64, 55.95, 55.66; IR V_{max} cm⁻¹: 3101.73 (N–H lactam), 2988.13 (C–H arom), 2797.78 (O–CH₃ stretch), 1702.07 (C=O stretch), 1610.93 (C=N stretch), 1550.36 (N–O stretch), 1343.65 (N–O stretch), 1207.07 (C–O stretch); *m/z* HRMS (APCI) found 393.0343, calcd for C₁₅H₁₃N₄O₅S₂: 393.0322 [M + H]⁺; Purity (HPLC): 88%.

(2E,5Z)-5-(2,4,6-trimethoxybenzylidene)-2-((5-nitrothiazol-2-yl)imino)thiazolidin-4-one (3o)

Black flakes; 42% yield; m.p.: 292–293°C; ¹H NMR (600 MHz, (D₆)DMSO) δ 7.63 – 7.54 (m, 2H, Ar-CH), 7.49 (t, *J* = 7.5 Hz, 1H, Ar-CH), 7.40 (t, *J* = 7.2 Hz, 1H, Ar-CH), 3.30 (s, 9H, 3 × CH₃); ¹³C NMR (151 MHz, (D₆)DMSO) δ 180.27, 178.86, 156.66, 134.53, 129.80, 129.34, 129.05, 128.99, 127.79, 45.33, 25.24, 23.47; IR *V*_{max} cm⁻¹: 3081.72 (N–H lactam), 2836.20 (O–CH₃ stretch), 1705.11 (C=O stretch), 1608.07 (C=N stretch), 1542.99 (N–O stretch), 1345.12 (N–O stretch), 1293.02 (C–O stretch); *m/z* HRMS (APCI) found 423.0450, calcd for C₁₆H₁₅N₄O₆S₂ 423.0428 [*M* + H]⁺; Purity (HPLC): 85%.

(2E,5Z)-5-(3-methoxybenzylidene)-2-((5-nitrothiazol-2-yl)imino)thiazolidin-4-one (3p)

Green-yellow powder; 54%; m.p.: 252°C; ¹H NMR (600 MHz, (D₆)DMSO) δ 13.14 (s, 1H, NH), 8.70 (s, 1H, thiazole-CH), 7.76 (s, 1H, CH), 7.48 (t, *J* = 8.2 Hz, 1H, Ar-CH), 7.19 (d, *J* = 7.4 Hz, 2H, Ar-CH), 7.10 – 7.04 (m, 1H, Ar-CH), 3.82 (s, 3H, CH₃); ¹³C NMR (151 MHz, (D₆)DMSO) δ 159.60, 143.36, 134.40, 130.38, 121.90, 116.06, 115.86, 55.25; IR *V*_{max} cm⁻¹: 3110.50 (N–H lactam), 2988.16 (C–H arom), 2797.54 (O–CH₃ stretch), 1720.46 (C=O stretch), 1603.05 (C=N stretch), 1569.55 (N–O stretch), 1345.01 (N–O stretch), 1232.32 (C–O stretch); *m/z* HRMS (APCI) found 363.0023, calcd for C₁₄H₁₁N₄O₂S₃ 363.0039 [*M* + H]⁺; Purity (HPLC, PDA, 280nm): 99%.

(2E,5Z)-5-(3,4-dichlorobenzylidene)-2-((5-nitrothiazol-2-yl)imino)thiazolidin-4-one (3q)

Green puffy powder; 35%; m.p.: 279–281°C; ¹H NMR (600 MHz, (D₆)DMSO) δ 8.70 (s, 1H, thiazole-CH), 7.92 (d, *J* = 1.8 Hz, 1H, Ar-CH), 7.84 (d, *J* = 8.4 Hz, 1H, Ar-CH), 7.77 (s, 1H, CH), 7.59 (dd, *J* = 8.4, 1.8 Hz, 1H, Ar-CH); ¹³C NMR (151 MHz, (D₆)DMSO) δ 143.39, 137.96, 132.07, 132.01, 131.42, 128.90, 119.62; IR *V*_{max} cm⁻¹: 3089.46 (N–H lactam), 2989.50 (C–H arom), 1729.79 (C=O stretch), 1698.65 (C=N stretch), 1579.35 (N–O stretch), 1345.73 (N–O stretch); *m/z* HRMS (APCI) found 400.9355, calcd for C₁₃H₇Cl₂N₄O₃S₂ 400.9331 [*M* + H]⁺; Purity (HPLC): 96%.

3.3.3. *In vitro* antitubercular evaluation

The antitubercular property of target compounds was established using the method reported by Beteck *et al.* (2019). In brief, a 10 ml culture of the gfp reporter Mtb strain was grown to an optical density (OD₆₀₀) of 0.6–0.7 in Middlebrook 7H9 medium supplemented with 0.03% casitone (CAS), 0.4% glucose, and 0.05% tyloxapol. Target compounds at 0.244–125 µM concentration range were added in 96-well plates and 50 ml of Mtb containing medium was introduced to each well. This was followed by sealing and incubation of the microplates at 37°C with 5% CO₂ and humidification. The antitubercular activity was determined with rifampicin (RIF) (2 x MIC₉₀) and 5% DMSO acting as the minimum, and maximum growth controls, respectively. On day 14, fluorescence readings at 485, and 520 nm were recorded for each well using a plate reader (FLUOstar OPTIMA, BMG LABTECH). These readings were standardised and used to generate dosage response curves with the help of the CDD Vault from Collaborative Drug Discovery. The minimal inhibitory concentration (MIC) was estimated using the Levenberg-Marquardt damped least-squares method and it is reported as the lowest concentration that inhibits the growth of more than 90% of the bacterial population [40].

3.3.4. *In vitro* antibacterial and antifungal evaluation

Starting from 32 µg/ml, eight-fold serial dilutions of each sample were prepared in 384-well, non-binding surface plates while keeping the final concentration of DMSO below 0.5%. Bacteria were cultured at 37°C overnight using Cation-Adjusted Mueller Hinton Broth (CAMHB) overnight and followed by 40-fold dilution, incubation at 37°C for 1.5–3 h.

Cultures at mid-log phase were diluted (CFU/ml measured by OD₆₀₀) and plated to each compound-containing well plate to attain a volume of 50 µl and a cell density of 5 x 10⁵ CFU/ml. Plates were incubated at 37°C for 18 h without shaking. Using a Tecan M1000 Pro monochromator plate reader, absorbance at 600 nm (OD₆₀₀) were recorded for each well and used to determine inhibition of bacterial growth. The minimum inhibitory concentration (MIC), defined as the lowest concentration at which > 80% of bacteria growth is inhibited, was

determined following CLSI guidelines. Compounds exhibiting MIC \leq 16 $\mu\text{g/mL}$ in either replicate ($n=2$) were classified as hits. *C. albicans* was cultured using Yeast Extract-Peptone Dextrose (YEPD) agar at 30°C for 3 days. A suspension of culture was made and subsequently diluted and added to each well of the compound-containing plates to give a final cell density of 2.5×10^3 CFU/mL and a volume of 50 μl . All plates were sealed and incubated for 36 h at 35°C, followed by addition of resazurin (0.001% final concentration) and incubating for additional 2 h at 35°C. Absorbance at 630 nm (OD_{630}) for each well was measured using a Biotek Multiflo Synergy HTX plate reader to determine growth inhibition.

3.3.5. *In vitro* cytotoxicity evaluation: resazurin assay

HEK-293 cells were counted manually in a Neubauer haemocytometer and then plated in 384-well compound-containing plates to give a density of 5×10^3 cells and a volume of 50 μl per well. Dulbecco's Modified Eagle Medium (DMEM) containing 10% foetal bovine serum was used as growth media. Compounds at 32 $\mu\text{g/ml}$ were added and incubated for 20 h at 37°C in 5% CO_2 , followed by the addition of resazurin (5 μl) and incubation for 3 more hours at 37°C in 5% CO_2 . The fluorescence of each well was recorded at 590 nm using a Tecan M1000 Pro monochromator plate reader and these data along with concentrations of compounds was used to generate the CC_{50} (concentration required to inhibit 50% cell growth) values.

3.3.6. *In vitro* haemolytic evaluation

Saline solution (NaCl, 0.9%) was used to wash human whole blood, after which the cells were re-suspended at concentration of 0.5×10^8 cells/ml and then added to the 384-well compound-containing plates to a final volume of 50 μl . The plates were shaken for ten minutes, they were then incubated at 37°C for 1 h. Plates were subsequently centrifuged at 1000 g for 10 min, after which the supernatant (25 μl) was transferred to a 384-well plate. Absorbance of the supernatant at 405 nm was recorded using a Tecan M1000 Pro monochromator plate reader, these data together with compounds concentrations were used to generate HC_{10} (concentration at which 10% of RBCs are haemolysed) values.

3.4. Conclusion

In this study, we successfully synthesised low molecular weight (< 500 Da), novel thiazolidin-4-one appended 5-nitrothiazole derivatives. The compounds were evaluated *in vitro* for antibacterial, antifungal, and overt cell toxicity. All compounds exhibited potent antitubercular activity, less than 5 μM . Most of the compounds showed potent activity against *S. aureus*, wherein SAR analyses suggest that the *ortho* substituted benzylidene moiety promotes activity against *S. aureus*. Notably, compound **3b** exhibited superior activity (< 0.25 $\mu\text{g/mL}$) against *methicillin-resistant S. aureus* compared to the standard (vancomycin; 1 $\mu\text{g/mL}$). With regards to antifungal activity, a few compounds showed low micromolar activity against *C. albicans*, with **3g** exhibiting comparable activity (\leq 0.25 $\mu\text{g/mL}$) to the standard fluconazole. Compounds in this study were not cytotoxic towards HEK-293 and human red blood cells. These compounds were generally inactive against Gram-negative bacteria and presented with insoluble problems. Future work will be aimed at overcoming these challenges.

3.5. Acknowledgements

This project received financial support from the National Research Foundation (NRF) Research Grant (grant no:137776) and MRC-SIR awarded to RMB. The views and opinions expressed herein are those of the authors and do not represent the views of NRF. The antitubercular screening was performed by Audrey Jordaan, under the supervision of Prof. Digby Warner, at the University of Cape Town in South Africa. The Wellcome Trust (UK) and The University of Queensland (Australia) are acknowledged for funding toward antimicrobial and cytotoxicity screening performed by COADD (The Community for Antimicrobial Drug Discovery). **Ethics:** The ethics committee of North-West University approved this project. Ethics number is N W U - 0 0 3 8 6-2 0 - A 1. Informed consent was obtained from participants or their next of kin.

3.6. Conflict of interest

The authors have no competing interest to declare.

3.7. Data availability statement

The data that support the findings of this study are available in the supplementary material (**Annexure A**).

REFERENCE LIST – CHAPTER 3

- [1] T. Togun, B. Kampmann, N.G. Stoker, M. Lipman, Anticipating the impact of the COVID-19 pandemic on TB patients and TB control programmes, *Ann. Clin. Microbiol. Antimicrob.* 19 (2020) art. #21.
- [2] WHO, Global tuberculosis report, World Health Organization, 2021a. Accessed from <https://www.who.int/publications/i/item/9789240037021> on 22/03/2022.
- [3] S.T. Dhumal, A.R. Deshmukh, L.D. Khillare, M. Arkile, D. Sarkar, R.A. Mane, Synthesis and Antitubercular activity of New Thiazolidinones with Pyrazinyl and Thiazolyl Scaffolds, *J. Heterocycl. Chem.* 54 (1) (2017) 125-130.
- [4] M.I. Islam, H. Seo, S. Kim, V.S. Sadu, K.-I. Lee, H.-Y. Song, Antimicrobial activity of IDD-B40 against drug-resistant *Mycobacterium tuberculosis*, *Sci. Rep.* 11 (2021) art. #740.
- [5] K. Viney, N.N. Linh, M. Gegia, M. Zignol, P. Glaziou, N. Ismail, T. Kasaeva, F. Mirzayev, New definitions of pre-extensively and extensively drug-resistant tuberculosis: update from the World Health Organization, *Eur. Respir. J.* 57 (4) (2021) art. #2100361.
- [6] K.N. Venugopala, C. Tratratt, M. Pillay, F.M. Mahomoodally, S. Bhandary, D. Chopra, M.A. Morsy, M. Haroun, B.E. Aldhubiab, M. Attimarad, A.B. Nair, N. Sreeharsha, R. Venugopala, S. Chandrashekarappa, O.I. Alwassil, B. Odhav, Anti-Tubercular Activity of Substituted 7-Methyl and 7-Formylindolizines and In Silico Study for Prospective Molecular Target Identification, *Antibiotics* 8 (4) (2019) art. #247.
- [7] C.E. Barry, Timing is everything for compassionate use of delamanid, *Nat. Med.* 21(3) (2015) 211.
- [8] K.T. Angula, L.J. Legoabe, R.M. Beteck, Chemical classes presenting novel antituberculosis agents currently in different phases of drug development: A 2010–2020 review, *Pharmaceuticals* 14 (5) (2021) art. #461.
- [9] O. Cars, S.J. Chandy, M. Mpundu, A.Q. Peralta, A. Zorzet, A.D. So, A.D., Resetting the agenda for antibiotic resistance through a health systems perspective. *Lancet Glob. Health* 9 (7) (2021) e1022-e1027.

- [10] O. Ayobami, S. Brinkwirth, T. Eckmanns, R. Markwart, Antibiotic resistance in hospital-acquired ESKAPE-E infections in low-and lower-middle-income countries: a systematic review and meta-analysis, *Emerg. Microbes & infect.* 11 (1) (2022) 443-451.
- [11] N.A. Nimer, Nosocomial Infection and Antibiotic-Resistant Threat in the Middle East, *Infect Drug Resist.* 15 (2022) 631-639.
- [12] CDC, HAI and Antibiotic Use Prevalence Survey, Centre for Disease Prevention and Control, 2022. Accessed from <https://www.cdc.gov/hai/eip/antibiotic-use.html> on 13/04/2022.
- [13] D.J. Morgan, L.L. Lomotan, K. Agnes, L. McGrail, M.C. Roghmann, M. C, Characteristics of healthcare-associated infections contributing to unexpected in-hospital deaths, *Infect. Control Hosp. Epidemiol.* 31 (8) (2010) 864-866.
- [14] E.R.M. Sydnor, T.M. Perl, Hospital epidemiology and infection control in acute-care settings, *Clin. Microbiol. Rev.* 24 (1) (2011) 141-73.
- [15] WHO, Global priority list of antibiotic-resistant bacteria to guide research, discovery, and development of new antibiotics, World Health Organization, 2021. Accessed from https://www.who.int/medicines/publications/WHO-PPL-Short_Summary_25Feb-ET_NM_WHO.pdf on 22/03/2022.
- [16] A. Shakya, H.R. Bhat, S.K. Ghosh, Update on Nitazoxanide: A Multifunctional Chemotherapeutic Agent, *Curr. Drug Discov. Technol.* 15 (3) (2018) 201-213.
- [17] P.S. Hoffman, G. Sisson, M.A. Croxen, K. Welch, W.D. Harman, N. Cremades, M.G. Morash, Antiparasitic drug nitazoxanide inhibits the pyruvate oxidoreductases of *Helicobacter pylori*, selected anaerobic bacteria and parasites, and *Campylobacter jejuni*, *Antimicrob. Agents Chemother.* 51 (3) (2007) 868-876.
- [18] L.P. De Carvalho, C.M. Darby, K.Y. Rhee, C. Nathan, Nitazoxanide Disrupts Membrane Potential and Intrabacterial Ph Homeostasis of *Mycobacterium tuberculosis*, *ACS Med. Chem. Lett.* 2 (11) (2011) 849-854.
- [19] P. Chahales, P.S. Hoffman, D.G. Thanassi, Nitazoxanide Inhibits Pilus Biogenesis by Interfering with Folding of the Usher Protein in the Outer Membrane, *Antimicrob. Agents Chemother.* 60 (4) (2016) 2028-2038.

- [20] T. Umumararungu, M.J. Mukazayire, M. Mpenda, M.F. Mukanyangezi, J.B. Nkuranga, J. Mukiza, E.O. Olawode, A review of recent advances in anti-tubercular drug development, *Indian J. Tuberc.* 67 (4) (2020) 539-559.
- [21] L.P. De Carvalho, G. Lin, X. Jiang, C. Nathan, Nitazoxanide kills replicating and nonreplicating *Mycobacterium tuberculosis* and evades resistance, *J. Med. Chem.* 52 (19) (2009) 5789-5792.
- [22] G. Kapoor, D.P. Pathak, R. Bhutani, R. Kant, Thiazolidinone as a pharmacologically active molecule, *J. Chem. Pharm.* 8 (4) (2016) 151-168.
- [23] N. Sahiba, A. Sethiya, J. Soni, D.K. Agarwal, S. Agarwal, Saturated Five-Membered Thiazolidines and Their Derivatives: From Synthesis to Biological Applications, *Top. Curr. Chem.* 378 (2020) art. #34.
- [24] M.M. Allawi, M.F. Mahdi, A.M. Raouf, Synthesis, preliminary pharmacological evaluation, molecular docking, and ADME studies of new 4-thiazolidinone derivatives bearing ketoprofen moiety targeting cyclooxygenase enzyme, *Egypt. J. Chem.* 64 (12) (2021) 7339-7350.
- [25] R. Nechak, S.A. Bouzroua, Y. Benmalek, L. Salhi, S.P. Martini, V. Morizur, E. Dunach, B.N. Kolli, Synthesis and Antimicrobial Activity Evaluation of Novel 4-Thiazolidinones Containing a Pyrone Moiety, *Synth. Commun.* 45 (2) (2015) 262-272.
- [26] P. Vicini, A. Geronikaki, M. Incerti, F. Zani, J. Dearden, M. Hewitt, 2-Heteroaryl-imino-5-benzylidene-4-thiazolidinones analogues of 2-thiazolylimino-5-benzylidene-4-thiazolidinones with antimicrobial activity: Synthesis and structure–activity relationship, *Bioorg. Med. Chem.* 16 (7) (2008) 3714-3724.
- [27] K. Omar, A. Geronikaki, P. Zoumpoulakis, C. Camoutsis, M. Soković, A. Ćirić, J. Glamočlija, Novel 4-thiazolidinone derivatives as potential antifungal and antibacterial drugs, *Bioorg. Med. Chem.* 18 (1) (2010) 426-432.
- [28] G. Aridos, S. Amirthaganesan, M.S. Kim, J.T. Kim, Y.T. Jeong, Synthesis, spectral and biological evaluation of some new thiazolidinones and thiazoles based on t-3-alkyl-r-2,c-6-diarylpiperidin-4-ones, *J. Med. Chem.* 44 (10) (2009) 4199-4210.

- [29] A. Mobinikhaledi, N. Foroughifar, M. Kalhor, M. Mirabolfathy, Synthesis and antifungal activity of novel 2-benzimidazolylimino-5-arylidene-4-thiazolidinones, *J. Heterocycl. Chem.* 47 (2010) 77-80.
- [30] M.L. Barreca, J. Balzarini, A. Chimirri, E.D. Clercq, L.D. Luca, H.D. Höltje, M. Höltje, A.-M. Monforte, P. Monforte, C. Pannecouque, Design, synthesis, structure– activity relationships, and molecular modeling studies of 2, 3-diaryl-1, 3-thiazolidin-4-ones as potent anti-HIV agents, *J. Med. Chem.* 45 (24) (2002) 5410-5413.
- [31] M.L. Barreca, A. Chimirri, L. De Luca, A.-M. Monforte, P. Monforte, A. Rao, M. Zappalà, J. Balzarini, E. De Clercq, C. Pannecouque, Discovery of 2, 3-diaryl-1, 3-thiazolidin-4-ones as potent anti-HIV-1 agents, *Bioorg. Med. Chem. Lett.* 11 (13) (2001) 1793-1796.
- [32] D. Havrylyuk, L. Mosula, B. Zimenkovsky, O. Vasylenko, A. Gzella, R. Lesyk, Synthesis and anticancer activity evaluation of 4-thiazolidinones containing benzothiazole moiety, *Eur. J. Med. Chem.* 45 (11) (2010) 5012-5021.
- [33] M. Mishchenko, S. Shtrygol, D. Kaminsky, R. Lesyk, Thiazole-bearing 4-thiazolidinones as new anticonvulsant agents, *Sci. Pharm.* 88 (1) (2020) art. #16.
- [34] P. Vicini, A. Geronikaki, K. Anastasia, M. Incerti, F. Zani, Synthesis and antimicrobial activity of novel 2-thiazolylimino-5-arylidene-4-thiazolidinones, *Bioorg. Med. Chem.* 14 (11) (2006) 3859-3864.
- [35] V.S. Gontijo, F.P.D. Viegas, C.J.C. Ortiz, M. De Freitas Silva, C.M. Damasio, M.C. Rosa, T.G. Campos, D.S. Couto, K.S. Tranches Dias, C. Viegas, Molecular Hybridization as a Tool in the Design of Multi-target Directed Drug Candidates for Neurodegenerative Diseases, *Curr. Neuropharmacol.* 18 (5) (2020) 348-407.
- [36] C.A. Lipinski, F. Lombardo, B.W. Dominy, P.J. Feeney, Experimental and computational approaches to estimate solubility and permeability in drug discovery and development settings, *Adv. Drug Deliv. Rev.* 23 (1-3) (1997) 3-25.
- [37] L.Z. Benet, C.M. Hosey, O. Ursu, T.I. Oprea, BDDCS, the Rule of 5 and drugability. *Adv. Drug Deliv. Rev.* 101 (2016) 89-98.

[38] D.F. Veber, S.R. Johnson, H.-Y. Cheng, B.R. Smith, K.W. Ward, K.D. Kopple, Molecular Properties That Influence the Oral Bioavailability of Drug Candidates, *J. Med. Chem.* 45 (12) (2002) 2615-2623.

[39] T. Hou, J. Wang, W. Zhang, X. Xu, ADME Evaluation in Drug Discovery. 6. Can Oral Bioavailability in Humans Be Effectively Predicted by Simple Molecular Property-Based Rules?, *J. Chem. Inf. Model.* 47 (2) (2007) 460-463.

[40] R.M. Beteck, R. Seldon, A. Jordaan, D.F. Warner, H.C. Hoppe, D. Laming, L.J. Legoabe, S.D. Khanye, Quinolone-isoniazid hybrids: synthesis and preliminary *in vitro* cytotoxicity and anti-tuberculosis evaluation, *MedChemComm.* 10 (2) (2019) 326-331.

CHAPTER 4: SUMMARY AND CONCLUSION

Tuberculosis (TB), a disease caused by *Mycobacterium tuberculosis* (*Mtb*), kills thousands of people each year despite the fact that it is preventable and curable with proper treatment. In 2020, 10 million people contracted TB, and it was responsible for 1.3 million deaths globally (WHO, 2021). The primary concerns about TB are as follows: (i) HIV co-infection; (ii) the predominance of drug-resistant *Mtb* strains leading to multidrug-resistant TB (MDR-TB) cases; (iii) the length of treatment and chemotherapy, which increases in the case of resistant TB; (iv) the toxicity of antitubercular drugs (Fang et al., 2019:1929; Woimo et al., 2017:2); and (v) latent-TB infection, which is thought to affect one-third of the world's population and serves as a reservoir for future TB infections (active TB) (Houben & Dodd, 2016:3).

Developing effective chemotherapeutic drugs with minimal toxicity and novel mechanisms of action to treat TB, particularly MDR-TB, has been an ongoing struggle since the discovery of the first antitubercular agent almost half a century ago. With the advent of MDR-TB, the utility of first-line drugs has been substantially reduced, rendering the majority of patient TB treatment outcomes unsatisfactory. Improving these outcomes in MDR-TB is further hampered in part by inadequate second-line drugs (WHO, 2019). MDR-TB treatment includes drugs with many side effects, which promotes patient noncompliance and treatment discontinuation. Patients who fail or default on TB treatment have a higher risk of death and develop additional complications. Furthermore, these patients accelerate the spread of drug-resistant *Mtb* within communities (Podewils et al., 2013:1).

Antimicrobial resistance is of high prevalence in hospital settings and is frequently related to ESKAPE pathogens. *Enterococcus faecium*, *Staphylococcus aureus*, *Klebsiella pneumoniae*, *Acinetobacter baumannii*, *Pseudomonas aeruginosa*, and *Enterobacter* spp. are the six hypervirulent, antimicrobial resistant bacteria represented by the abbreviation ESKAPE (Orosz et al., 2022:27). These pathogens are associated with potentially fatal hospital-

acquired infections (HAIs), such as catheter-associated urinary tract infections, central line-associated bloodstream infections, ventilator-associated pneumonia, and surgical site infections in critically ill and immunocompromised patients (CDC, 2014). The prevalence of HAIs is rising at an alarming rate for a number of reasons, including the emergence of new infectious diseases and the reappearance of previously eradicated infectious diseases; the rise in antimicrobial resistance; and the lengthening of patients' duration of stay in hospitals while they receive specialised care, *i.e.*, ICU patients (Nouri et al., 2020:2365).

When compared to their susceptible counterparts, ESKAPE pathogens result in much worse clinical outcomes (Kamurai et al., 2020:1). Higher mortality and morbidity rates, as well as increased healthcare costs, are some of the major consequences of HAIs caused by ESKAPE pathogens (Ma et al., 2020:3). Furthermore, despite the plethora of antibiotics accessible for clinical use, the principles of evolution and natural selection, as well as antibiotic misuse, have all contributed to the development and spread of drug-resistance among these pathogens (Wang et al., 2020:1). This jeopardises modern medicine's accomplishments, and in the absence of effective antibiotics for the prevention and treatment of HAIs, medical procedures such as organ transplants may become considerably riskier and more futile in the future (WHO, 2020). In fact, if no new antibiotics are developed or discovered by 2050, it is anticipated that there will be no effective antibiotics available to treat infections caused by resistant bacteria like ESKAPE pathogens (Vivas et al., 2019). To avert this eventuality, novel antimicrobial drugs to combat the rise in antimicrobial resistance are urgently required.

It has been shown that the drug nitazoxanide (a 5-nitrothiazole based drug) has potent inhibitory activity against both replicating and non-replicating *Mtb* via a unique mechanism of action (MOA), which seems to prevent resistance (De Carvalho et al., 2009:5789–5792). Recent studies also demonstrated that a RIF–NTZ combination was successful in eradicating latent *Mtb* strains in as little as 28 to 35 days, in contrast to the approximately 6 month time frame required by other antitubercular drug combinations employed in human treatment.

Nitazoxanide is therefore indicated to be useful as a suitable lead compound in designing novel antitubercular drugs with a short development time (Iacobino et al., 2019:1-4; Umumararungu et al., 2020:550).

The thiazolidin-4-one scaffold is referred to as a "wonder nucleus" because it demonstrates a wide variety of biological activities, including those that are anti-tuberculous, antibacterial, anti-inflammatory, anticarcinogenic, and antiprotozoal, amongst others (Mech et al., 2021:1). In the field of medicinal chemistry, thiazolidin-4-ones are well-known examples of privileged scaffolds, and they have become the focus of many studies as potential scaffolds for the synthesis of novel drugs. For example, it is a well-known fact that modifying the C2 and C5 positions of the thiazolidin-4-one scaffold often results in the generation of compounds with optimised biological activity (Molina et al., 2021:130). Also, Vicini et al. (2006:3863) reported that C5-benzylidene substituted thiazolidin-4-one analogues had considerably increased antibacterial activity when compared to counterparts in which the C5 position is unsubstituted.

In this study, target compounds (see **Fig. 4.1**) containing a 5-nitrothiazole moiety appended to thiazolidin-4-one, were conceptualised, synthesised, characterised (through ^1H NMR, ^{13}C NMR, FTIR, HRMS, and HPLC), and biologically evaluated *in vitro*.

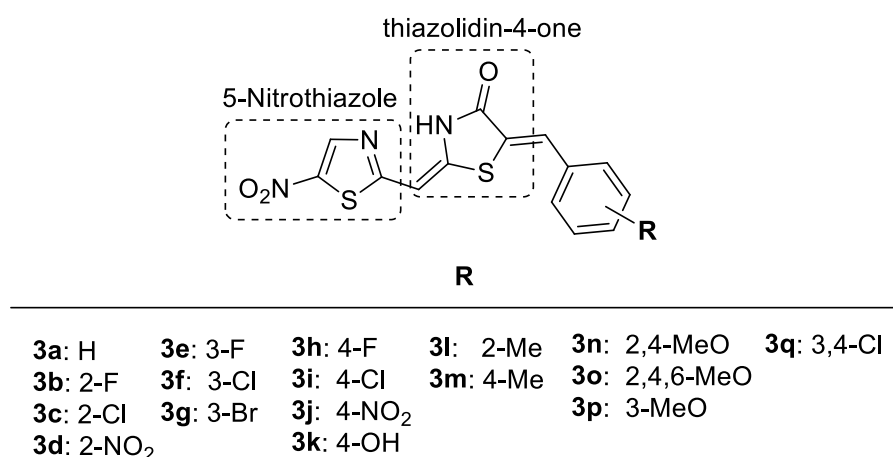


Figure 4.1 General structure of target compounds (**3a – 3j**)

The compounds in this study were generally active against the *gfp* reporter strain of *Mtb* (cultured in Middlebrook 7H9 medium), with potent MIC₉₀ values (the lowest concentration of compound needed to inhibit the growth of more than 90% of *Mtb*) in the range of < 0.244–2.004 μM. Comparing the MIC₉₀ value of parent intermediate **2** (31.25 μM) against the values of target compounds **3a – 3q**, suggests that appending on to **2** a benzylidene moiety bearing electron withdrawing– (EWG) or electron donating groups (EDG) is essential for antitubercular activity.

Target compounds were also evaluated for antimicrobial activities against some ESKAPE pathogens and compounds **3a**, **3b**, **3c**, **3d**, **3e**, **3g**, **3i**, **3l**, **3m**, and **3p** demonstrated significant activity against *S. aureus*, with MIC₈₀ values (the lowest concentration at which > 80% of bacterial growth was inhibited) in the range of 2–8 μg/ml. However, the compounds were generally inactive against Gram-negative ESKAPE pathogens (*Enterococcus faecium*, *Klebsiella pneumoniae*, *Acinetobacter baumannii*, *Pseudomonas aeruginosa*), probably owing to the lack of penetration through the highly lipophilic cell walls of these bacteria. Furthermore, the compounds were inactive against methicillin-resistant *Staphylococcus aureus* (MRSA) (except for **3b**), suggesting that penicillin binding protein might be a probable target for this series. Compound **3b**, demonstrated sub-micromolar activity against MSRA (MIC < 0.25 μg/ml), indicating an alternative target from penicillin binding protein. It is also worth noting that **3b** exhibited superior activity against the reference drug vancomycin (1 μg/ml) for MSRA activity. Furthermore, the SAR of the target compounds (**3a – 3q**) demonstrated that substitution in the *ortho* positions of the C5-benzylidene moiety favoured *S. aureus* activity.

In addition to antitubercular and antimicrobial screening, target compounds were evaluated for antifungal activity against *C. albicans*. Six compounds displayed varying inhibitory concentrations, including **3a** (4 μg/ml), **3b** (4 μg/ml), **3e** (16 μg/ml), **3g** (≤ 0.25 μg/ml), **3h** (32 μg/ml), and **3q** (32 μg/ml). It is noteworthy to mention that **3g** exhibit comparable activity to the reference drug fluconazole (0.12 μg/ml).

Cell toxicity against HEK-293 cells (cultured in Dulbecco's Modified Eagle Medium) and haemolysis against human red blood cells were also investigated. The target compounds herein reported displayed no cytotoxicity nor haemolytic activity ($HC_{10}/HC_{50} > 32 \mu\text{g/ml}$).

Collectively, the study's aims and objectives were met, and the results indicate the successful synthesis (utilising a molecular hybridization approach) and antimicrobial evaluation of 17 novel nitrothiazole-thiazolidinone hybrids (**3a – 3q**) with a molecular weight (MW) of less than 500 Da. Moreover, these hybrids may be considered as possible oral drug candidates according to Lipinski's Rule of 5 (based on *in silico* evaluation). However, lack of solubility in commercially available solvents has been identified as a limitation for this series of compounds, which will be addressed in future work. The findings of this study warrant further investigation and optimisation as potential lead compounds for overcoming and treating resistant pathogens associated with TB and HAIs.

Table 4.1 Target compounds with the best MIC values against evaluated pathogens

Pathogen	Target compound	MIC
<i>Mycobacterium tuberculosis</i>	3c, 3g, 3h, 3i, 3l, 3n, 3q	< 0.24 μM
<i>Staphylococcus aureus</i>	3b, 3d, 3g, 3l, 3m	2 $\mu\text{g/ml}$
Methicillin-resistant <i>S. aureus</i>	3b	< 0.25 $\mu\text{g/ml}$
<i>Candida albicans</i>	3g	\leq 0.25 $\mu\text{g/ml}$

REFERENCE LIST – CHAPTER 4

CDC (Centre for Disease Prevention and Control). 2014. *Types of Healthcare-associated Infections*. <https://www.cdc.gov/hai/infectiontypes.html> Date of access: 07 May. 2022.

De Carvalho, L.P.S., Lin, G., Jiang, X. & Nathan, C. 2009. Nitazoxanide kills replicating and nonreplicating *Mycobacterium tuberculosis* and evades resistance. *Journal of Medicinal Chemistry*, 52(19): 5789-5792. <https://doi.org/10.1021/jm9010719>

Fang, X.-H., Shen, H.-H., Hu, W.-Q., Xu, Q.-Q., Jun, L., Zhang, Z.-P., ... Wu, G.-C. 2019. Prevalence of and factors influencing anti-tuberculosis treatment non-adherence among patients with pulmonary tuberculosis: a cross-sectional study in Anhui province, Eastern China. *International Medical Journal of Experimental and Clinical Research*, 25: 1928-1935. doi:10.12659/MSM.913510

Iacobino, A., Giannoni, F., Pardini, M., Piccaro, G. & Fattorini, L. 2019. The combination rifampin-nitazoxanide, but not rifampin-isoniazid-pyrazinamide-ethambutol, kills dormant *Mycobacterium tuberculosis* in hypoxia at neutral pH. *Antimicrobial Agents and Chemotherapy*, 63(7), e00273-19. doi:10.1128/AAC.00273-19

Kamurai, B., Mombeshora, M. & Mukanganyama, S. 2020. Repurposing of drugs for antibacterial activities on selected ESKAPE bacteria *Staphylococcus aureus* and *Pseudomonas aeruginosa*. *International Journal of Microbiology*, 2020, art. #8885338. <https://doi.org/10.1155/2020/8885338>

Ma, Y.X., Wang, C.Y., Li, Y.Y., Li, J., Wan, Q.Q., Chen, J.H., ... Niu, L.N. 2020. Considerations and caveats in combating ESKAPE pathogens against nosocomial infections. *Advanced Science*, 7, art. #1901872. doi:10.1002/adv.201901872

Mech, D., Kurowska, A. & Trotsko, N. 2021. The bioactivity of thiazolidin-4-ones: A short review of the most recent studies. *International Journal of Molecular Sciences*, 22(21), art. #11533. doi:10.3390/ijms222111533

Molina, D.A., Ramos, G.A., Zamora-Vélez, A., Gallego-López, G.M., Rocha-Roa, C., Gómez-Marin, J.E. & Cortes, E. 2021. *In vitro* evaluation of new 4-thiazolidinones on

invasion and growth of *Toxoplasma gondii*. *International Journal for Parasitology: Drugs and Drug Resistance*, 16: 129-139. <https://doi.org/10.1016/j.ijpddr.2021.05.004>

Nouri, F., Karami, P., Zarei, O., Kosari, F., Alikhani, M.Y., Zandkarimi, E., ... Taheri, M. 2020. Prevalence of common nosocomial infections and evaluation of antibiotic resistance patterns in patients with secondary infections in Hamadan, Iran. *Infection and Drug Resistance*, 13: 2365-2374. doi:10.2147/IDR.S259252

Orosz, L., Lengyel, G., Ánosi, N., Lakatos, L. & Burián, K. 2022. Changes in resistance pattern of ESKAPE pathogens between 2010 and 2020 in the clinical center of University of Szeged, Hungary. *Acta Microbiologica et Immunologica Hungarica*, 69(1): 27-34. doi:10.1556/030.2022.01640

Podewils, L.J., Gler, M.T. S., Quelapio, M.I. & Chen, M.P. 2013. Patterns of treatment interruption among patients with multidrug-resistant TB (MDR TB) and association with interim and final treatment outcomes. *PloS One*, 8(7), e70064. <https://doi.org/10.1371/journal.pone.0070064>

Umumararungu, T., Mukazayire, M.J., Mpenda, M., Mukanyangezi, M.F., Nkuranga, J.B., Mukiza, J. & Olawode, E.O. 2020. A review of recent advances in anti-tubercular drug development. *Indian Journal of Tuberculosis*, 67(4): 539-559. <https://doi.org/10.1016/j.ijtb.2020.07.017>

Vicini, P., Geronikaki, A., Anastasia, K., Incerti, M. & Zani, F. 2006. Synthesis and antimicrobial activity of novel 2-thiazolylimino-5-arylidene-4-thiazolidinones. *Bioorganic & Medicinal Chemistry*, 14(11): 3859-3864. <https://doi.org/10.1016/j.bmc.2006.01.043>

Vivas, R., Barbosa, A.A.T., Dolabela, S.S. & Sona, J. 2019. [Multidrug-resistant bacteria and alternative methods to control them: An Overview] [Abstract]. *Microbial Drug Resistance*, 25(6): 890-908. <https://doi.org/10.1089/mdr.2018.0319>

Wang, C.-H., Hsieh, Y.-H., Powers, Z.M. & Kao, C.-Y. 2020. Defeating antibiotic-resistant bacteria: exploring alternative therapies for a post-antibiotic era. *International Journal of Molecular Sciences*, 21(3), art. #1061. doi:10.3390/ijms21031061

WHO (World Health Organization). 2020. *Antibiotic resistance*. <https://www.who.int/news-room/fact-sheets/detail/antibiotic-resistance> Date of access: 02 Jun. 2022.

WHO (World Health Organization). 2021. *Global tuberculosis report 2021*.
<https://www.who.int/teams/global-tuberculosis-programme/tb-reports/global-tuberculosis-report-2021> Date of access: 09 Mar. 2022.

Woimo, T.T., Yimer, W.K., Bati, T. & Gesesew, H.A. 2017. The prevalence and factors associated for anti-tuberculosis treatment non-adherence among pulmonary tuberculosis patients in public health care facilities in South Ethiopia: a cross-sectional study. *BMC Public Health*, 17(1), art. #269. <https://doi.org/10.1186/s12889-017-4188-9>

ANNEXURE A: SUPPLEMENTARY MATERIAL FOR CHAPTER 3

**Nitrothiazole-thiazolidinone hybrids: Synthesis
and *in vitro* antimicrobial evaluation**

SUPPORTING DATA FOR *IN SILICO* PREDICTIONS

Table 1: Prediction of distribution and absorption properties of **2** and **3a – 3j**

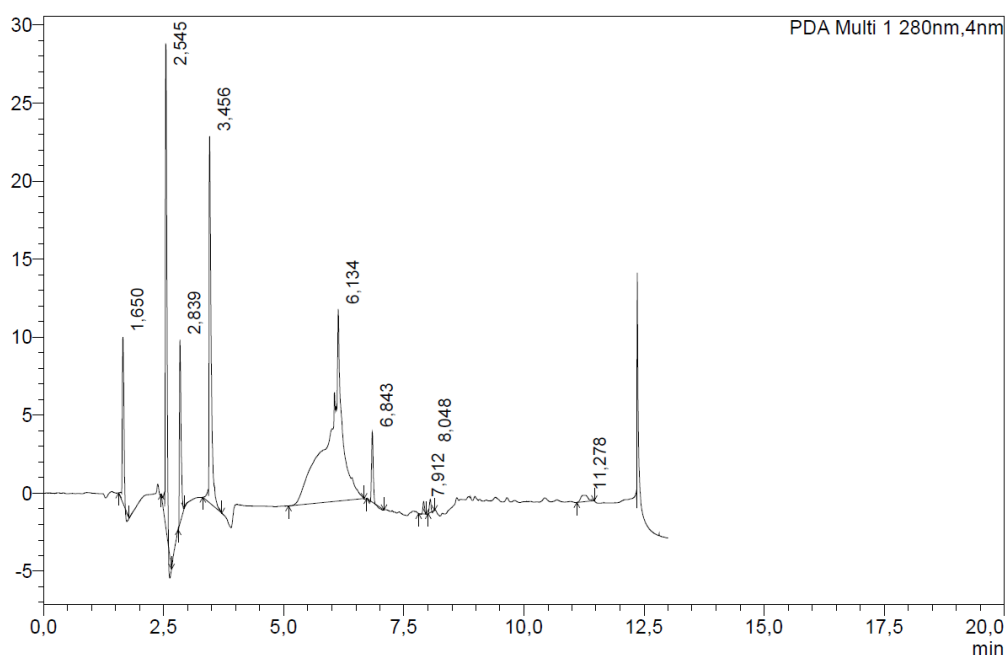
ID	GI Absorption	BBB permeant	P-gp substrate	CYPP450				
				CYP1A2	CYP2C19	CYP2C9	CYP2D6	CYP3A4
2	Low	No	No	✓	X	X	X	X
3a	Low	No	No	✓	✓	✓	X	X
3b	Low	No	No	✓	✓	X	X	X
3c	Low	No	No	✓	✓	X	X	X
3d	Low	No	No	✓	✓	X	X	X
3e	Low	No	No	✓	✓	X	X	X
3f	Low	No	No	✓	✓	✓	X	X
3g	Low	No	No	✓	✓	✓	X	X
3h	Low	No	No	✓	✓	X	X	X
3i	Low	No	No	✓	✓	✓	X	X
3j	Low	No	No	✓	✓	X	X	X
3k	Low	No	No	✓	✓	✓	X	✓
3l	Low	No	No	✓	✓	✓	X	✓
3m	Low	No	No	✓	✓	✓	X	✓
3n	Low	No	No	✓	✓	✓	X	✓
3o	Low	No	No	✓	✓	✓	✓	✓
3p	Low	No	No	✓	✓	✓	X	✓
3q	Low	No	No	✓	✓	✓	X	✓

SUPPORTING DATA FOR CHEMISTRY, CHARACTERIZATION AND SYNTHESIS

Blank HPLC test

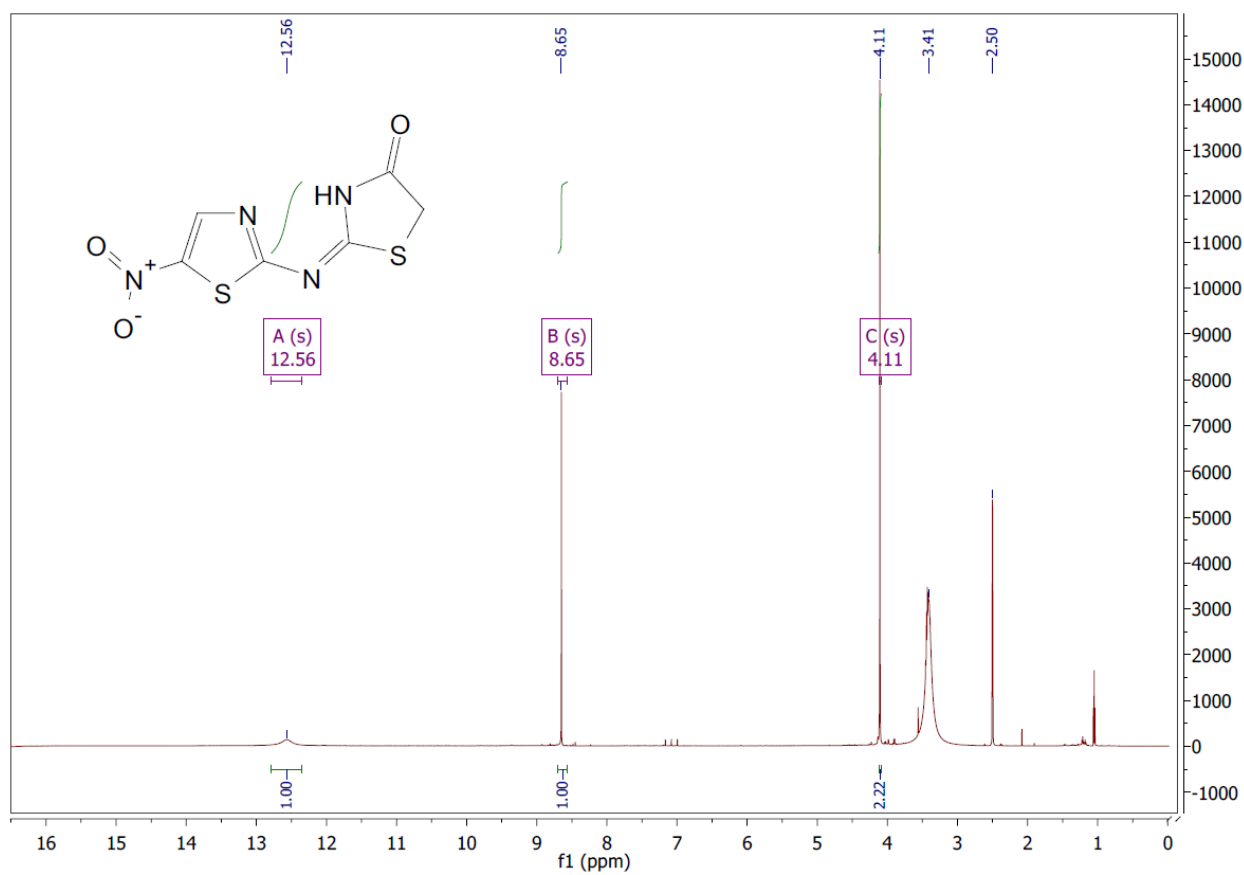
A blank experimental HPLC control analysis using just acetonitrile (solvent) was conducted to rule out any visibly undesirable peaks that may be present in the HPLC data of the test compounds owing to solvent or column impurities. The HPLC data of parent intermediate **2** and hybrid-target compounds **3a – 3j** with identical peaks to the blank were excluded from the calculation (AUC) of purity for each individual compound.

Blank HPLC result (Solvent: Acetonitrile)

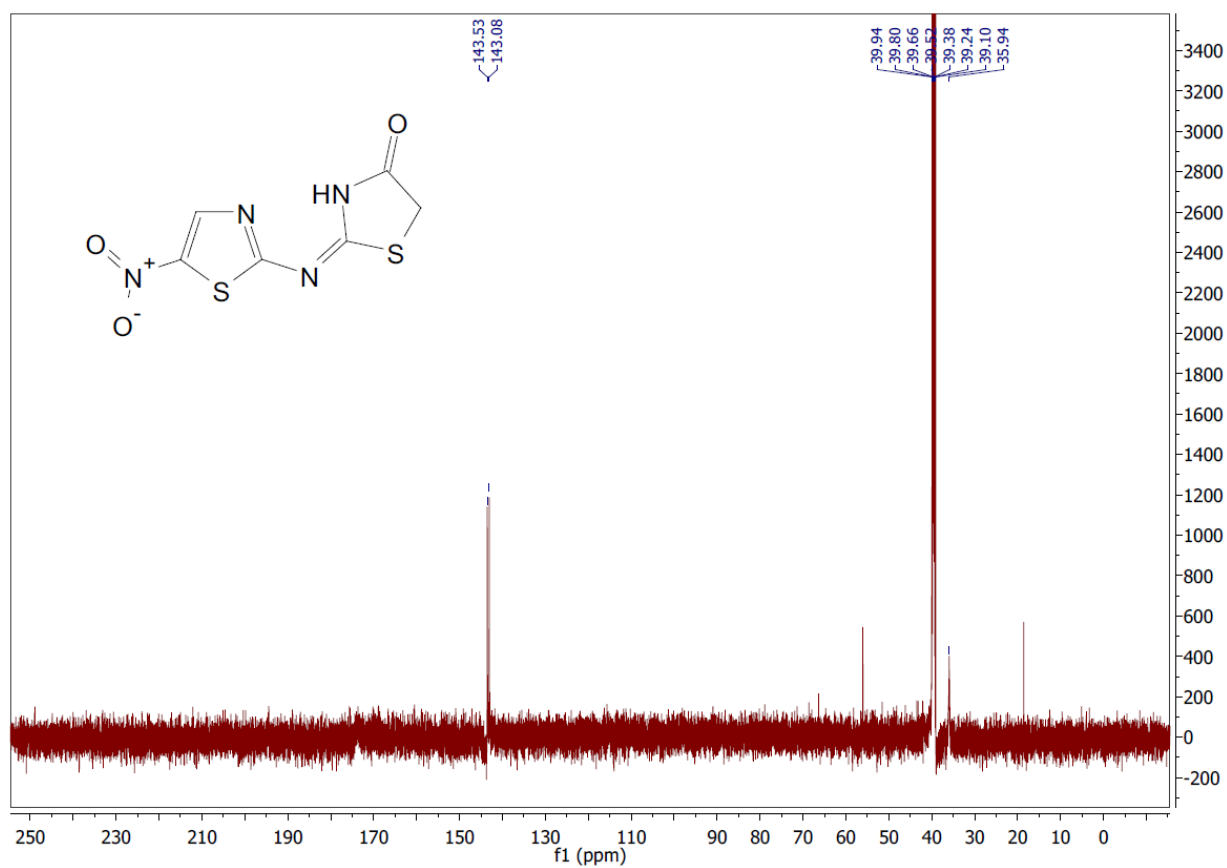


(E)-2-((5-nitrothiazol-2-yl)imino)thiazolidin-4-one (2)

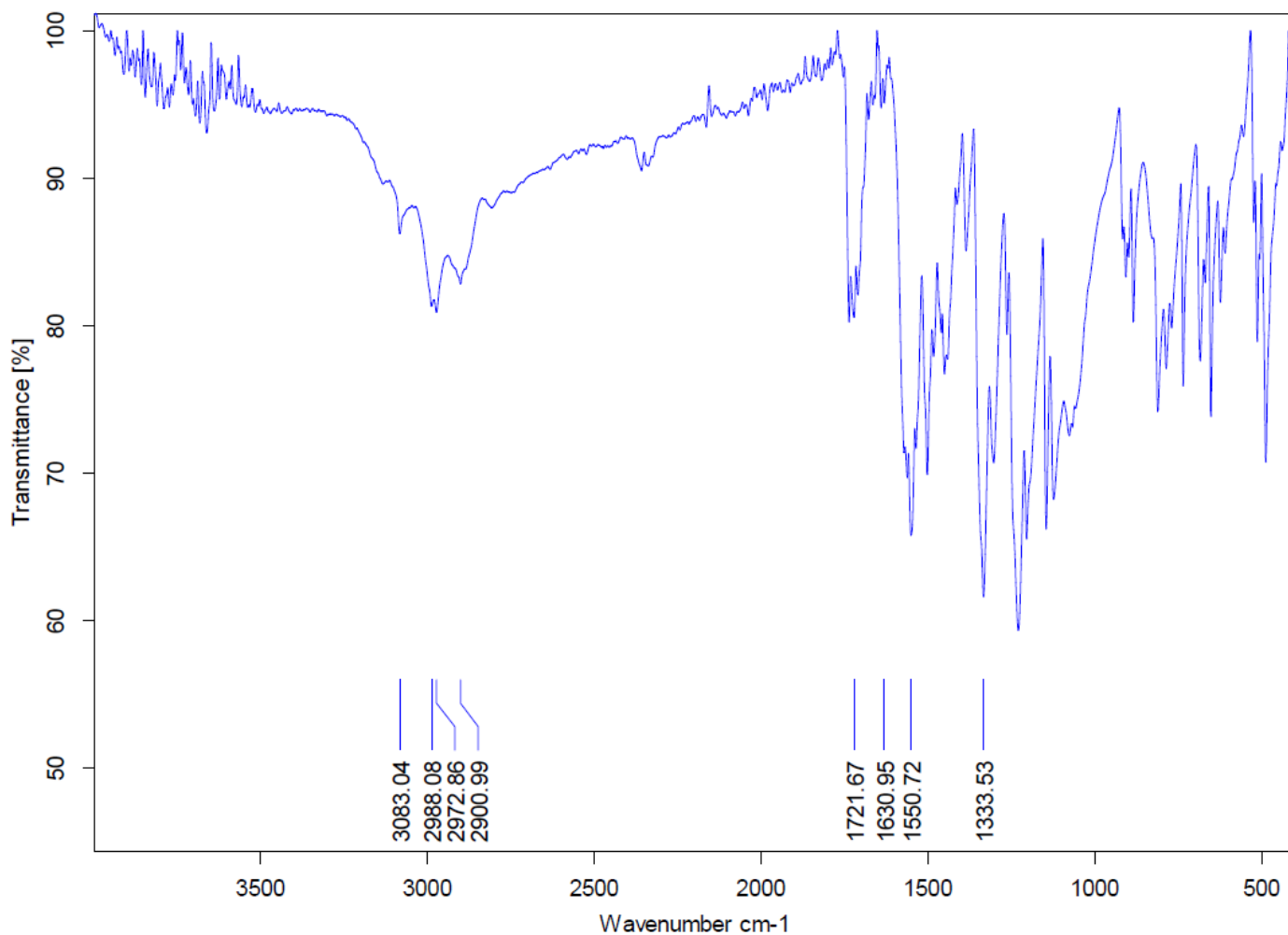
¹H NMR



¹³C NMR



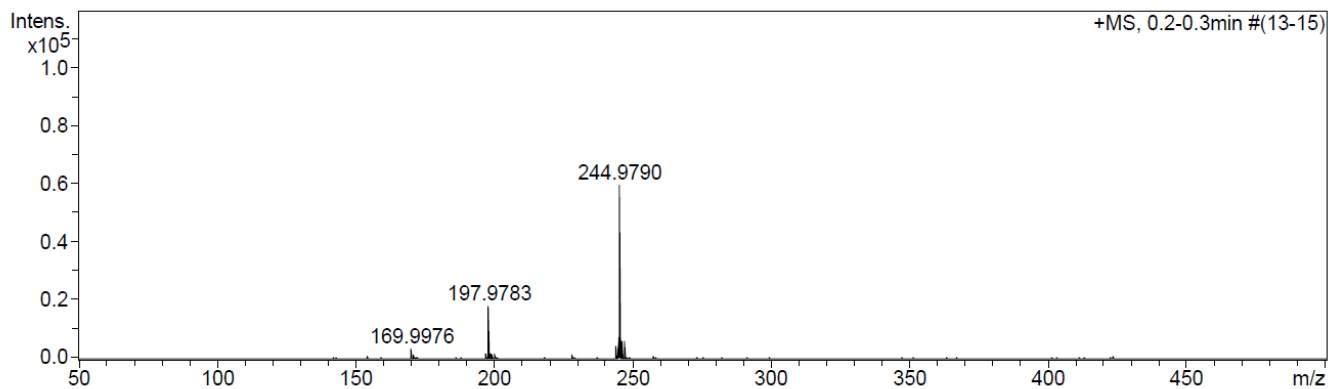
FTIR



HRMS

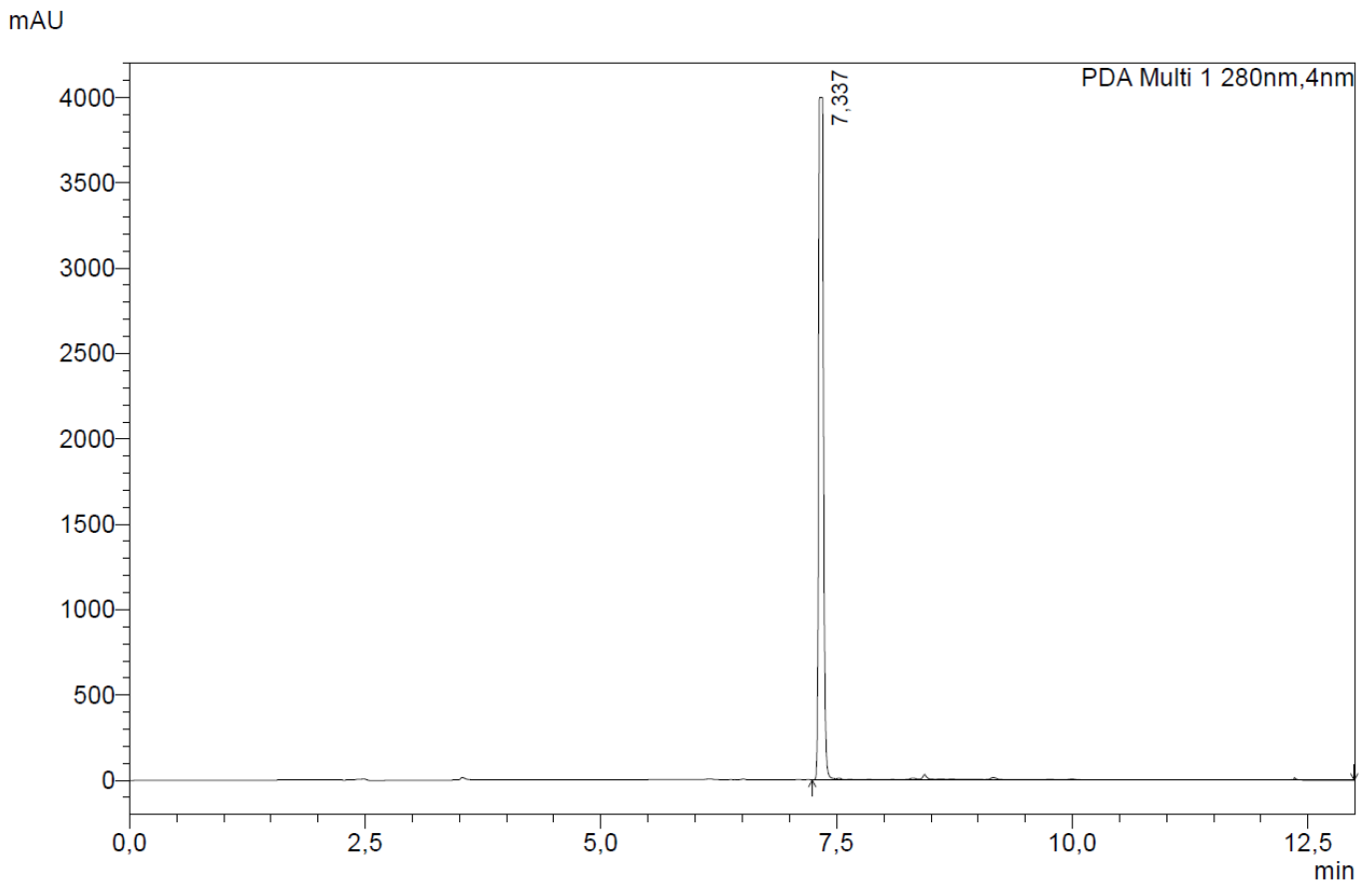
Acquisition Parameter

Source Type	APCI	Ion Polarity	Positive	Set Nebulizer	1.8 Bar
Focus	Not active	Set Capillary	4500 V	Set Dry Heater	200 °C
Scan Begin	50 m/z	Set End Plate Offset	-500 V	Set Dry Gas	8.0 l/min
Scan End	1600 m/z	Set Collision Cell RF	150.0 Vpp	Set Divert Valve	Waste



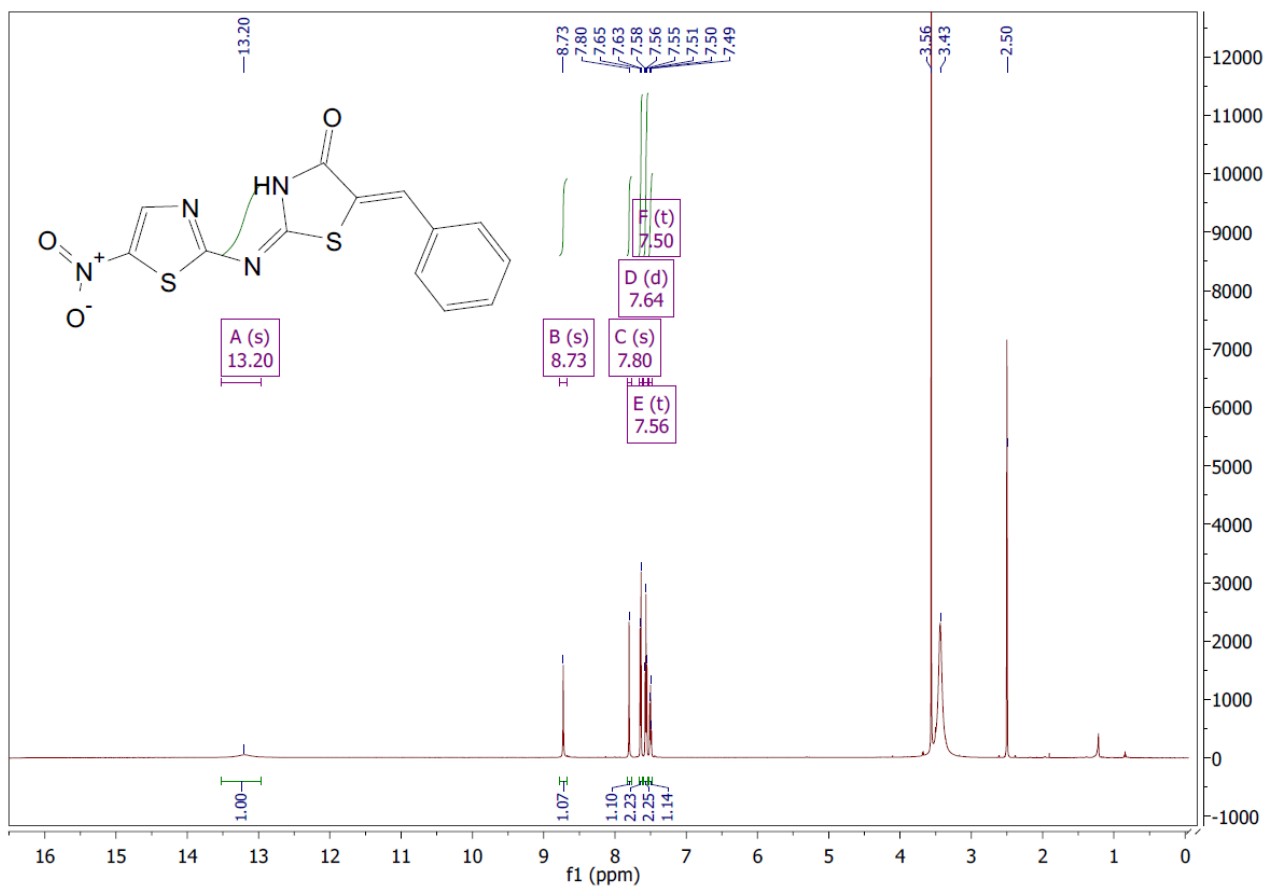
Meas. m/z	#	Formula	Score	m/z	err [mDa]	err [ppm]	mSigma	rdb	e ⁻ Conf	N-Rule
244.9790	1	C ₆ H ₅ N ₄ O ₃ S ₂	100.00	244.9798	0.8	3.1	3.1	6.5	even	ok

HPLC

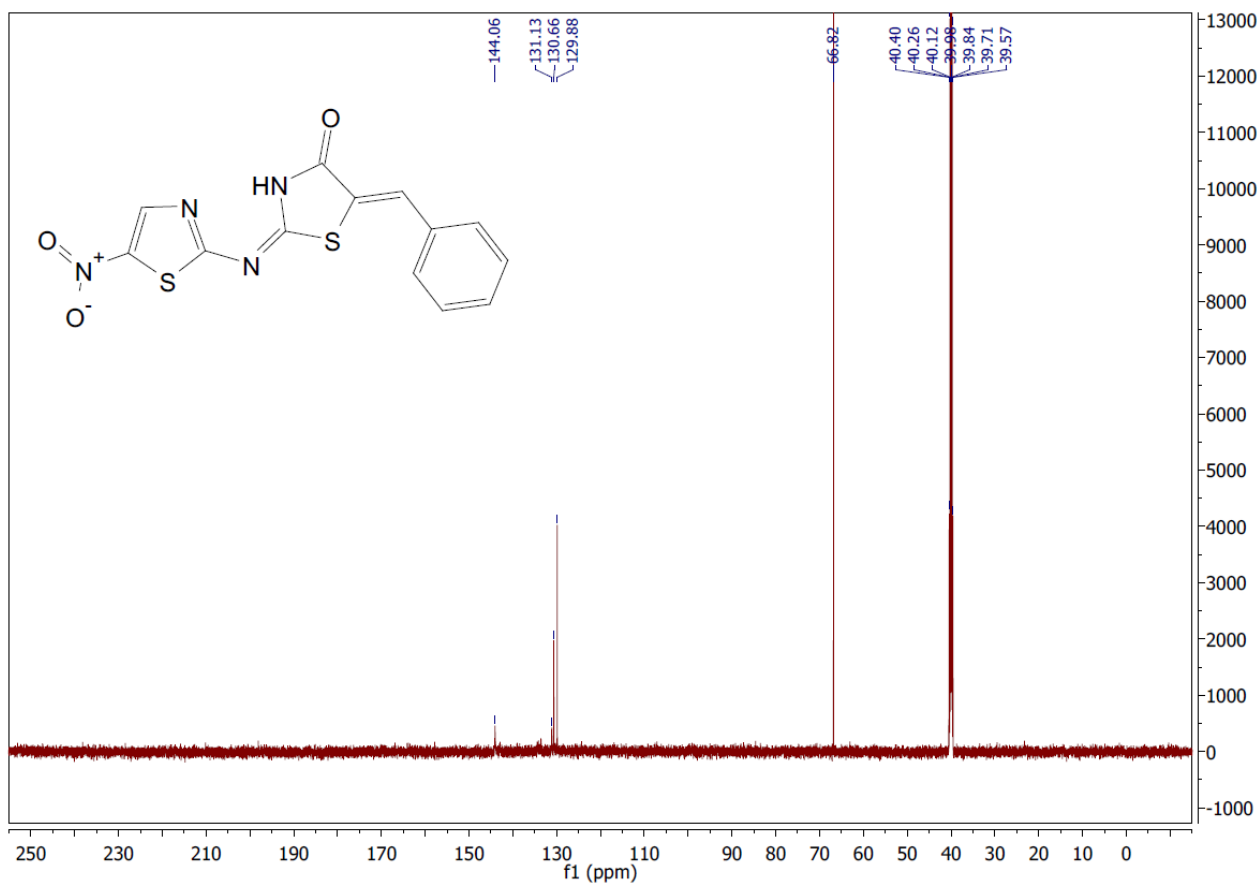


(2E,5Z)-5-benzylidene-2-((5-nitrothiazol-2-yl)imino)thiazolidin-4-one (**3a**)

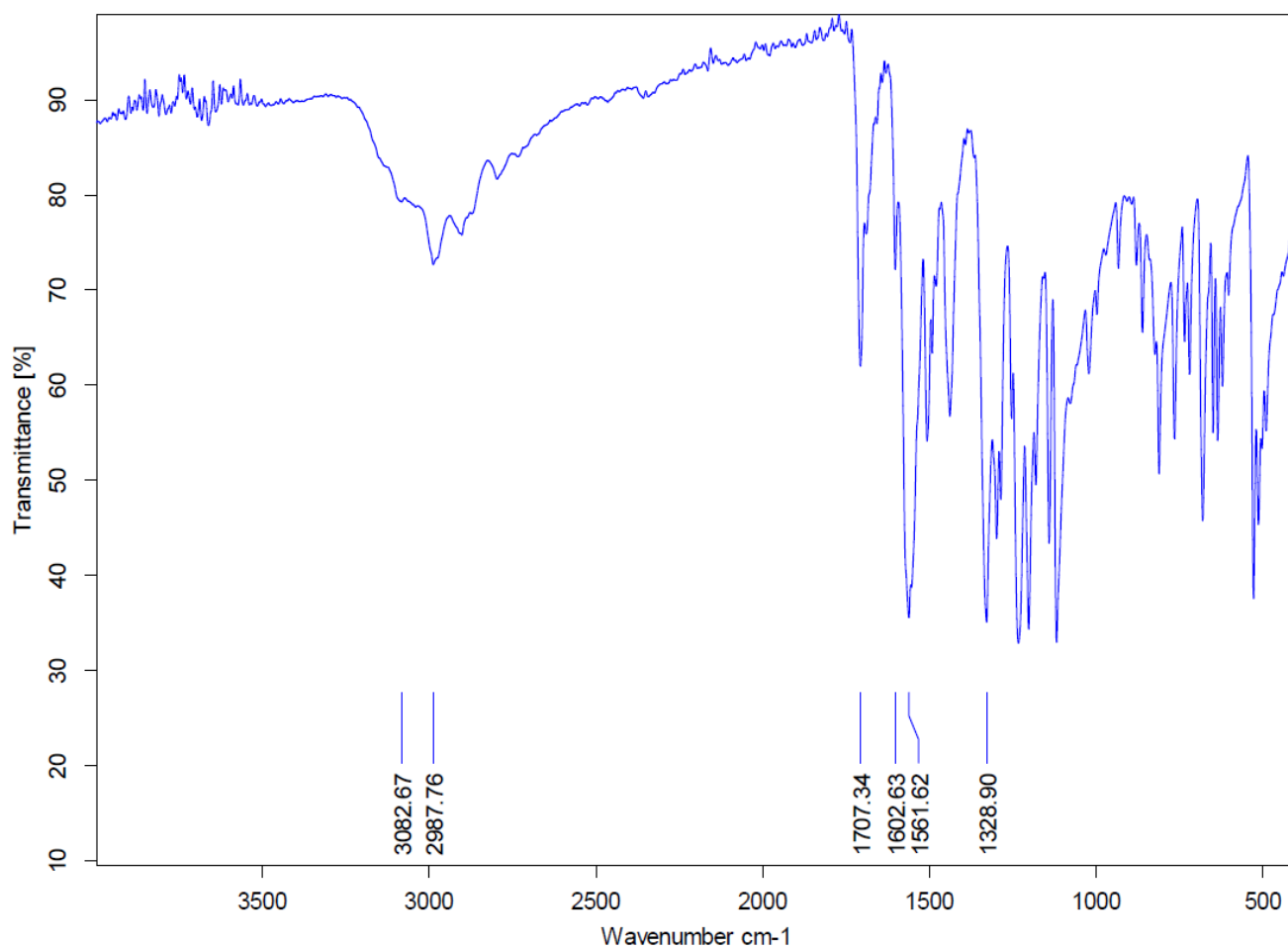
¹H NMR



¹³C NMR



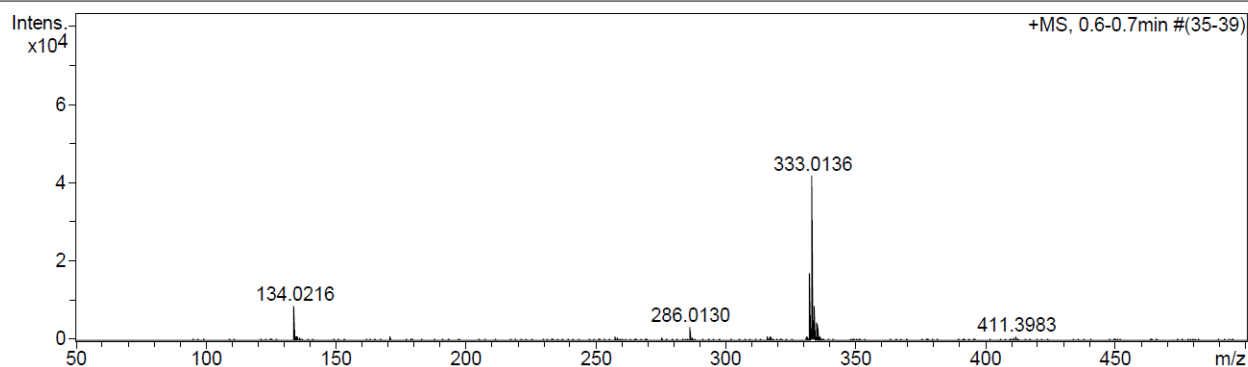
FTIR



HRMS

Acquisition Parameter

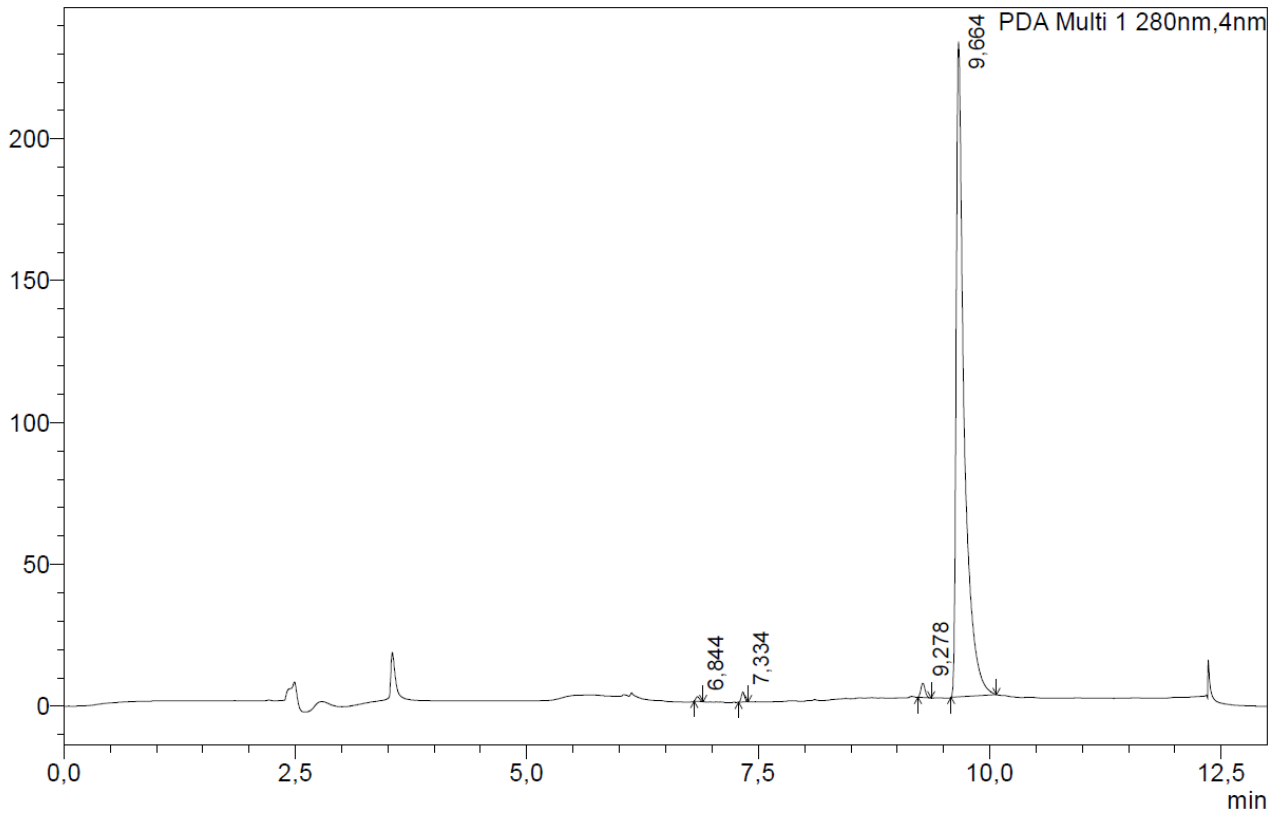
Source Type	APCI	Ion Polarity	Positive	Set Nebulizer	1.8 Bar
Focus	Not active	Set Capillary	4500 V	Set Dry Heater	200 °C
Scan Begin	50 m/z	Set End Plate Offset	-500 V	Set Dry Gas	8.0 l/min
Scan End	1600 m/z	Set Collision Cell RF	150.0 Vpp	Set Divert Valve	Waste



Meas. m/z	#	Formula	Score	m/z	err [mDa]	err [ppm]	mSigma	rdb	e ⁻ Conf	N-Rule
134.0216	1	C ₈ H ₆ S	19.04	134.0185	-3.2	-23.7	2.4	6.0	odd	ok
	2	C ₅ H ₁₀ S ₂	100.00	134.0218	0.2	1.4	25.2	1.0	odd	ok
	3	C ₇ H ₄ NO ₂	32.73	134.0237	2.0	15.0	27.1	6.5	even	ok
	4	C ₅ H ₂ N ₄ O	68.15	134.0223	0.7	4.9	32.0	7.0	odd	ok
333.0136	1	C ₁₃ H ₉ N ₄ O ₃ S ₂	100.00	333.0111	-2.5	-7.5	16.7	11.5	even	ok

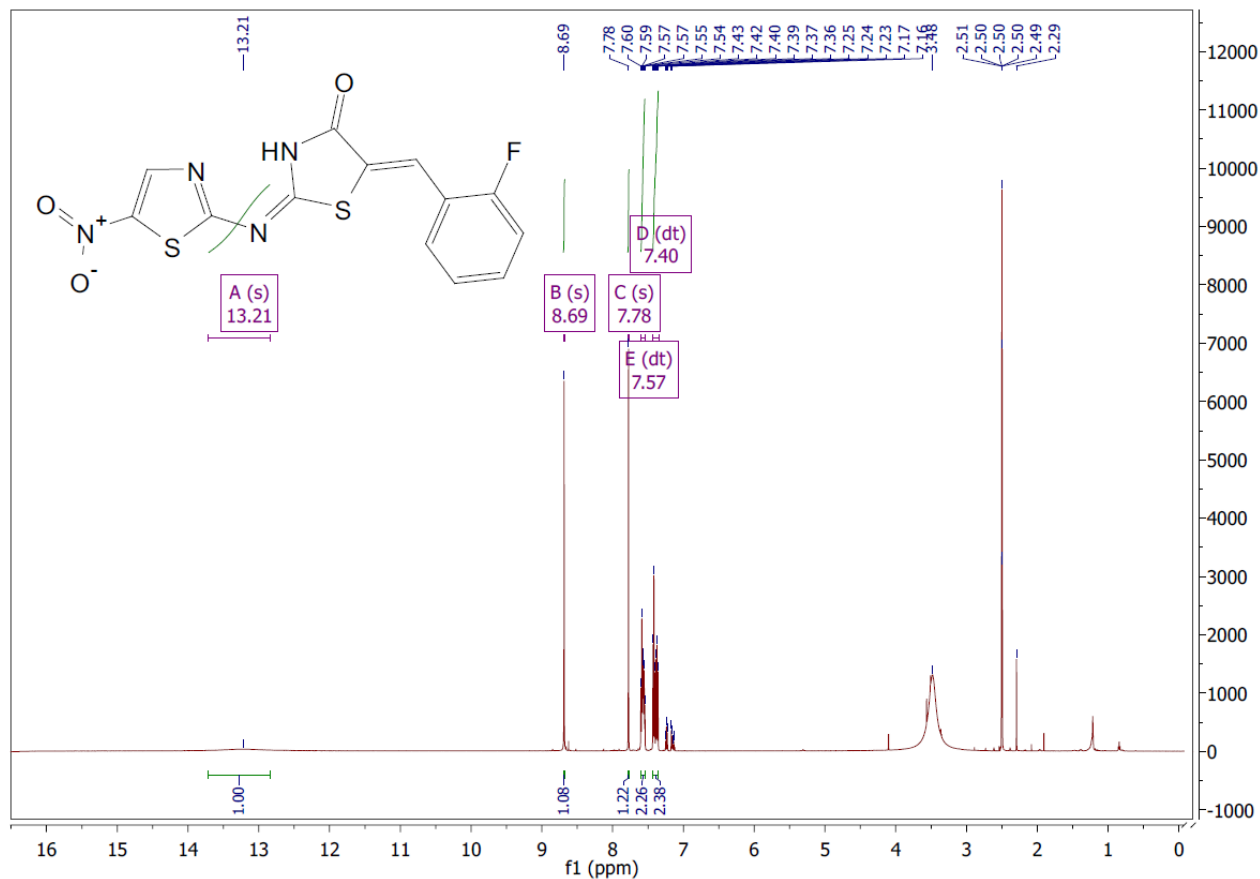
HPLC

mAU

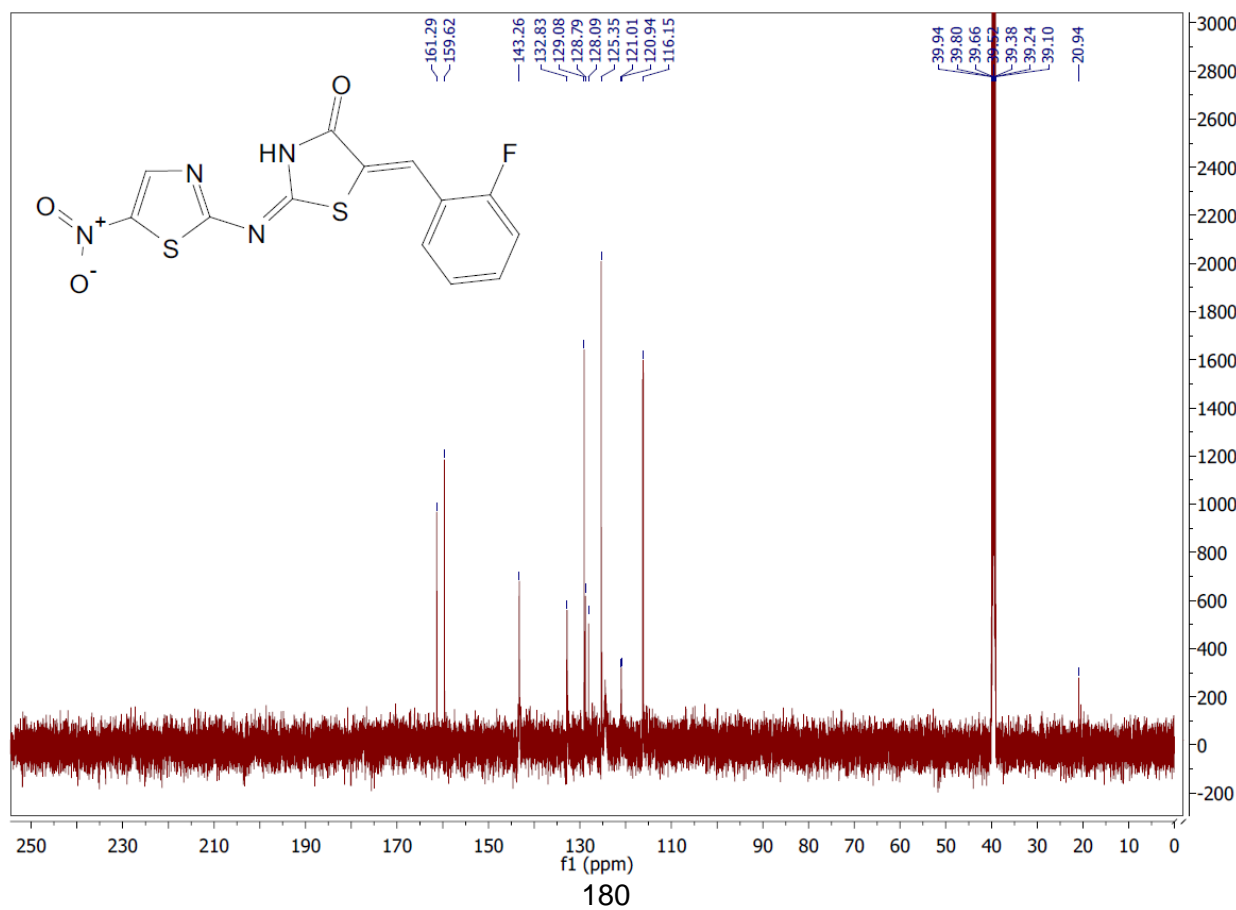


(2E,5Z)-5-(2-fluorobenzylidene)-2-((5-nitrothiazol-2-yl)imino)thiazolidin-4-one (**3b**)

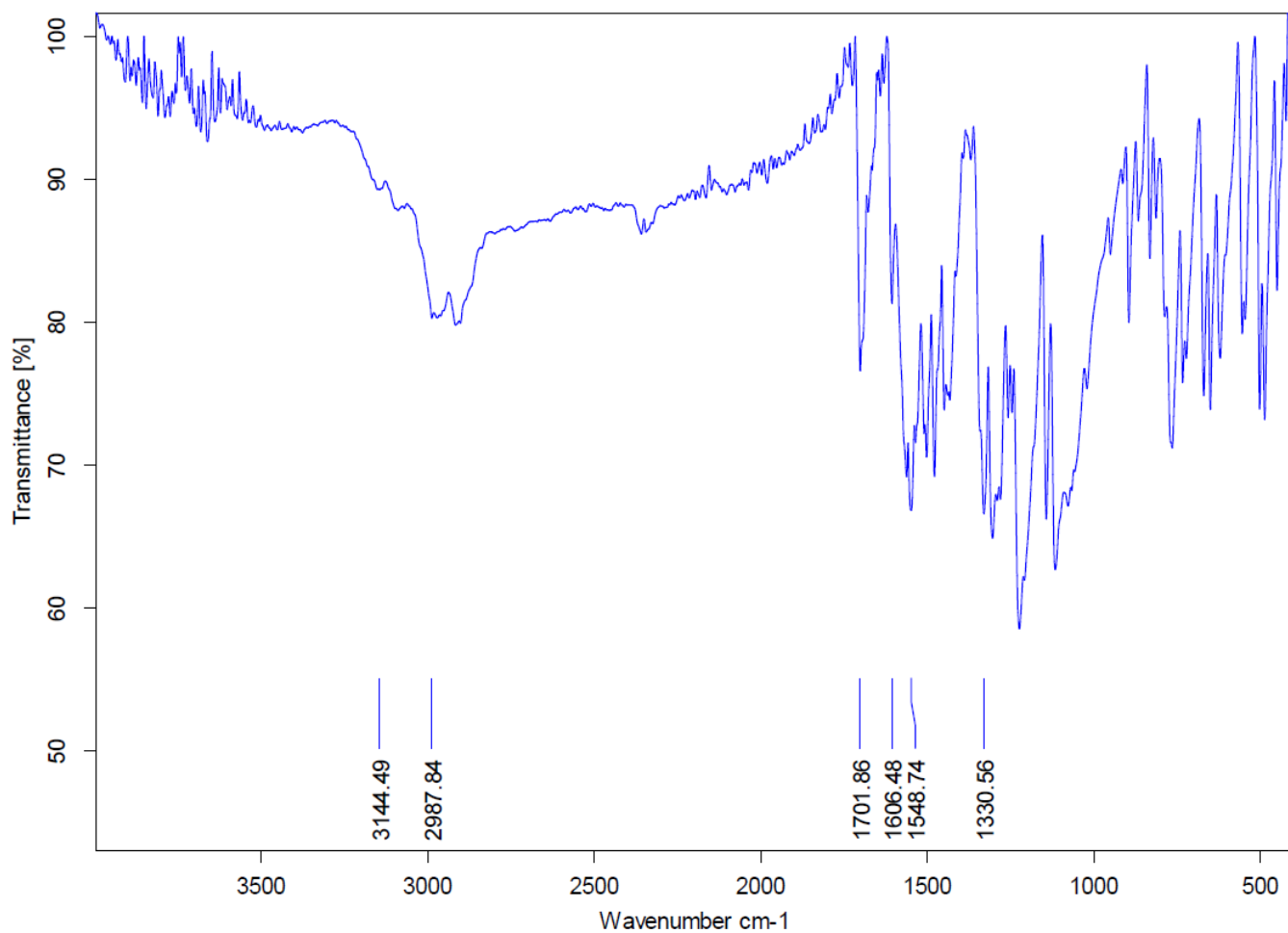
¹H NMR



¹³C NMR



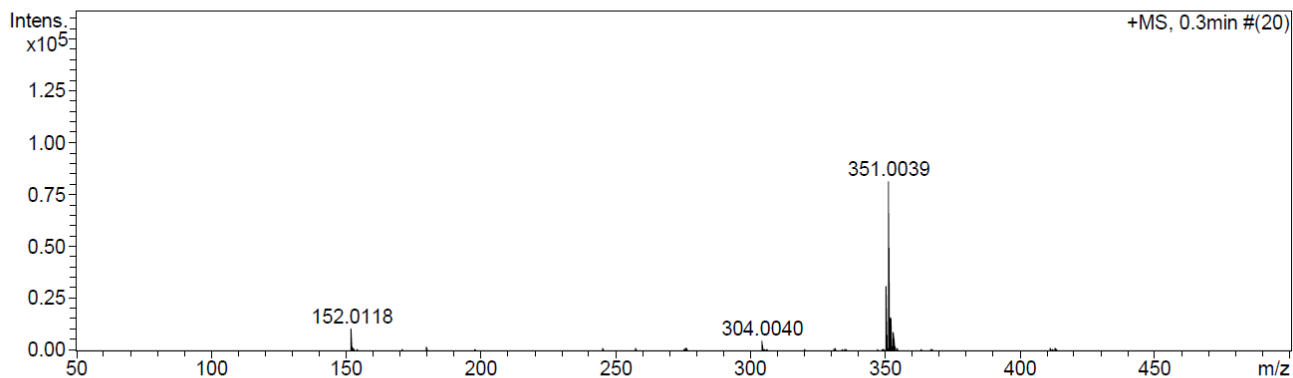
FTIR



HRMS

Acquisition Parameter

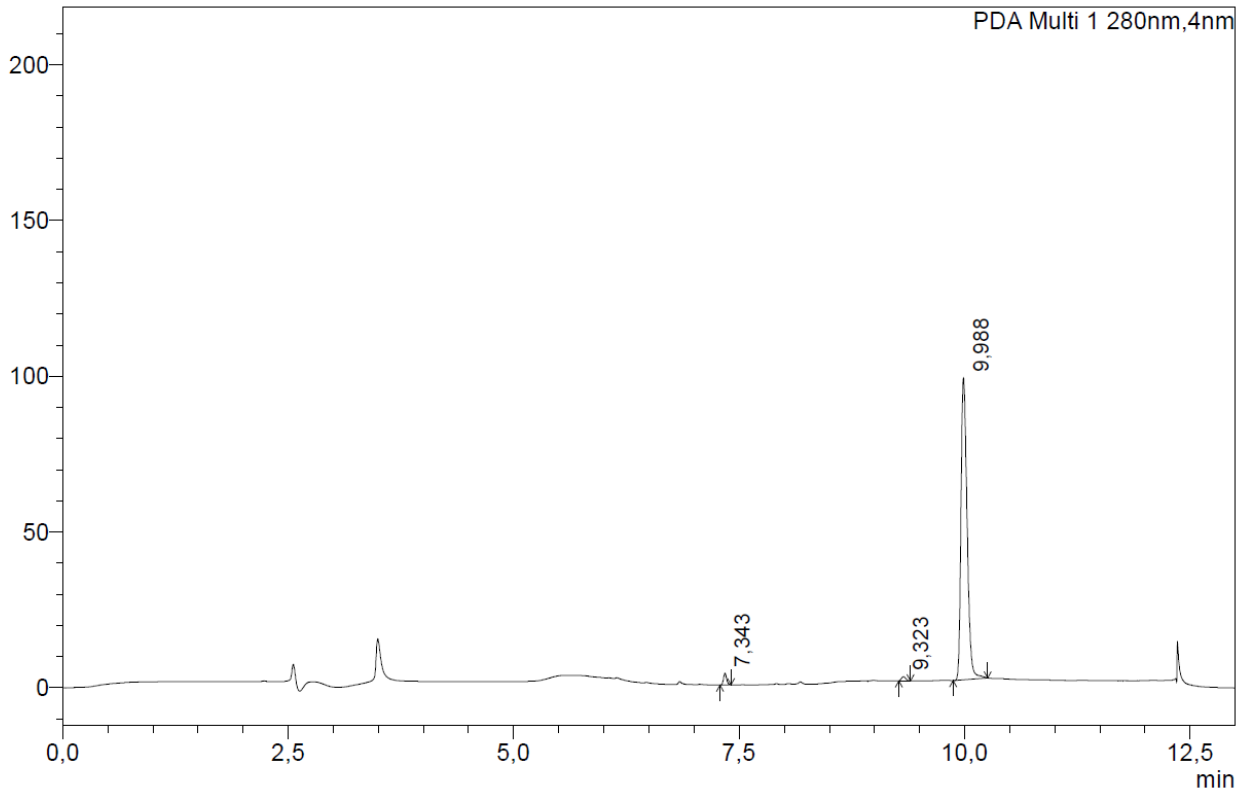
Source Type	APCI	Ion Polarity	Positive	Set Nebulizer	1.8 Bar
Focus	Not active	Set Capillary	4500 V	Set Dry Heater	200 °C
Scan Begin	50 m/z	Set End Plate Offset	-500 V	Set Dry Gas	8.0 l/min
Scan End	1600 m/z	Set Collision Cell RF	150.0 Vpp	Set Divert Valve	Waste



Meas. m/z	#	Formula	Score	m/z	err [mDa]	err [ppm]	mSigma	rdb	e ⁻ Conf	N-Rule
351.0039	1	C ₁₃ H ₈ FN ₄ O ₃ S ₂	32.03	351.0016	-2.3	-6.6	14.1	11.5	even	ok
	2	C ₁₃ H ₁₁ N ₄ O ₂ S ₃	100.00	351.0039	-0.1	-0.2	24.4	10.5	even	ok

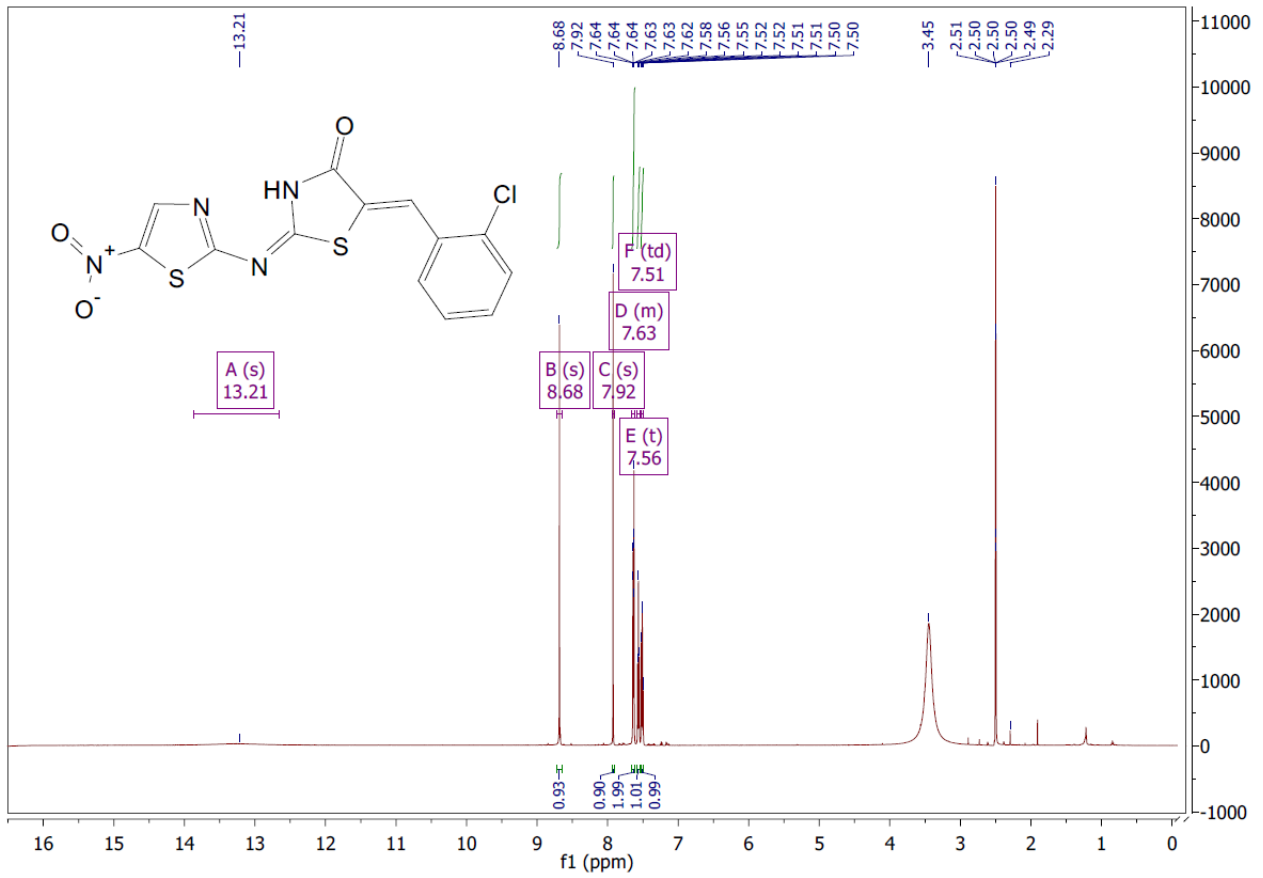
HPLC

mAU

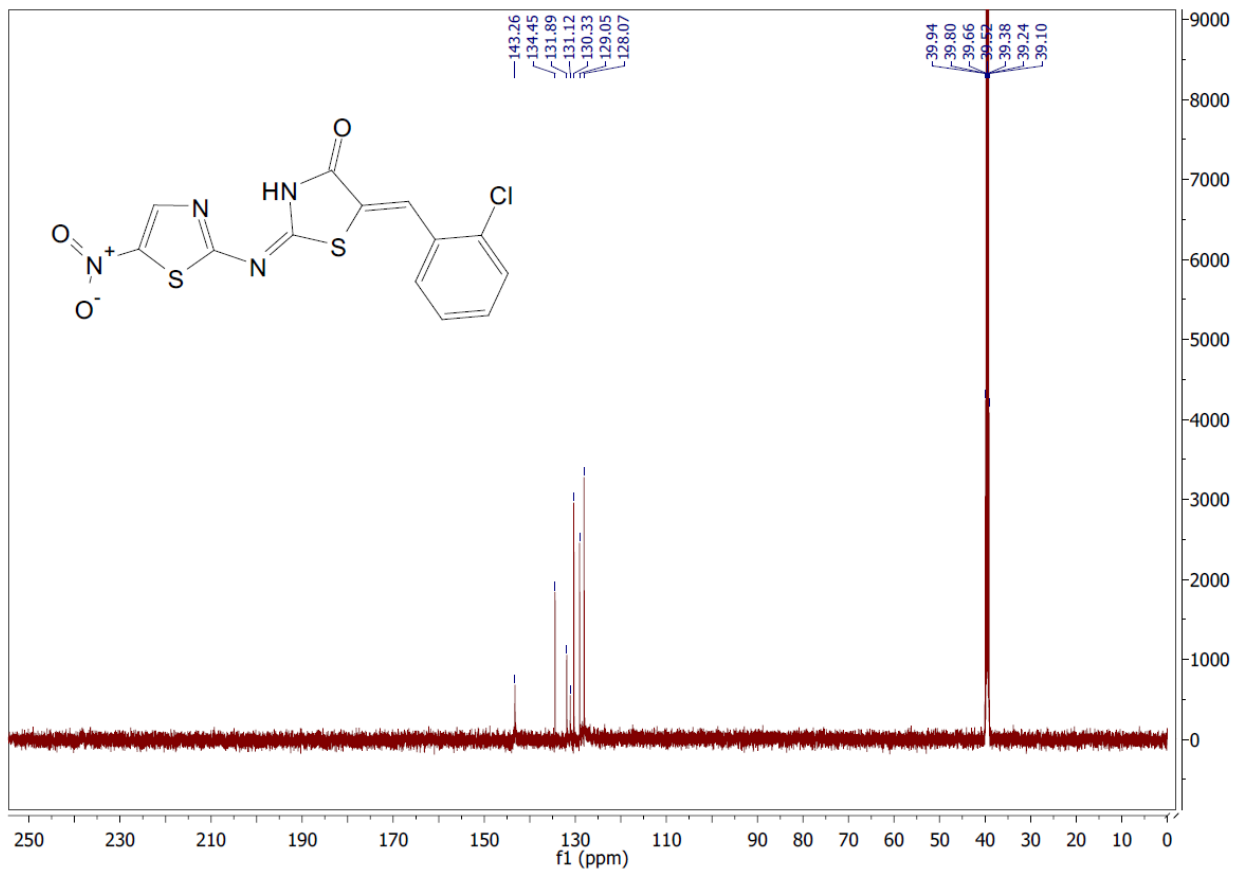


(2E,5Z)-5-(2-chlorobenzylidene)-2-((5-nitrothiazol-2-yl)imino)thiazolidin-4-one (**3c**)

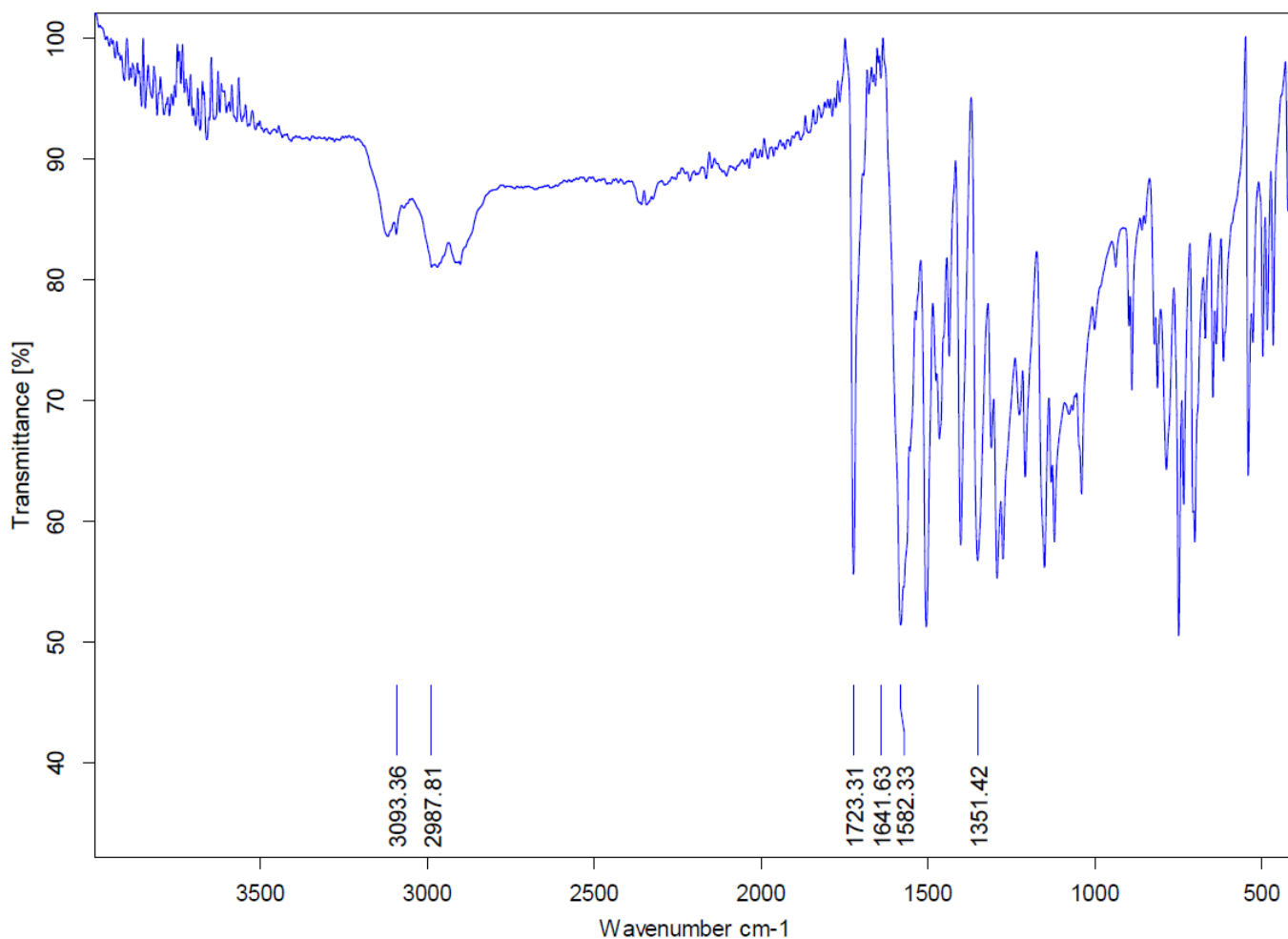
¹H NMR



¹³C NMR



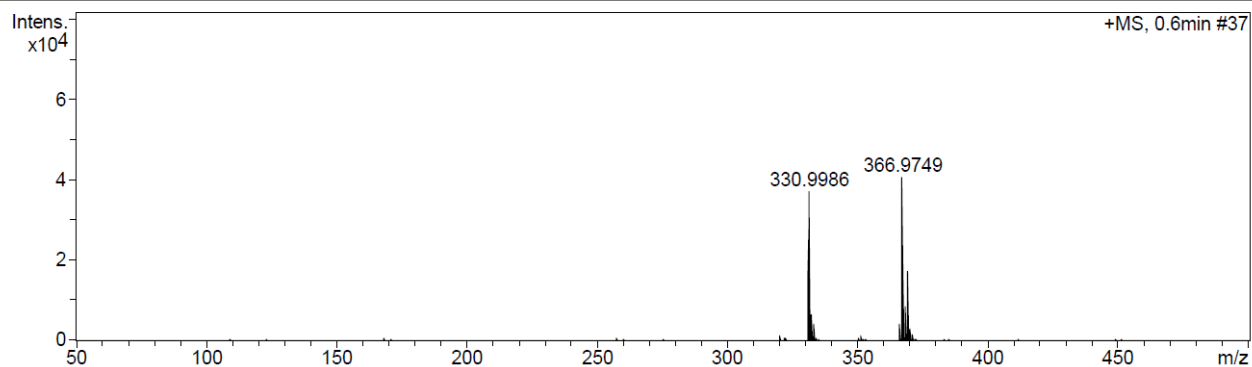
FTIR



HRMS

Acquisition Parameter

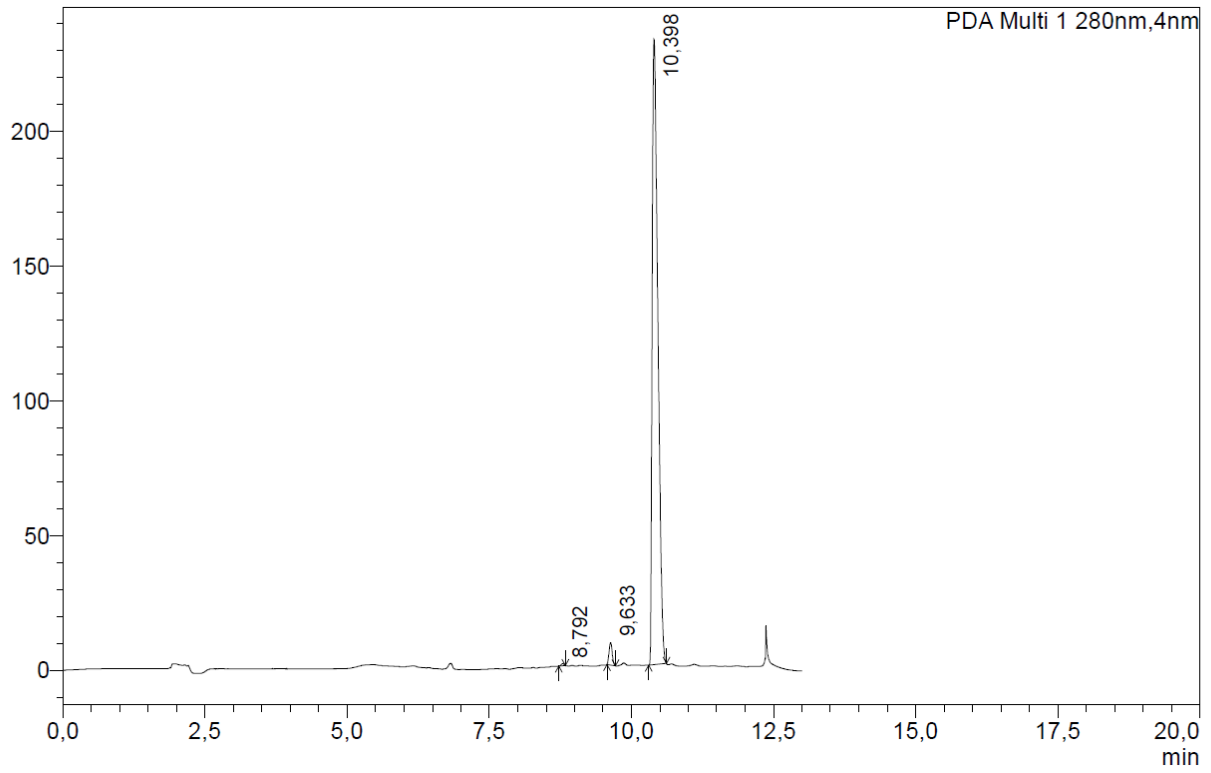
Source Type	APCI	Ion Polarity	Positive	Set Nebulizer	1.8 Bar
Focus	Not active	Set Capillary	4500 V	Set Dry Heater	200 °C
Scan Begin	50 m/z	Set End Plate Offset	-500 V	Set Dry Gas	8.0 l/min
Scan End	1600 m/z	Set Collision Cell RF	150.0 Vpp	Set Divert Valve	Waste



Meas. m/z	#	Formula	Score	m/z	err [mDa]	err [ppm]	mSigma	rdb	e ⁻ Conf	N-Rule
330.9986	1	C 13 H 7 N 4 O 3 S 2	15.65	330.9954	-3.2	-9.7	8.0	12.5	even	ok
	2	C 10 H 11 N 4 O 3 S 3	100.00	330.9988	0.2	0.5	22.0	7.5	even	ok
	3	C 12 H 12 Cl N 2 O 3 S 2	0.70	330.9972	-1.4	-4.1	131.2	7.5	even	ok
366.9749	1	C 13 H 8 Cl N 4 O 3 S 2	100.00	366.9721	-2.8	-7.6	16.0	11.5	even	ok

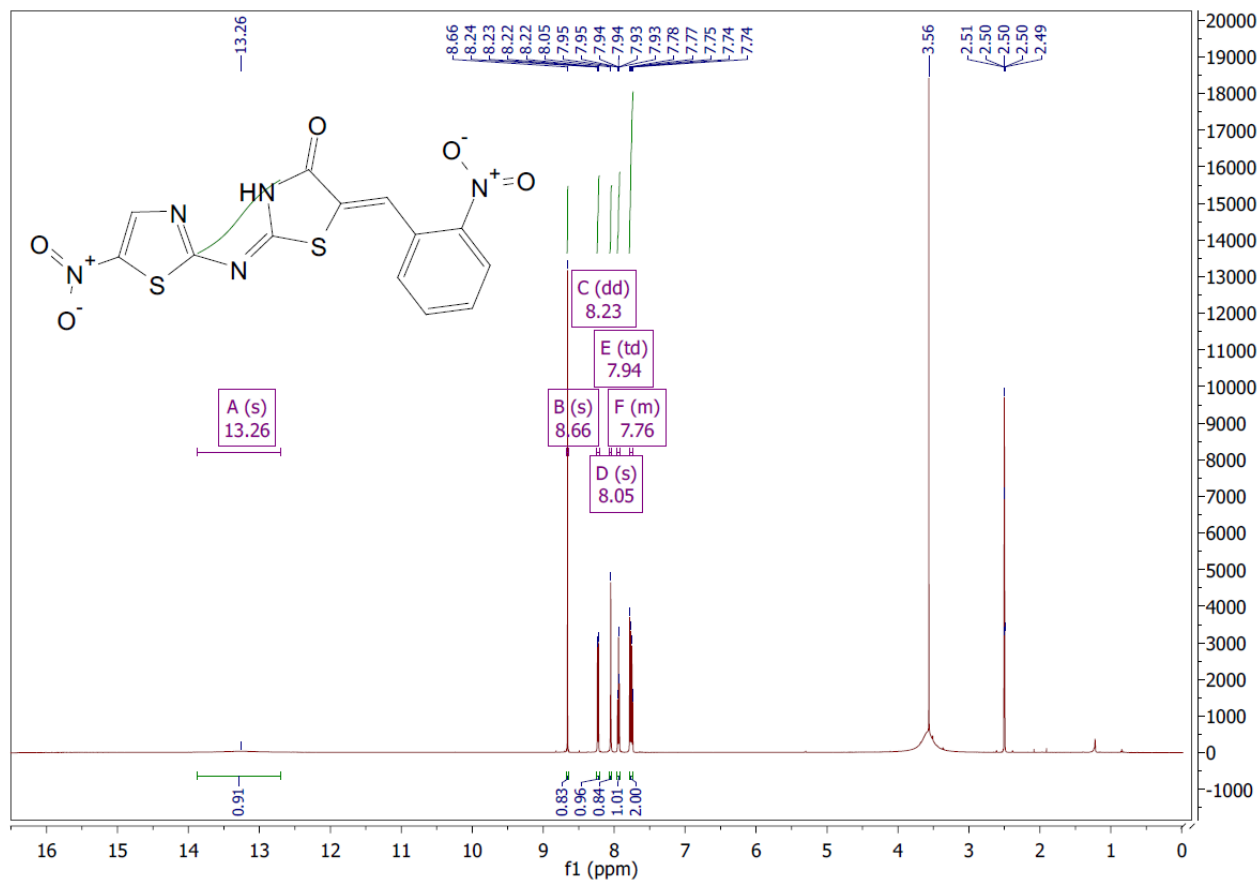
HPLC

mAU

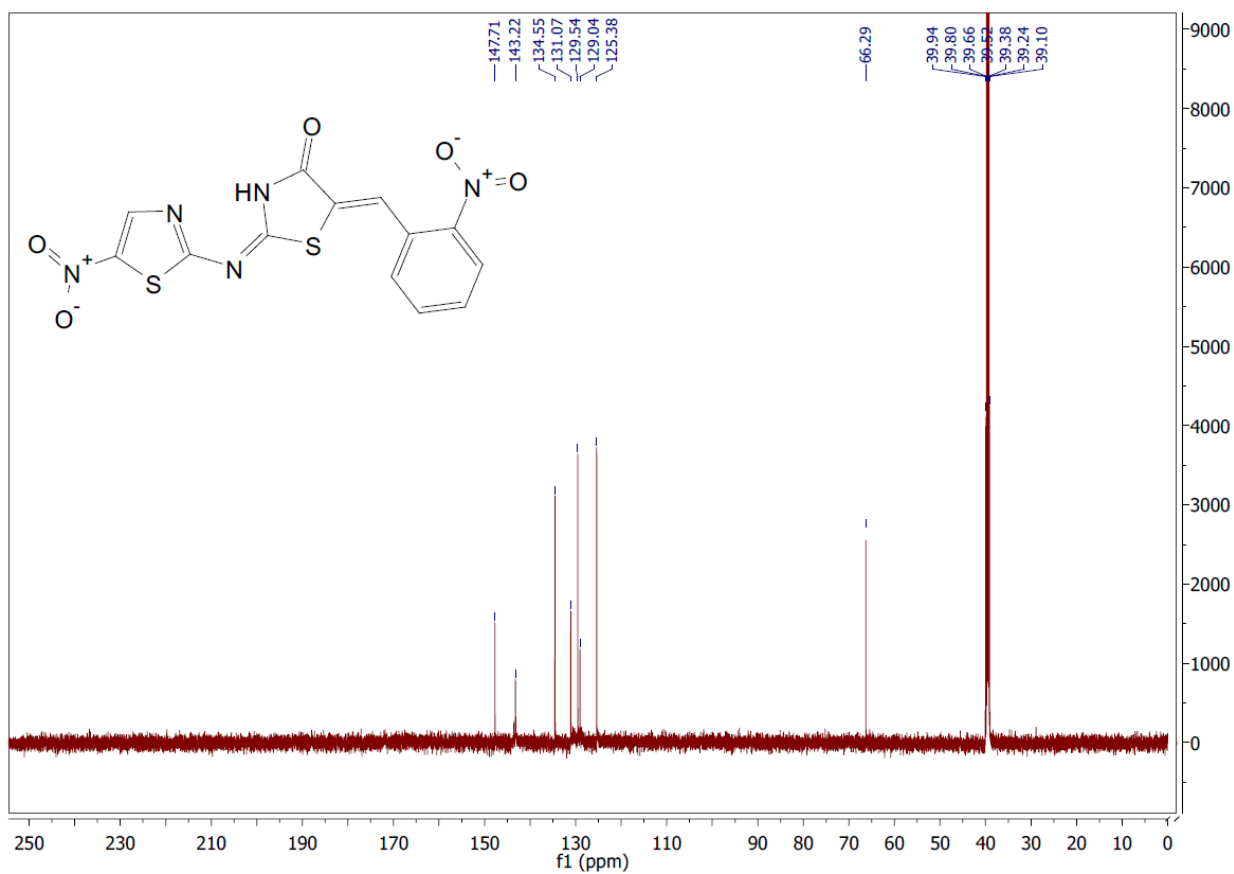


(2*E*,5*Z*)-5-(2-nitrobenzylidene)-2-((5-nitrothiazol-2-yl)imino)thiazolidin-4-one (**3d**)

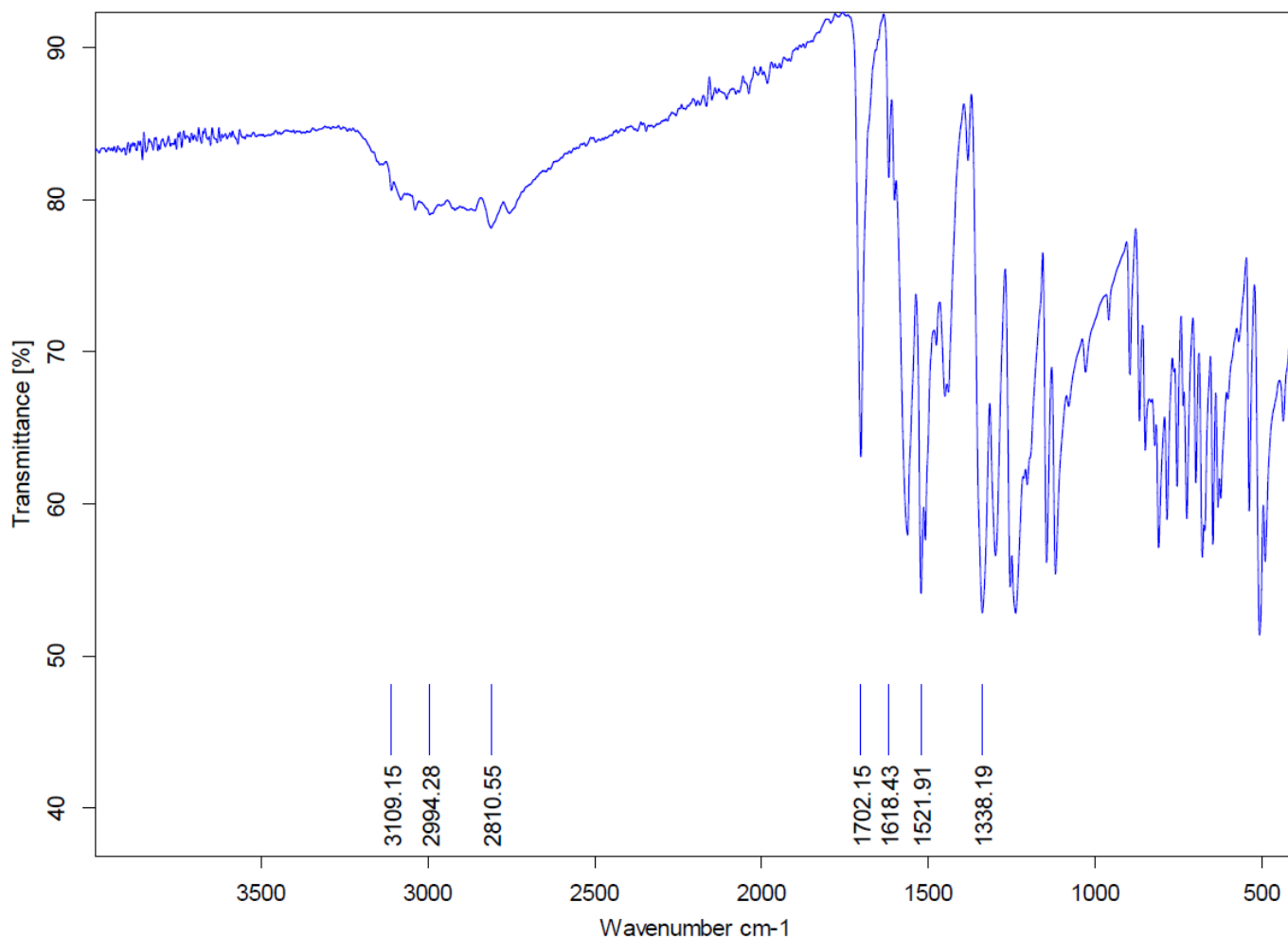
¹H NMR



¹³C NMR



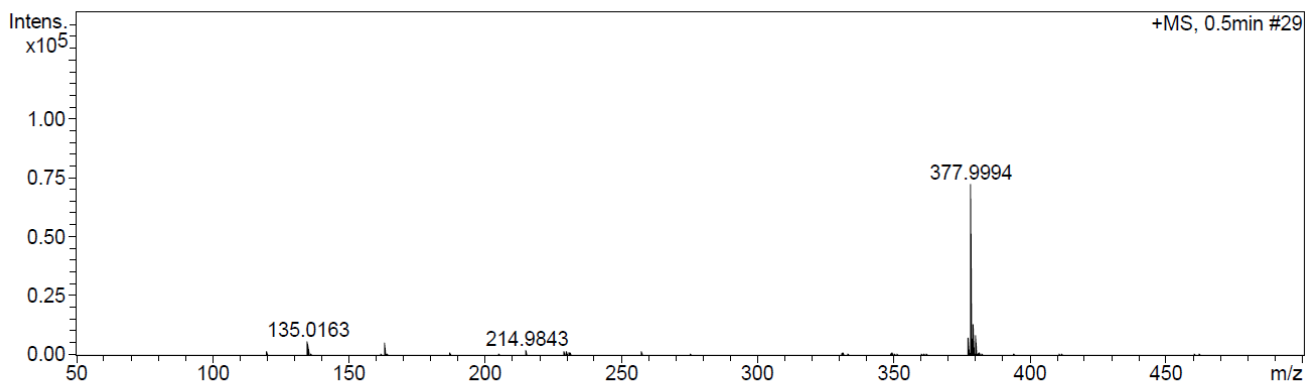
FTIR



HRMS

Acquisition Parameter

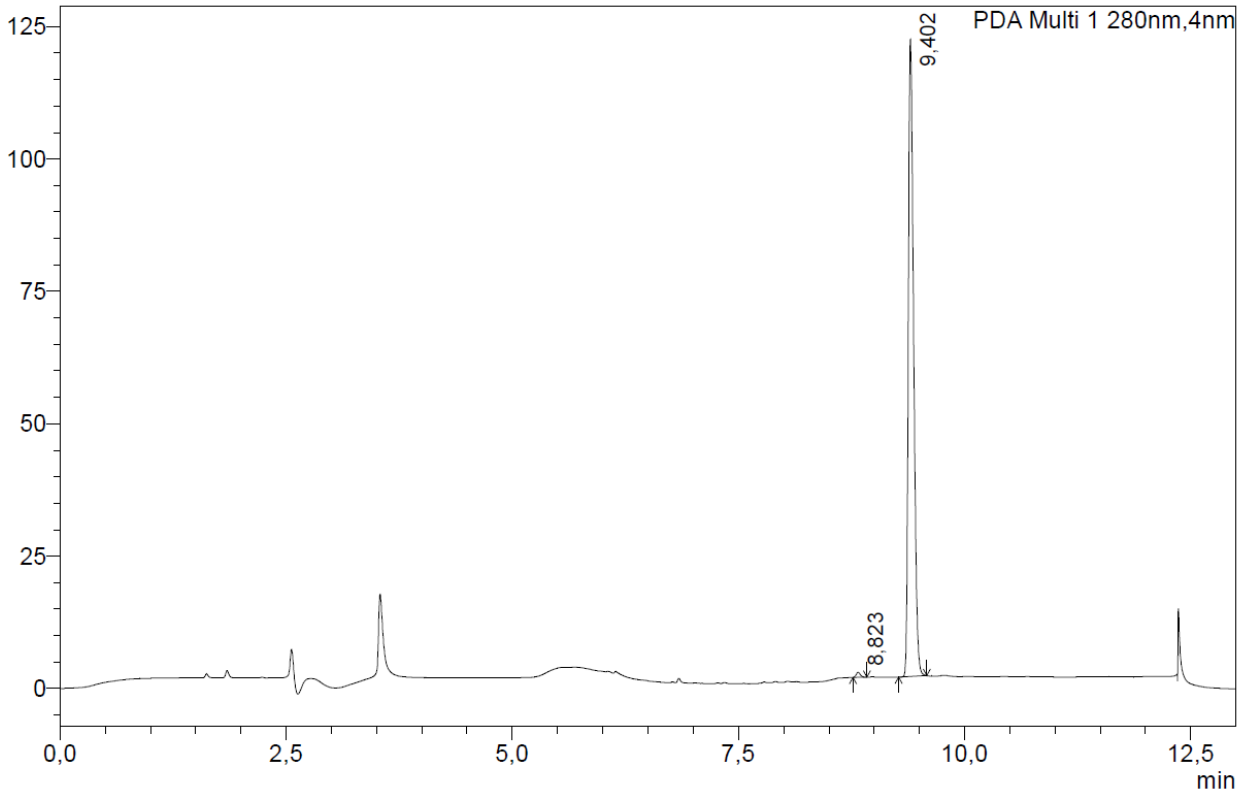
Source Type	APCI	Ion Polarity	Positive	Set Nebulizer	1.8 Bar
Focus	Not active	Set Capillary	4500 V	Set Dry Heater	200 °C
Scan Begin	50 m/z	Set End Plate Offset	-500 V	Set Dry Gas	8.0 l/min
Scan End	1600 m/z	Set Collision Cell RF	150.0 Vpp	Set Divert Valve	Waste



Meas. m/z	#	Formula	Score	m/z	err [mDa]	err [ppm]	mSigma	rdb	e ⁻ Conf	N-Rule
377.9994	1	C ₁₃ H ₈ N ₅ O ₅ S ₂	100.00	377.9961	-3.3	-8.7	3.8	12.5	even	ok

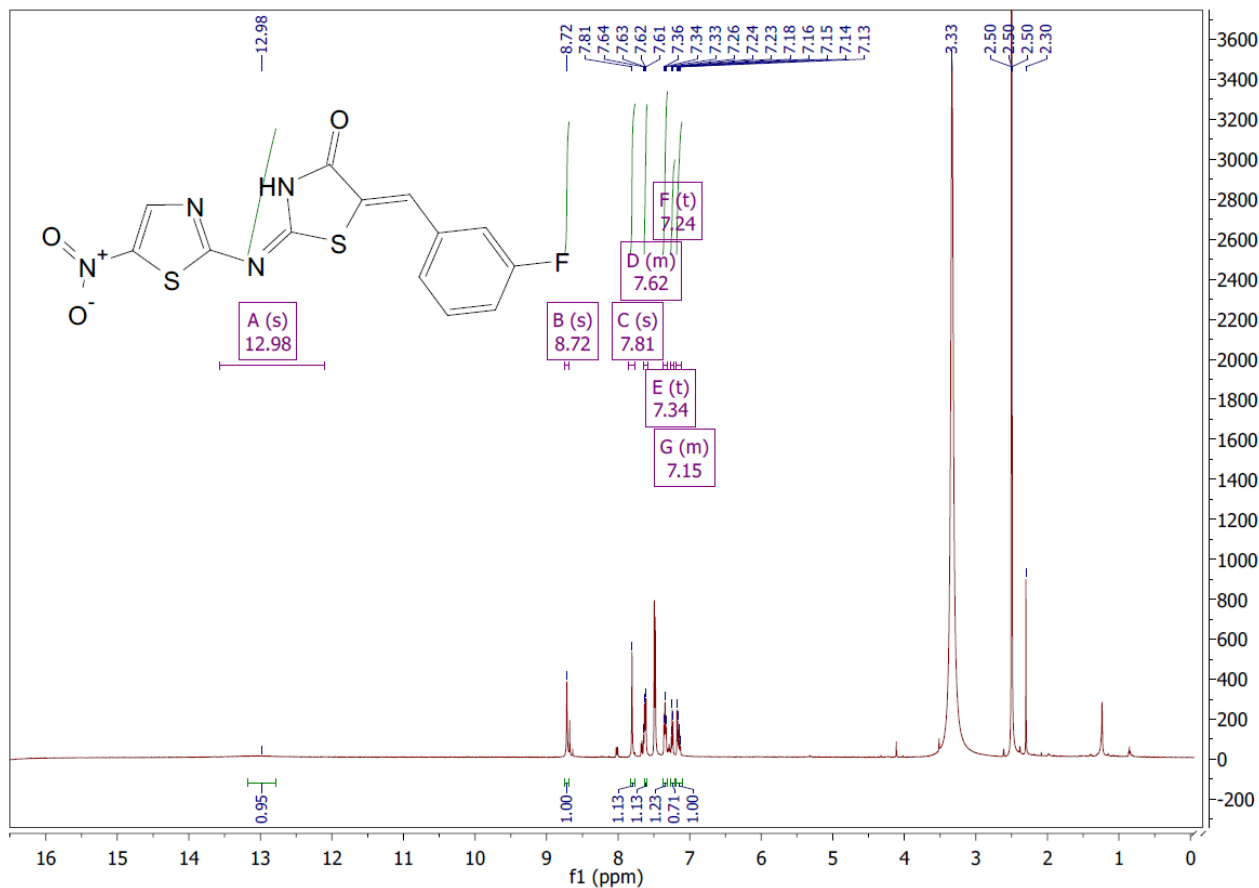
HPLC

mAU

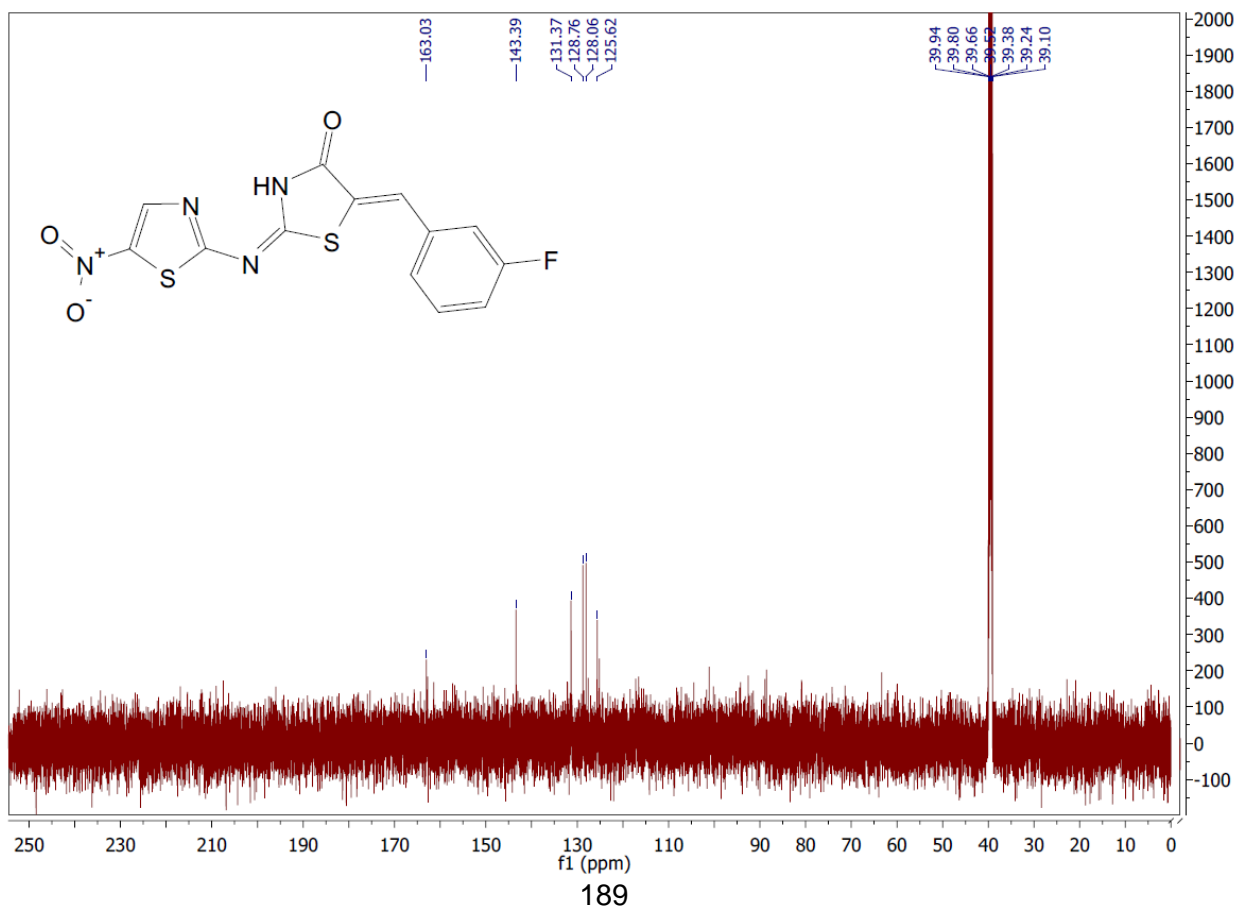


(2E,5Z)-5-(3-fluorobenzylidene)-2-((5-nitrothiazol-2-yl)imino)thiazolidin-4-one (**3e**)

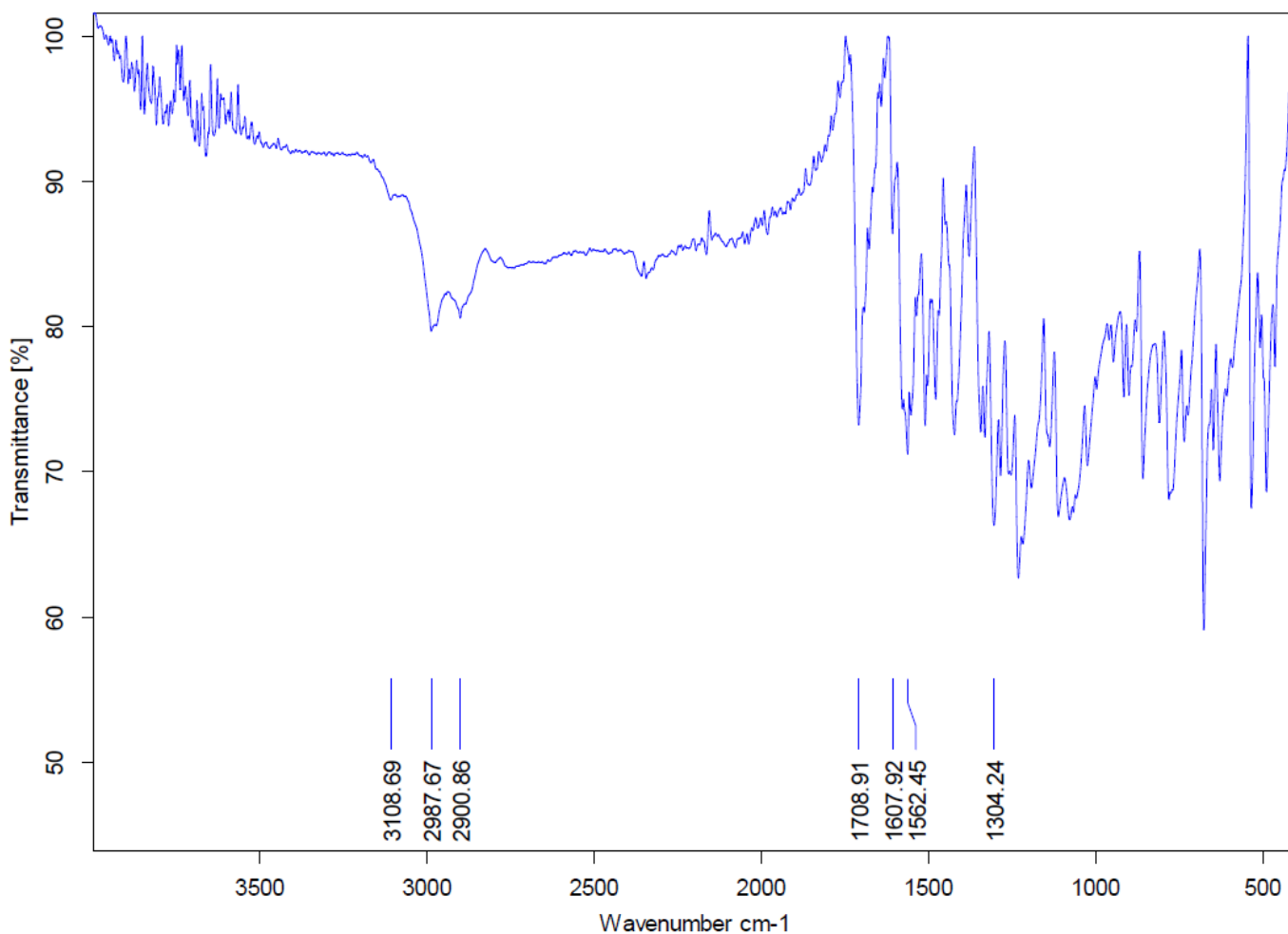
¹H NMR



¹³C NMR



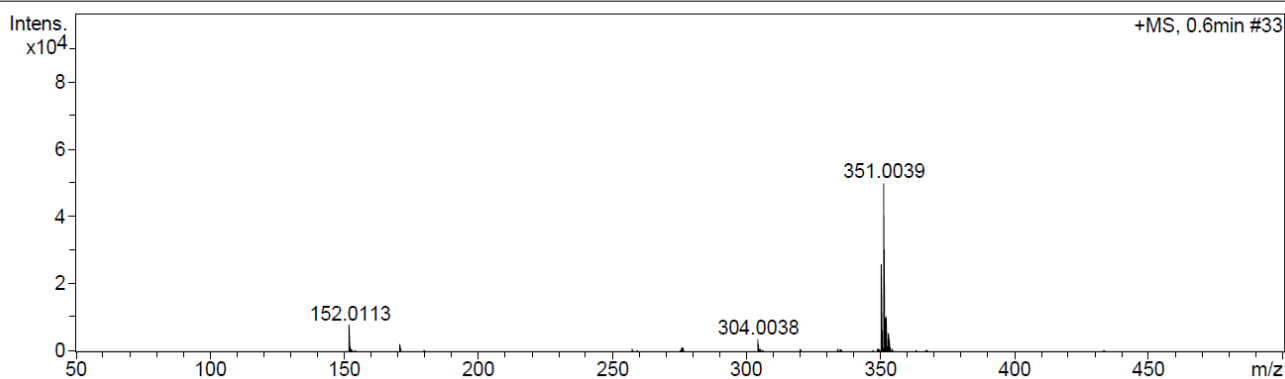
FTIR



HRMS

Acquisition Parameter

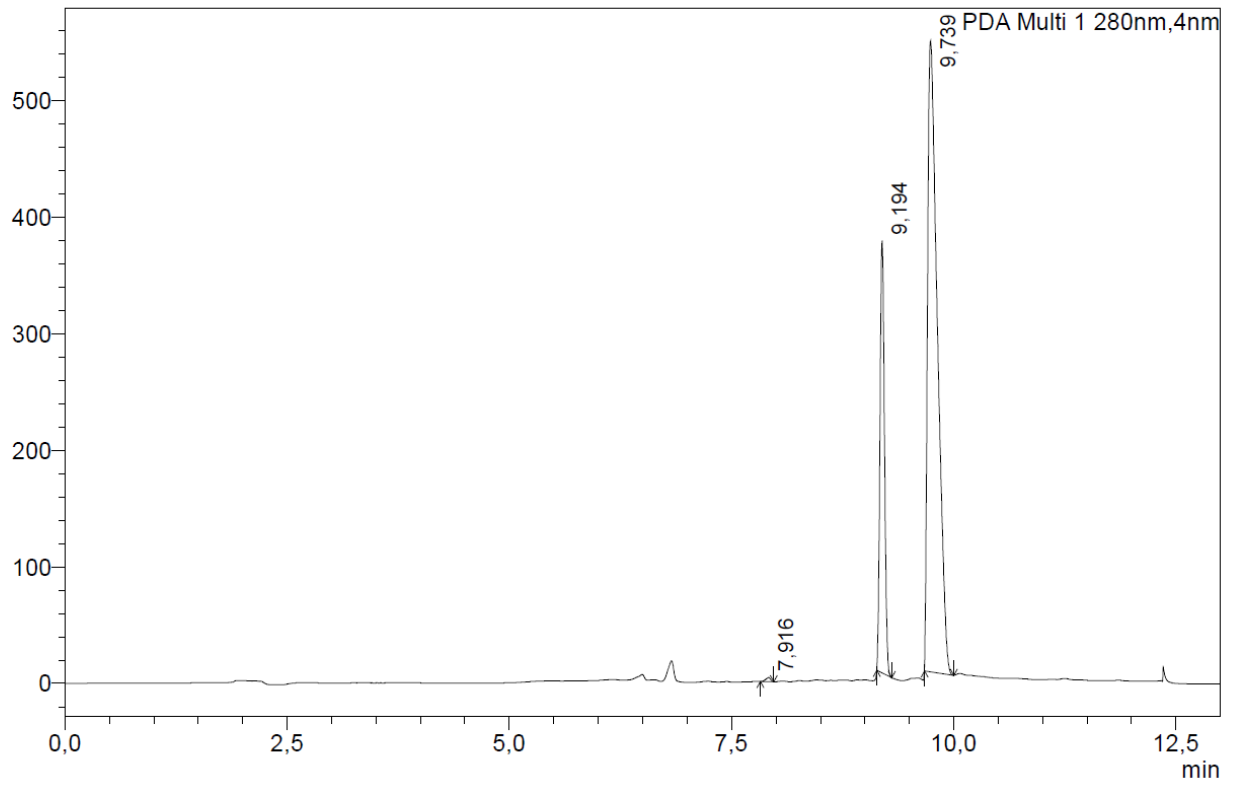
Source Type	APCI	Ion Polarity	Positive	Set Nebulizer	1.8 Bar
Focus	Not active	Set Capillary	4500 V	Set Dry Heater	200 °C
Scan Begin	50 m/z	Set End Plate Offset	-500 V	Set Dry Gas	8.0 l/min
Scan End	1600 m/z	Set Collision Cell RF	150.0 Vpp	Set Divert Valve	Waste



Meas. m/z	#	Formula	Score	m/z	err [mDa]	err [ppm]	mSigma	rdb	e ⁻ Conf	N-Rule
351.0039	1	C ₁₃ H ₈ FN ₄ O ₃ S ₂	29.12	351.0016	-2.3	-6.6	22.3	11.5	even	ok
	2	C ₁₃ H ₁₁ N ₄ O ₂ S ₃	100.00	351.0039	-0.1	-0.2	27.8	10.5	even	ok

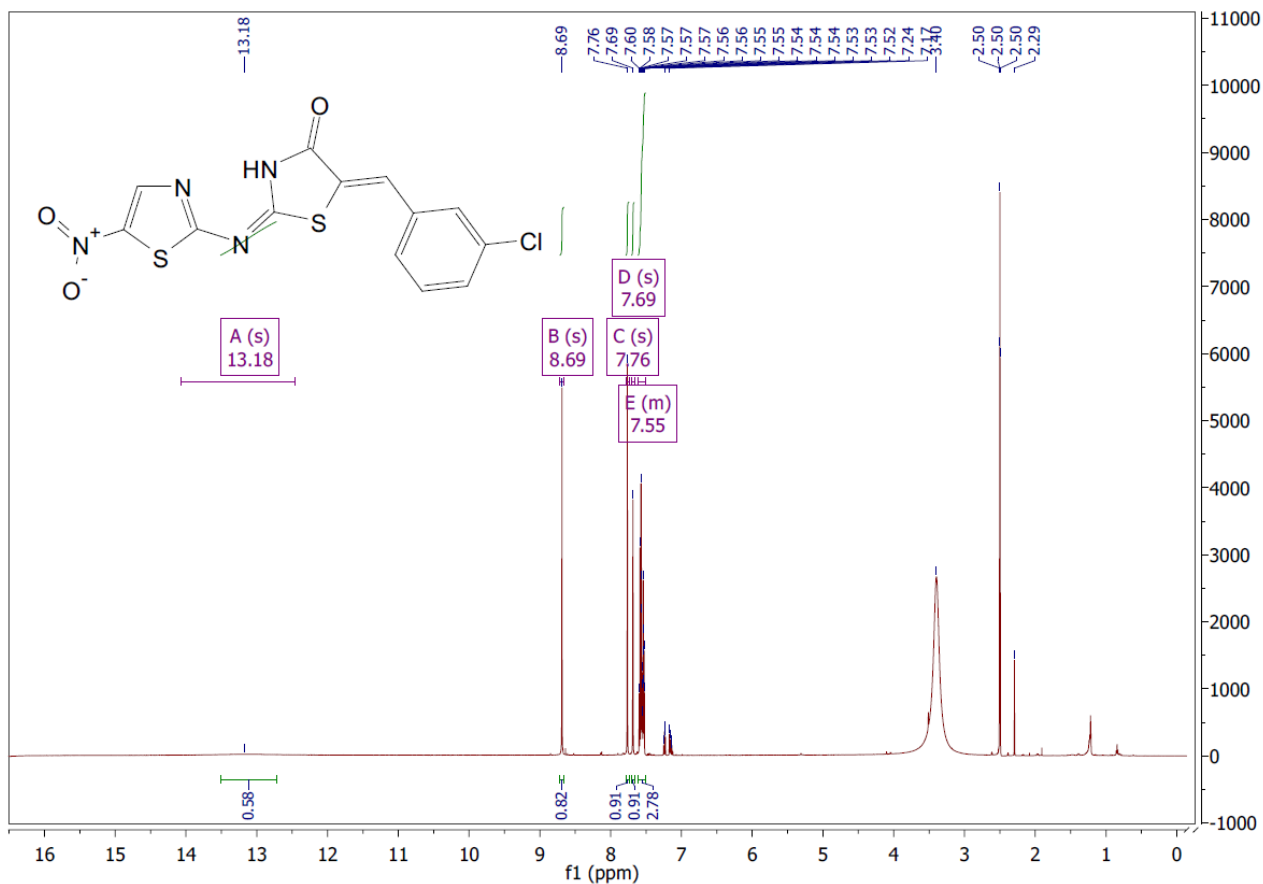
HPLC

mAU

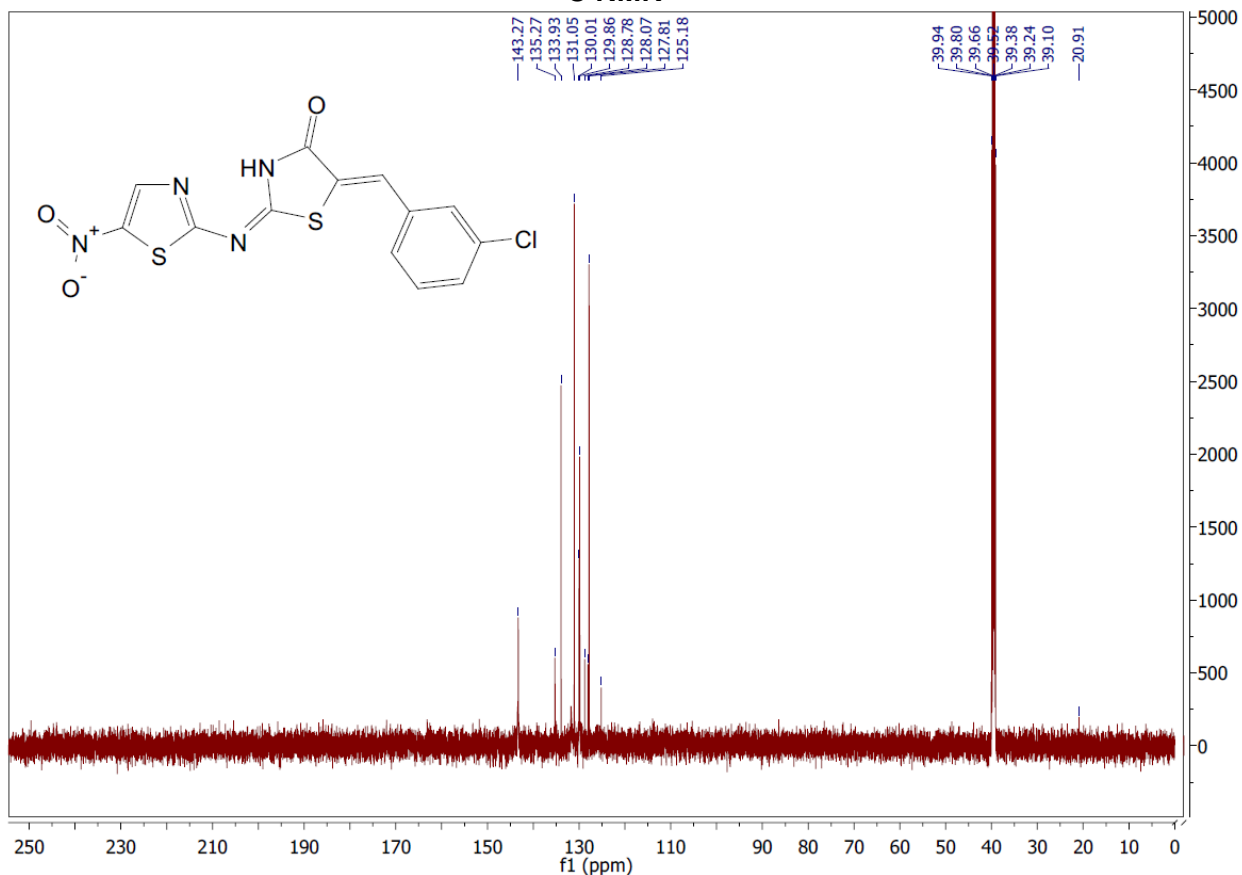


(2E,5Z)-5-(3-chlorobenzylidene)-2-((5-nitrothiazol-2-yl)imino)thiazolidin-4-one (**3f**)

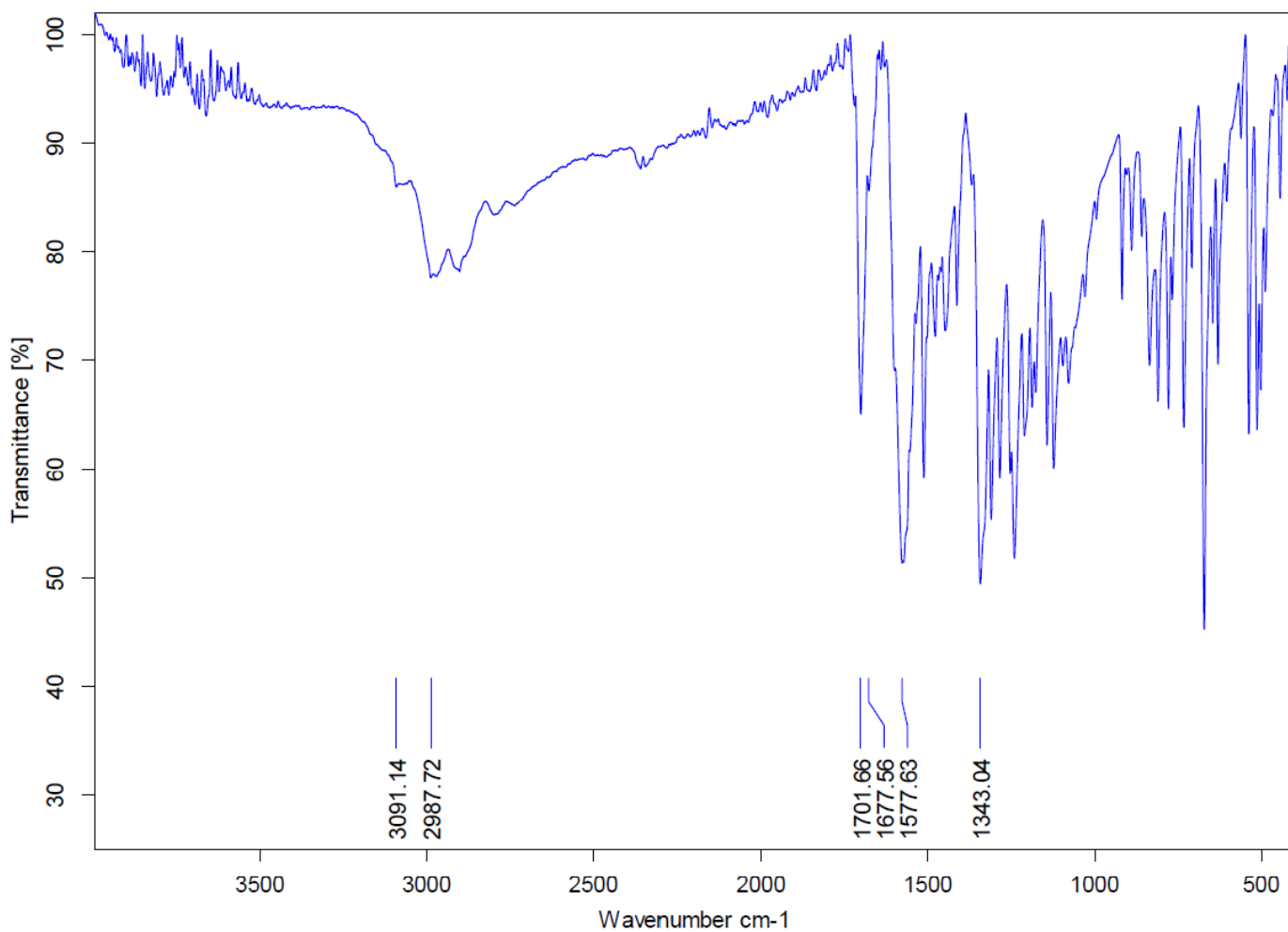
¹H NMR



¹³C NMR



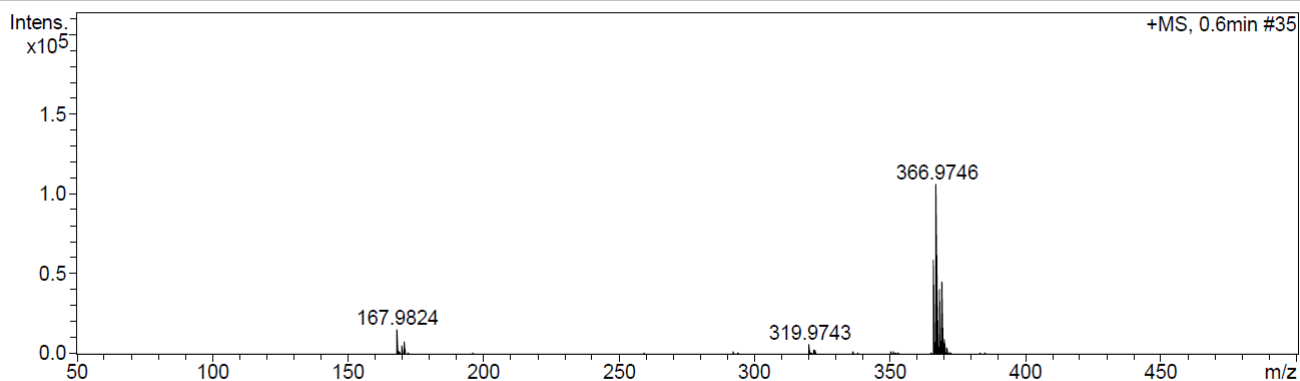
FTIR



HRMS

Acquisition Parameter

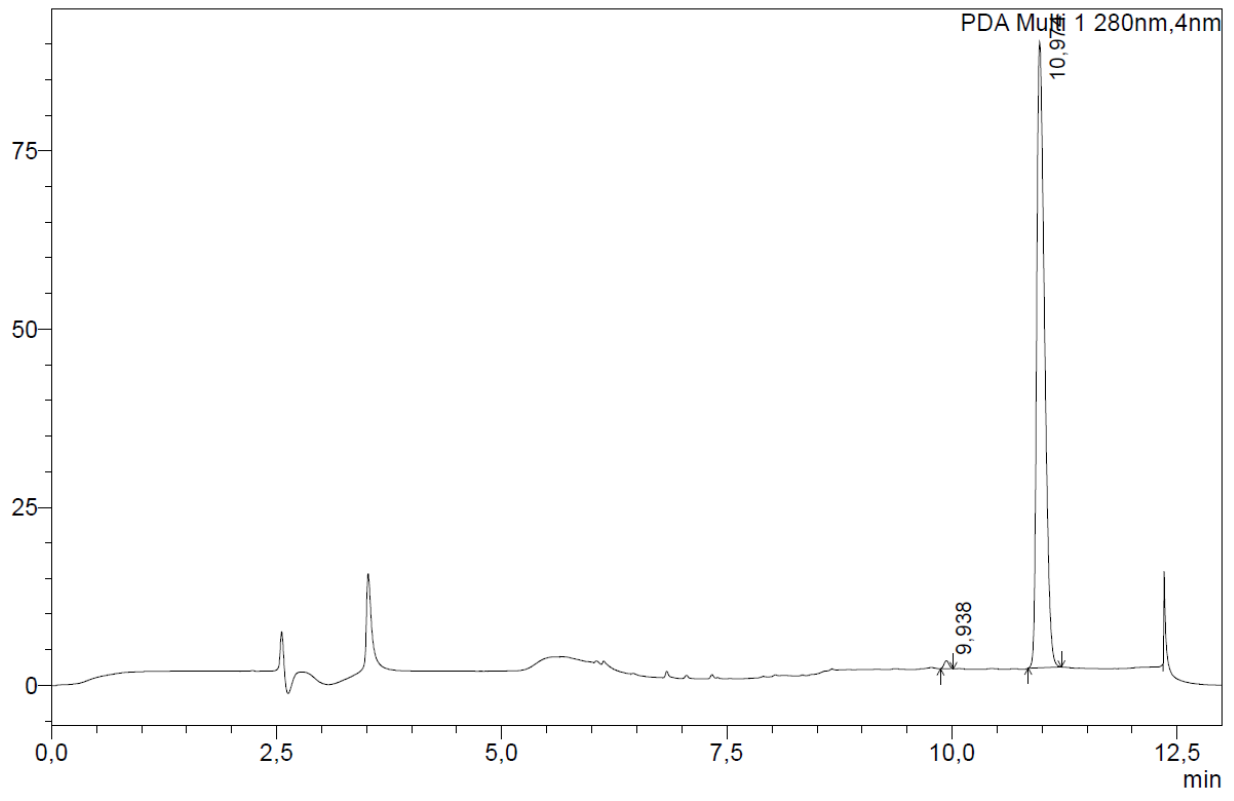
Source Type	APCI	Ion Polarity	Positive	Set Nebulizer	1.8 Bar
Focus	Not active	Set Capillary	4500 V	Set Dry Heater	200 °C
Scan Begin	50 m/z	Set End Plate Offset	-500 V	Set Dry Gas	8.0 l/min
Scan End	1600 m/z	Set Collision Cell RF	150.0 Vpp	Set Divert Valve	Waste



Meas. m/z	#	Formula	Score	m/z	err [mDa]	err [ppm]	mSigma	rdb	e ⁻ Conf	N-Rule
366.9746	1	C ₁₃ H ₈ CIN ₄ O ₃ S ₂	100.00	366.9721	-2.5	-6.7	85.2	11.5	even	ok

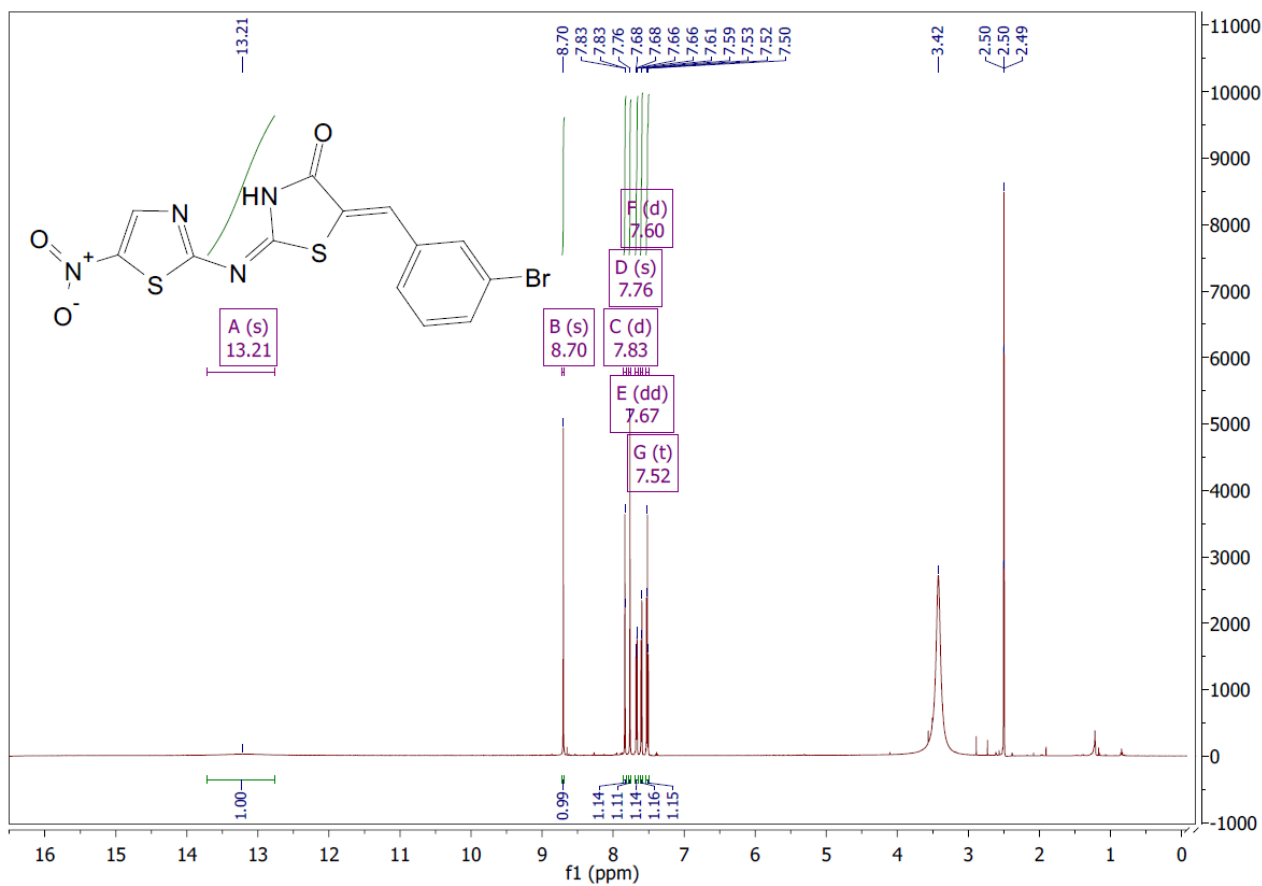
HPLC

mAU

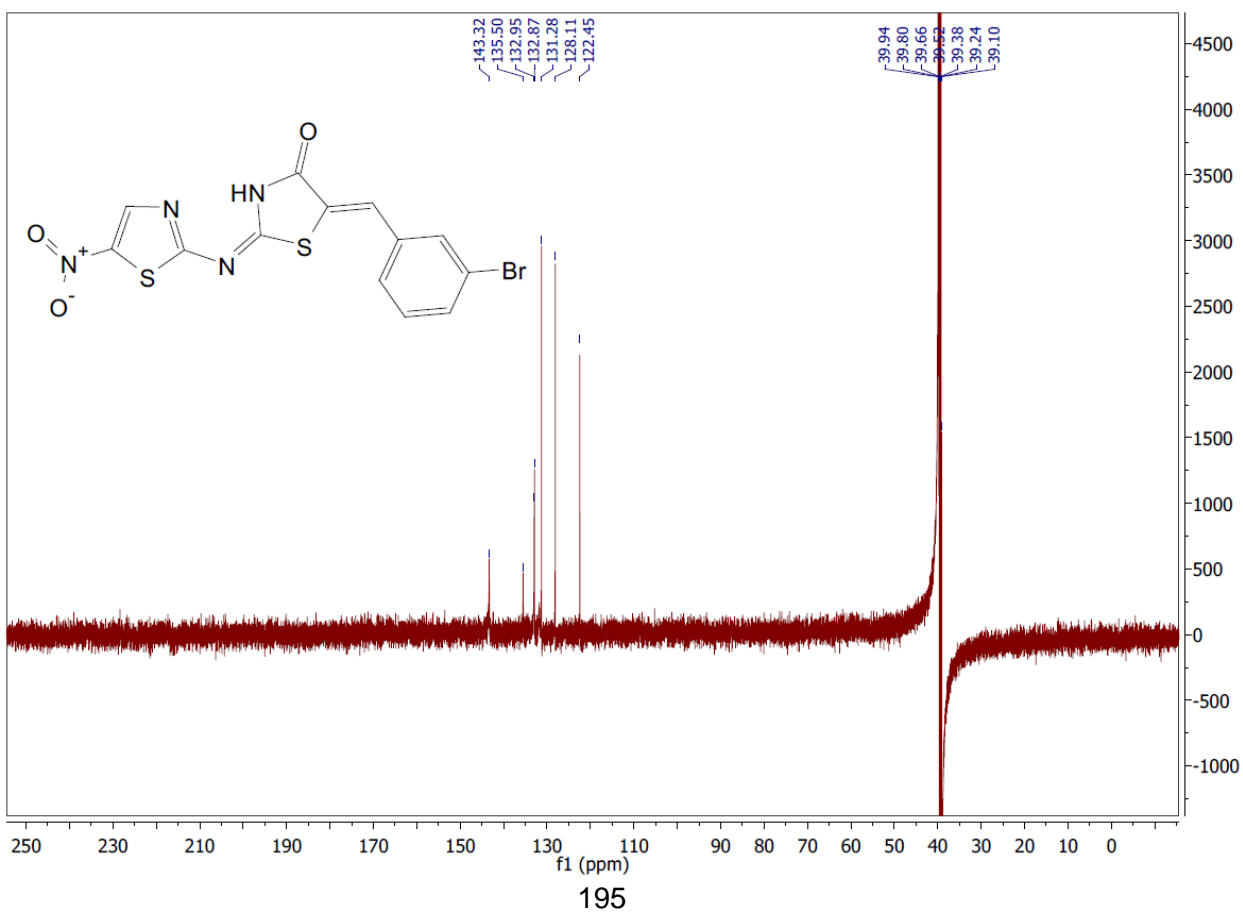


(2E,5Z)-5-(3-bromobenzylidene)-2-((5-nitrothiazol-2-yl)imino)thiazolidin-4-one (**3g**)

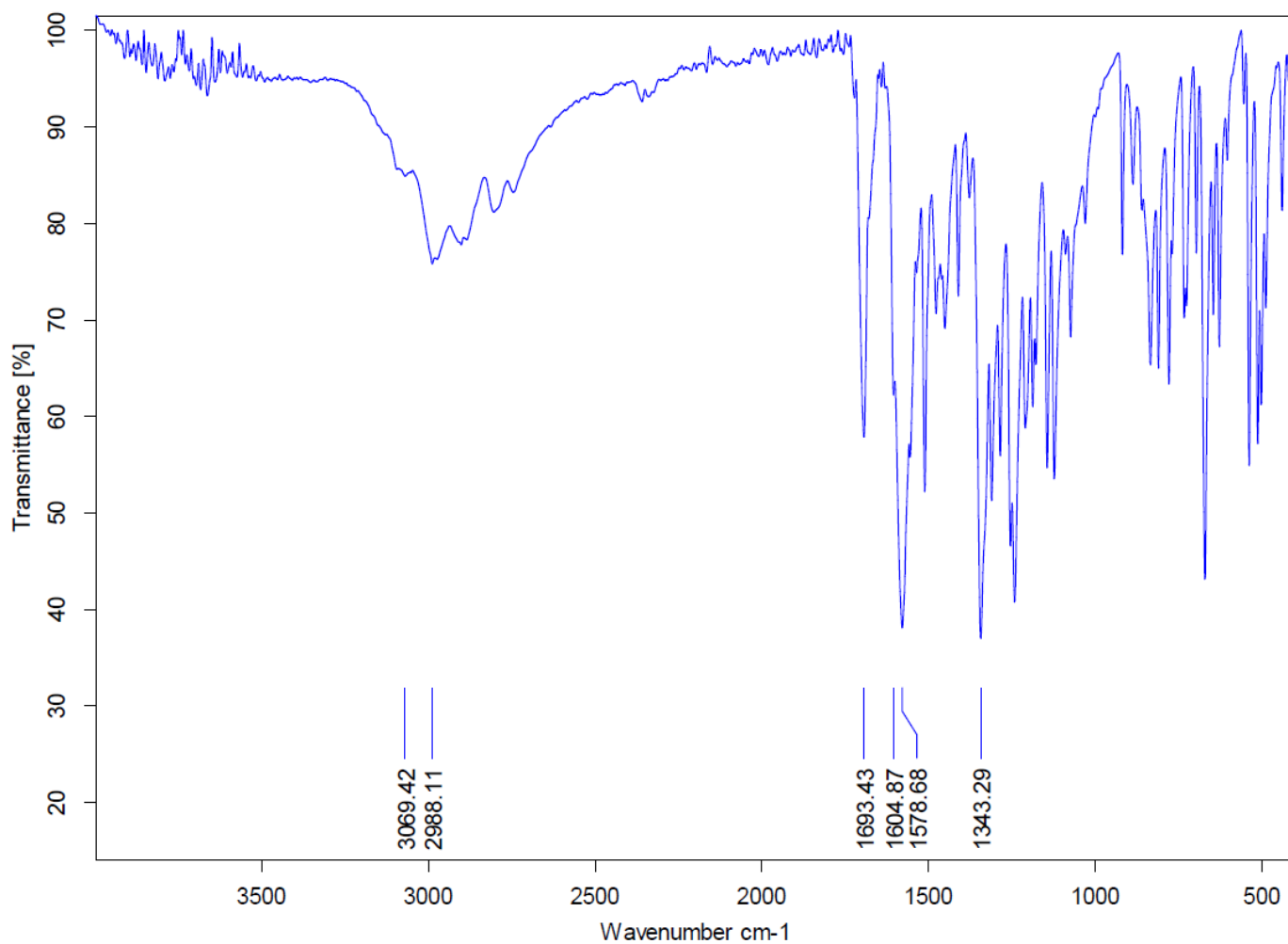
¹H NMR



¹³C NMR



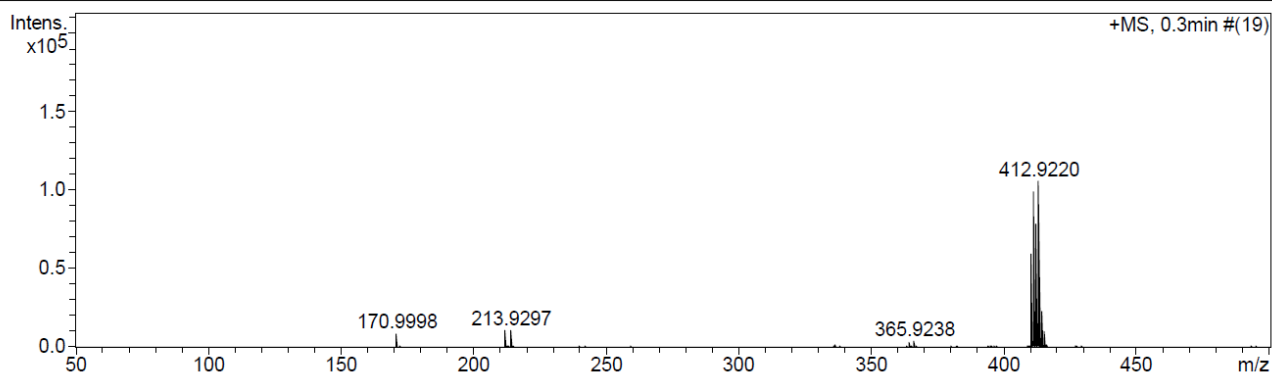
FTIR



HRMS

Acquisition Parameter

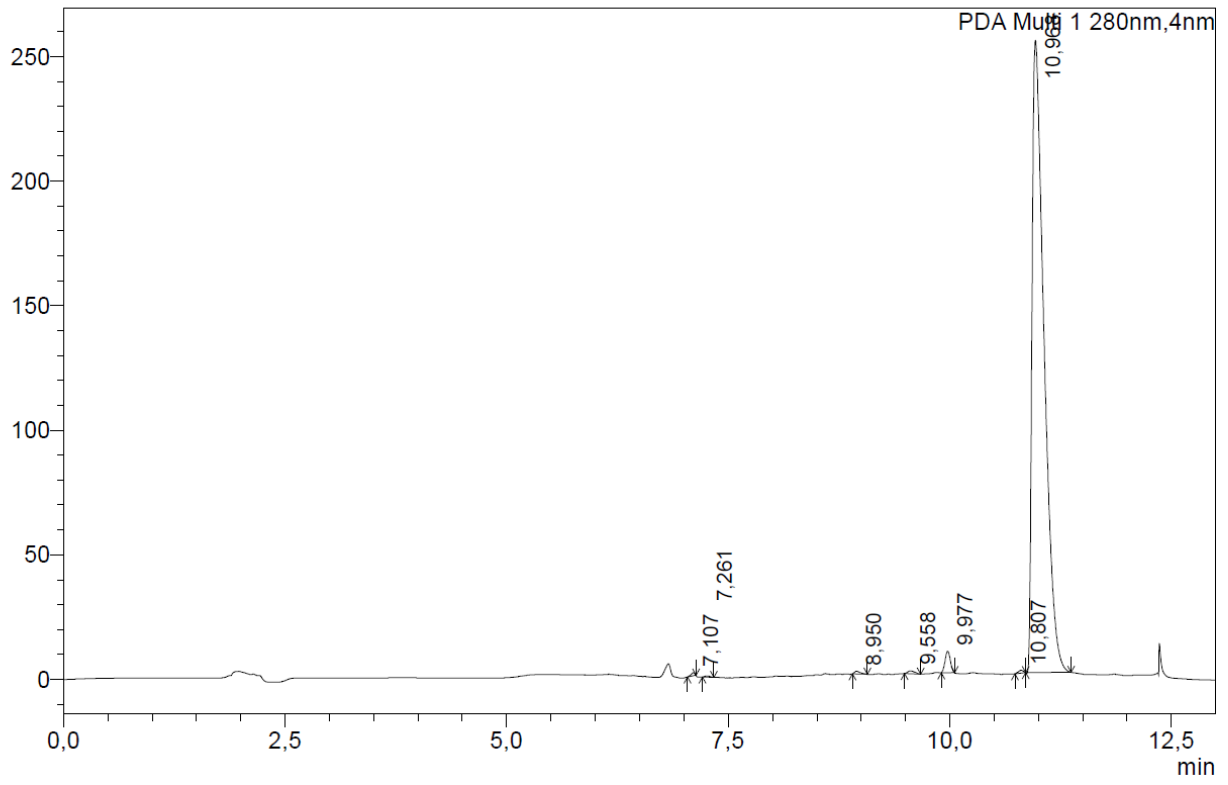
Source Type	APCI	Ion Polarity	Positive	Set Nebulizer	1.8 Bar
Focus	Not active	Set Capillary	4500 V	Set Dry Heater	200 °C
Scan Begin	50 m/z	Set End Plate Offset	-500 V	Set Dry Gas	8.0 l/min
Scan End	1600 m/z	Set Collision Cell RF	150.0 Vpp	Set Divert Valve	Waste



Meas. m/z	#	Formula	Score	m/z	err [mDa]	err [ppm]	mSigma	rdb	e ⁻ Conf	N-Rule
409.9169	1	C 13 H 7 Br N 4 O 3 S 2	100.00	409.9137	-3.1	-7.6	502.1	12.0	odd	ok
410.9241	1	C 13 H 8 Br N 4 O 3 S 2	100.00	410.9216	-2.6	-6.3	238.9	11.5	even	ok

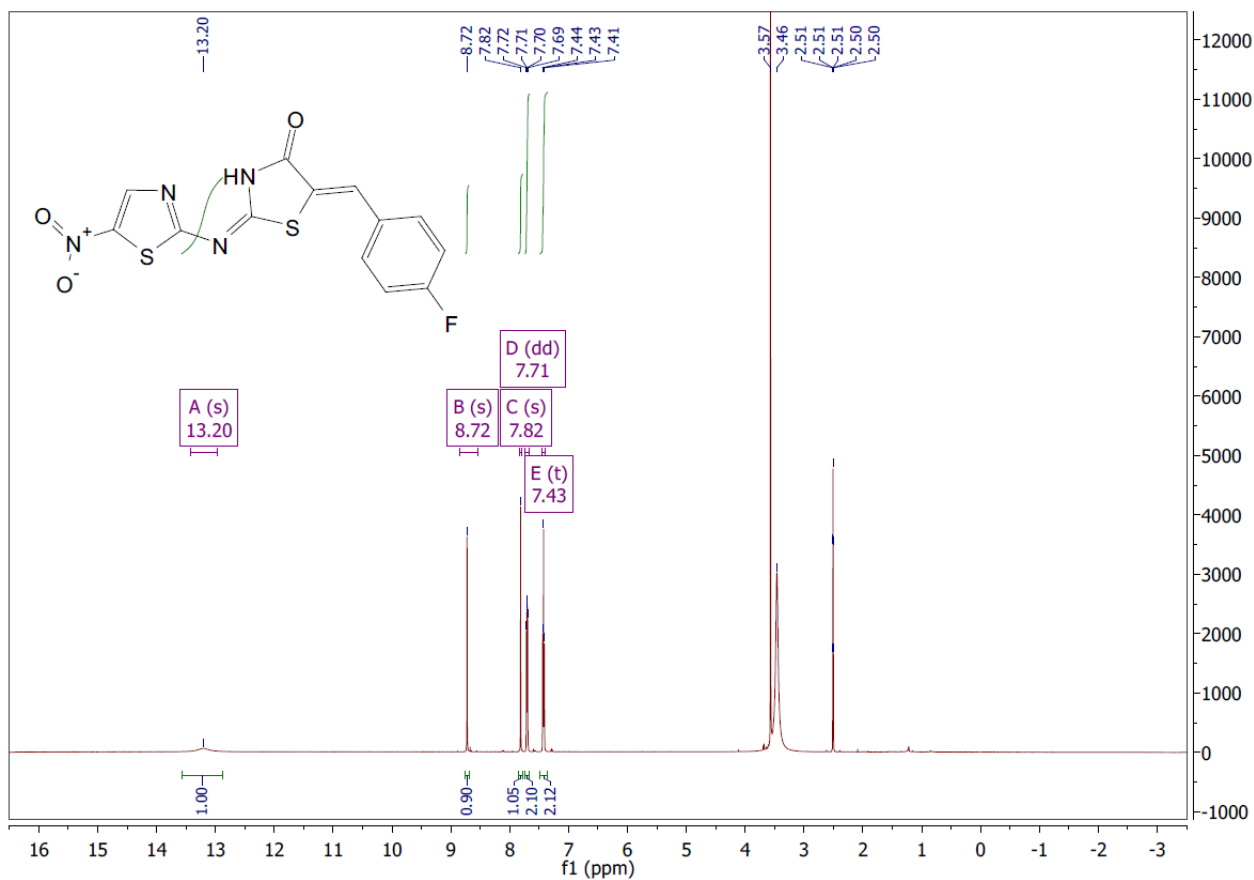
HPLC

mAU

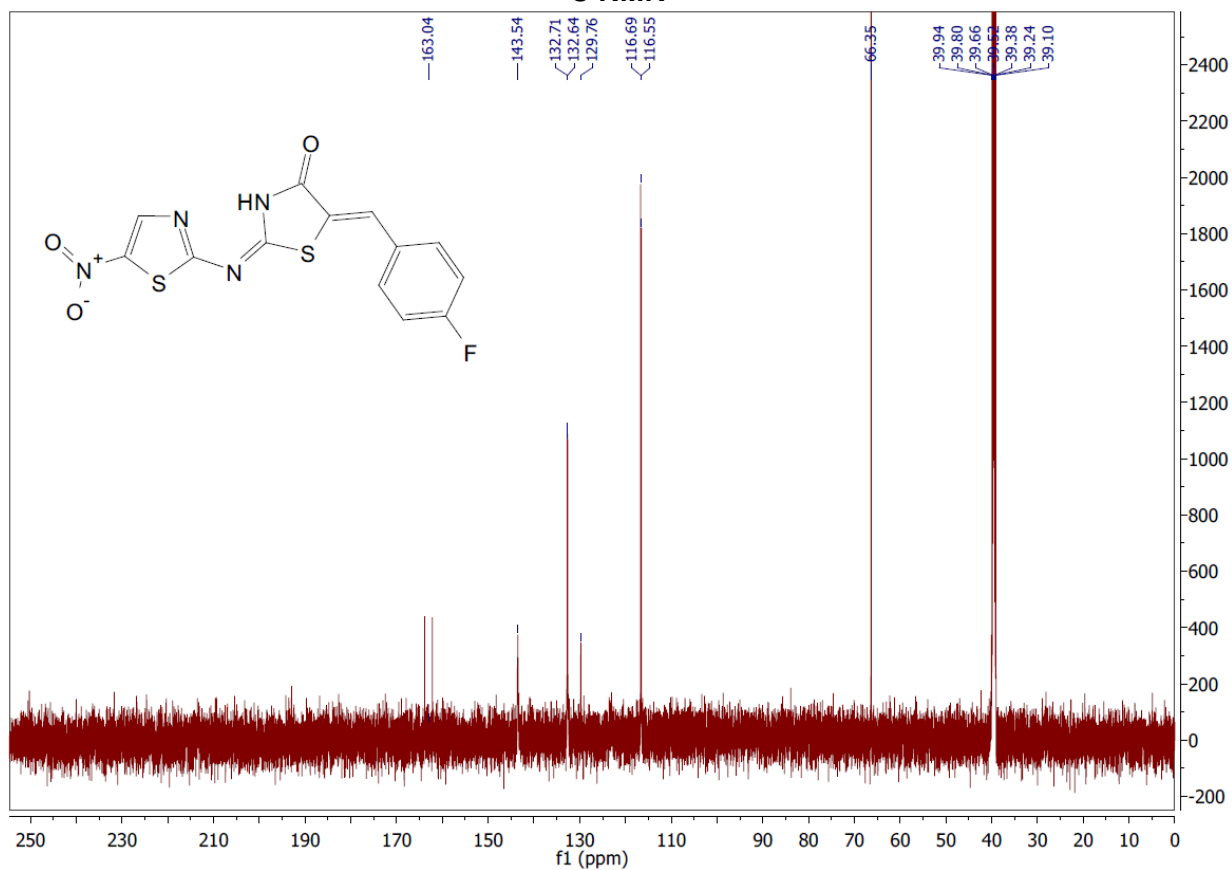


(2E,5Z)-5-(4-fluorobenzylidene)-2-((5-nitrothiazol-2-yl)imino)thiazolidin-4-one (**3h**)

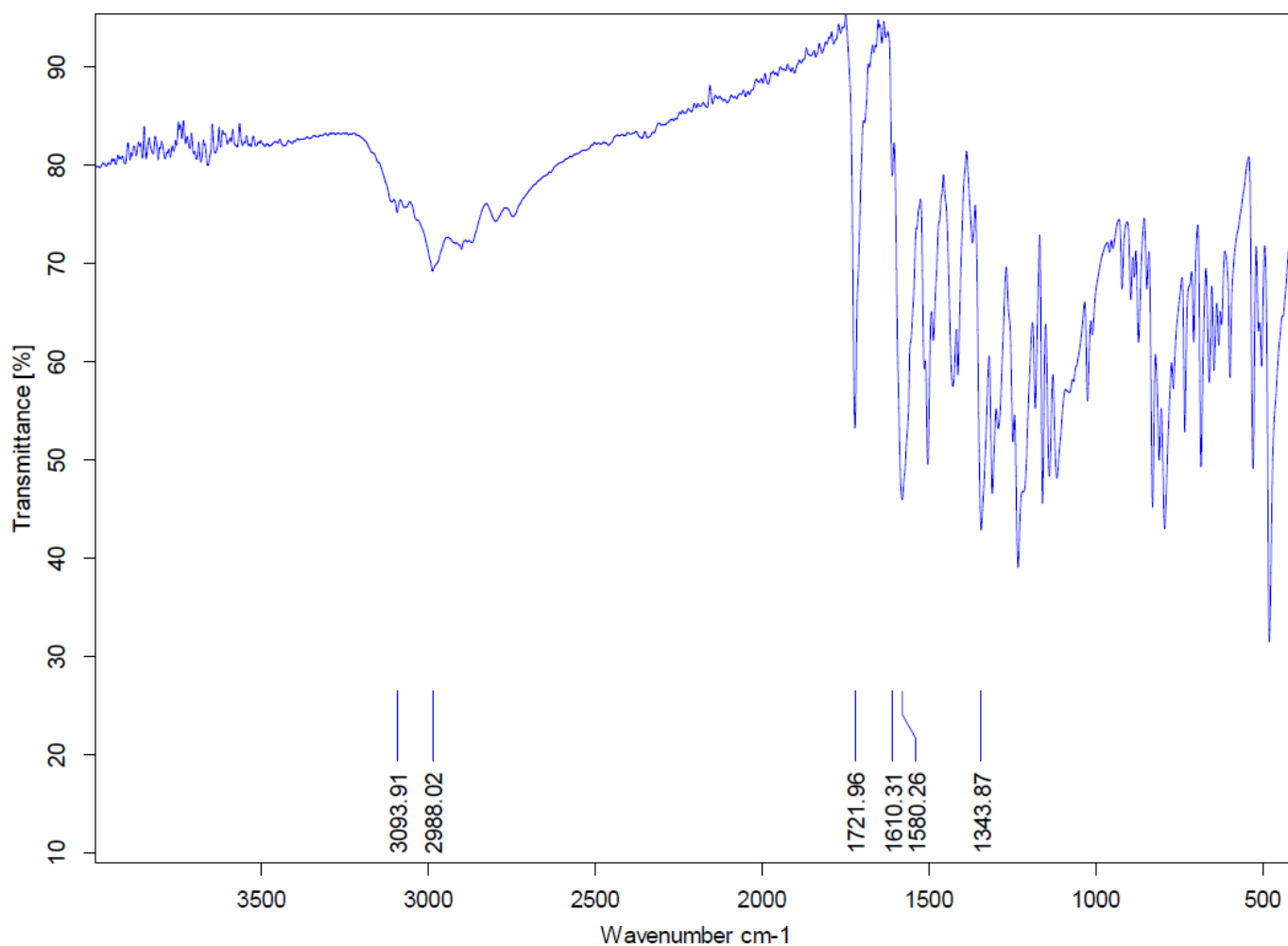
¹H NMR



¹³C NMR



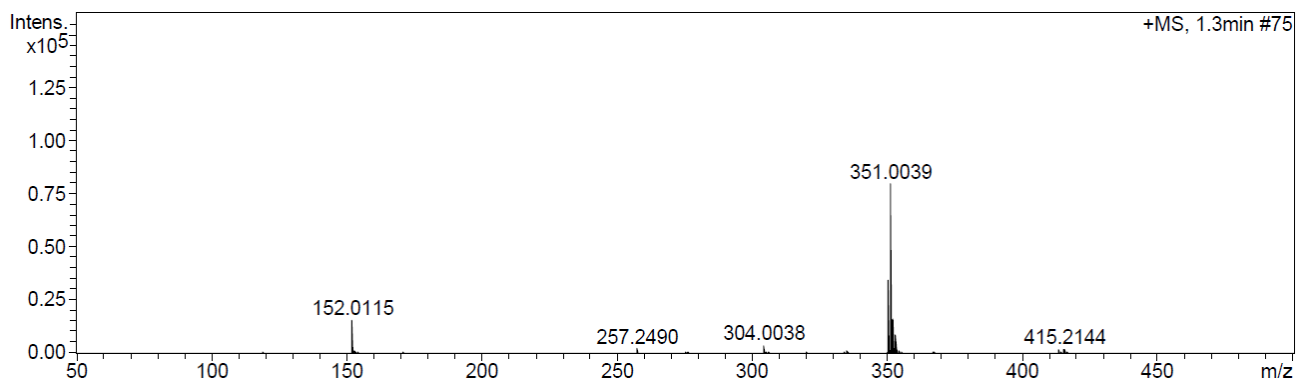
FTIR



HRMS

Acquisition Parameter

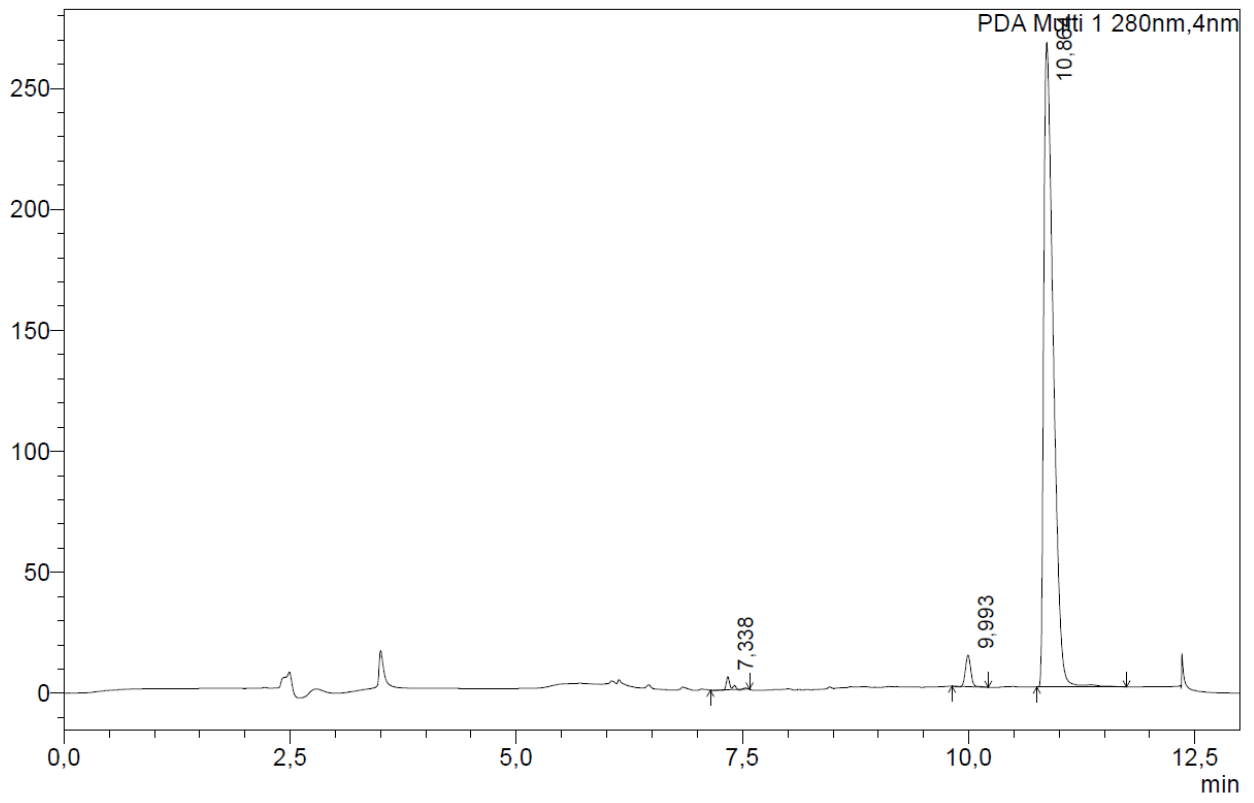
Source Type	APCI	Ion Polarity	Positive	Set Nebulizer	1.8 Bar
Focus	Not active	Set Capillary	4500 V	Set Dry Heater	200 °C
Scan Begin	50 m/z	Set End Plate Offset	-500 V	Set Dry Gas	8.0 l/min
Scan End	1600 m/z	Set Collision Cell RF	150.0 Vpp	Set Divert Valve	Waste



Meas. m/z	#	Formula	Score	m/z	err [mDa]	err [ppm]	mSigma	rdb	e ⁻ Conf	N-Rule
351.0039	1	C ₁₃ H ₈ FN ₄ O ₃ S ₂	100.00	351.0016	-2.2	-6.4	16.5	11.5	even	ok

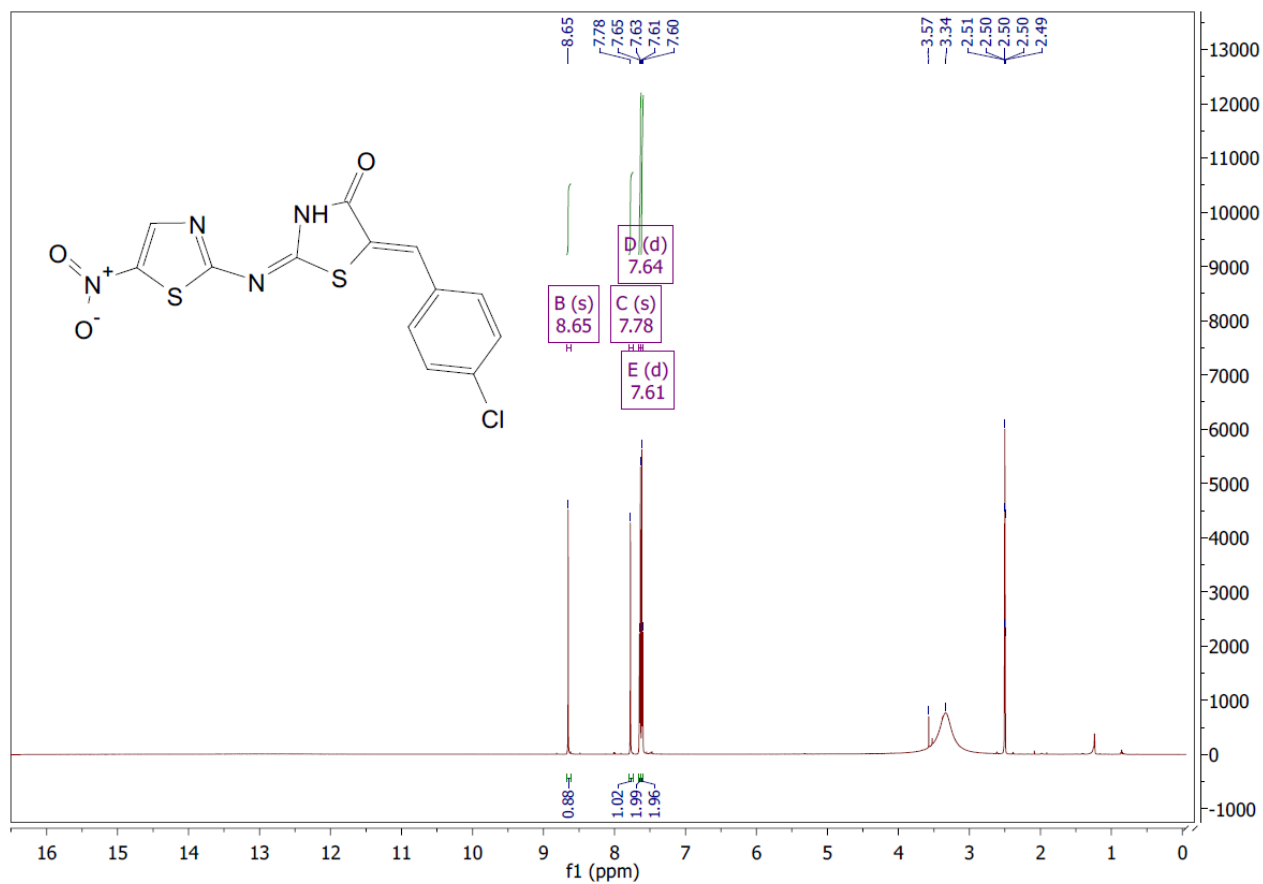
HPLC

mAU

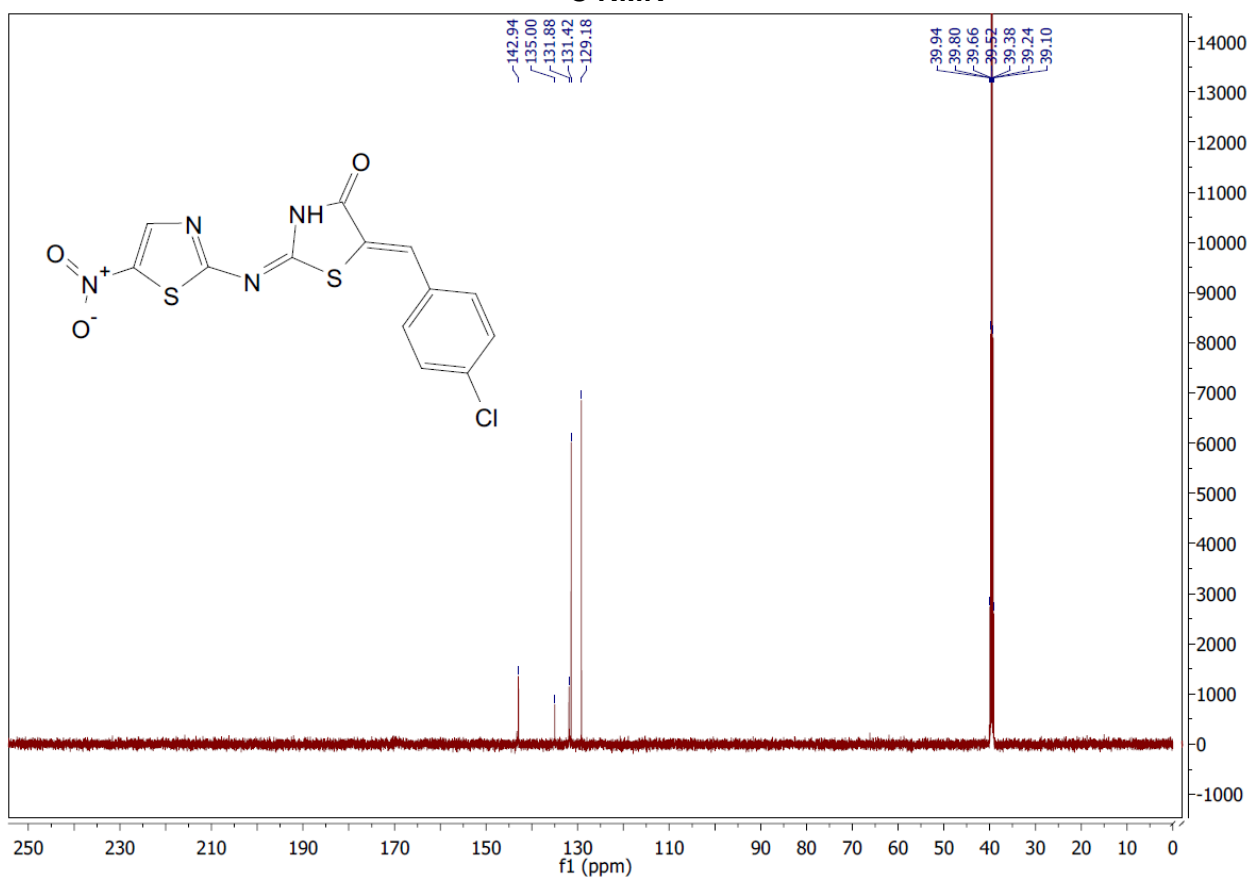


(2E,5Z)-5-(4-chlorobenzylidene)-2-((5-nitrothiazol-2-yl)imino)thiazolidin-4-one (**3i**)

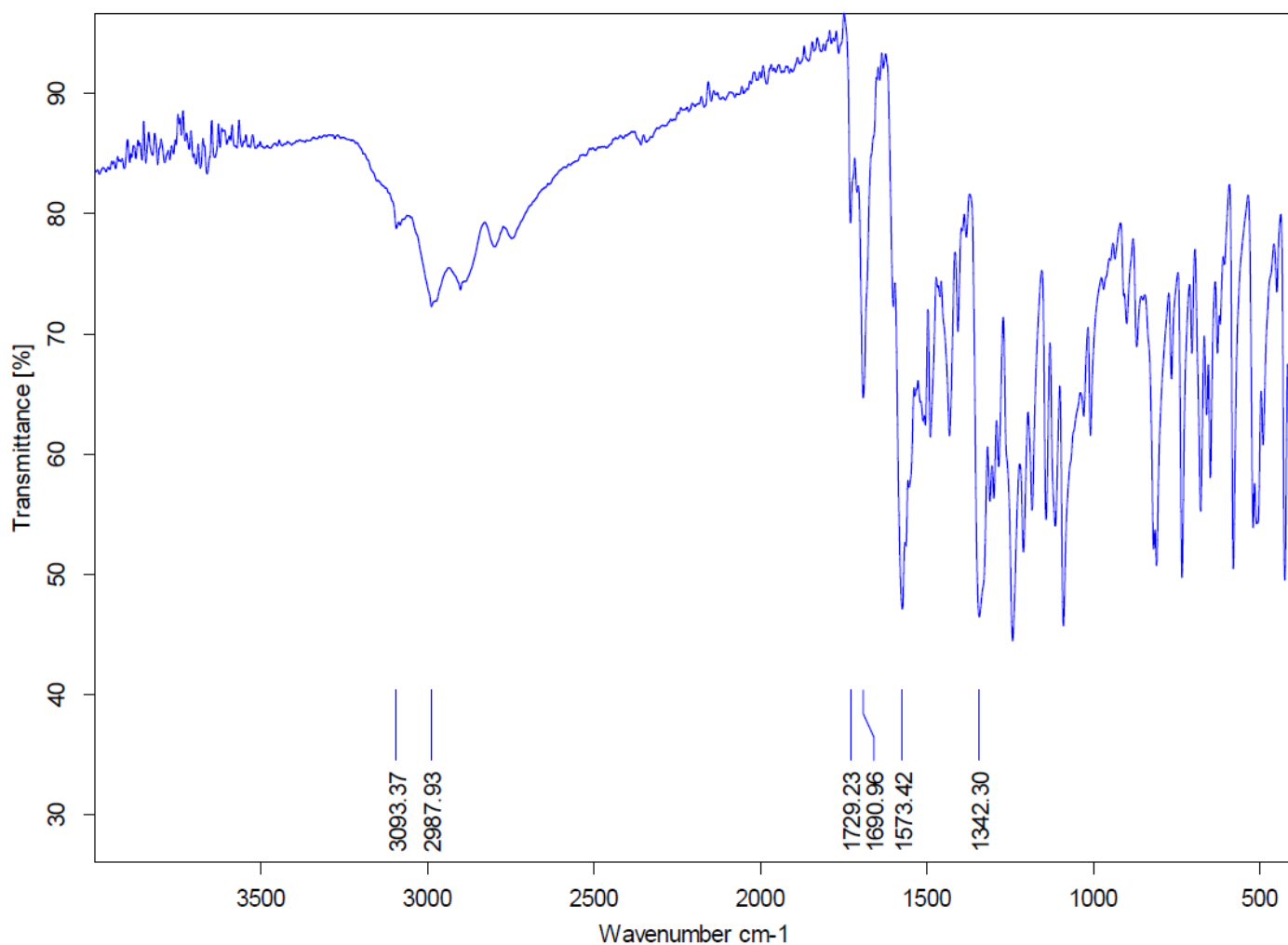
¹H NMR



¹³C NMR



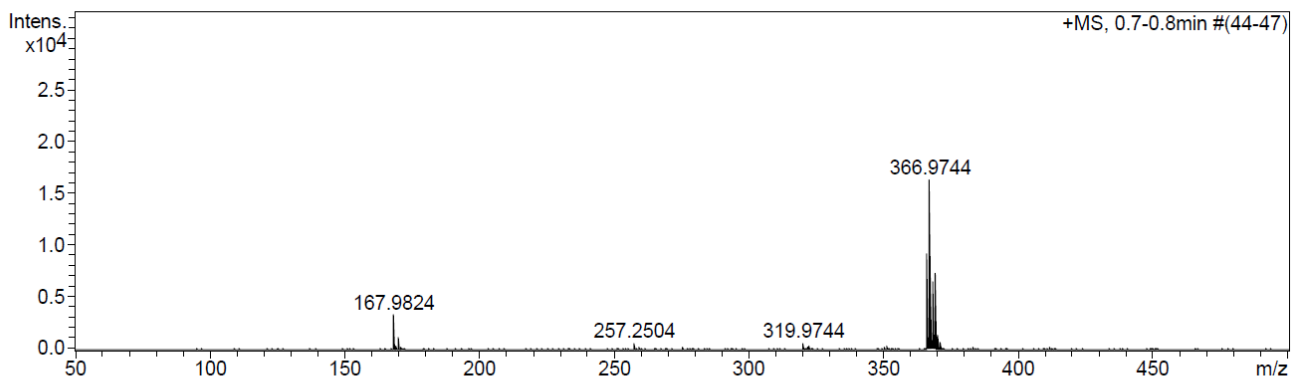
FTIR



HRMS

Acquisition Parameter

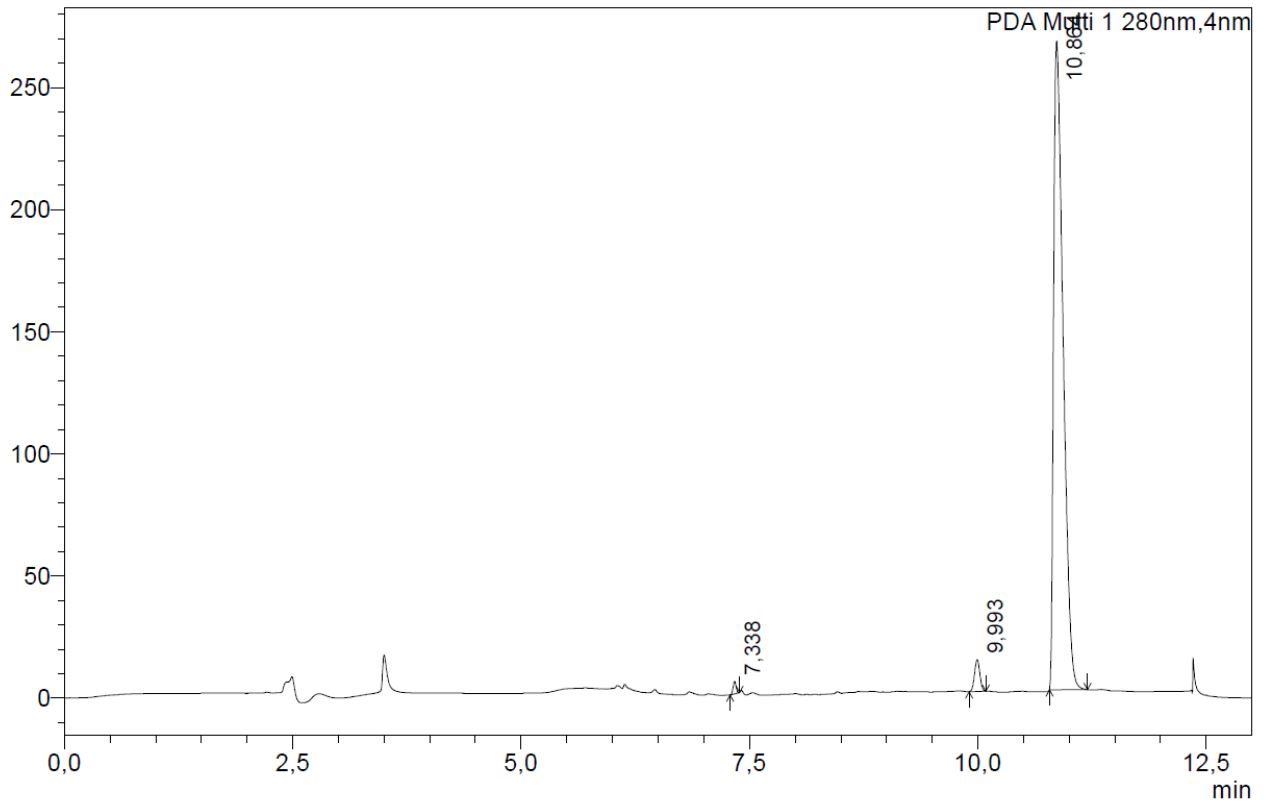
Source Type	APCI	Ion Polarity	Positive	Set Nebulizer	1.8 Bar
Focus	Not active	Set Capillary	4500 V	Set Dry Heater	200 °C
Scan Begin	50 m/z	Set End Plate Offset	-500 V	Set Dry Gas	8.0 l/min
Scan End	1600 m/z	Set Collision Cell RF	150.0 Vpp	Set Divert Valve	Waste



Meas. m/z	#	Formula	Score	m/z	err [mDa]	err [ppm]	mSigma	rdb	e ⁻ Conf	N-Rule
366.9744	1	C ₁₃ H ₈ ClN ₄ O ₃ S ₂	100.00	366.9721	-2.3	-6.2	93.4	11.5	even	ok

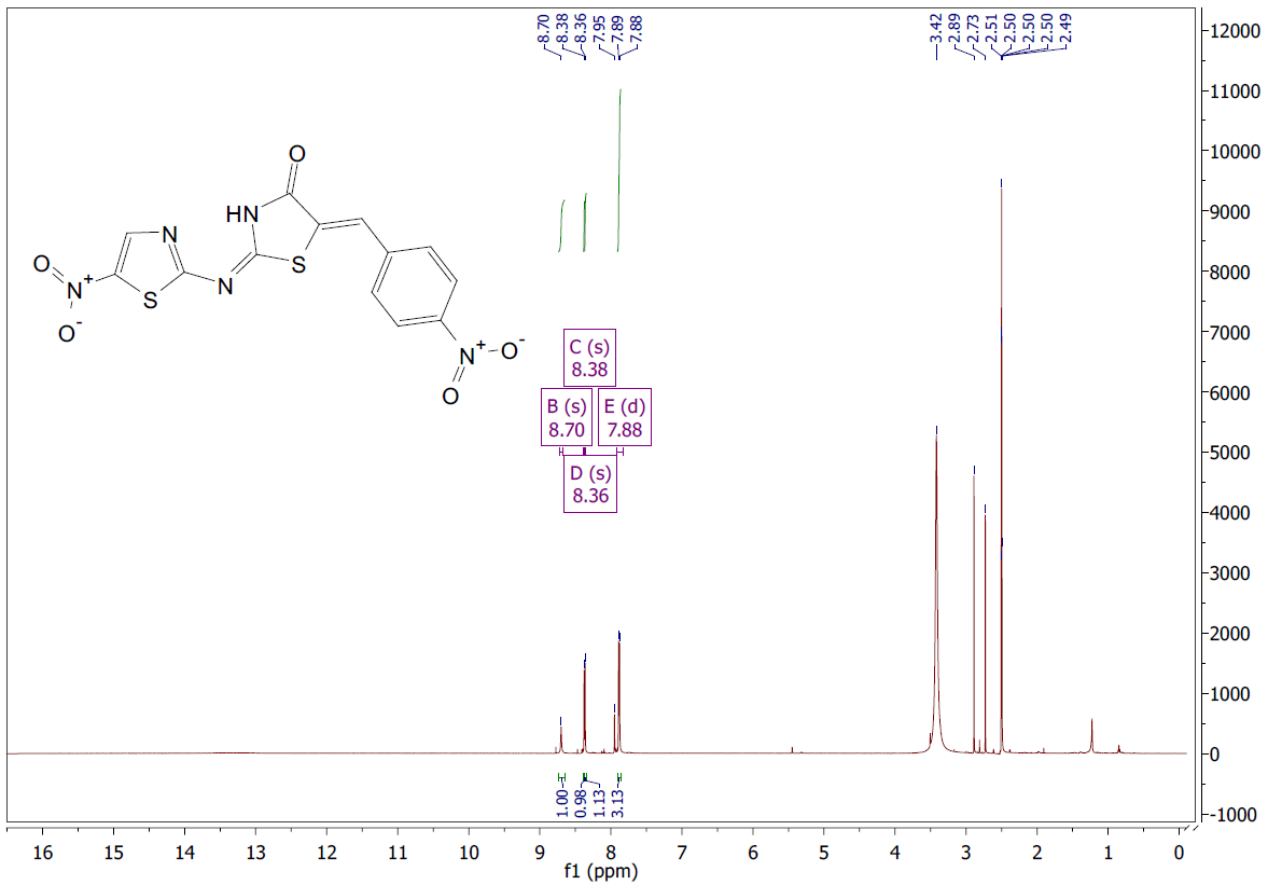
HPLC

mAU

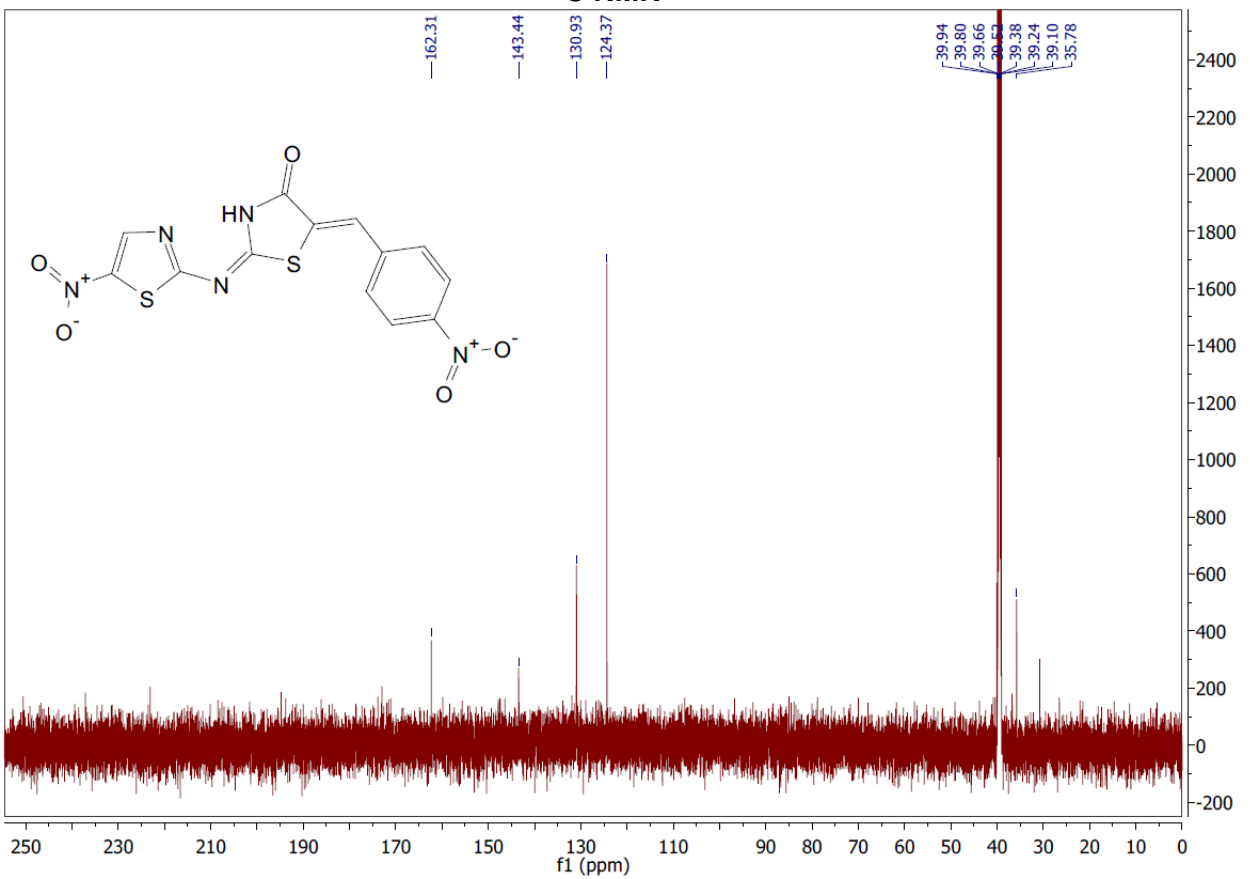


(2E,5Z)-5-(4-nitrobenzylidene)-2-((5-nitrothiazol-2-yl)imino)thiazolidin-4-one (**3j**)

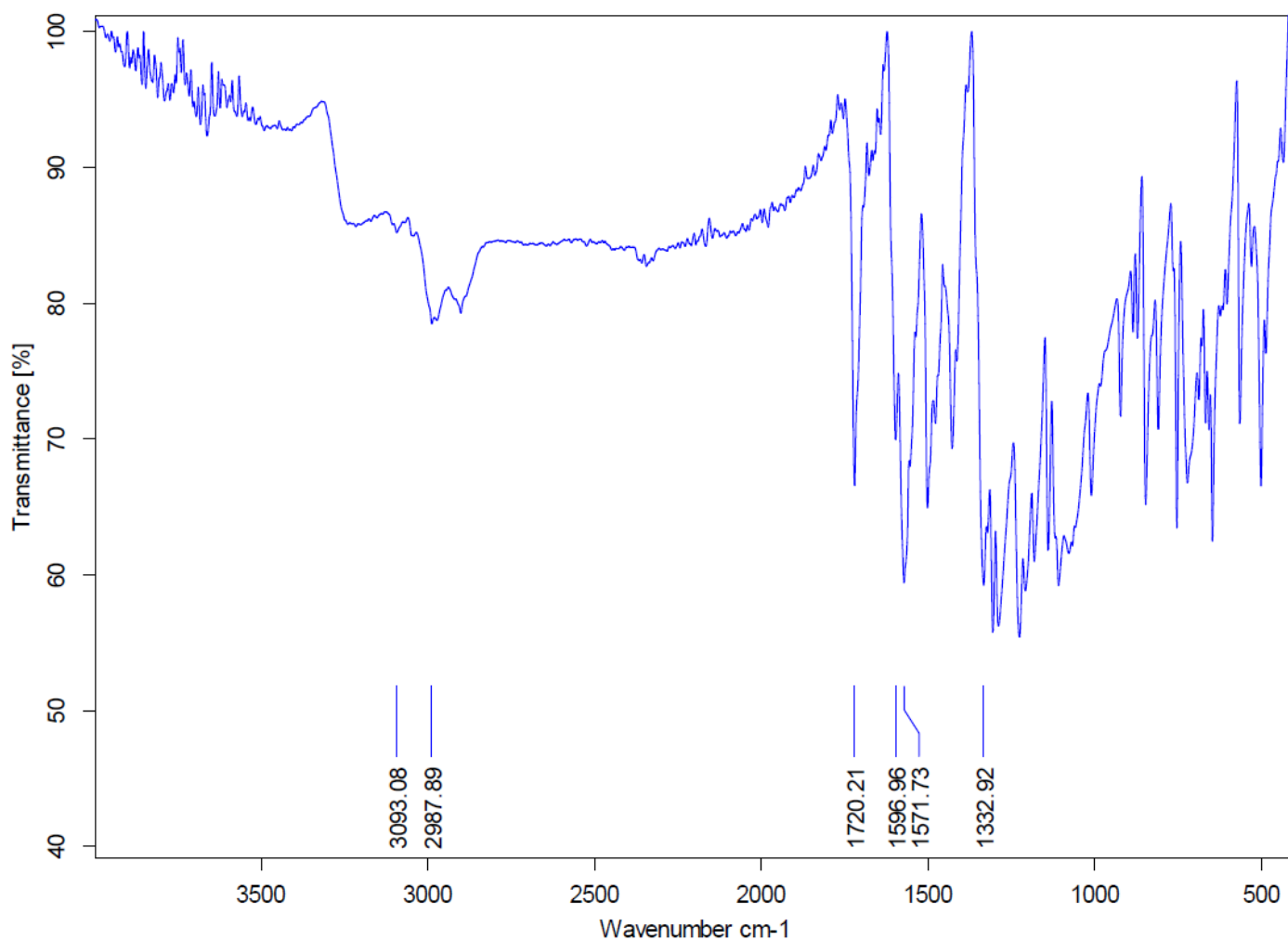
¹H NMR



¹³C NMR



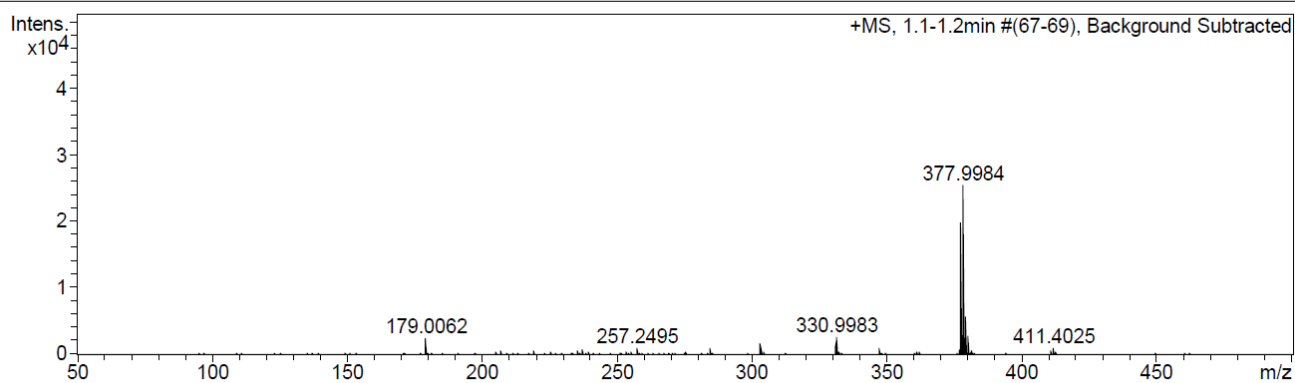
FTIR



HRMS

Acquisition Parameter

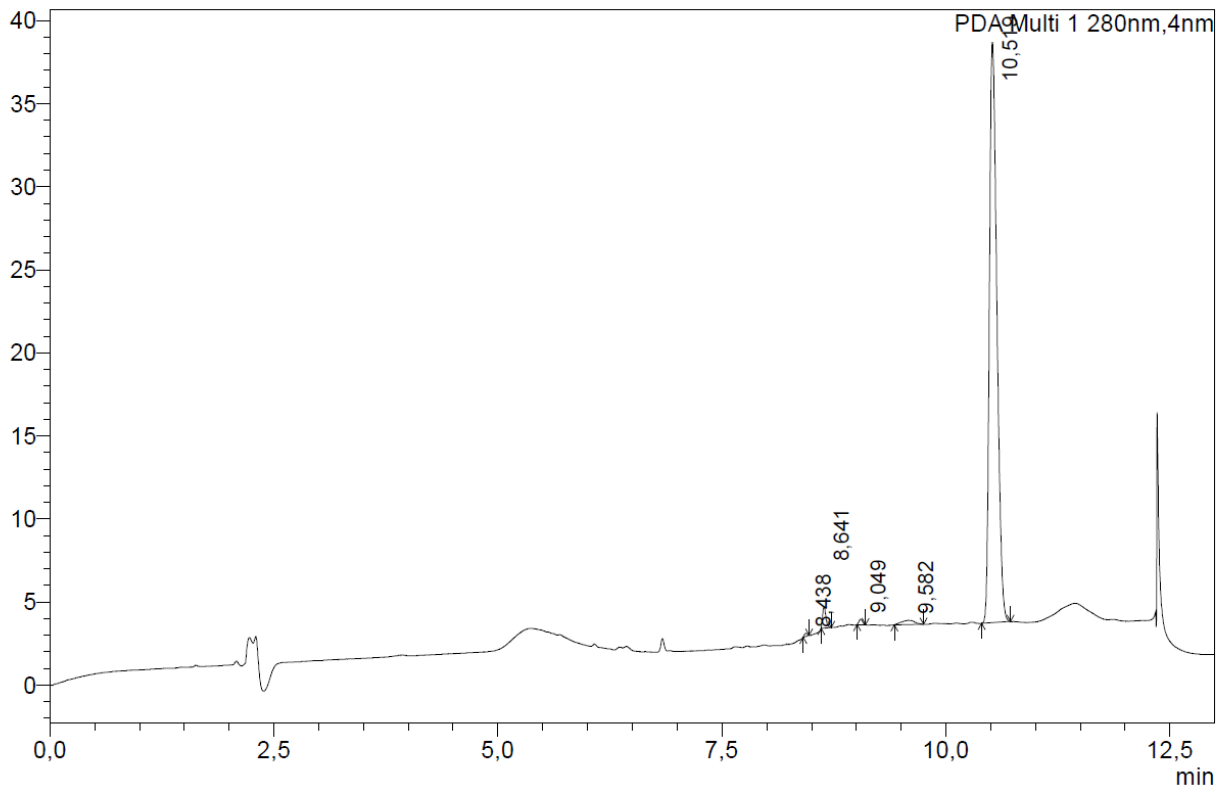
Source Type	APCI	Ion Polarity	Positive	Set Nebulizer	1.8 Bar
Focus	Not active	Set Capillary	4500 V	Set Dry Heater	200 °C
Scan Begin	50 m/z	Set End Plate Offset	-500 V	Set Dry Gas	8.0 l/min
Scan End	1600 m/z	Set Collision Cell RF	150.0 Vpp	Set Divert Valve	Waste



Meas. m/z	#	Formula	Score	m/z	err [mDa]	err [ppm]	mSigma	rdb	e ⁻ Conf	N-Rule
377.9984	1	C ₁₃ H ₈ N ₅ O ₅ S ₂	100.00	377.9961	-2.2	-5.9	25.6	12.5	even	ok

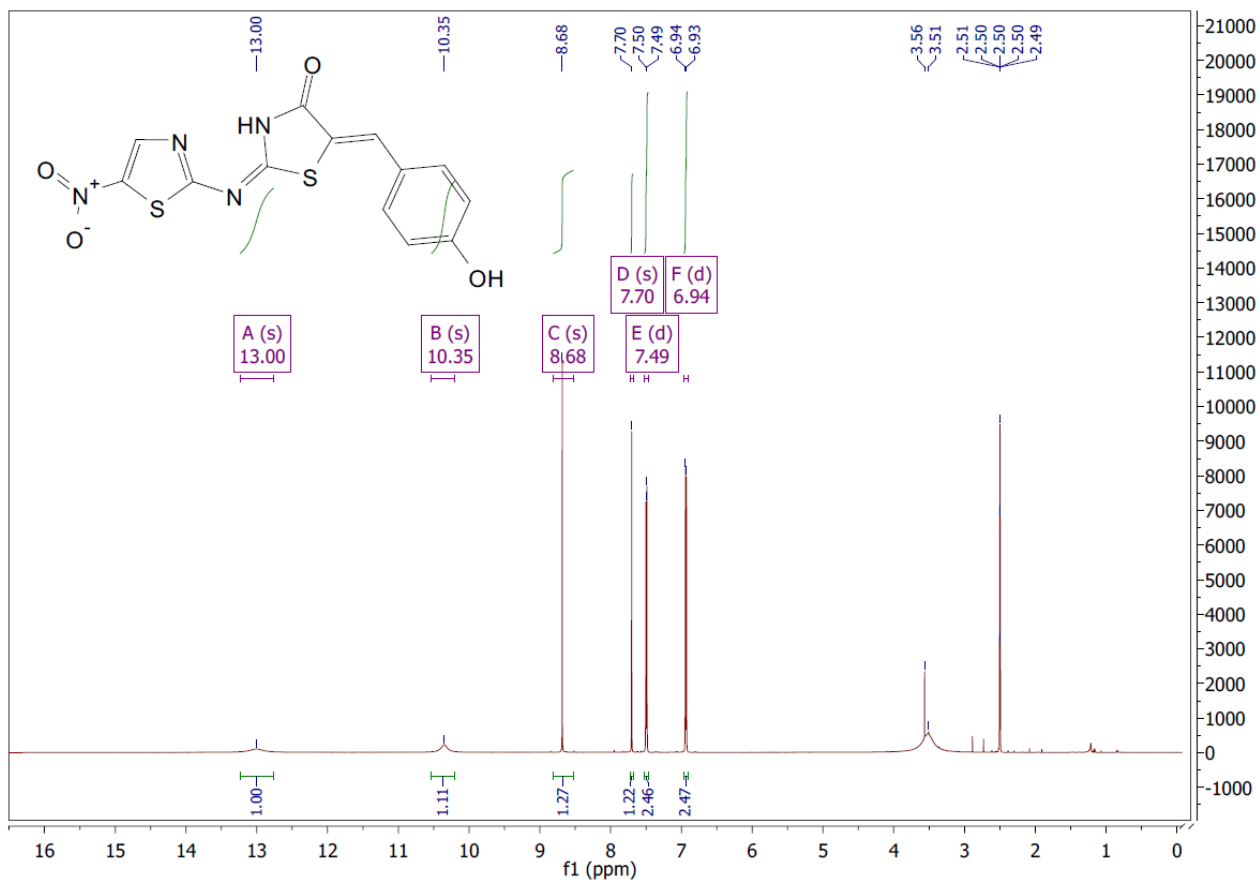
HPLC

mAU

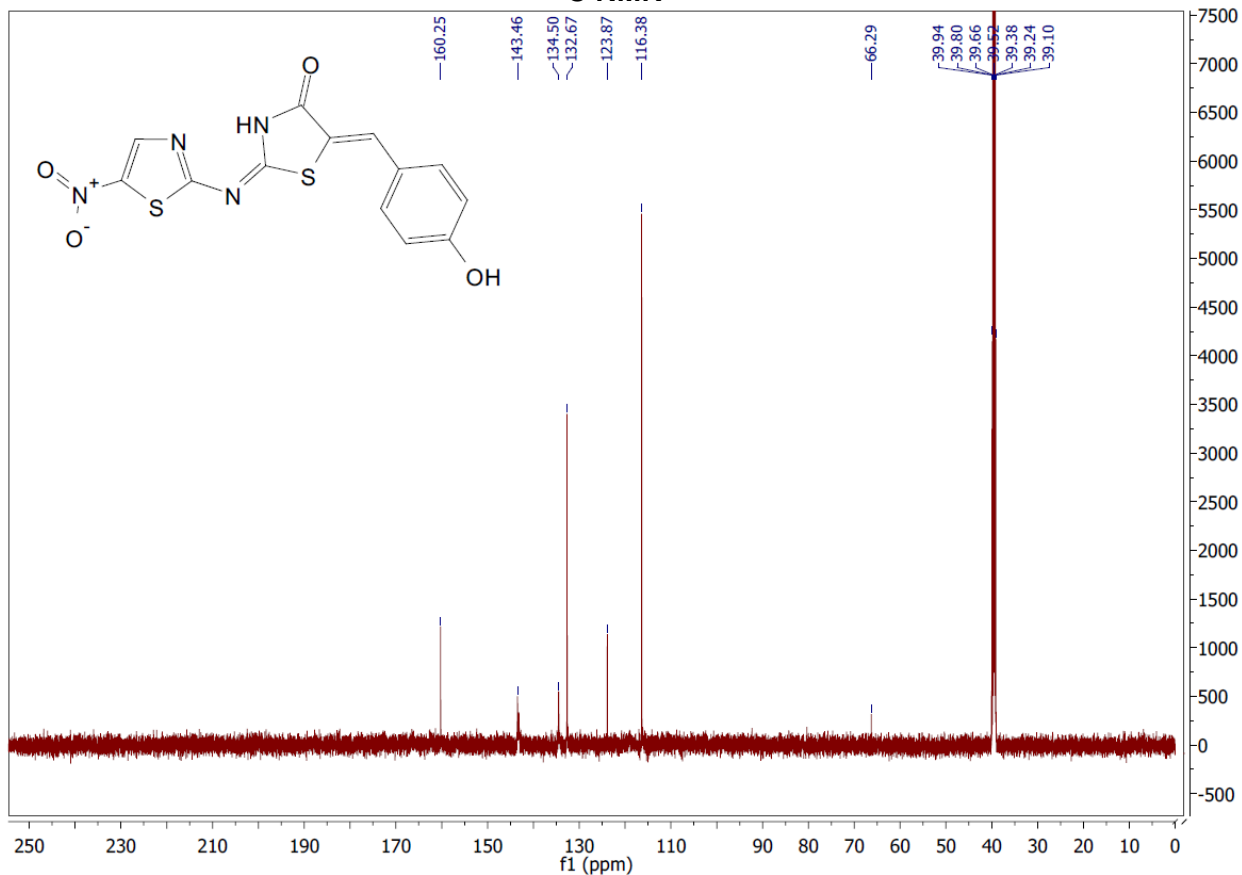


(2E,5Z)-5-(4-hydroxybenzylidene)-2-((5-nitrothiazol-2-yl)imino)thiazolidin-4-one (**3k**)

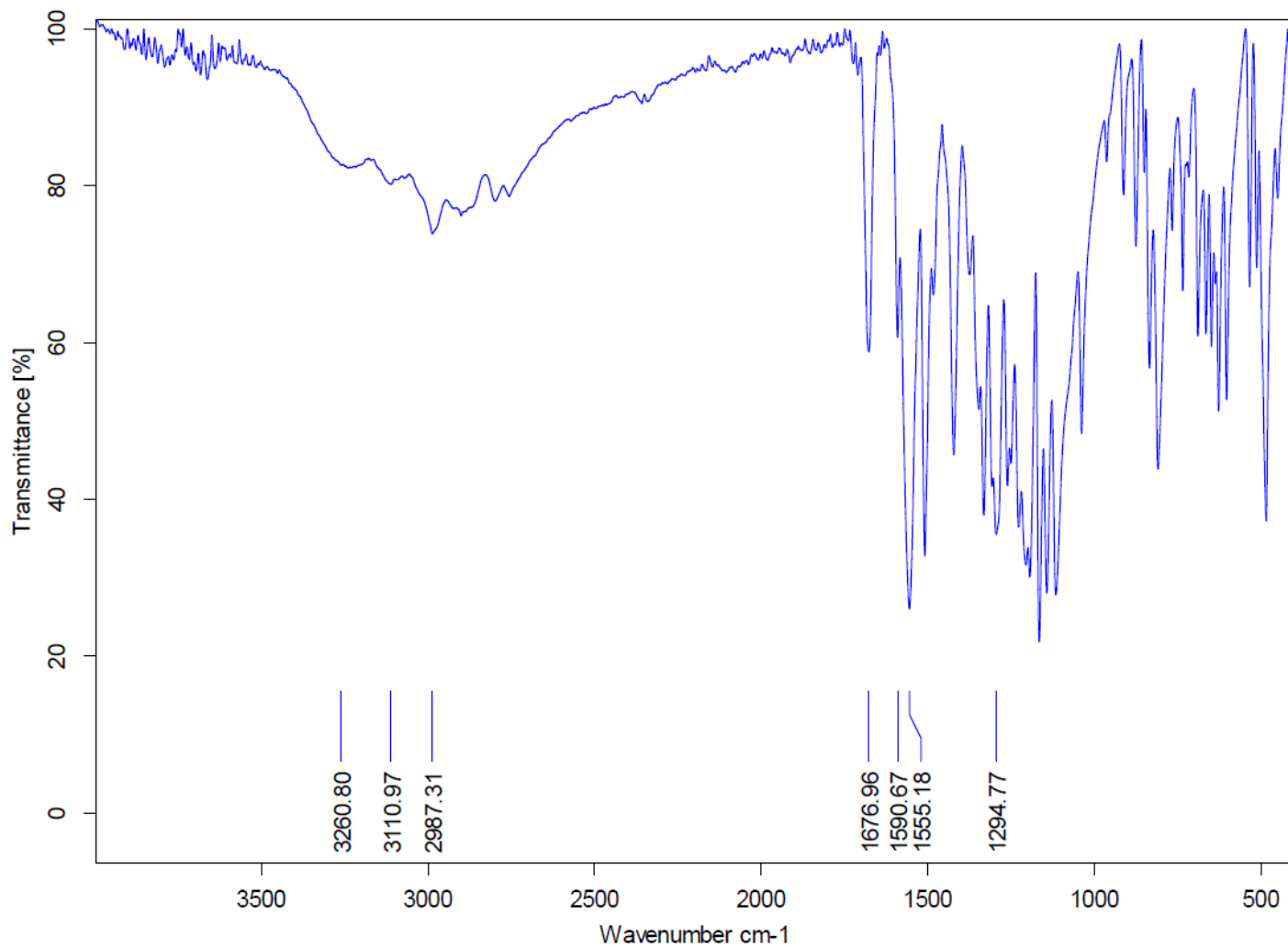
¹H NMR



¹³C NMR



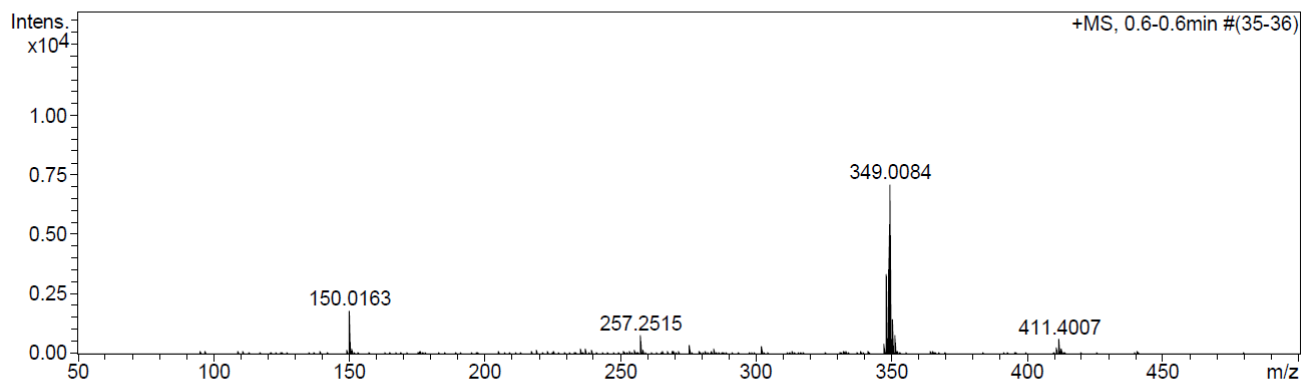
FTIR



HRMS

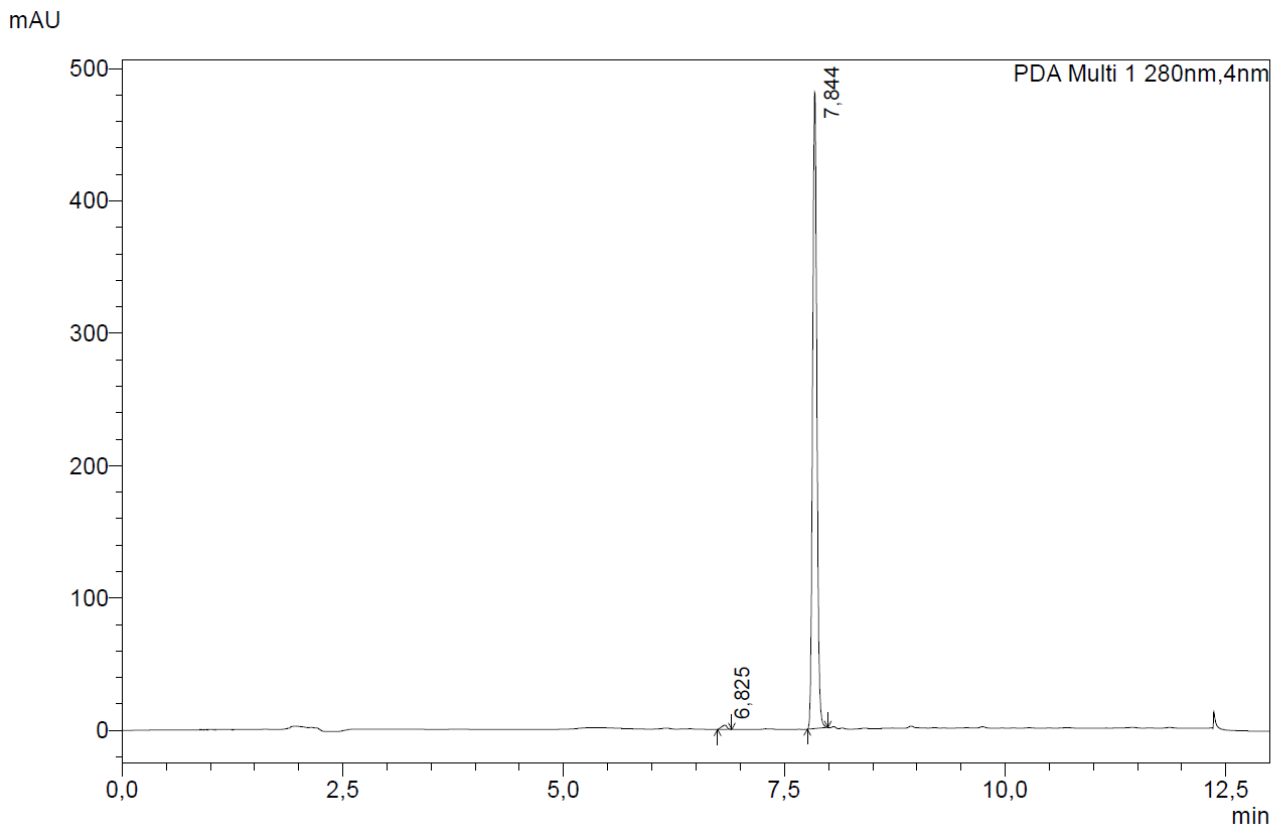
Acquisition Parameter

Source Type	APCI	Ion Polarity	Positive	Set Nebulizer	1.8 Bar
Focus	Not active	Set Capillary	4500 V	Set Dry Heater	200 °C
Scan Begin	50 m/z	Set End Plate Offset	-500 V	Set Dry Gas	8.0 l/min
Scan End	1600 m/z	Set Collision Cell RF	150.0 Vpp	Set Divert Valve	Waste



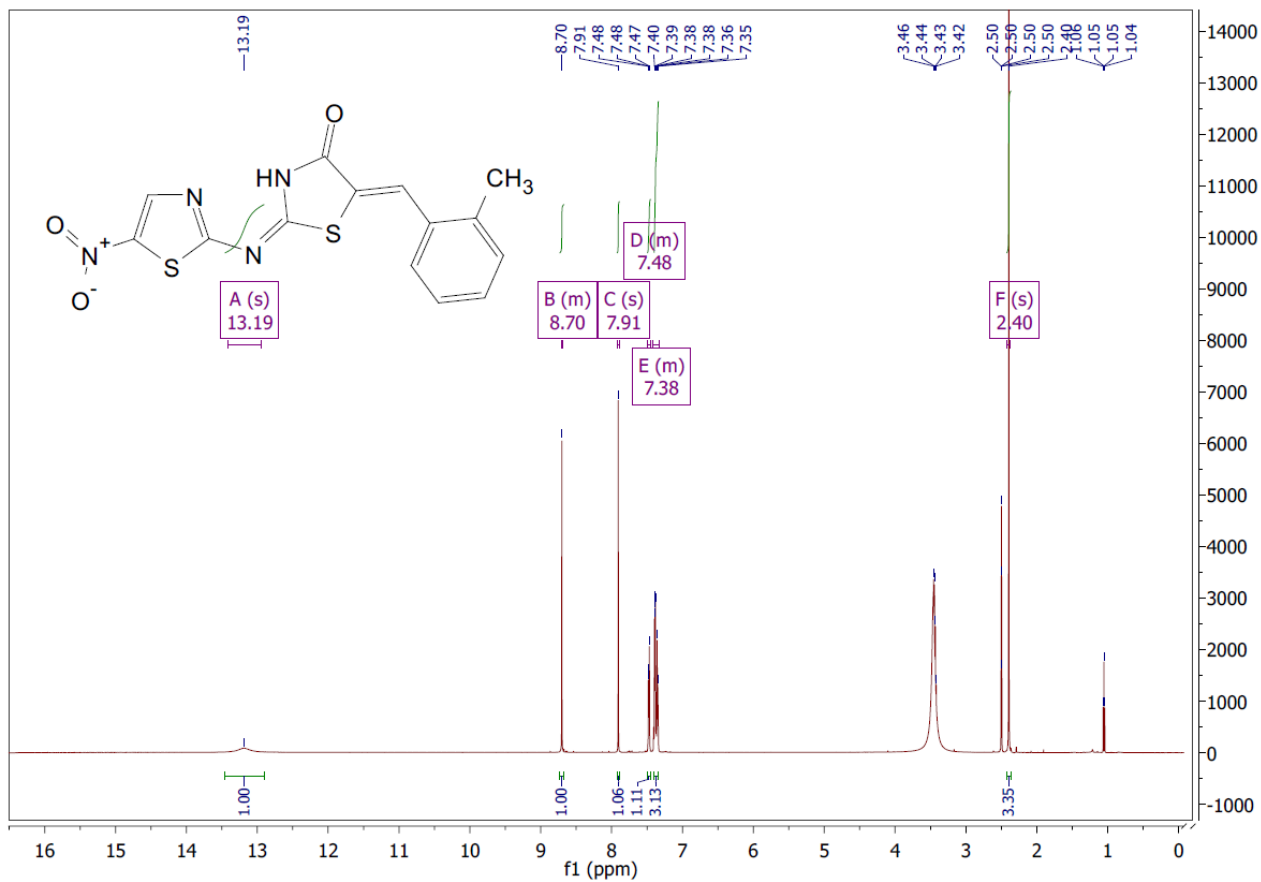
Meas. m/z	#	Formula	Score	m/z	err [mDa]	err [ppm]	mSigma	rdb	e ⁻ Conf	N-Rule
349.0084	1	C ₁₃ H ₉ N ₄ O ₄ S ₂	100.00	349.0060	-2.4	-6.9	19.1	11.5	even	ok

HPLC

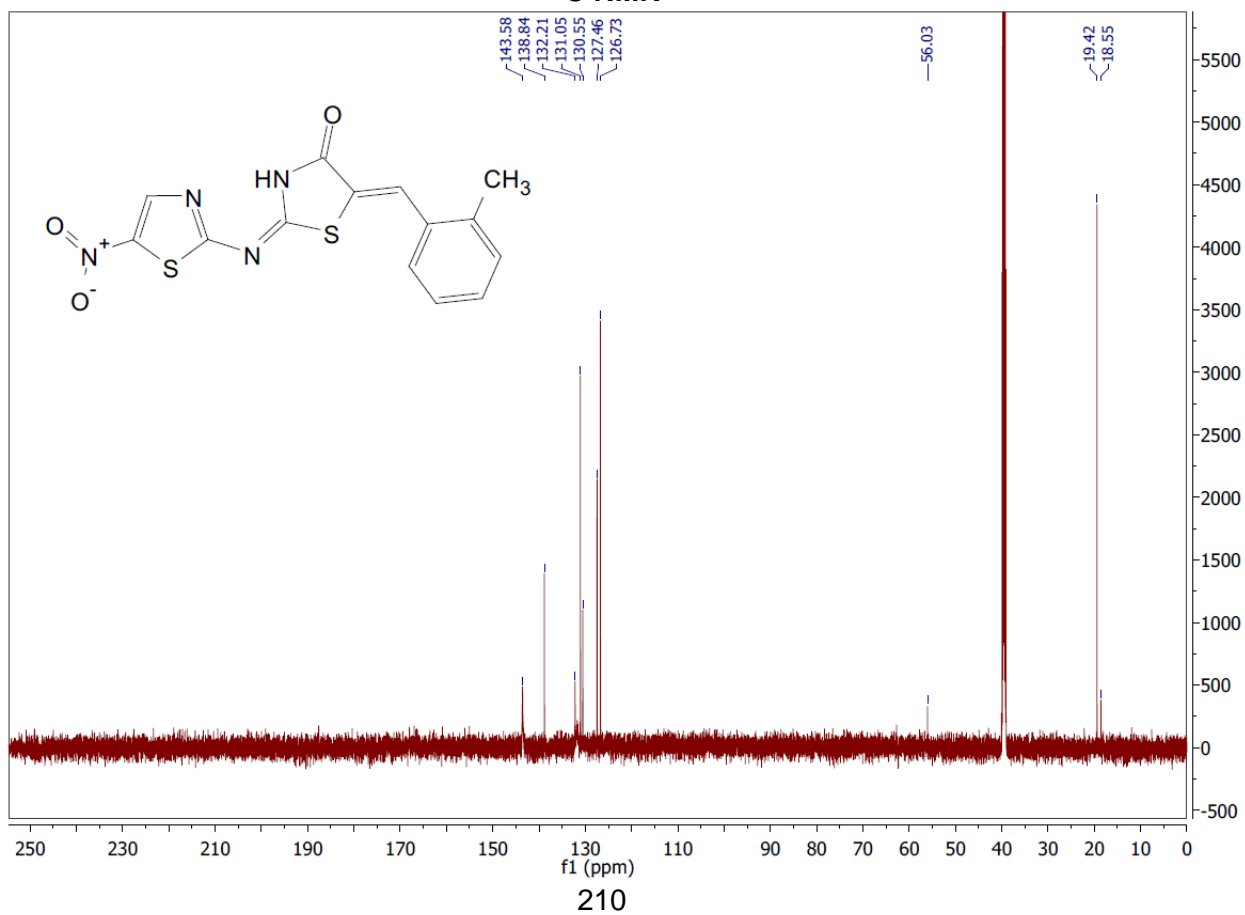


(2E,5Z)-5-(2-methylbenzylidene)-2-((5-nitrothiazol-2-yl)imino)thiazolidin-4-one (**3I**)

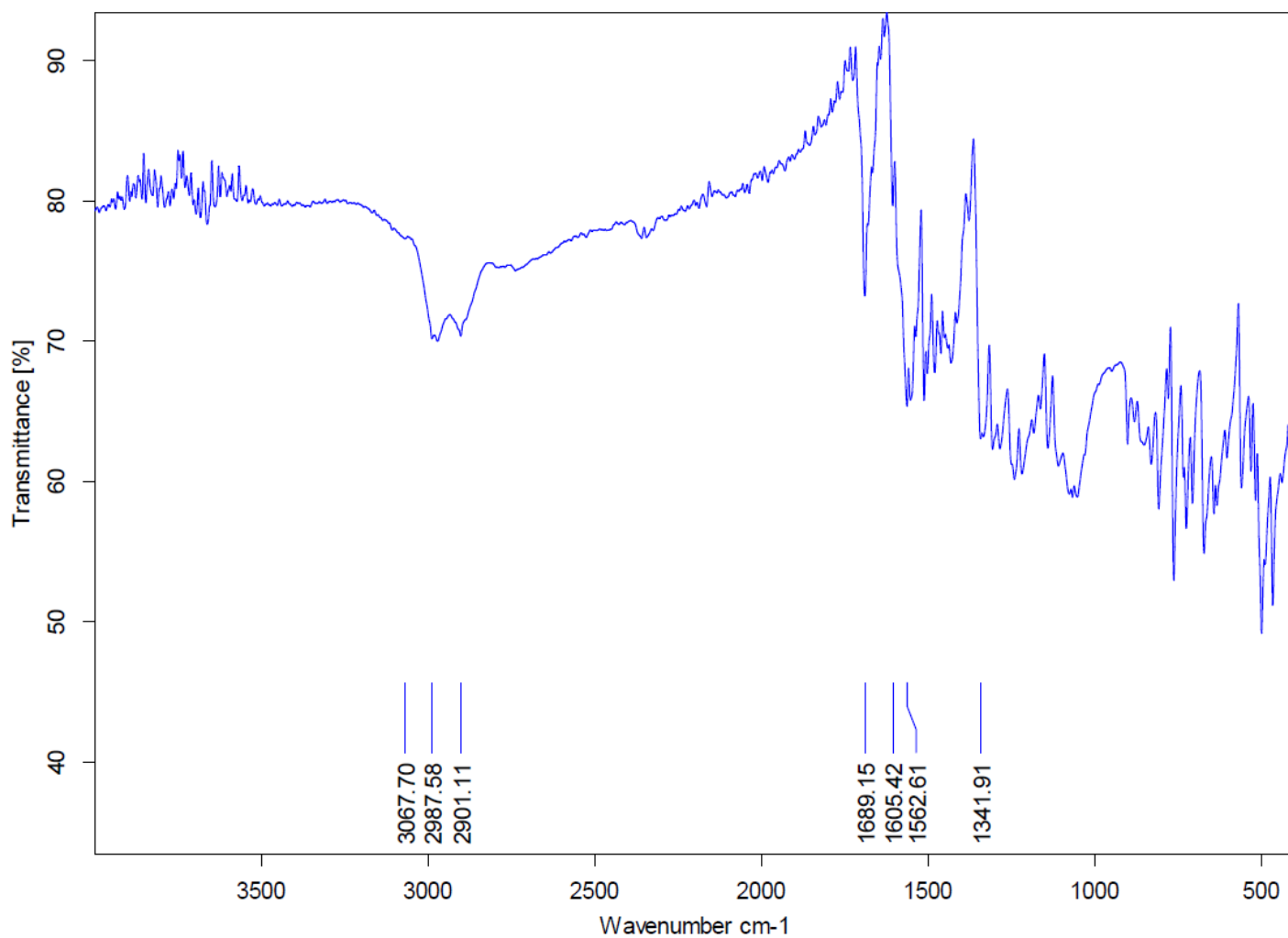
¹H NMR



¹³C NMR



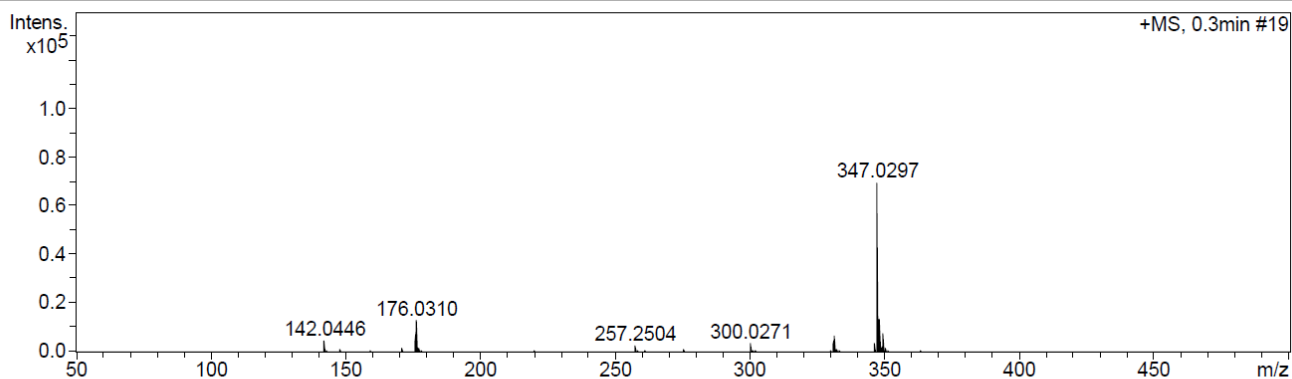
FTIR



HRMS

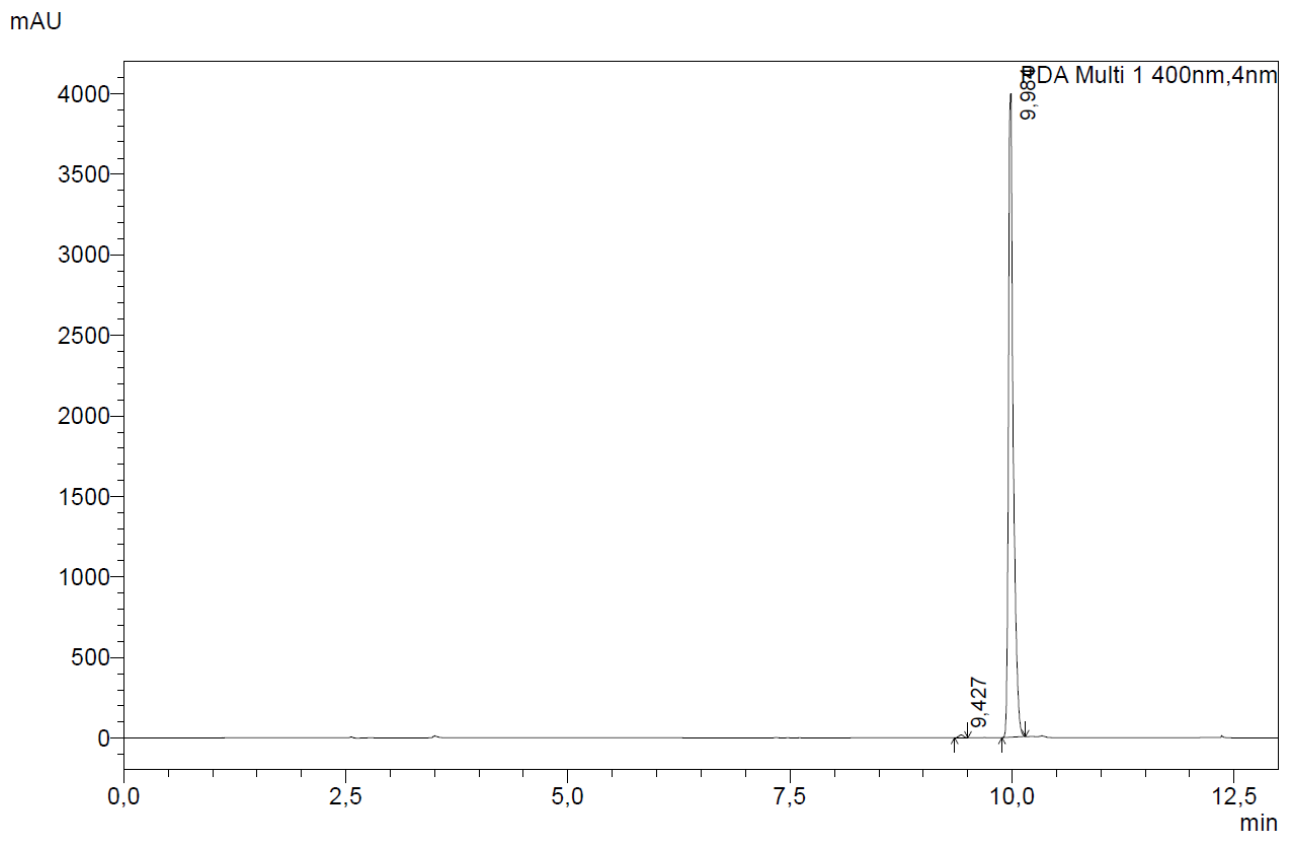
Acquisition Parameter

Source Type	APCI	Ion Polarity	Positive	Set Nebulizer	1.8 Bar
Focus	Not active	Set Capillary	4500 V	Set Dry Heater	200 °C
Scan Begin	50 m/z	Set End Plate Offset	-500 V	Set Dry Gas	8.0 l/min
Scan End	1600 m/z	Set Collision Cell RF	150.0 Vpp	Set Divert Valve	Waste



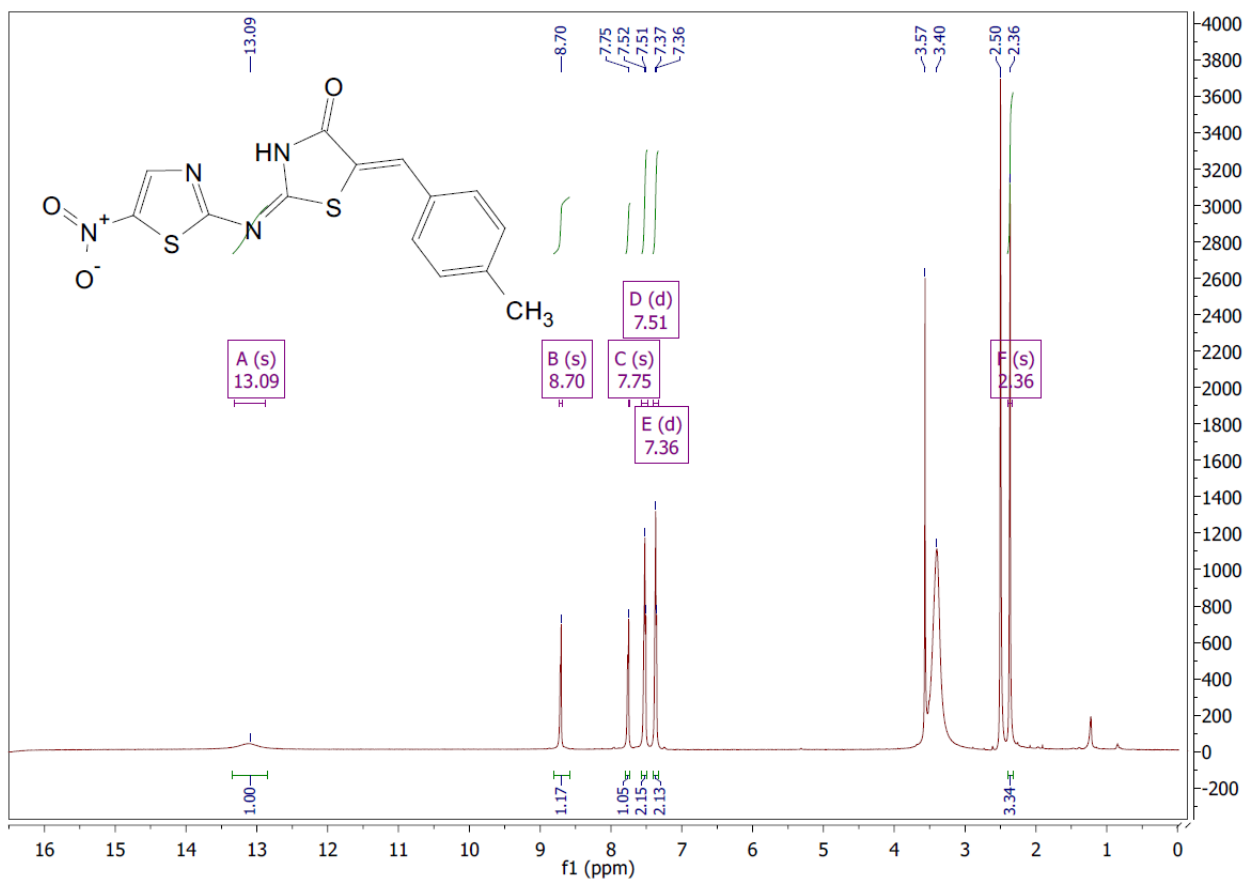
Meas. m/z	#	Formula	Score	m/z	err [mDa]	err [ppm]	mSigma	rdb	e ⁻ Conf	N-Rule
347.0297	1	C 14 H 11 N 4 O 3 S 2	100.00	347.0267	-3.0	-8.7	7.2	11.5	even	ok

HPLC

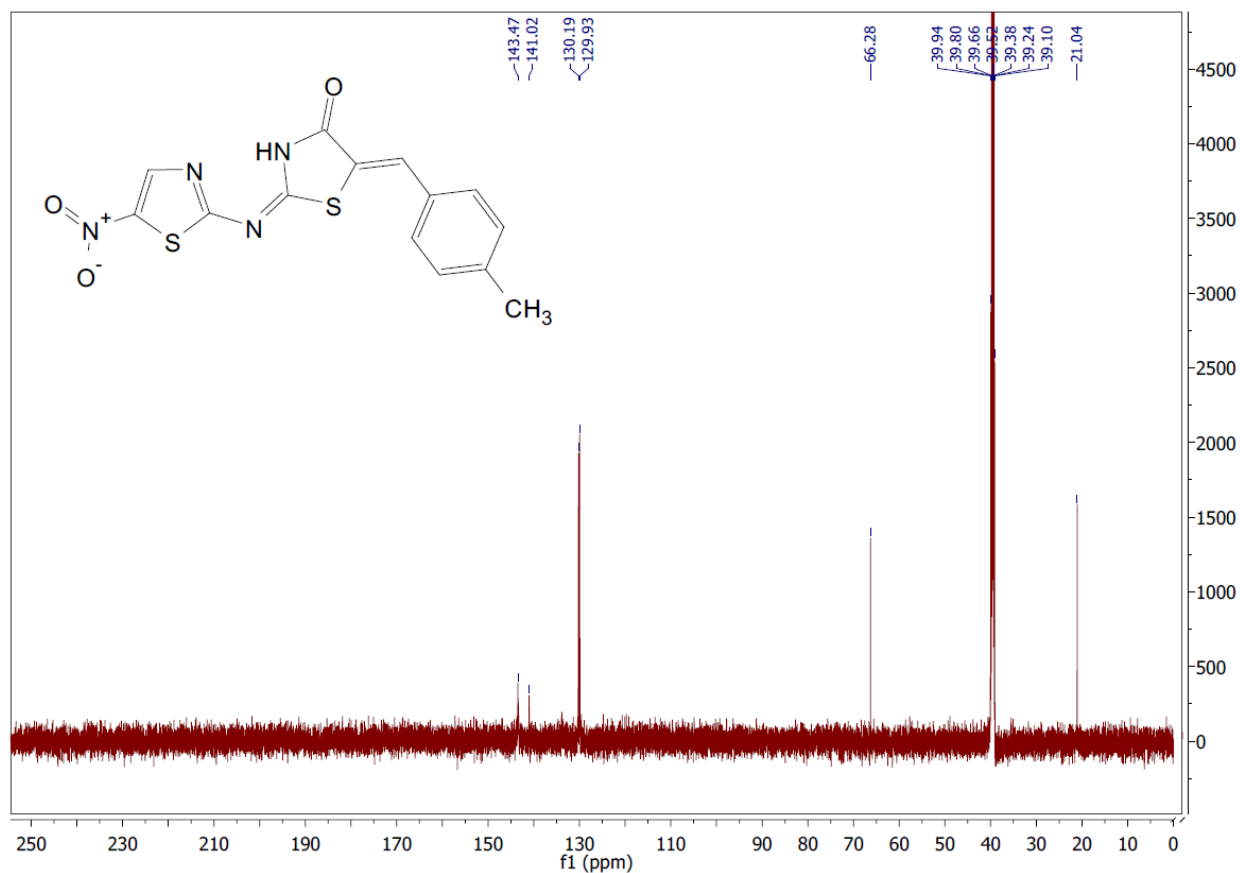


(2E,5Z)-5-(4-methylbenzylidene)-2-((5-nitrothiazol-2-yl)imino)thiazolidin-4-one (**3m**)

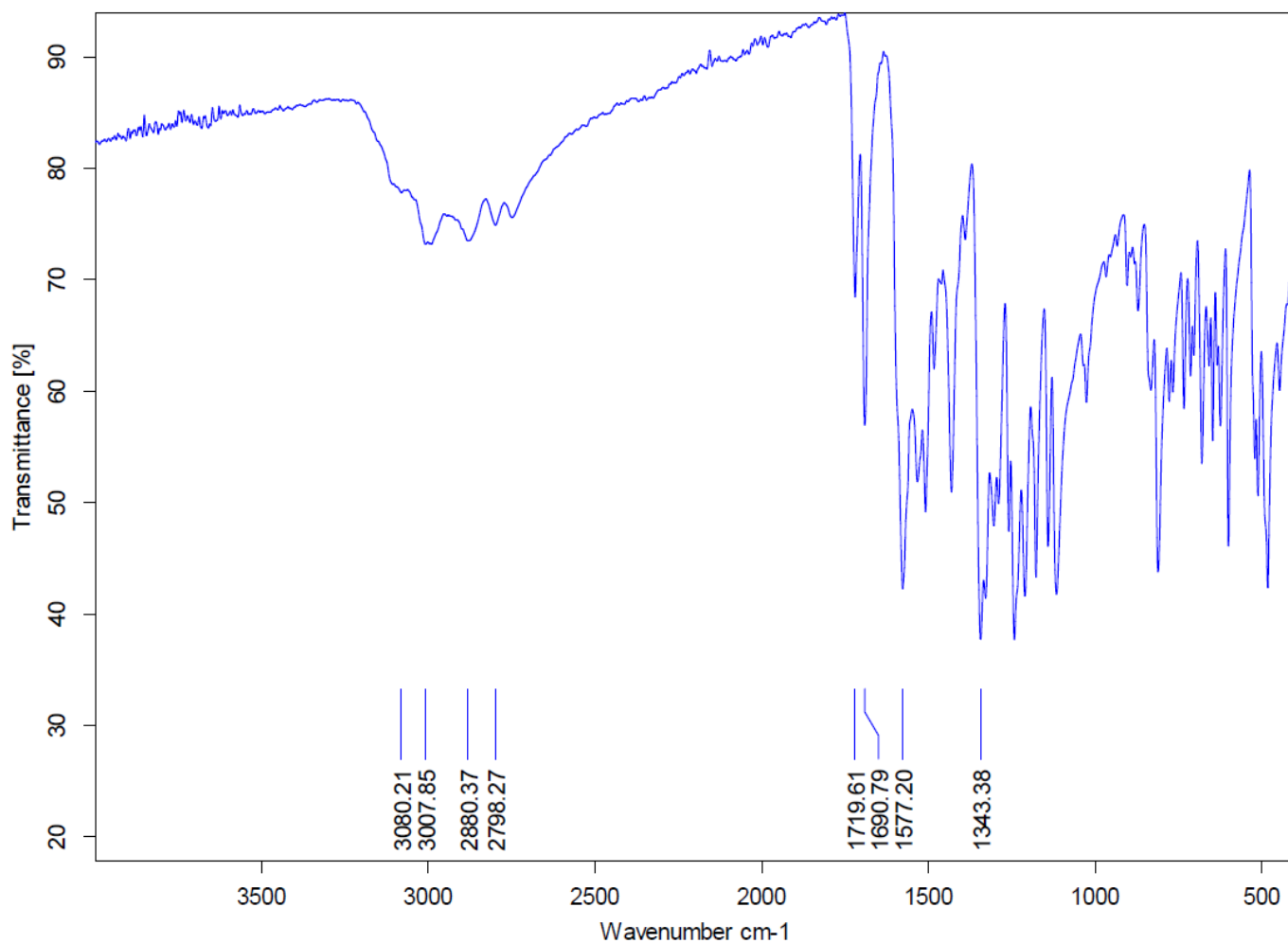
¹H NMR



¹³C NMR



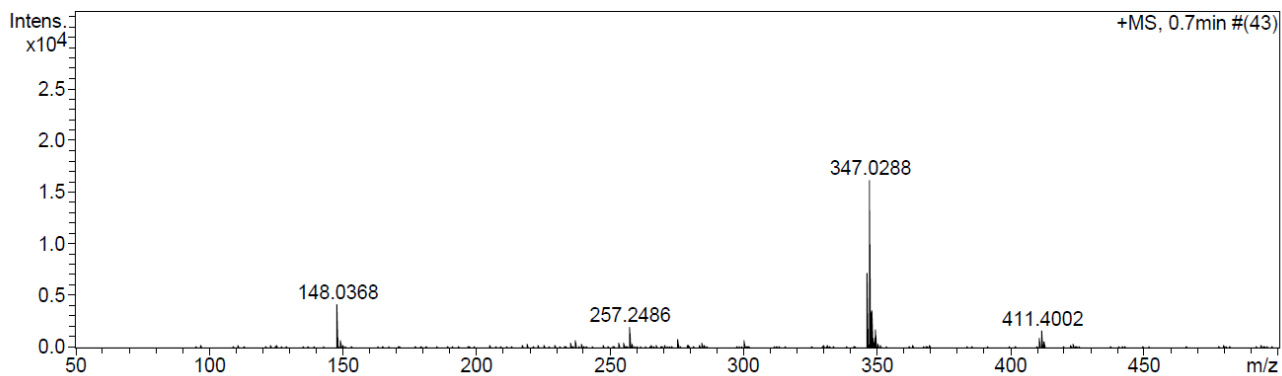
FTIR



HRMS

Acquisition Parameter

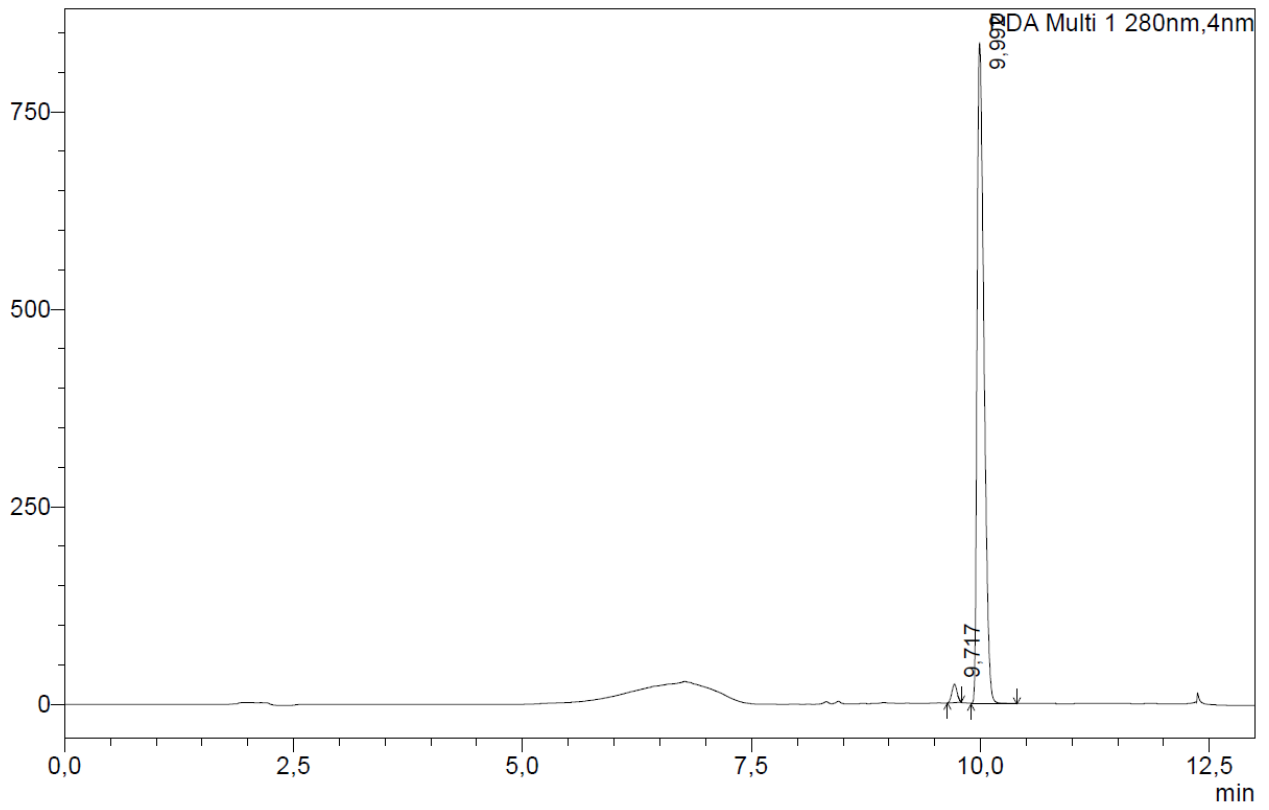
Source Type	APCI	Ion Polarity	Positive	Set Nebulizer	1.8 Bar
Focus	Not active	Set Capillary	4500 V	Set Dry Heater	200 °C
Scan Begin	50 m/z	Set End Plate Offset	-500 V	Set Dry Gas	8.0 l/min
Scan End	1600 m/z	Set Collision Cell RF	150.0 Vpp	Set Divert Valve	Waste



Meas. m/z	#	Formula	Score	m/z	err [mDa]	err [ppm]	mSigma	rdb	e ⁻ Conf	N-Rule
347.0288	1	C ₁₄ H ₁₁ N ₄ O ₃ S ₂	100.00	347.0267	-2.1	-6.0	24.3	11.5	even	ok

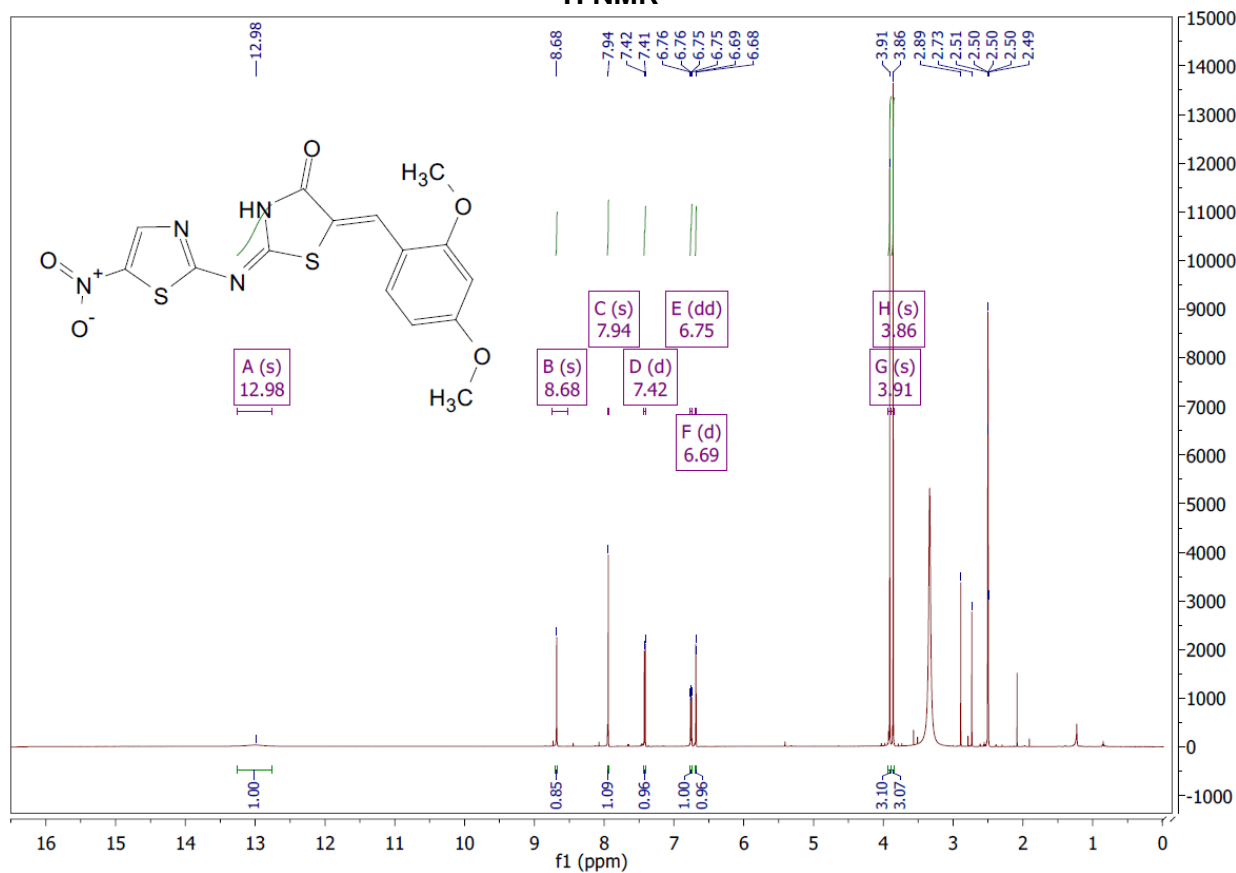
HPLC

mAU

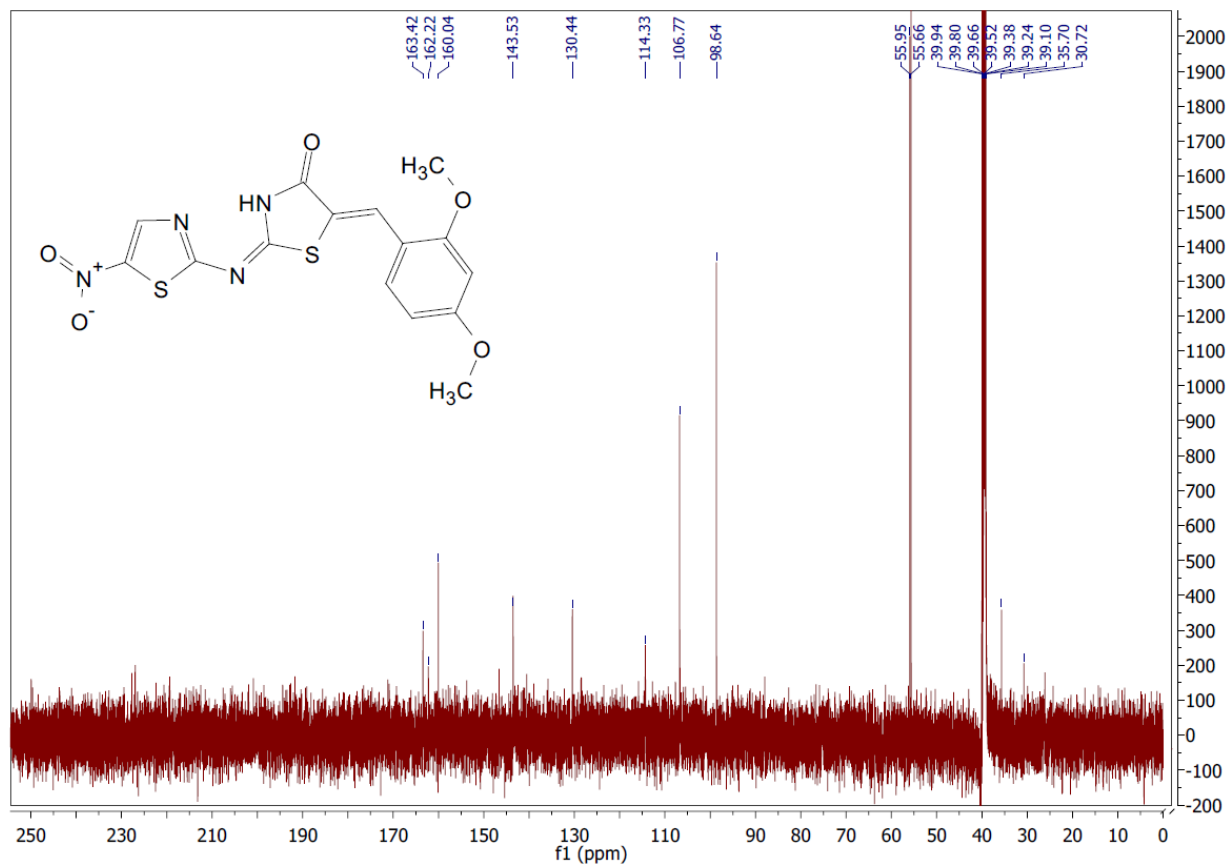


(2E,5Z)-5-(2,4-dimethoxybenzylidene)-2-((5-nitrothiazol-2-yl)imino)thiazolidin-4-one (**3n**)

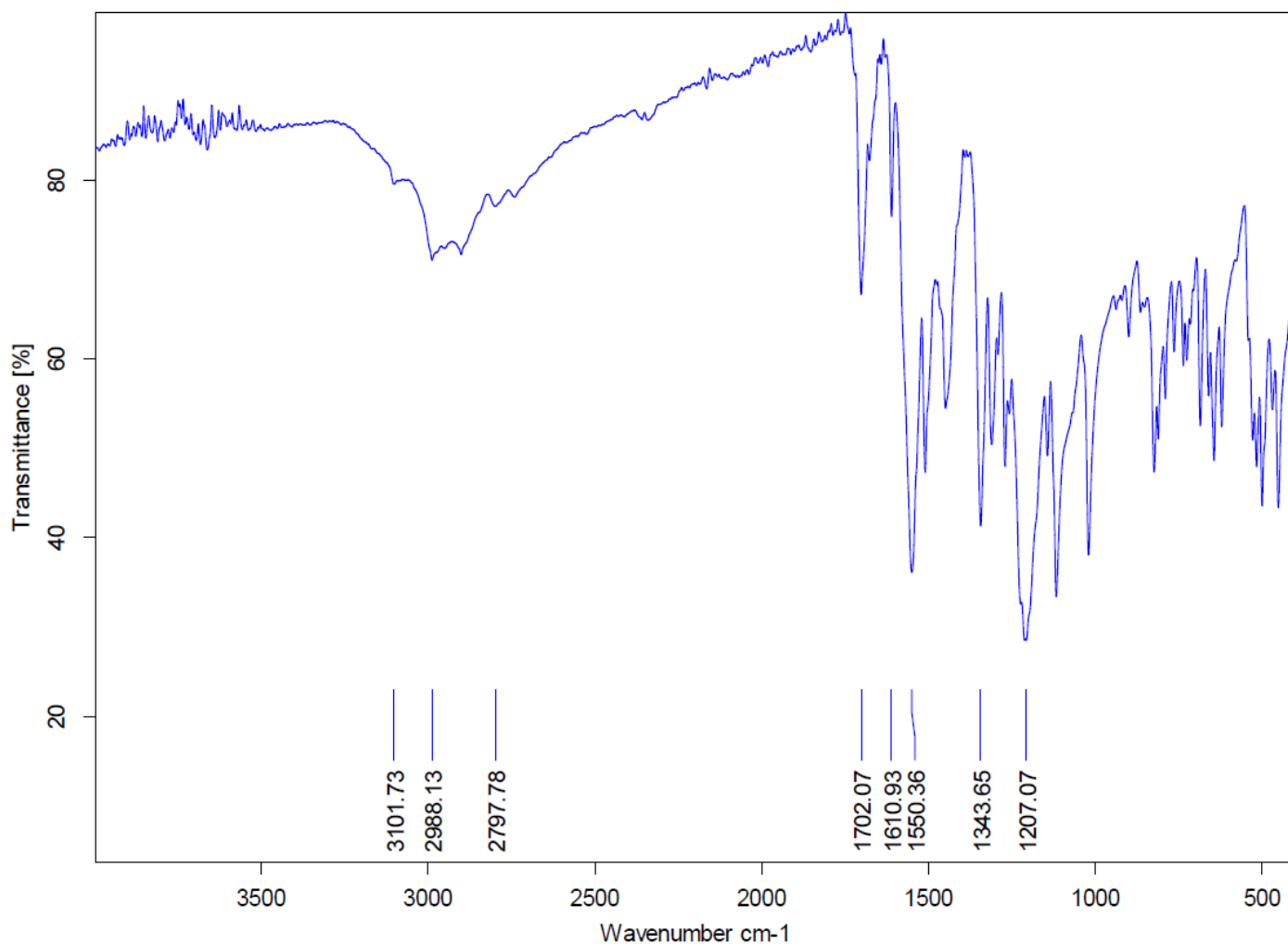
¹H NMR



¹³C NMR



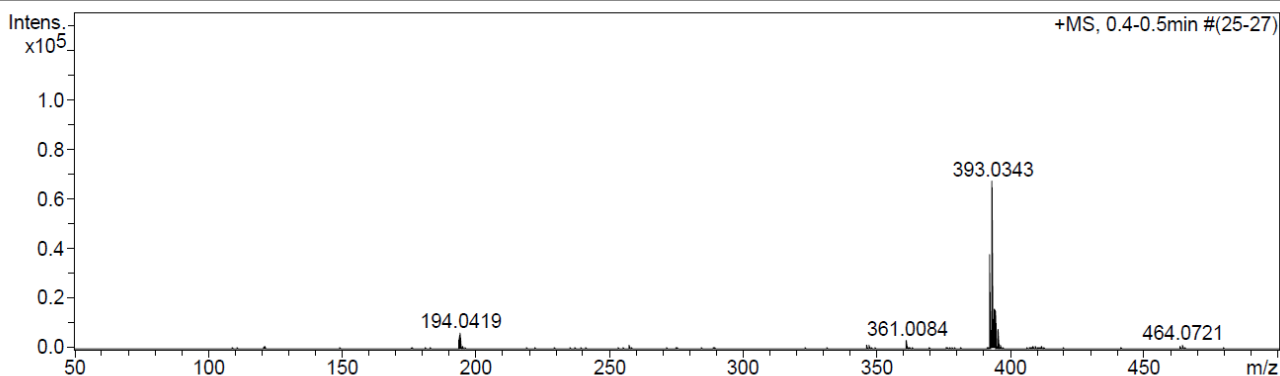
FTIR



HRMS

Acquisition Parameter

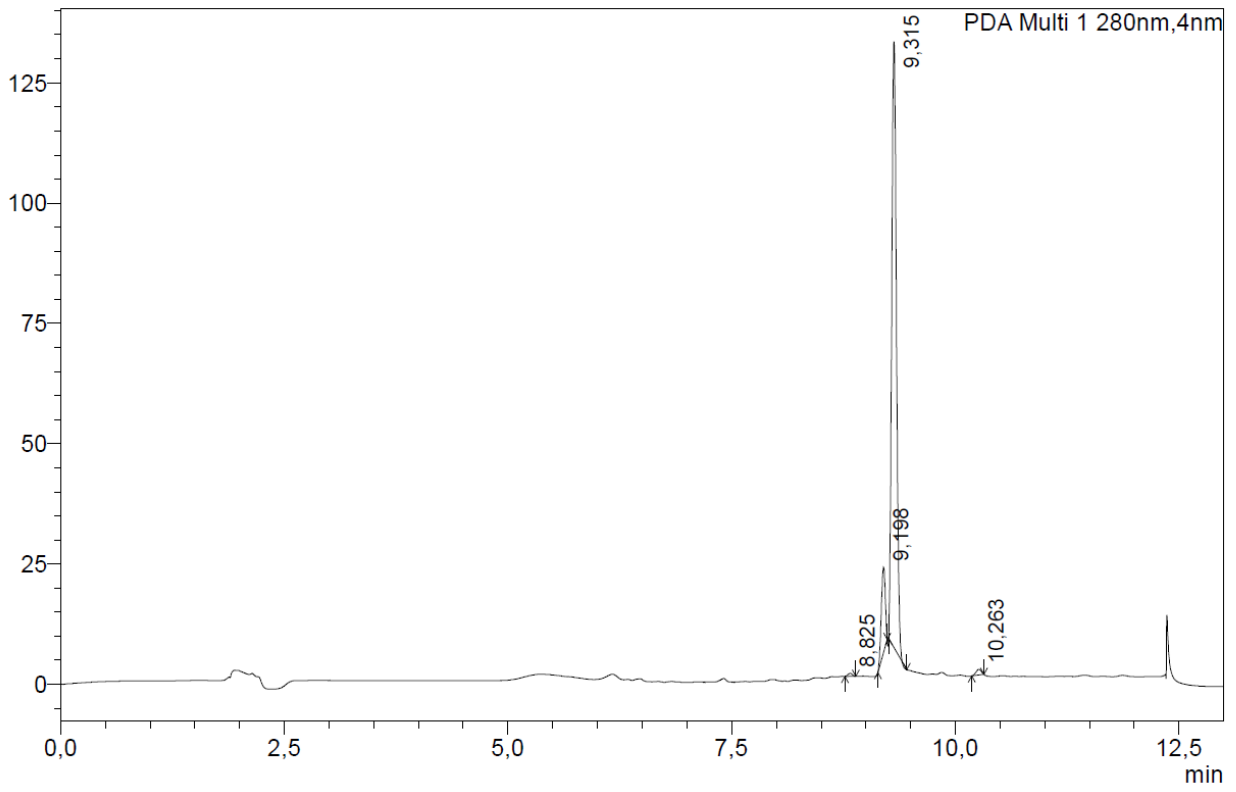
Source Type	APCI	Ion Polarity	Positive	Set Nebulizer	1.8 Bar
Focus	Not active	Set Capillary	4500 V	Set Dry Heater	200 °C
Scan Begin	50 m/z	Set End Plate Offset	-500 V	Set Dry Gas	8.0 l/min
Scan End	1600 m/z	Set Collision Cell RF	150.0 Vpp	Set Divert Valve	Waste



Meas. m/z	#	Formula	Score	m/z	err [mDa]	err [ppm]	mSigma	rdb	e ⁻ Conf	N-Rule
392.0274	1	C ₁₂ H ₁₆ N ₄ O ₅ S ₃	100.00	392.0277	0.3	0.8	424.2	7.0	odd	ok
	2	C ₁₅ H ₁₂ N ₄ O ₅ S ₂	0.01	392.0244	-3.1	-7.8	466.0	12.0	odd	ok
393.0343	1	C ₁₅ H ₁₃ N ₄ O ₅ S ₂	100.00	393.0322	-2.1	-5.3	23.8	11.5	even	ok

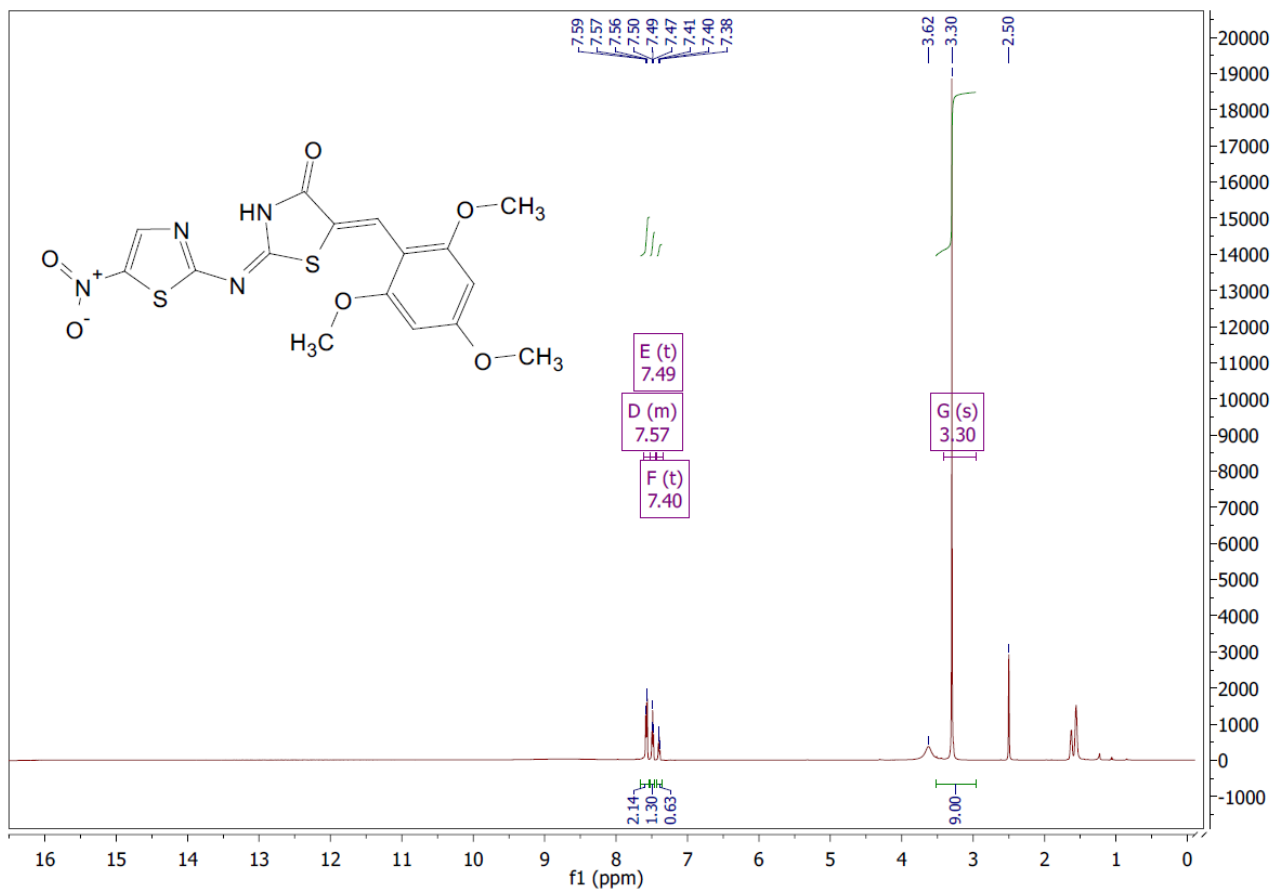
HPLC

mAU

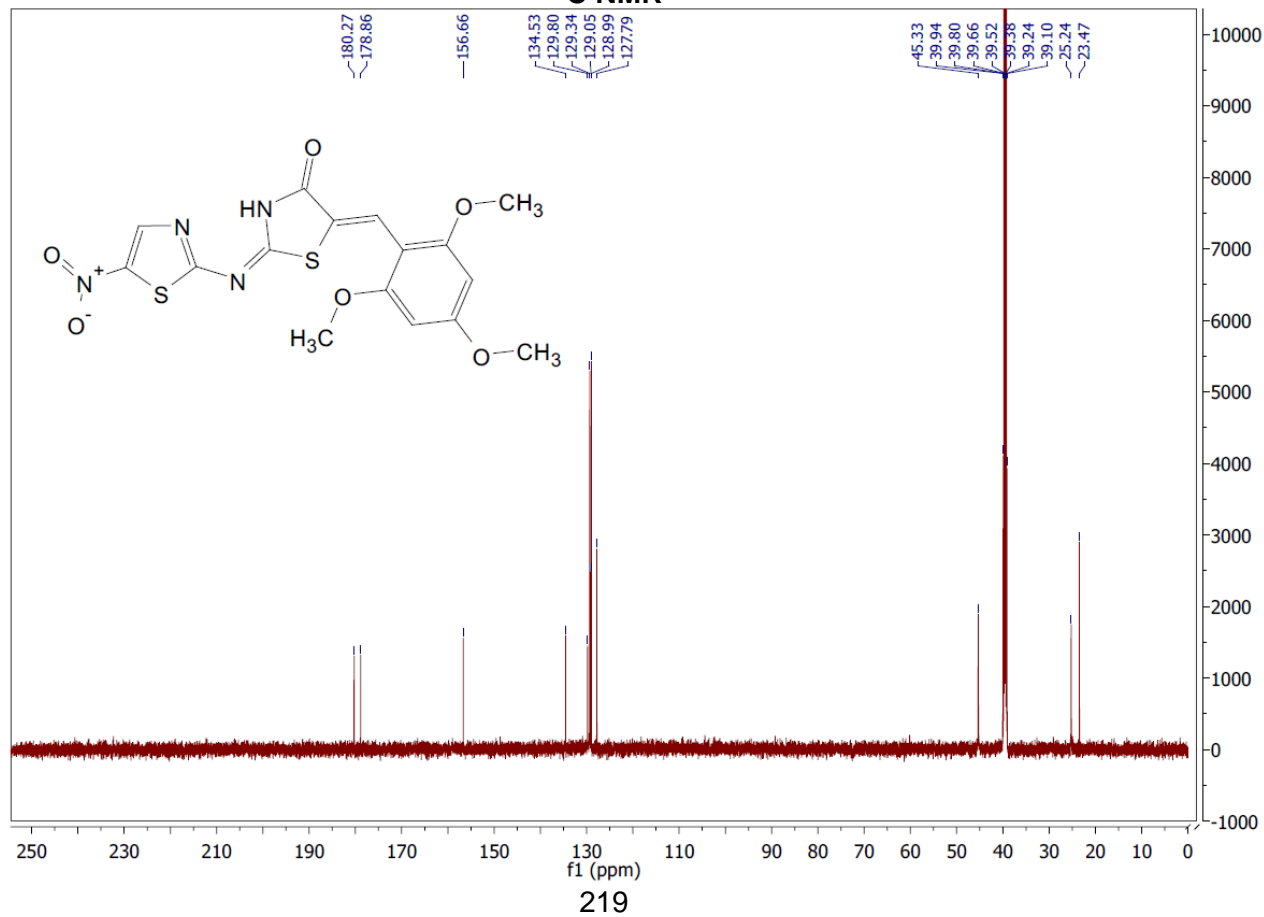


(2E,5Z)-5-(2,4,6-trimethoxybenzylidene)-2-((5-nitrothiazol-2-yl)imino)thiazolidin-4-one (**3o**)

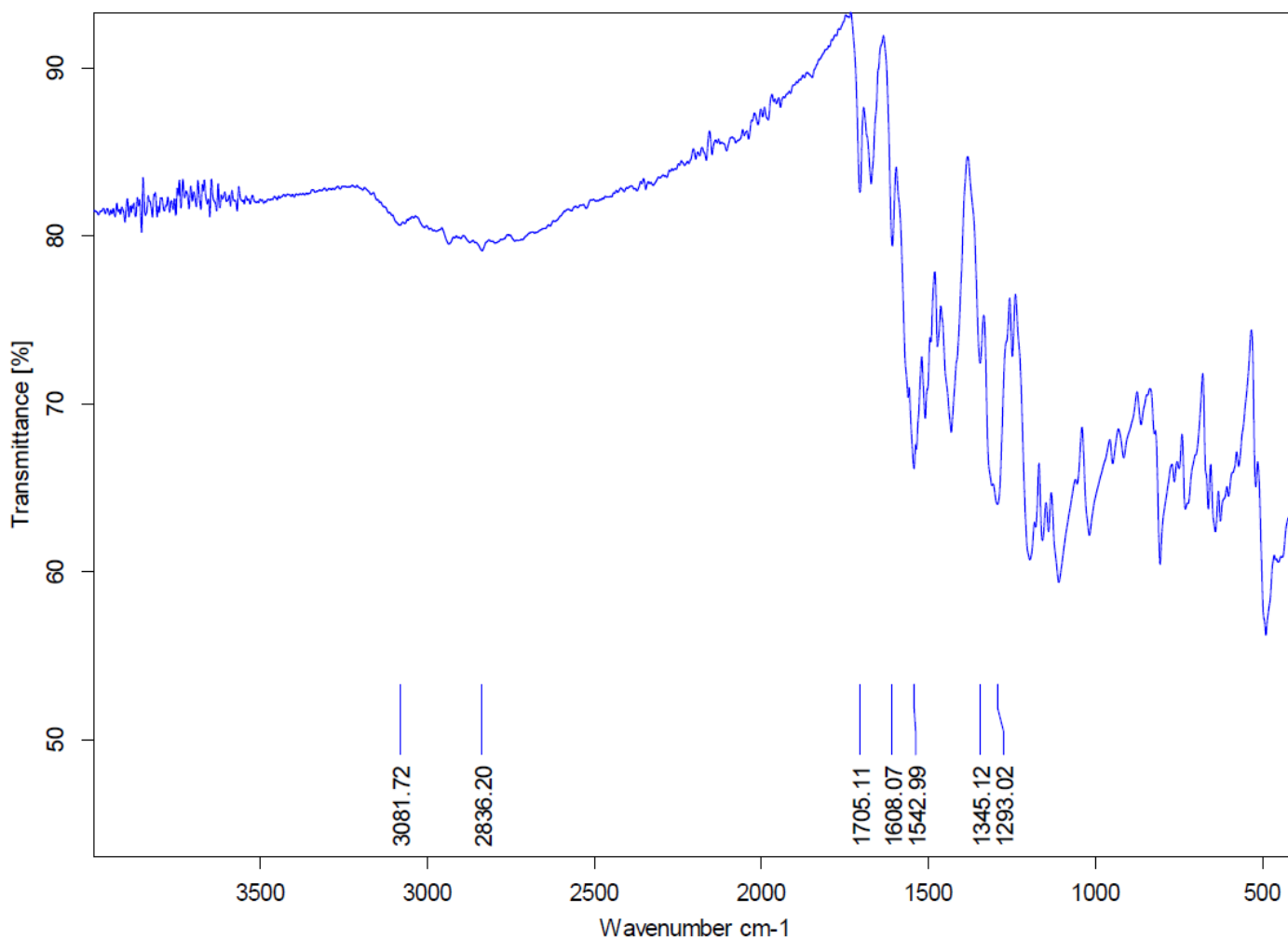
¹H NMR



¹³C NMR



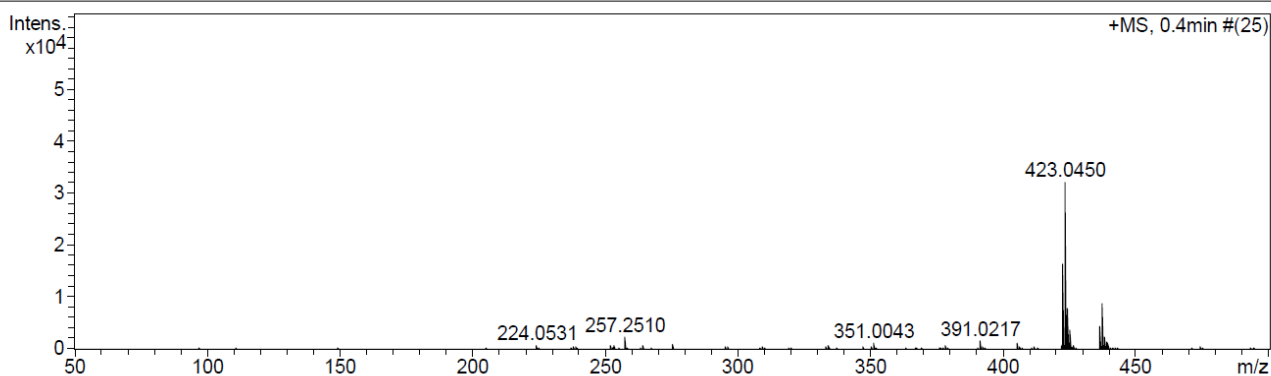
FTIR



HRMS

Acquisition Parameter

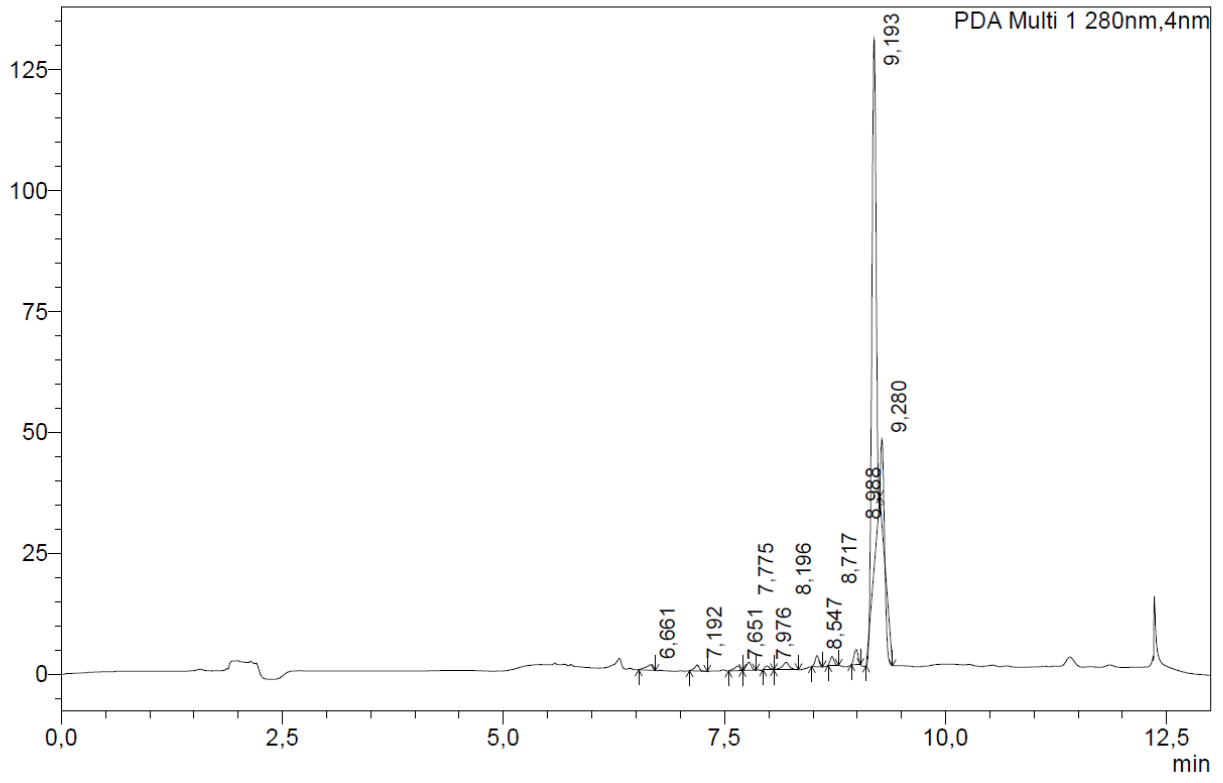
Source Type	APCI	Ion Polarity	Positive	Set Nebulizer	1.8 Bar
Focus	Not active	Set Capillary	4500 V	Set Dry Heater	200 °C
Scan Begin	50 m/z	Set End Plate Offset	-500 V	Set Dry Gas	8.0 l/min
Scan End	1600 m/z	Set Collision Cell RF	150.0 Vpp	Set Divert Valve	Waste



Meas. m/z	#	Formula	Score	m/z	err [mDa]	err [ppm]	mSigma	rdb	e ⁻ Conf	N-Rule
423.0450	1	C 16 H 15 N 4 O 6 S 2	100.00	423.0428	-2.2	-5.3	21.6	11.5	even	ok

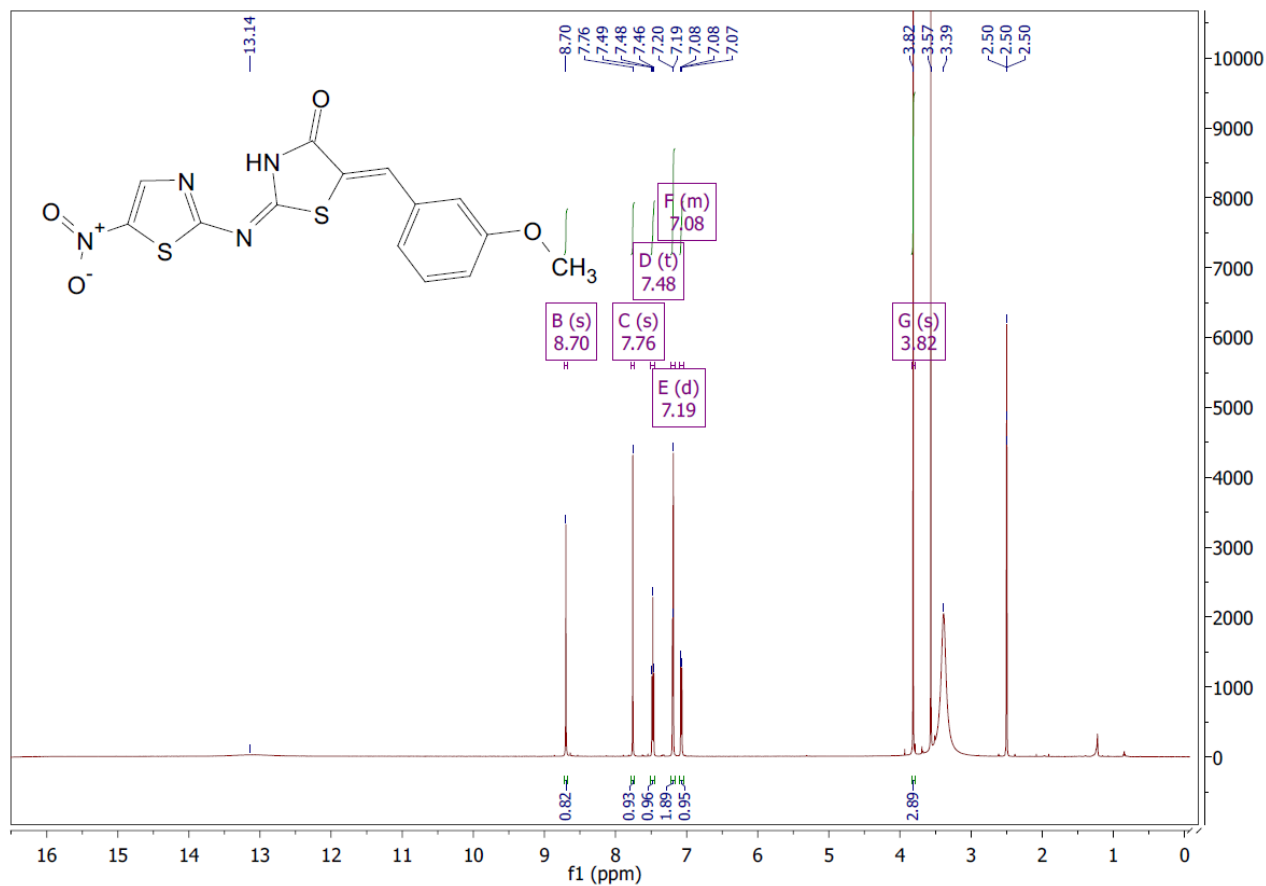
HPLC

mAU

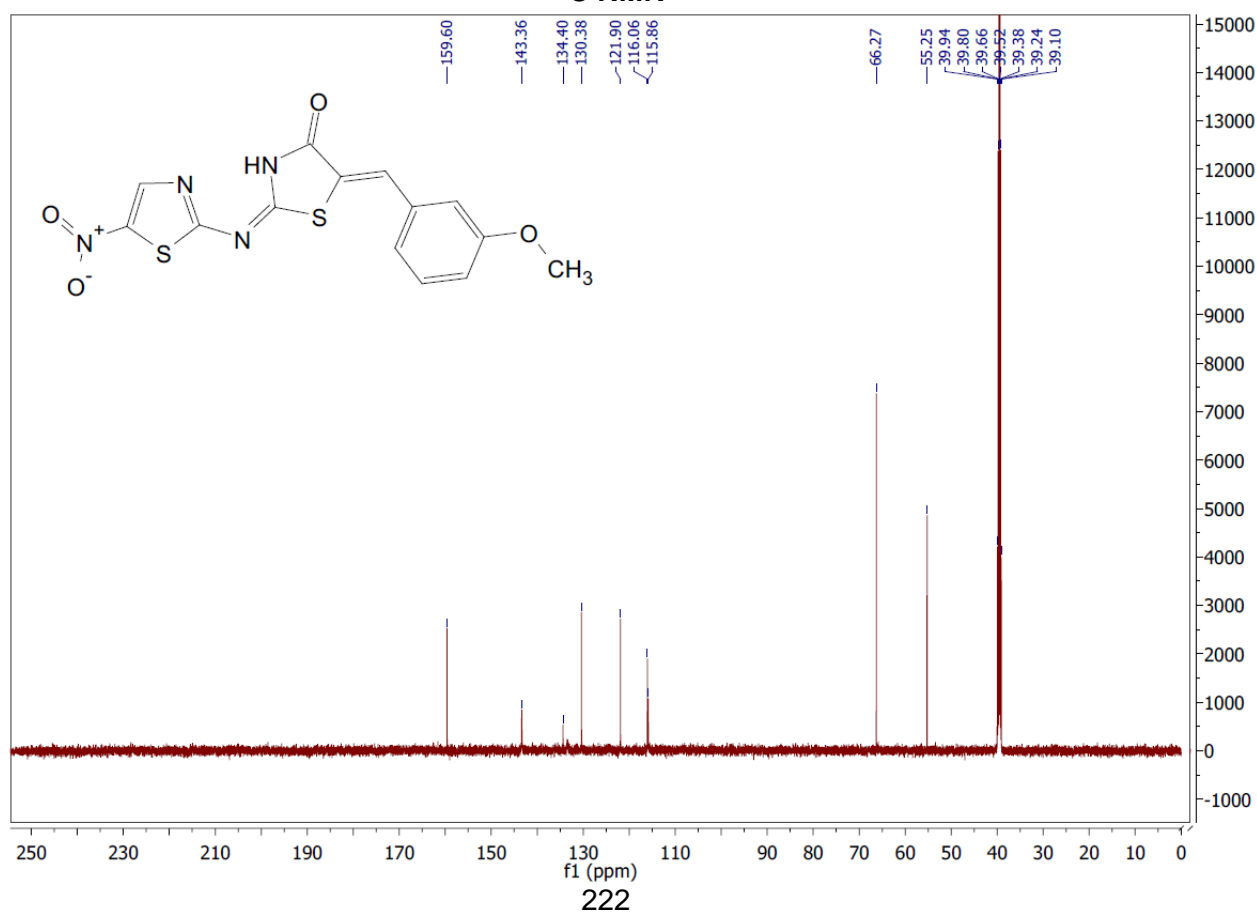


(2E,5Z)-5-(3-methoxybenzylidene)-2-((5-nitrothiazol-2-yl)imino)thiazolidin-4-one (**3p**)

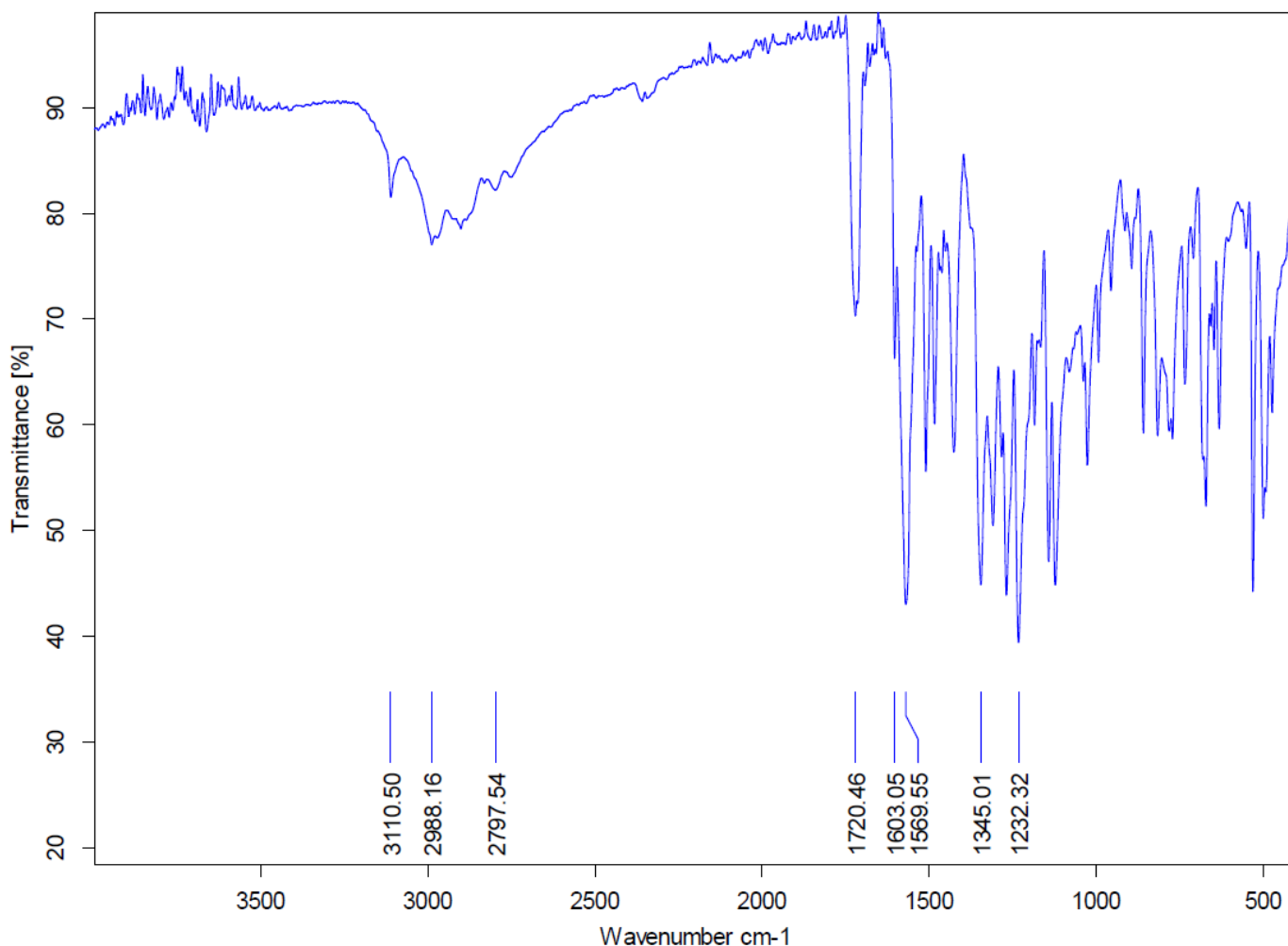
¹H NMR



¹³C NMR



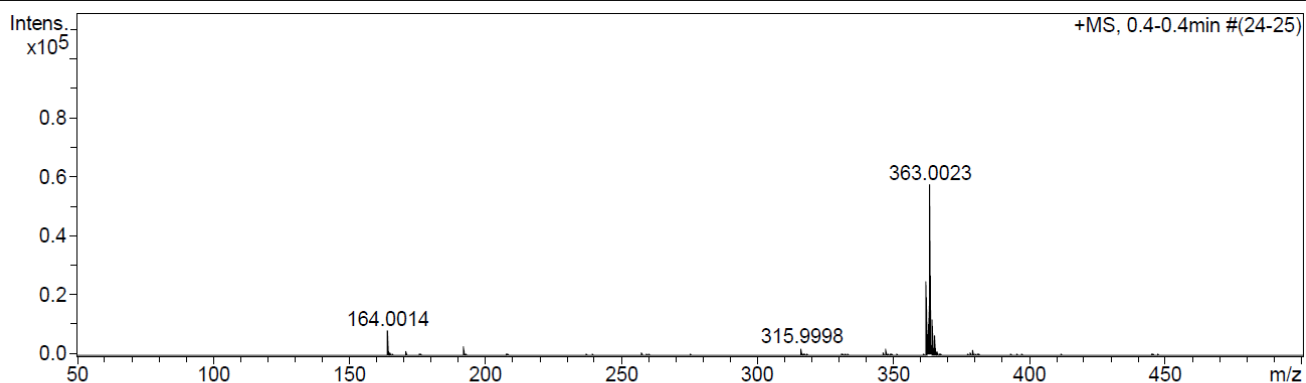
FTIR



HRMS

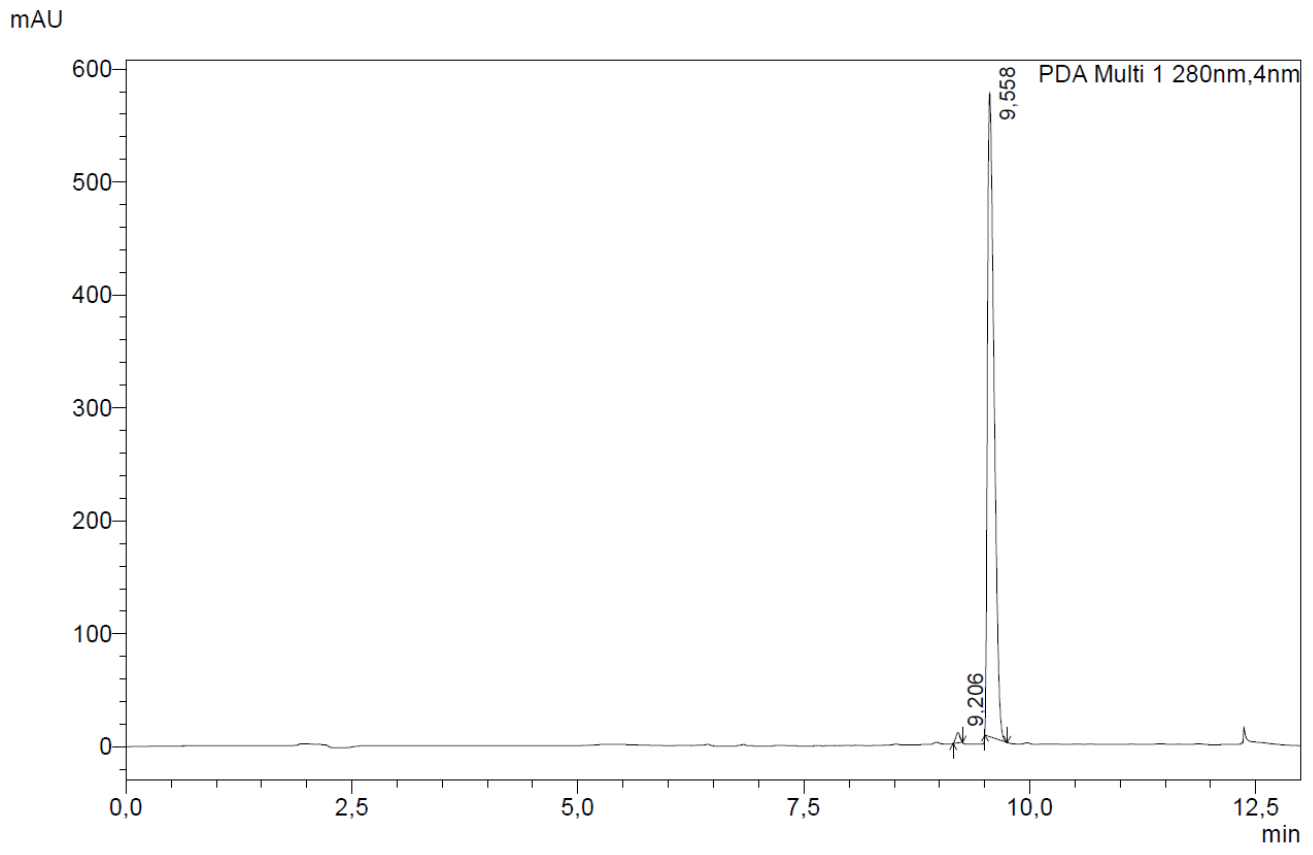
Acquisition Parameter

Source Type	APCI	Ion Polarity	Positive	Set Nebulizer	1.8 Bar
Focus	Not active	Set Capillary	4500 V	Set Dry Heater	200 °C
Scan Begin	50 m/z	Set End Plate Offset	-500 V	Set Dry Gas	8.0 l/min
Scan End	1600 m/z	Set Collision Cell RF	150.0 Vpp	Set Divert Valve	Waste



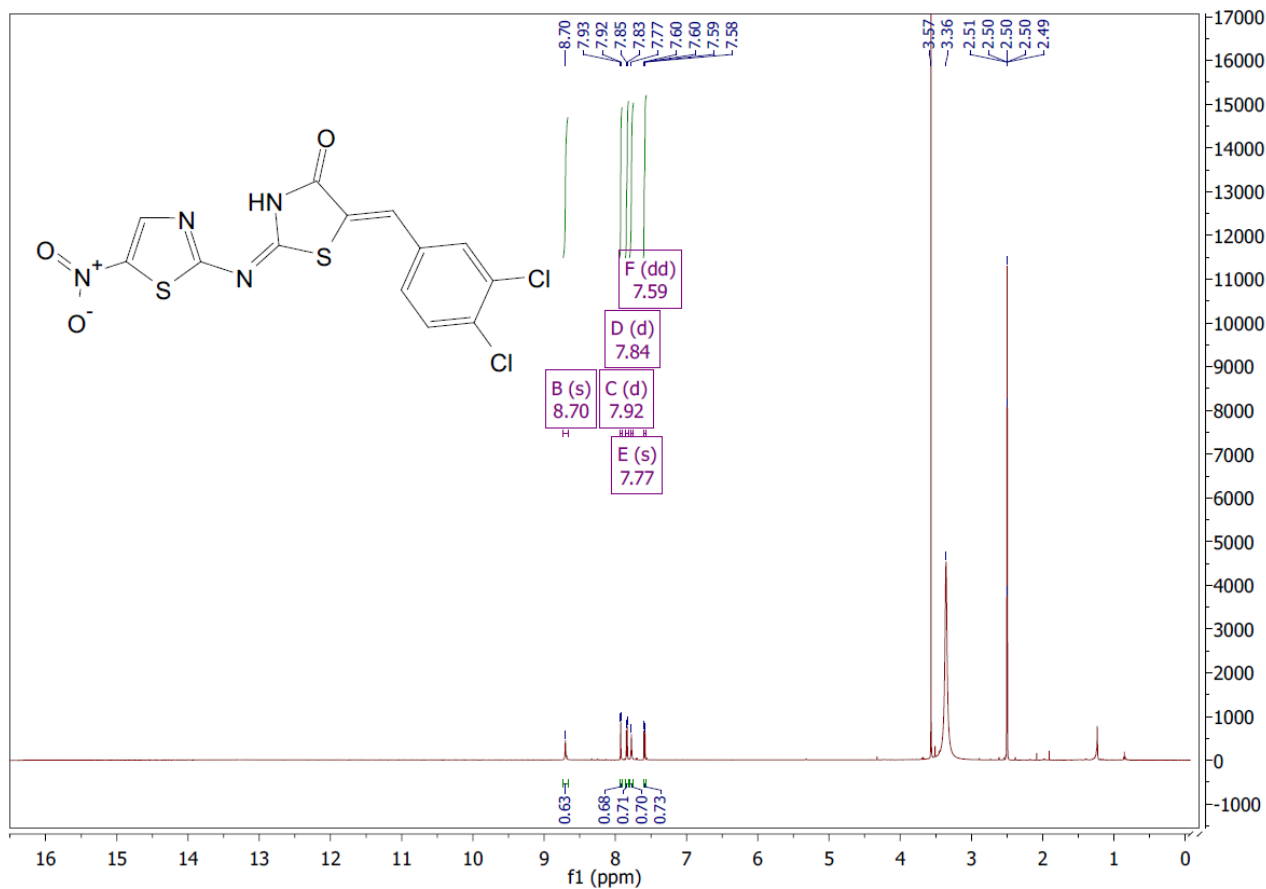
Meas. m/z	#	Formula	Score	m/z	err [mDa]	err [ppm]	mSigma	rdb	e ⁻ Conf	N-Rule
363.0023	1	C ₁₄ H ₁₁ N ₄ O ₂ S ₃	100.00	363.0039	1.5	4.3	21.4	11.5	even	ok

HPLC

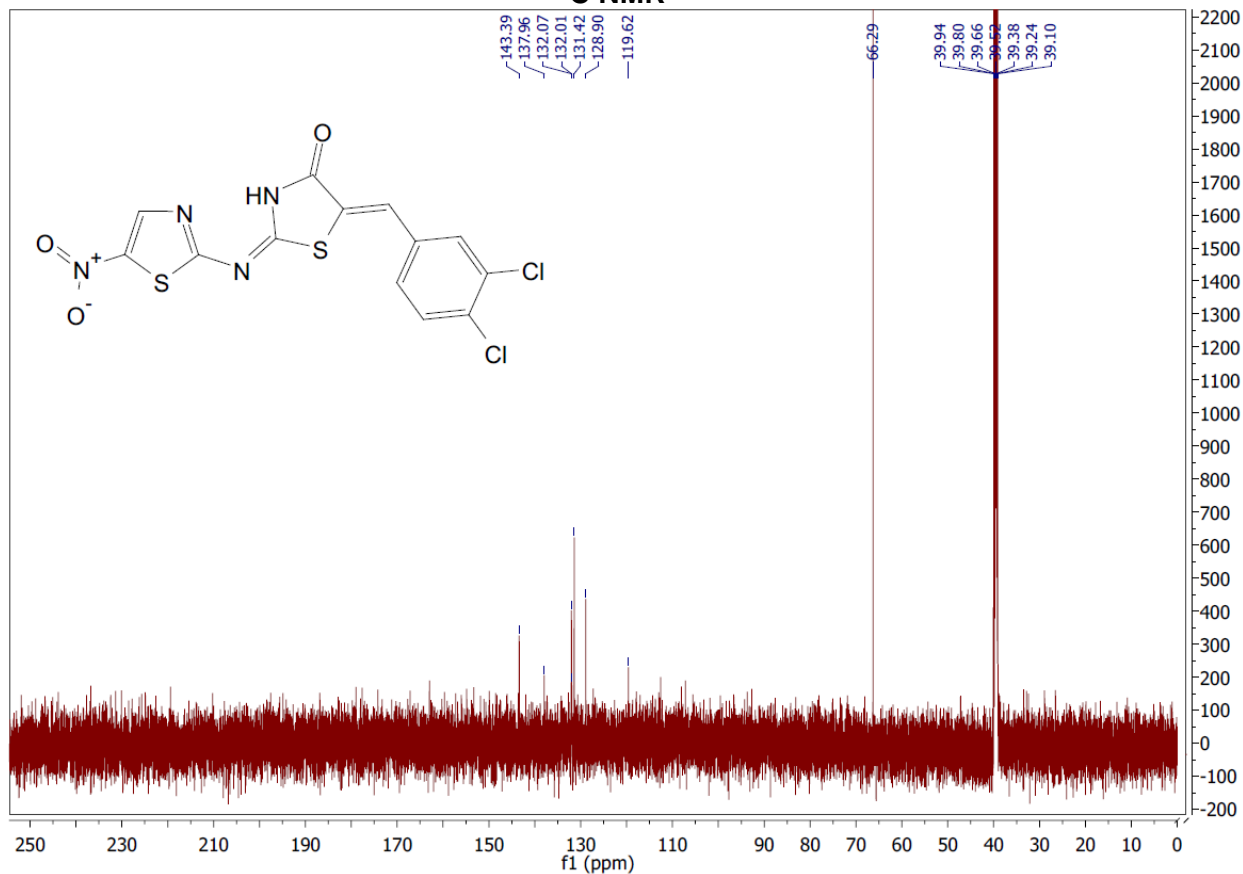


(2E,5Z)-5-(3,4-dichlorobenzylidene)-2-((5-nitrothiazol-2-yl)imino)thiazolidin-4-one (**3q**)

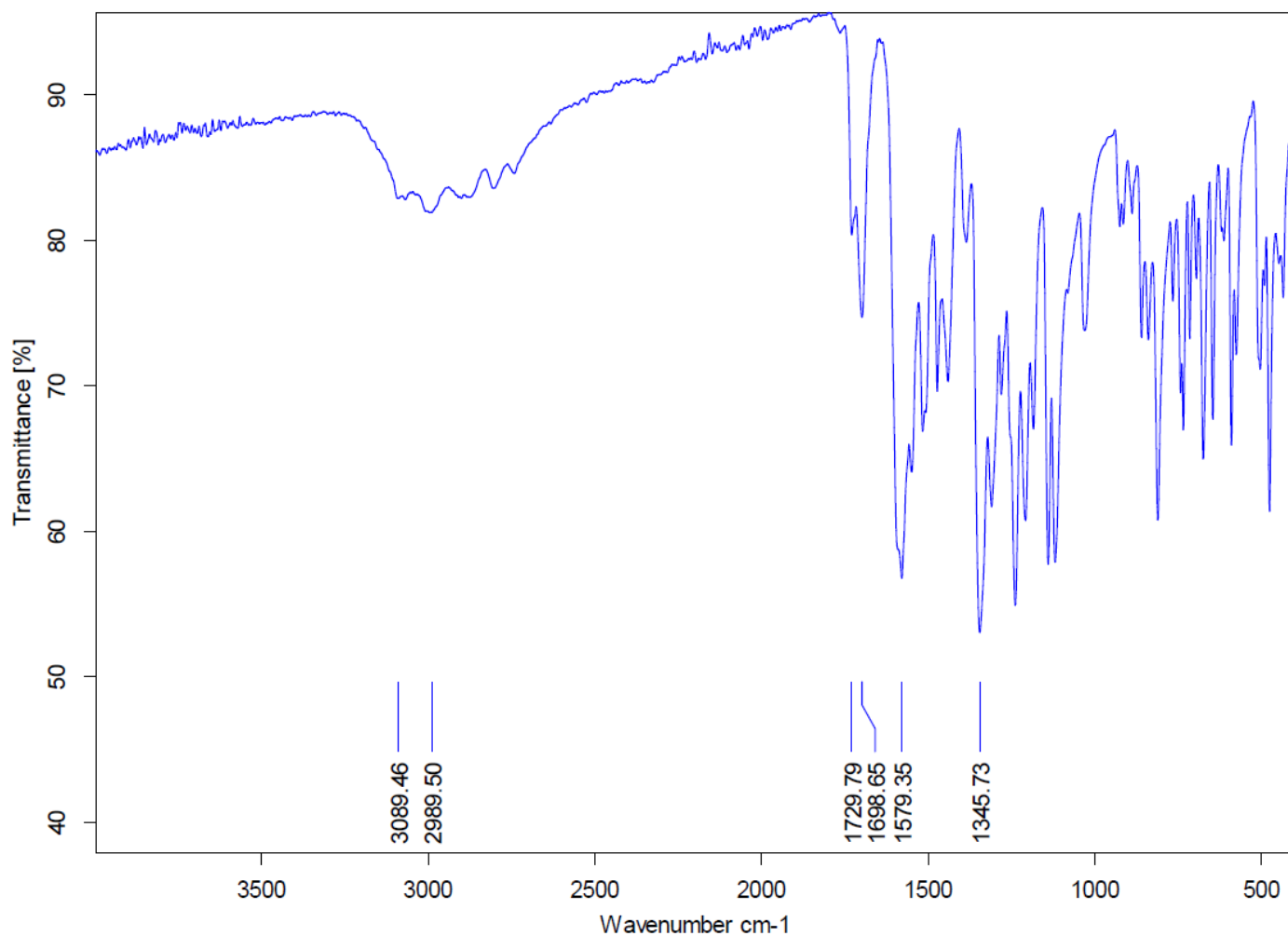
¹H NMR



¹³C NMR



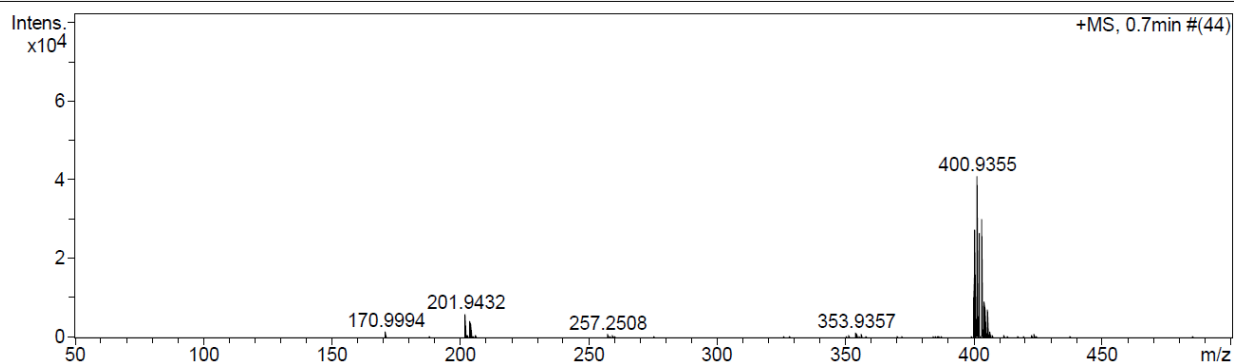
FTIR



HRMS

Acquisition Parameter

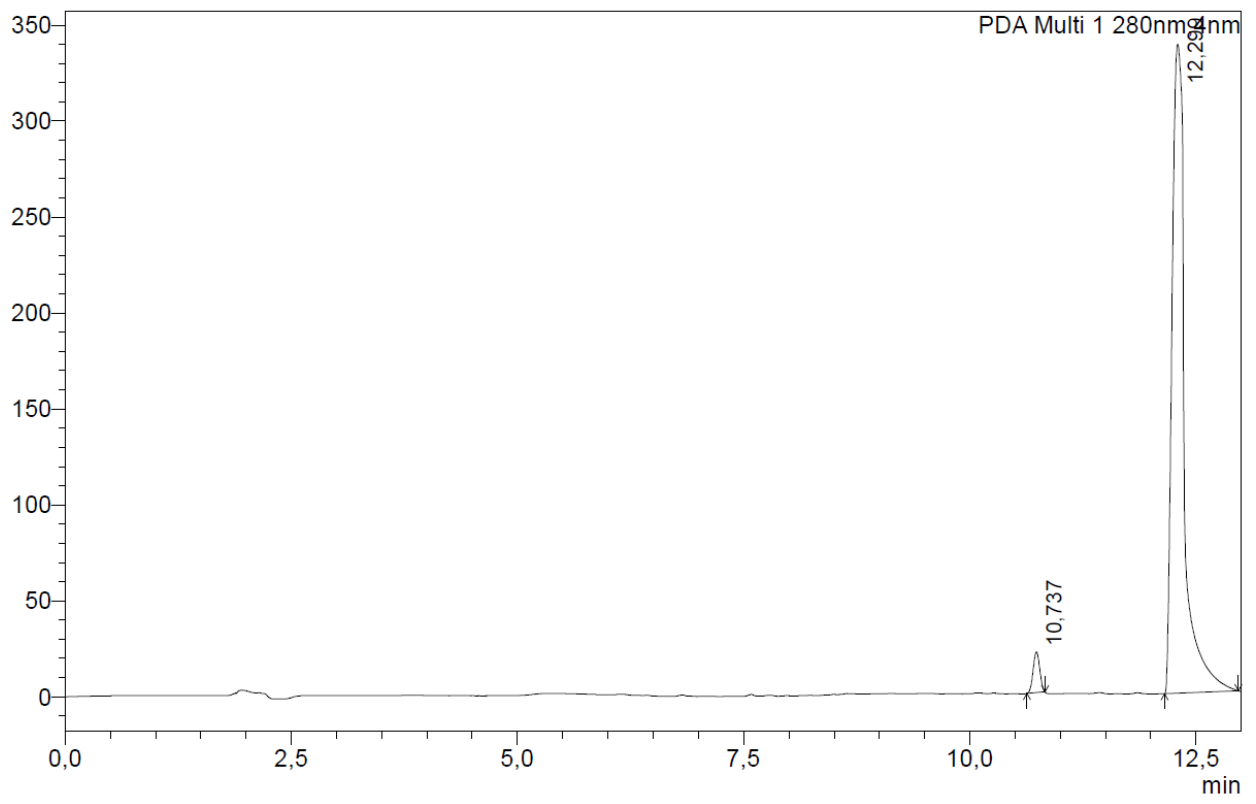
Source Type	APCI	Ion Polarity	Positive	Set Nebulizer	1.8 Bar
Focus	Not active	Set Capillary	4500 V	Set Dry Heater	200 °C
Scan Begin	50 m/z	Set End Plate Offset	-500 V	Set Dry Gas	8.0 l/min
Scan End	1600 m/z	Set Collision Cell RF	150.0 Vpp	Set Divert Valve	Waste



Meas. m/z	#	Formula	Score	m/z	err [mDa]	err [ppm]	mSigma	rdb	e ⁻ Conf	N-R rule
399.9286	1	C ₁₃ H ₆ Cl ₂ N ₄ O ₃ S ₂	100.00	399.9253	-3.3	-8.3	414.1	12.0	odd	ok
400.9355	1	C ₁₃ H ₇ Cl ₂ N ₄ O ₃ S ₂	100.00	400.9331	-2.4	-5.9	182.9	11.5	even	ok

HPLC

mAU



ANNEXURE B: PERMISSIONS AND LICENSES

LICENSES FOR ADAPTED & USED FIGURES:

ELSEVIER LICENSE

TERMS AND CONDITIONS

Jun 13, 2022

This Agreement between Pharmacen –Dylan Hart ("You") and Elsevier ("Elsevier") consists of your license details and the terms and conditions provided by Elsevier and Copyright Clearance Center.

License Number	5327300878455
License date	Jun 13, 2022
Licensed Content Publisher	Elsevier
Licensed Content Publication	Trends in Microbiology
Licensed Content Title	<i>Mycobacterium tuberculosis</i>
Licensed Content Author	Anastasia Koch, Valerie Mizrahi
Licensed Content Date	Jun 1, 2018
Licensed Content Volume	26
Licensed Content Issue	6
Licensed Content Pages	2
Start Page	555
End Page	556
Type of Use	reuse in a thesis/dissertation

Portion	figures/tables/illustrations
Number of figures/tables/illustrations	1
Format	both print and electronic
Are you the author of this Elsevier article?	No
Will you be translating?	No
Title	Mr
Institution name	North-West University, Potchefstroom
Expected presentation date	Aug 2022
Order reference number	DHFIG1
Portions	Granuloma formation
Requestor Location	Pharmacien North-West University Pharmaceutical Chemistry Potchefstroom, North West 2520 South Africa Attn: Dylan Hart
Publisher Tax ID	ZA 4110266048
Total	0.00 USD

This work is licensed under a [Creative Commons Attribution-NonCommercial 4.0 International License](#).

Authors who publish with Medical Journal of Indonesia agree to the following terms:

1. Authors retain copyright and grant Medical Journal of Indonesia right of first publication with the work simultaneously licensed under a [Creative Commons Attribution-NonCommercial License](#) that allows others to remix, adapt, build upon the work non-commercially with an acknowledgment of the work's authorship and initial publication in Medical Journal of Indonesia.
2. Authors are permitted to copy and redistribute the journal's published version of the work non-commercially (e.g., post it to an institutional repository or publish it in a book), with an acknowledgment of its initial publication in Medical Journal of Indonesia.

a. License grant.

1. Subject to the terms and conditions of this Public License, the Licensor hereby grants You a worldwide, royalty-free, non-sublicensable, non-exclusive, irrevocable license to exercise the Licensed Rights in the Licensed Material to:
 - A. reproduce and Share the Licensed Material, in whole or in part, for NonCommercial purposes only; and
 - B. produce, reproduce, and Share Adapted Material for NonCommercial purposes only.
2. Exceptions and Limitations. For the avoidance of doubt, where Exceptions and Limitations apply to Your use, this Public License does not apply, and You do not need to comply with its terms and conditions.
3. Term. The term of this Public License is specified in Section [6\(a\)](#).
4. Media and formats; technical modifications allowed. The Licensor authorizes You to exercise the Licensed Rights in all media and formats whether now known or hereafter created, and to make technical modifications necessary to do so. The Licensor waives and/or agrees not to assert any right or authority to forbid You from making technical modifications necessary to exercise the Licensed Rights, including technical modifications necessary to circumvent Effective Technological Measures. For purposes of this Public License, simply making modifications authorized by this Section [2\(a\)\(4\)](#) never produces Adapted Material.
5. Downstream recipients.

SPRINGER NATURE LICENSE
TERMS AND CONDITIONS

Jan 12, 2023

This Agreement between Pharmacen -- Dylan Hart ("You") and Springer Nature ("Springer Nature") consists of your license details and the terms and conditions provided by Springer Nature and Copyright Clearance Center.

License Number	5466431207745
License date	Jan 12, 2023
Licensed Content Publisher	Springer Nature
Licensed Content Publication	Molecular Diversity
Licensed Content Title	Design, synthesis, and anticancer activity of novel 4-thiazolidinone-phenylaminopyrimidine hybrids
Licensed Content Author	Aslı Türe et al
Licensed Content Date	Apr 23, 2020
Type of Use	Thesis/Dissertation
Requestor type	academic/university or research institute
Format	print and electronic
Portion	figures/tables/illustrations
Number of figures/tables/illustrations	1

Will you be translating?	no
Circulation/distribution	1000 - 1999
Author of this Springer Nature content	no
Title	Mr
Institution name	North-West University, Potchefstroom
Expected presentation date	Jan 2023
Order reference number	DHFIG2
Portions	Fig 2 - Keto/enol and amine/imine
	Pharmacien 6 Elephant Walk
Requestor Location	Richards Bay, Kwa-Zulu-Natal 3900 South Africa Attn: Dylan Hart
Total	0.00 USD
Terms and Conditions	